THE APPLICATION OF CFD TO BUILDING ANALYSIS AND DESIGN: A COMBINED APPROACH OF AN IMMERSIVE CASE STUDY AND WIND TUNNEL TESTING

Daeung Kim

Dissertation submitted to the Faculty of the Virginia Polytechnic Institute and State University in partial fulfillment of the requirements for the degree of

Doctor of Philosophy
in
Architecture and Design Research

James R. Jones, Chair
Robert P. Schubert
Elizabeth J. Grant
Demetri P. Telionis
Saad A. Ragab

December 11, 2013
Blacksburg, Virginia

Keywords: Computational Fluid Dynamics, building design, design assistance tool, immersive case study, wind tunnel tests

THE APPLICATION OF CFD TO BUILDING ANALYSIS AND DESIGN: A COMBINED APPROACH OF AN IMMERSIVE CASE STUDY AND WIND TUNNEL TESTING

Daeung Kim

ABSTRACT

Computational Fluid Dynamics (CFD) can play an important role in building design. For all aspects and stages of building design, CFD can be used to provide more accurate and rapid predictions of building performance with regard to air flow, pressure, temperature, and similar parameters.

Generally, the process involved in conducting CFD analyses is relatively complex and requires a good understanding of how best to utilize computational numerical methods. Moreover, the level of skill required to perform an accurate CFD analysis remains a challenge for many professionals particularly architects. In addition, the user needs to input a number of different items of information and parameters into the CFD program in order to obtain a successful and credible solution.

This research seeks to improve the general understanding of how CFD can best be used as a design assistance tool. While there have been a number of quantitative studies suggesting CFD may be a useful tool for building related airflow assessment, few researchers have explored the more qualitative aspects of CFD, in particular developing a better understanding of the procedures required for the proper application of CFD to whole building analysis. This study therefore adopted a combined qualitative and quantitative methodology, with the researcher immersing himself into a case study approach and defining several lessons-learned that are documented and shared. This research will assist practicing architects and architecture students to better understand the application of CFD to building analysis and design.

DEDICATION

In my memory, my father didn't say much, but I could feel your love.
While I am finishing this journey, I miss you the most and I won't forget your smile at the airport when I left for the United States.
Without your support and encouragement, I couldn't get to the end of this journey.
With my full respect, I dedicate this dissertation to you, my father,

Chun-Hwan Kim (1949 – 2010).

I also dedicated my dissertation to my family in South Korea:

My dear mom, for her greatest sacrifices and praying;

My lovely wife, Gajin Moon and our first baby, for care, support and patience;

My sister, Boram Kim, for her support;

Parents-in-law, for their support and encouragement

I love you all.

ACKNOWLEDGEMENTS

I would like to thank my supervisor, Dr. James R. Jones, for his guidance, assistance, encouragement, and patience. During my journey, his insightful guidance showed me the way to go forward. In addition, his way of conducting research made me to realize what the researcher's role is between Architecture and Engineering. Without his advice and support, I couldn't complete this journey. Thank you, Jim. Your thoughtful guidance always reminds me of the famous quotes from the movie "Dead Poets Society". That is "Oh Captain, My Captain."

I would also like to thank the members of my committee. Thank you, Dr. Elizabeth Grant, for your insightful ideas. Thank you, Prof. Robert Schubert, for your support and advice. Thank you, Dr. Saad Ragab, for your advice in conducting CFD simulation and kindness. Thank you, Dr. Demetri Telionis.

I am also thankful to CD-adapco, Computer-aided engineering company, for providing the academic license for the CFD simulation package "STAR-CCM+" without a charge.

Many thanks to my colleagues, Naif Altahlawi, Kongkun Charoenvisal, Bandar Alkahlan, Mohammed Aloshan, Vidya Gowda and Ana Jaramillo, for their warm words and support.

A special thanks to Heejin Jung, who is one of my best friends in Blacksburg, for his support and wishes.

TABLE OF CONTENTS

LIST OF FIGURES

APPENDICES

LIST OF EQUATIONS

APPENDICES

LIST OF TABLES

APPENDICES

1. INTRODUCTION

1.1. Background

Natural disasters such as cyclones, earthquakes, floods and landslides strike various parts of the world every year. In the United States alone, these cause hundreds of deaths and cost billions of dollars in disaster aid annually. According to the preliminary report issued by NOAA's National Climatic Data Center (Graumann et al., 2005), Hurricane Katrina has been the most expensive natural disaster in recent U.S. history. Although only a Category 3 hurricane, Katrina caused massive devastation along the central Gulf Coast states of the U.S. and was responsible for more than 1,800 deaths.

Wind fluctuations during high wind events can have a serious effect on building envelopes, often with serious consequences such as roof failures (Morrison & Kopp, 2011) because wind uplift pressure makes roof membranes flutter or rapidly flap up and down (Baskaran et al., 2009). According to Blessing et al. (2009), the resulting loss of roofing leads to rainwater intrusion, interior restoration and occupant displacement. Moreover, roofing elements separated by high winds become wind-borne debris that then cause further damage to other structures downwind. Suaris and Irwin (2010) found that the uplift pressure generated by corner vortices can create very high intermittent suction. Aerodynamic loads on the roof and walls of a low building are characterized by the interaction of wind flow with the surface of the building and this interaction depends primarily on the building geometry and flow characteristics (Stathopoulos, 1984). However, architects and engineers seldom consider these issues but instead tend to focus primarily on design and structural aspects related to elements such as walls, overhangs, foundation and roofing when designing buildings.

Managing the risk to buildings from wind requires detailed information on the type and magnitude of the wind loads that buildings are likely to be exposed to. Recent attempts to minimize damage due to high winds have been devoted to developing more reliable estimates of wind effects on buildings. For example, Tieleman et al. (1998) used a 1:50 scale model of the

WERFL experimental building in the wind load test facility at Clemson University to examine how the pressure coefficient varied with horizontal turbulence intensity, the small-scale turbulence parameter and the streamwise and lateral turbulence integral scale. Chen and Zhou (2007) investigated the equivalent static wind loads on low-rise buildings based on full-scale measurements, while wind-induced torsional loads on low rise buildings were reported by Elsharawy et al. (2012), who assessed the effectiveness of three national building codes and standards, namely ASCE 7 (United States), NBCC (Canada), and EN 1991-14 (Australia). Ho et al. (2005) studied the effect of the surroundings on wind loads on flat roof low buildings, examining several cases of similar buildings with different types of immediate surroundings.

Traditionally, this information has been gathered using a combination of wind tunnel tests and full-scale measurements. However, these field studies can be both time-consuming and costly so Computational Fluid Dynamics (CFD) methods are becoming more widely accepted as an alternative tool for predicting turbulent flow over buildings and thus informing their design. CFD methods are convenient to access for design practice and can simulate the flow field about a building and predict parameters of interest such as velocity, pressure, and temperature fields (Alexander et al., 1997). CFD techniques are now commonly applied in a number of industries.

1.2. Wind tunnel tests

Wind tunnels have been employed extensively for both industry and research applications over the past 50 years. Varying greatly in scale and geometry, some facilities are large enough to house and test small aircraft while others are miniaturized to accommodate the flow generators used in the calibration of small sensors (Morrison & Kopp, 2011). Wind tunnels are used to study the flow of air over objects of interest, the forces acting on them, and their interaction with the flow and have been employed to verify aerodynamic theories and facilitate the design of aircraft, as well as to develop new aircraft, wind turbines and other designs that involve complex interactions with an airflow (Hernandez et al., 2013).

On Mar 23 – 24, 2012, wind tunnel testing was conducted at the IBHS in Richburg, SC to investigate the performance of roof vent systems developed by Virginia Tech and Acrylife Inc. For this study, the data from these wind tunnel tests were utilized to validate the results of the CFD modeling.

1.3. CFD simulations for building design

Due to the time and cost issues involved in wind tunnel testing, CFD is now widely employed for the prediction of flow fields. The first CFD techniques were introduced in the early 1950s, made possible by the advent of the digital computer (Chung, 2002). CFD is a computer-based mathematical modeling tool capable of dealing with fluid flow problems and predicting physical fluid flows and heat transfer (Versteeg & Malalasekera, 1995). While traditionally thought of as exclusively for use in aerodynamic research, CFD analysis is now being applied in many other fields, including marine engineering, electrical and electronic engineering, biomedical engineering, chemical engineering, environmental engineering, wind engineering, hydrology, oceanography, meteorology, and nuclear power (Versteeg & Malalasekera, 1995). As the range of CFD applications continues to increase, new techniques have been introduced that facilitate its use in both architectural engineering and HVAC (heating ventilating and air conditioning) design (Zhang et al., 2009). It is particularly useful for building design and analyses, where it has been applied with considerable success (Murakami, 1998). There are now numerous commercial CFD software packages that are targeted specifically toward building applications.

CFD is used intensively as a tool for evaluating the indoor environment of a building and its interaction with the building envelope, as well as for analyzing the outdoor environment surrounding the building (Blocken et al., 2009). For the prediction of external wind flows, CFD can be used to analyze wind loading on buildings, bridges, and street canyons. For example, Sengupta et al. (2008) simulated the effects of microburst and tornadic winds to quantify the resulting aerodynamic loading on a building in order to investigate the peak loads and stresses at various locations on a roof and then compared the results to the corresponding values for the guidelines specified in ASCE 7-05. In a study examining pedestrian wind comfort, Janssen et al.

(2013) compared and evaluated various wind comfort criteria to highlight the importance of standardizing the wind comfort assessment procedure using CFD techniques. For their research on predicting pollutant dispersion, Gousseau et al. (2011) employed CFD to investigate pollutant concentrations in streets and on building surfaces surrounding the source. CFD has also been applied to test proposed natural ventilation, mixed-mode ventilation, and HVAC systems in buildings (Hooff & Blocken, 2012; Balocco & Lio, 2011; Bangalee et al., 2012; Chiang et al., 2012), which generally involves the prediction of air temperature, velocity, and relative humidity, among other parameters. CFD techniques have been used to simulate the spread of fire and smoke through large-volume spaces (Huang et al., 2009) as well as being applied in clean rooms and buildings in order to protect against biochemical and radioactive agents and provide contamination control (Rui et al., 2008). Figure 1.1 shows several examples of CFD applications that enhance building performance.

According to Wainwright and Mulligan (2004), CFD offers a number of advantages compared to traditional wind tunnel testing. Not only can CFD generate full-scale simulations as opposed to scale models of many physical simulations, it also provides more extensive data than can be measured in the lab and its results can be visualized clearly and in great detail. On the other hand, CFD also has several drawbacks and issues. Knowledge and experience of fluid mechanics are required to evaluate CFD results critically and a good understanding of how a CFD code functions for a particular application is essential if the results are to be meaningful. In addition, the cost of purchasing a commercial CFD package is high and a high-performance computer is required.

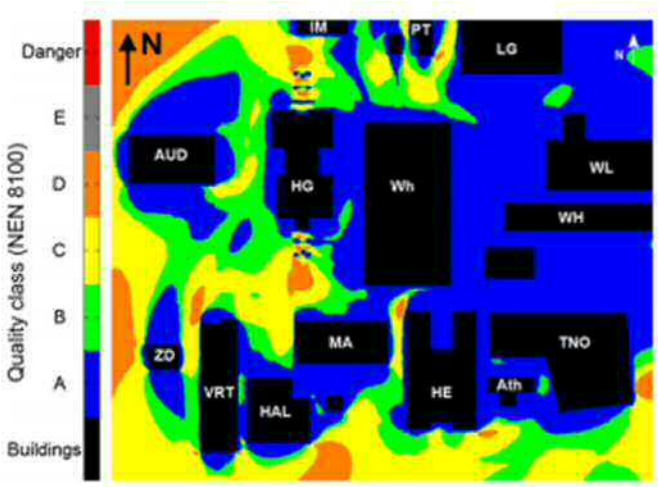

a. Assessment of pedestrian wind comfort (Janssen et al., 2013)

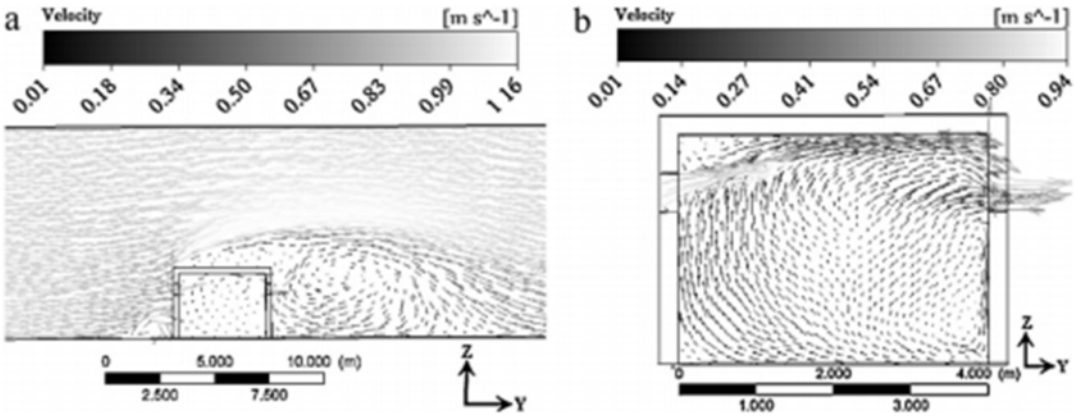

b. Prediction of natural ventilation (Bangalee et al., 2012)

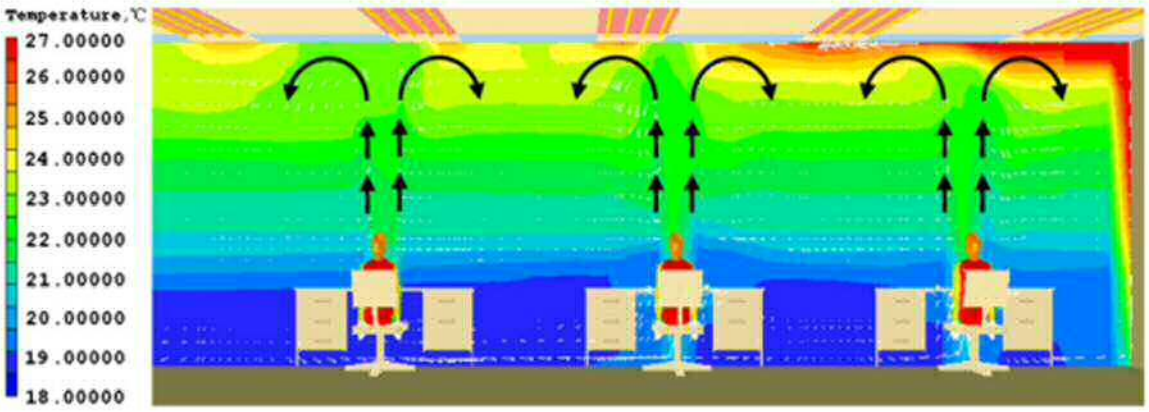

c. Investigation of HVAC system for indoor environment (Chiang et al., 2012)

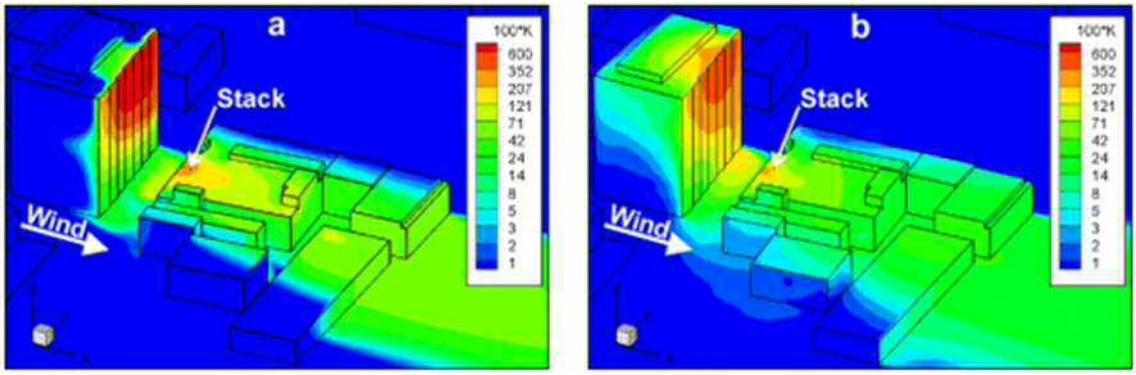

d. Prediction of pollutant dispersion (Gousseau et al., 2011)

Figure 1.1 - Various CFD applications for building design

1.4. General use of CFD as a design assistance tool

According to the AIA (American Institute of Architects), design and construction projects typically involve several phases (*The five phases of design*, the AIA).

In the first stage, the most important decisions are made. In this stage, discussions regarding the project requirements are conducted, with stakeholders presenting their expectations for aspects such as the number of rooms, functions and occupants to the design team. These discussions enable the scope of the design project to be outlined. Once the object to be built has been defined, the next step is to create schematic designs. During the schematic design stage, study drawings, documents, or other media that illustrate the concepts of the design and include spatial relationships, scale, and form for the owner to review are developed. The third step is design development. In this phase, the initial designs from the second phase are developed further by adding details of the project's mechanical, electrical, plumbing, and structural elements, and architectural documents are provided. After the design development phase is complete, construction documents are prepared. Once the construction documents are finalized, the general contractor or builder who will undertake the actual construction is hired (*The five phases of design*, the AIA).

During the schematic phase, CFD is often employed to calculate airflows in and around the buildings. Based on the calculated results, it typically determines whether the design needs to be modified. In order to achieve satisfactory indoor and outdoor environmental conditions for the building, these steps will be repeated iteratively as often as necessary to achieve a satisfactory result (Glicksman, & Lin, 2006).

As indicated above, CFD techniques are now commonly used as a design assistance tool. The results from CFD simulations during the schematic design stage can help architects or designers to improve the indoor and outdoor environment for the planned building at the schematic design stage. Figure 1.2 shows the architectural design process when CFD simulation is used.

This study demonstrates the use of the CFD process as a design assistance tool for building design and provides recommendations to ensure the effective use of CFD simulation results.

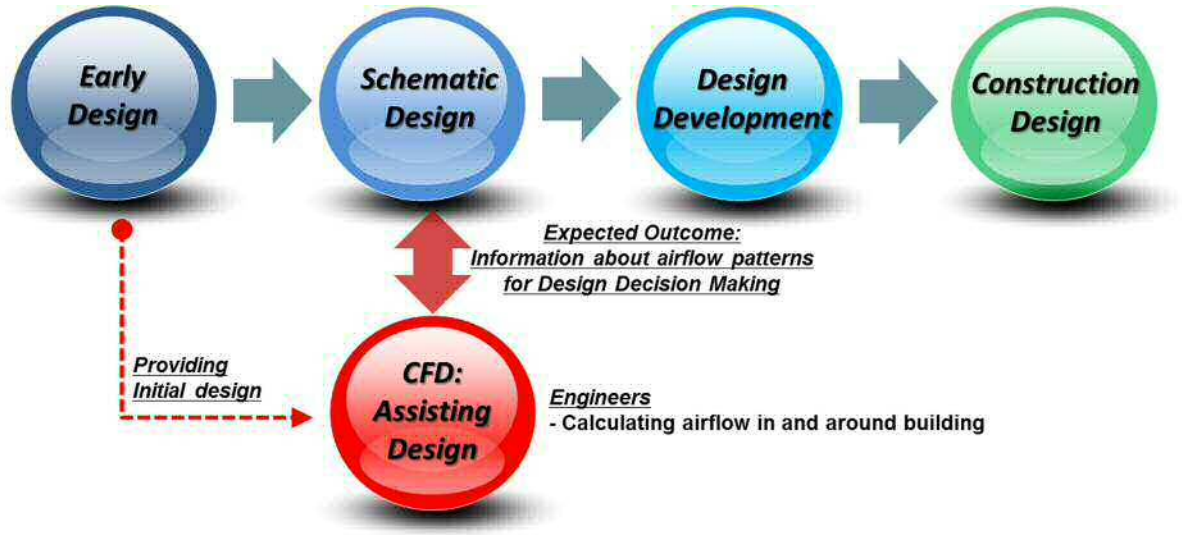

Figure 1.2 - Architectural design process with CFD simulation

1.5. Problem statement

The demand for new, easier to use CFD applications continues to increase and many commercial CFD codes are now available that are designed to be used by non-CFD experts. Many architects have begun to take advantage of CFD techniques as a design assistance tool because CFD analyses can provide detailed information throughout all stages of the design process, providing a flexible and interactive design environment for design decision making. However, there are several potential pitfalls that users need to constantly bear in mind. First, CFD is difficult to use in the architectural design process because of its relatively complicated process and time consuming aspects such as the generation of complex geometries. Second, various calculation conditions, such as the size of the computational domain, grid resolution, boundary conditions, selection of the turbulence model, and so on must be set by the user. As Ferziger (1990) pointed out, the selection of boundary conditions is not a simple matter in the numerical solution of turbulent flow. Third, although many CFD publications on building performance have focused on the quantitative aspects of the problem, far fewer have reported qualitative investigations into the effectiveness of adopting CFD as a design assistance tool. Instead, most numerical studies have conducted straightforward quantitative comparisons of model predictions against experimental observations.

Understanding the CFD process and its limitations is crucial if it is to become a dependable tool for design and analyses. By considering the challenges described above and how they relate to the needs of architects, the findings of this study will assist designers. Although some preliminary quantitative procedures are used, the main focus of this study is on the qualitative aspects of the problem in order to bridge the gap between architecture and engineering.

1.6. Scope of research

1.6.1. Primary goal

This research seeks to improve our understanding of how best to utilize CFD as a design assistance tool for architecture. While a number of quantitative studies have suggested that CFD may be a useful tool for building related airflow assessment (Ramponi & Blocken, 2012; Lo et al., 2013; Hooff & Blocken, 2013), there have been few studies exploring the more qualitative aspects of CFD, including the development of suitable procedures for the proper application of CFD to whole building analysis. Adopting a combined qualitative and quantitative investigation, in the course of which the researcher immersed himself in the case study approach for analyzing wind effects on building roofs, enabled him to develop a set of lessons-learned that can be documented and shared. This research thus applied a combined method using both qualitative and quantitative techniques to maximize the effective use of CFD as a design assistance tool and to minimize any inaccuracies related to its application for building design in the schematic design stage.

1.6.2. Research objectives

A thorough literature review and journal analysis of the key computational parameters and conditions involved in CFD analyses of wind flow around buildings was conducted for this study. These selected parameters were examined and validated utilizing the data gathered during wind tunnel tests conducted at the IBHS. Results of a sensitivity analysis comparing CFD to wind tunnel data were then used to inform the immersive case study. The observations were gathered and discussed in the context of the themes that emerged from the data during the case studies. Throughout this process, lessons-learned were documented. The outcome was a rich description of the simulation process and a summary of lessons-learned to inform the practice of those using CFD for building airflow analysis.

1.7. Significance

The significance and unique contribution of this research is that it considered the challenges of CFD simulation from a designer's point of view. Its findings include a comprehensive set of recommendations to guide the use of CFD for the prediction of building performance that are expected to provide a greatly improved understanding of how to apply CFD methods to best effect during the building design process.

1.8. Limitations

In order to predict air flow in and around a building, CFD analyzes the air velocity, temperature, contaminant concentrations, and amount of turbulence around that building by solving a set of mathematical equations. It is therefore necessary to conduct mathematical modeling at the outset to establish the necessary computational inputs. Unlike other building simulations such as energy simulations, CFD requires users to have some knowledge of mathematical modeling and experience with numerical methods. In addition, the CFD modeling approach relies on physical models such as turbulence. However, computational domains for outdoor environment studies can be very large and the boundary conditions are not always well-known (Blocken et al., 2011). This may lead to very large computational errors in the simulation results. It is difficult for non-experts or architects to conduct CFD simulations.

Moreover, this research employed a qualitative approach using case study methods. For this approach, the primary instrument of data collection and analysis is the researcher. However, it is difficult for case study researchers to act as trained observers. In addition, the research outcome is generally heavily dependent on the researcher's own instincts and abilities.

In this research, the critical computational inputs were established through case study methods. As a building designer, it is not always easy to completely understand mathematical equations and physical models in real world. The computational inputs utilized were those established by previous researchers and reported in the literature, particularly the findings of studies

investigating wind flow in building applications using CFD techniques. Less rigorous commercial CFD codes are available that can be used in building practice and for analyses of the built environment. These commercial codes include advanced techniques that automate much of the data specification process for common situations. Moreover, the limitations of case study methods can be overcome by employing iterative methods such as the document analysis and an immersive approach.

1.9. Dissertation outline

Chapter Two presented the qualitative research approach to provide an in-depth description of the CFD process as a design assistance tool. A review of the qualitative research method and the case study approach was presented in this chapter. For this approach, the research design, data collection, case study evidence and the validity were presented in detail.

In order to choose the initial computational parameters for CFD simulation at the early design stage, best practice guidelines were briefly reviewed in Chapter Three and a set of computational parameters for wind flows around buildings reviewed. However these selected parameters were not sufficient to ensure credibility, and therefore the ten-steps approach was employed. The characteristics of this approach were summarized in Chapter Four. In this chapter, four journal articles related to the application of CFD for wind flows around buildings were analyzed using the ten-steps approach in order to obtain specific computational parameters.

Computational results should be validated with experimental data whenever possible to ensure their credibility and reliability. For this validation and to inform the CFD simulation process, wind tunnel testing was conducted at the IBHS wind facility. An overview of these wind tunnel tests and their results were presented in Chapter Five.

Using the computational parameters from Chapters Three and Four, three sensitivity analyses were conducted and these were presented in Chapter Six. CFD simulations were compared with

the wind tunnel testing at the IBHS as described in Chapter Five. These results included the velocity and pressures along the centerline and on the roof of the building.

The computational parameters selected in Chapters Three to Six were employed in the case study. The wind flow behaviors on the roof surface of a low-rise building with several building configurations, including various building heights, aspect ratios and parapet wall heights were investigated in Chapter Seven. For the case study, some computational parameters were subsequently reselected based on these results.

The computational parameters from Chapters Six and Seven were analyzed and are categorized under two themes in Chapter Eight. Discussions of the CFD process for wind flow around buildings considering the accuracy and the effective use of CFD in the schematic design stage were presented in this chapter.

Chapter Nine was devoted to a set of the lessons-learned from the present study. In Chapter Ten, the conclusions and some recommendations were made for future research.

2. QUALITATIVE RESEARCH APPROACH

The main goal of this research is to provide an in-depth description of the CFD process in order to improve our understanding of its use as a design assistance tool. This chapter outlines the rationale supporting the utility of qualitative research methods and the case study approach and describes the case study research design and methods used for this study. Multiple case study methods are explored and the case selection process, methods of data collection and analysis of the collected data are described.

2.1. Qualitative research method

This research makes use of qualitative research methodologies to understand the process of applying CFD tools to issues related to building design as a decision-support tool following the recommendations provided by Linda Groat and David Wang. In their book *Architectural Research Methods*, Groat and Wang address the "generic" definition of qualitative research originally stated by Norman Denzin and Yvonne Lincoln as follows:

> Qualitative research is multi-method in focus, involving an interpretive, naturalistic approach to its subject matter. This means that qualitative researchers study things in their natural settings, attempting to make sense of, or interpret, phenomenon in terms of the meanings people bring to them. Qualitative research involves the studied use and collection of a variety of empirical materials (Denzin & Lincoln, 1998, as quoted in Groat & Wang, 2002, p. 176).

This definition implies that the value of the research is precisely due to its ability to highlight trends embedded in the context of the academic departments the subjects are a part of. They ground their work in the empirical realities of their observations and interviews, while at the same time making it clear that they, as researchers, play an important role in interpreting and making sense of that data. Researchers aim to present a holistic portrayal of the setting or phenomenon under study as the respondents themselves understand it. Groat and Wang also pointed out that the strategy of qualitative research consists of first-hand encounters with a

specific context and thus involves gaining an understanding of how people in real-world situations 'make sense' of their environment and themselves using a variety of tactics. They provide the following summary of the attributes of qualitative research design, based on previous researchers' descriptions:

Holistic. The goal of qualitative research is to gain a holistic (systematic, encompassing, integrated) overview of the context under study.
Prolonged Contact. Qualitative research is conducted through an intense and/or prolonged contact with a 'field' or life situation.
Open Ended. Qualitative research tends to be more open-ended in both theoretical conception and research design than other research strategies.
Researcher as Measurement Device. Since there is relatively little use of standardized measures such as survey questionnaires, the researcher is essentially the main measurement device in the study.
Analysis Through Words. Since an emphasis on descriptive numerical measures and inferential statistics is typically eschewed, the principal mode of analysis is through words, whether represented in visual displays or through narrative devices.
Personal Informal Writing Stance. In contrast to the typical journal format of experimental or correlational studies, the writing style of qualitative work is typically offered in a personal informal writing stance that lessens the distance between the writer and the reader (Groat &Wang, 2002, p. 179).

This description goes a long way towards describing the aims and strategies of the present research. Here, the actions will be those components of the lessons related to the CFD simulation that most accurately reflect the reality and the understanding of its application. Groat and Wang (2002) conclude that the major strengths of qualitative research follow from its capacity to take in the rich qualitative information available in real-life circumstances and settings. Based on this qualitative research method, a direct means of achieving this is as a participant observer directly involved in the prediction of building design and systems in order to answer the research question concerning the applicability of the CFD technique. In addition to the information

gleaned as a participant observer and through direct observation of a CFD case study for building design and systems, information that addresses the research question will be gathered through the researcher's practice as an architect. It is through this practice that a participant observer can gain a more comprehensive understanding of what lessons can be learned about the utility of CFD as a decision-support technique.

2.2. Utilizing the case study approach

This qualitative study is concerned with improving our understanding of CFD as a technique for studying airflow around buildings. In order to perform this study, a case study approach was adopted. According to Rowley (2002), case studies as a research method or strategy have traditionally been considered as lacking rigor and objectivity comparing with other social research methods. However, in spite of this skepticism they are widely accepted by researchers in many fields since they can offer insights that might not be achieved with other approaches. Rowley (2002) also mentioned that case studies have often been considered a useful tool for the preliminary, exploratory stage of a research project in order to provide a basis for the development of the 'more structured' tools that are necessary in surveys and experiments. Robert Yin quotes a useful definition of case studies given by an earlier researcher in his book *Case Study Research* (1994):

> The essence of a case study, the central tendency among all types of case study, is that it tries to illuminate a decision or set of decisions: why they were taken, how they were implemented, and with what result (Schramm, 1971, quoted in Yin, 1994, p.17).

He explores the concept further to provide an alternative definition:

> A case study is an empirical inquiry that investigates a contemporary phenomenon within its real-life context, especially when the boundaries between phenomenon and context are not clearly evident (Yin, 1994, p.18).

Yin (1994) emphasized that an important strength of case studies is their ability to facilitate an investigation into a phenomenon in its context. Thus, the replication of the phenomenon in a laboratory or experimental setting is no longer necessary to achieve a better understanding of the phenomena, making the case study method a valuable way of looking at the world around us. Moreover, case study research can be based on any mix of quantitative and qualitative approaches and can utilize multiple data sources, including direct/participant observations, interviews, and documents (Rowley, 2002).

The goal of this study has been to improve our understanding of the use of CFD as an architectural design tool. Many researchers have shown that CFD studies can provide useful information, demonstrating good statistical and quantitative reliability between experiments and simulations (Ramponi & Blocken, 2012; Hooff & Blocken, 2012; Chavez et al, 2011; Blocken et al, 2008), and the increasing use of CFD has led to it being applied for a wide range of purposes in built environments. However, real-world projects may involve conditions or parameters that are either unfamiliar or too complex to apply to different situations. To determine the limits that should be applied to restrict the scope of its use, the applicability of CFD will be studied in the context of wind flow over a roof by adopting a case study strategy.

2.3. Overview of case study approach

The case study performed for this research was designed to obtain a holistic description of the CFD modeling process in the context of wind flow around a building. The following sections will discuss, in turn, the guidelines for data collection, analysis, and the decision-making process regarding which evidence to pursue and information to collect among the available data.

2.4. Case study research design

The design of a case study encompasses the logic that connects the data to be collected and the conclusions to be drawn to the initial questions addressed by the study. This ensures that there is a clear view of what is to be achieved by the case study. This process includes defining the basic

components of the investigation, such as the research questions and propositions, determining how validity and reliability will be established, and selecting an appropriate case study design (Rowley, 2002).

Among these components, the research question is perhaps the most significant element in determining the most appropriate research approach. Who, what and where questions can be investigated through documents, archival analysis, surveys and interviews (Yin, 1994). As mentioned previously, this study is based on the CFD modeling process. However, issues concerning the credibility and acceptance of CFD results remain due to its complexity and the number of computational parameters. Thus, the research questions guiding this case study are:

1) What computational parameters are used in the context of the CFD analysis of wind flow around a building?
2) How has the wind tunnel testing informed the CFD modeling process?
3) How are the credibility and reliability of the CFD results determined?
4) What CFD tool is most appropriate to support architectural design decision making? and
5) How can CFD modeling be integrated with the architectural design process?

According to Yin (1994), the design of a case study can be classified along two dimensions, reflecting the number of case studies contributing to the design, and the number of units in each case study, respectively. It is important to make a distinction between single case and multiple case designs. A single case design is appropriate when the case is closely linked to an established theory for some reason. This might occur when the case provides a critical test of a well-established theory, for example, or where the case is extreme, unique, or has something special to reveal. In the case of a multiple case design, the more cases that can be included to establish or refute a theory, the more robust the resulting research outcomes. In a multiple case design cases should be chosen carefully in order to produce either similar or contrasting results.

For this study, a multiple case design was employed. Each case was investigated using a conceptual framework to include as wide a range as possible of contextual factors and outcomes

to be explored and compared. The context of interest for the case studies focused on the wind flow around a building. Multiple sources of evidence, including documents, participant observation, archival records and artifacts, were collected to ensure the strength of the case study methodology.

2.5. Selection of the cases

After taking the decision to adopt a multiple case study design for this study, the next issue was the number of cases that should be included in the research project. Cases are typically selected purposively to maximize learning about the research questions, in contrast to the quantitative ideal of a random sample that is statistically representative of a larger population (Patton, 2002; Yin, 1994). With regard to the sample size, Patton argued that "There are no rules for sample size in qualitative inquiry. Sample size depends on what you want to know, the purpose of the inquiry, what's at stake, what will be useful, what will have credibility, and what can be done with the available time and resources" (2002, p. 244). Yin (1994) suggested that the decision on sample size should reflect the number of replications of both literal and theoretical aspects of the problem and that this replication is one of the most powerful ways to ensure the high credibility of the results. In order to identify patterns of similarity, the sample size will be determined based on the literal replication.

Another important consideration in selecting the cases to be included in a multiple case design is the specific sampling strategy utilized (Patton, 2002). Patton suggested that "Because research and evaluations often serve multiple purposes, more than one qualitative sampling strategy may be necessary . . . The sampling strategy must be selected to fit the purpose of the study, the resources available, the questions being asked, and the constraints being faced" (2002, p. 242)." In order to achieve a better understanding of the problem and the research questions, cases were therefore selected purposefully for this case study (Cresswell, 2009). Three cases were selected and each case conducted a CFD simulation in order to examine wind flow on the roof surface with several building configurations including the building height, aspect ratio and parapet wall heights. The three cases are presented in Table 2.1.

Table 2.1- Overview of the three case projects

Cases	Projects
Case A	An investigation of wind flow on a roof with two different building heights
Case B	A comparisons of wind flow on the roof surface with two different building aspect ratios
Case C	A comparisons of wind flow on the roof surface of a low-rise building with three different parapet walls

2.6. Objectives of the case study

In order to address the study's overarching research questions, a set of substantive research objectives was developed to achieve a robust, holistic description of the CFD simulation for the investigation of wind flow around buildings in the architectural design process. Figure 2.1 showed an overview of the major components of the case study design. In this figure, the objectives provided a roadmap for data collection and analysis, guiding decisions on what documentary evidence to pursue and what information to gather through participant observation during two design stages. The objectives are:

1) Early design stage

- In order to reproduce wind flow around buildings using CFD, computational parameters were selected through document analysis and the sensitivity tests.
- Best practice guidelines were reviewed to select computational parameter for wind flow around buildings (Chapter 3).
- Four journal articles were analyzed in order to achieve specific computational parameters for wind flow around buildings (Chapter 4).
- The sensitivity of selected computational parameters from best practice guidelines and the analysis of journal articles were analyzed using the data of wind tunnel tests at the IBHS (Chapter 5 & 6).

- The chosen computational parameters through Chapter 4 to 7 were applied and analyzed through case studies (Chapter 7).

2) Schematic design stage

- The computational parameters of the early stage were categorized and analyzed under two categories (Chapter 8):

a) What are the computational parameters to maximize the accuracy of the CFD modeling? and,

b) What are the computational parameters for the effective use of CFD as a design assistance tool regarding time consuming aspects and easy use of CFD?

- Through research process, lessons-learned to inform CFD process for building design were documented (Chapter 9).

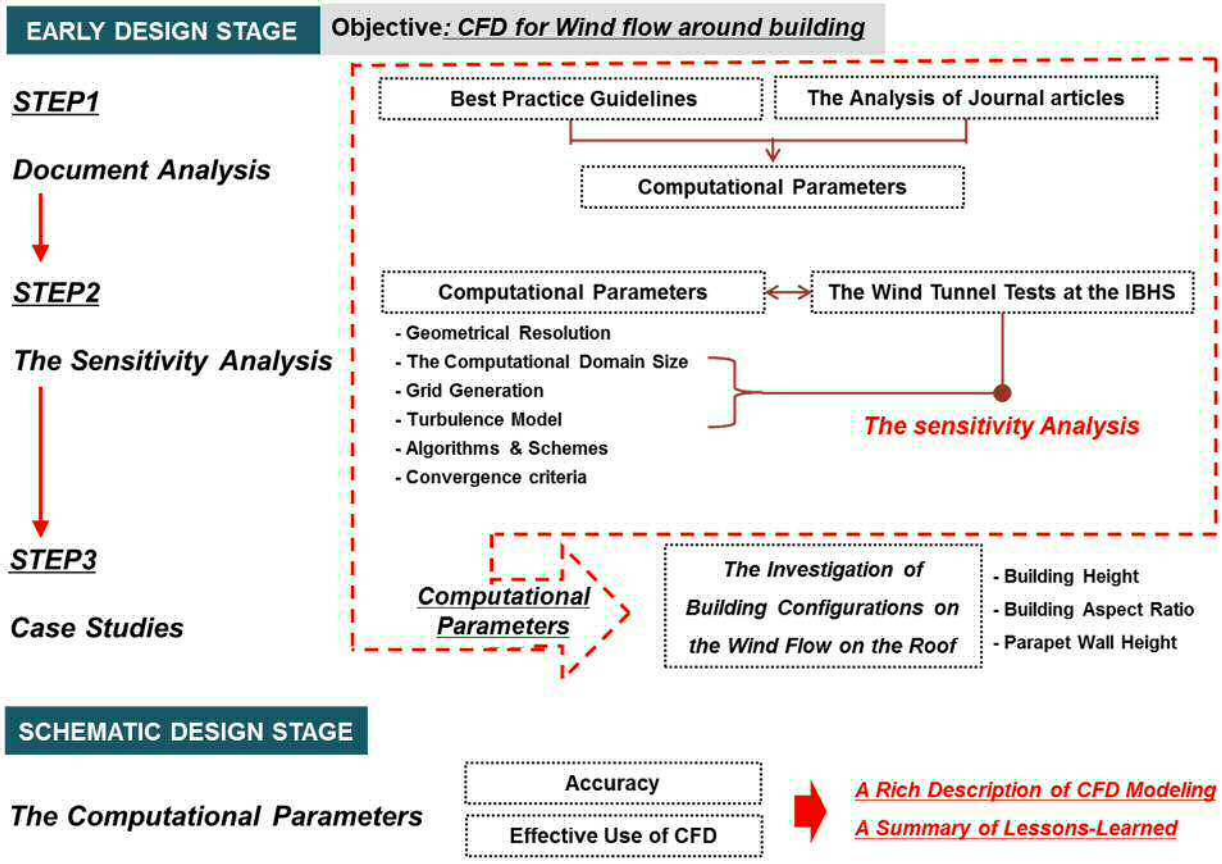

Figure 2.1 - Overview of the case study design

2.7. Data collection

Typically, case studies draw on multiple sources of evidence including documents, archival records, interviews, direct observation, participant observation, and physical artifacts. Each of these different sources requires a different approach and is likely to produce a different kind of insight (Yin, 1994).

This section introduces the methods used to collect the evidence for this case study during two design stages. First, documents including studies, reports and practice guidelines related to CFD investigations of wind flow around a building were reviewed and analyzed. In the context of wind flow around a building, information on the computational parameters used and how these have influenced the results were gathered. Second, participant observation was conducted, conducting the CFD analysis, and any relevant physical artifacts or archival records were also obtained. For the observation, the data were collected with the researcher as a passive observer, immersing him into each case. For the specific data collection, the evidence for this case study was obtained from the following four sources:

Documents – Studies, evaluations of the computational parameters for CFD applications of wind flow around a building.
Archival records –Statistical or survey data from the result of CFD analyses validated quantitatively.
Participant observation – The researcher's first-hand knowledge of CFD modeling was important due to his personal experience of making decisions regarding computational parameters.
Physical Artifacts – The visualization of wind flow speed or pressures by CFD simulations.

Among those different types of evidence, participant observation implies an active engagement with individuals in their natural setting. For the participant observation, an immersive approach was therefore employed. An immersive approach consists of introducing people into a simplified situation to facilitate the observation of their various behaviors. The immersion continues the

idea of a controlled set-up from the laboratory methodology but also builds on the importance of rich contextual situations advocated by the situated methodology (Sester et al., 2013). For this study, participant observation involved recording impressions and descriptions in the form of a set of field notes describing the CFD modeling process.

For the document collection, the best CFD practice guidelines were reviewed in order to provide initial inputs for the computational parameters. To obtain a specific understanding of CFD analysis in the context of wind flow around a building, four papers published in academic journals were collected and analyzed using the ten iterative steps approach in order to provide more detailed computational parameters. The best practice guidelines are presented in Chapter 3 and an analysis of four selected papers using the ten steps approach is presented in Chapter 4.

2.8. Analysis of case study evidence

Cresswell contended that "The process of data analysis involves making sense out of text and image data. It involves preparing the data for analysis, conducting different analyses, moving deeper and deeper into understanding the data, representing the data, and making an interpretation of the larger meaning of the data" (2009, p. 183). Unlike statistical analysis, qualitative analysis depends on an investigator's own style of rigorous empirical thinking, accompanied with a presentation of the evidence and a consideration of alternative interpretations (Yin, 1994). For the analysis in this study, data collected from the examination of documentation and observations including field notes were stored and organized under categories based on emergent themes. The data gathered in the course of the participant observation were given more weight in the analysis than were the data extracted from the document reviews.

2.9. Validity of the study

Cresswell also noted that "Validity is one of the strengths of qualitative research, and it is based on determining whether the findings are accurate from the standpoint of the researcher, the

participant, [or] of the readers of an account" (2009, p. 191). In this research, established procedures were employed to enhance the credibility:

- Data triangulation across multiple evidence sources was used during data collection and analysis to strengthen the information and to assess patterns (Yin, 1994)
- Self-reflection was used during the data collection process for the participant observation to create an open and honest narrative (Cresswell, 2009).

2.10. Researcher's Role

The researcher is the sole investigator in this study. Since 2005, I have regularly performed CFD simulations to analyze wind flow in and around buildings. The two and a half years' experience gained during my master's research and the 5 years I have spent studying for my Ph.D. have given me a deep understanding of its intricacies, enabling me to appreciate how CFD applications can best be used in the context of built environments. Conducting this multiple case study will allow me to immerse myself into the case studies in order to collect evidence based on my CFD experience. Based on my observations of the creation and modification of CFD models in analyzing wind flow on buildings, the findings of this research will help designers gain a better understanding of the utility of CFD applications for building design.

3. BEST PRACTICE GUIDELINES FOR CFD

When performing a simulation, the user typically chooses select target variables, the approximate form of the governing equations, the turbulence model, the level of detail in the geometrical representation of the buildings, the size of the computational domain, the type and resolution of the computational grid, the boundary conditions, the discretization schemes, and the iterative convergence criteria. Since the results of CFD simulations can be highly sensitive to the wide range of computational parameters, these parameters must be carefully considered by the user (Blocken & Gualtieri, 2012). It is also increasingly necessary to establish generally recognized and accepted quality assurance criteria for evaluating CFD results as a result of the rapid development of CFD and the increasing complexity of the geometrical and physical conditions of CFD simulations (Hirsch, 2006). The past decade has seen the development and publication of several important best practice guideline documents to assist in this process (Blocken et al., 2012).

3.1. Overview of best practice guidelines

In the late 1970s and 80s, CFD investigations into issues such as the effects of the size of the computational domain, the grid resolution, the boundary conditions and the turbulence model on the computational results. These studies have all contributed to the introduction of best practice guidelines for CFD in urban aerodynamics (Blocken et al., 2012).

Since 2000, several best practice guidelines have been published. ERCOFTAC's Special Interest Group on "Quality and Trust in Industrial CFD" published best practice guidelines for achieving high-quality industrial CFD using RANS equations (Casey & Wintergerste, 2000). These guidelines focused on helping less experienced CFD users and experienced users moving to a new application area. To ensure the accuracy of CFD in wind engineering applications, Franke et al. (2004) summarized the results of CFD simulations in the built environment, focusing particularly on the mean velocities and turbulence obtained using steady RANS simulations in order to deduce recommendations on the proper use of CFD. Franke et al. (2007) then went on to

publish best practice guidelines for CFD simulations of flows in urban environments based on published guidelines and recommendations dealing with applications of the steady RANS simulations and included a consideration of other turbulence models such as unsteady RANS and LES. A set of guidelines for CFD prediction were also provided by the Architectural Institute of Japan (AIJ) that focused on the pedestrian wind environment around buildings. Tominaga et al.'s (2008) AIJ guidelines on this topic utilized steady RANS equations. In a parallel project, Tamura et al. (2008) published another AIJ guide that examined the numerical prediction of wind loads on buildings based on the use of LES simulations.

3.2. Recommendations for the use of CFD for wind around buildings

Best practice guidelines provide valuable information on how the CFD applications should be used in order to avoid or at least reduce user errors caused by the incorrect use of CFD and a lack of experience or resources (Franke et al., 2007). A number of best practice guidelines have been published that classify proper computational conditions for the CFD resolution of wind around buildings. Three of these were reviewed for this study: "Best practice guidelines for the CFD simulation of flows in the urban environment" (Franke et al., 2007), "AIJ guidelines for practical applications of CFD to pedestrian wind environment around buildings" (Tominaga et al., 2008), and "Best practice guidelines" (Casey & Wintergerste, 2000) since their recommendations are widely used in current CFD studies focusing on wind flows around elements in the built environment (Chavez et al., 2011; Ramponi & Blocken, 2012; Blocken & Persoon, 2009; Hooff & Blocken, 2012; Chavez et al., 2012; Balogh et al., 2012; Karava et al., 2012; Blocken et al., 2008; Lateb et al., 2013; Hooff et al., 2012; Cheung & Liu 2011; Hertwig et al., 2012; Moonen et al., 2012; Blocken et al., 2012; Montazeri & Blocken, 2013; Hooff & Blocken, 2010; Blocken & Gualtier, 2012).

Sections 3.2.1 through 3.2.6 in this chapter briefly highlight and explain the recommendation for CFD conditions related to wind around buildings based on the works cited above.

3.2.1. Geometrical representation

According to Franke et al. (2007), wind flow patterns are greatly influenced by the distribution of buildings or topography and the central region of interest should be represented with as much as possible. They also suggest that simulations be performed both with and without details of a small region around the region of interest to limit the consideration of details and thus avoid the need for increased computational resources. Moreover, those buildings located away from the center region can be represented by simple blocks. However, Tominaga et al. (2008) mention specifically that the area of a radius 1- 2H from the building of interest should be reproduced as accurately as possible, where the height of the building of interest is H. They also recommend that at least one additional street block in each direction around the region of interest should be clearly reproduced. Figure 3.1 shows and example of a high-resolution computational domain taken from Blocken et al. (2012), who created the computational domain and reproduced building geometries satisfying the best practice guidelines recommended by both COST (Franke et al., 2007) and AIJ (Tominaga et al., 2008).

For the geometrical representation, the central region of interest (the area of a radius 1 -2 H from the building of interest) is reproduced as accurately as possible and buildings located away from the region of interest are represented by simple blocks. In addition, at least one additional street block in each direction around the region of interest should be represented.

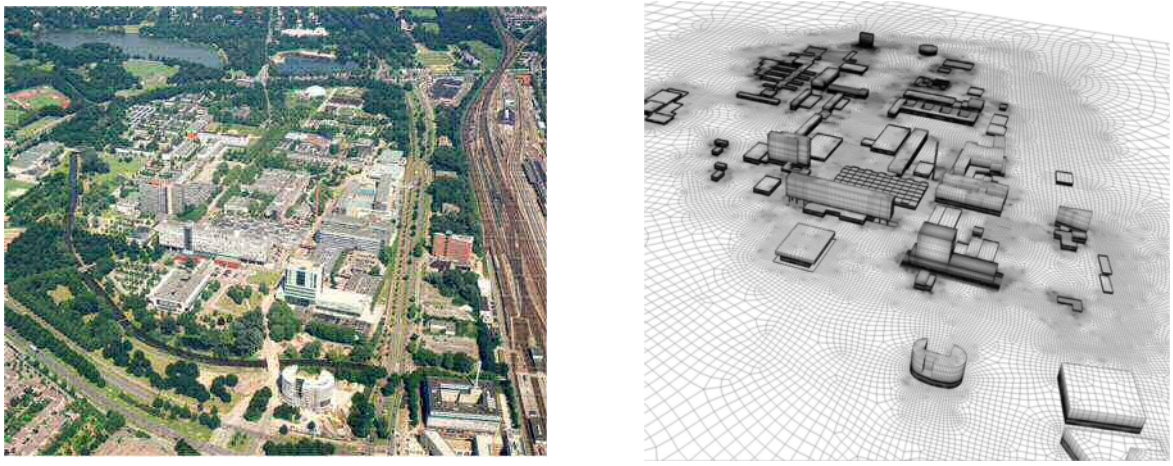

a. Aerial view of the geometry for CFD resolution

b. Corresponding high-resolution computational grid

Figure 3.1 - An example of geometric resolution (Blocken et al., 2012)

3.2.2. The computational domain

Generally, the size of the entire computational domain depends on the targeted area and the boundary conditions. For a single building, the distance from the top of the building to the top of the computational domain should be at least 5H with a maximum blockage of 3%, where H is the building height. For the lateral boundary, 2.3H is required between the building's sidewalls and the edge of the computational domain. 5H is also considered to be the minimum for the inflow boundary when the approach flow profiles are well known. If the approach flow profiles are not provided, a larger distance is required in order to establish a realistic flow profile. For the outflow boundary, at least 15H behind the building is suggested (Franke et al., 2007). Tominaga et al. (2008) suggest 5H for the lateral boundary and 10H for the outflow boundary, but their other boundary condition recommendations are similar to those of Franke et al. (2007).

For the case of urban areas with multiple buildings, COST (Franke et al., 2007) suggests $5H_{max}$ for both the top boundary and the lateral boundary, where H_{max} is the height of the tallest building. They also mentioned the size of the computational domain in the case of the boundary layer wind tunnel. However, if the height of the wind tunnel is much larger than $6H_{max}$, a lower

height of the computational domain can be employed. For the lateral boundary, if the distance of the lateral walls of the wind tunnel from the built area is much larger than $5H_{max}$, a smaller extent of the computational domain can be used.

Figure 3.2 shows the dimensions of the computational domain specified by Lateb et al. (2013), who employed the COST guidelines (Franke et al., 2007). Here, the top and the lateral boundaries are 5H away from the building and the outflow boundary is 20H downwind from the building to allow adequate flow development.

Therefore, 5H for the top and the lateral boundary is recommended in both the case of a single building and urban areas with multiple buildings when H is the height of the tallest building. In addition, 5H and 15H can be used for the upstream and the downstream length respectively.

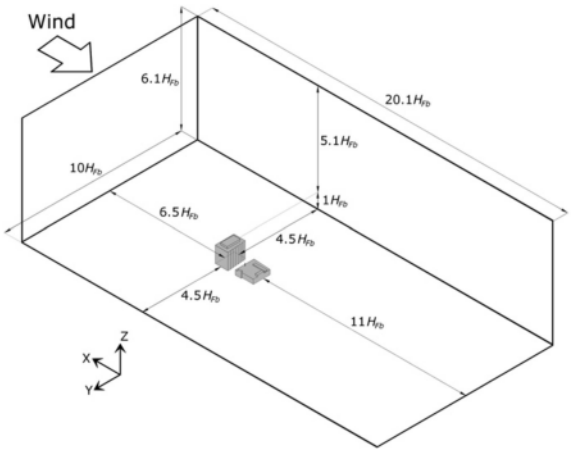

Figure 3.2 - Dimensions of the domain grid (Lateb et al., 2013)

3.2.3. Computational grid

With regard to the geometry of the region of interest, the computational grids that discretize the computational domain should be fine enough to provide an adequate resolution of the geometrical and expected flow features (Casey & Wintergerste, 2000). Generally, the greater the number of cells the better the CFD results, but as the number of cells increases, the calculation time also increases. The maximum number of cells that can be created for the solution depends

on the computing resources available. According to the AIJ guidelines (Tominaga et al., 2008), the grid resolution must be at least 1/10 the building scale within the region that includes the evaluation points around the building of interest. COST (Franke et al., 2007) also recommends a minimum of 10 cells per building side and at least 10 cells per cube root of building volume should be used for the initial grid resolution.

To boost the accuracy of the simulation, local grid refinement can be used. Some commercial codes provide algorithms to adjust the local grid resolution according to numerical criteria obtained from the flow solution. However this accuracy comes at a cost, as any increase in the number of cells also increases the computer storage required and the run-time of the simulation. Thus, it is important to determine the optimum mesh size taking into account the available computer storage and run-time (Casey & Wintergerste, 2000). Casey and Wintergerste also provide some recommendations for the choice of grids and the grid design:

1) Choose a suitable global topology for the mesh to help satisfy the skewness, aspect ratio and expansion ratio.
2) The computational domain should be chosen to capture all the relevant flow and geometrical features.
3) Use local grid refinement to capture fine geometrical details.
4) Avoid highly skewed cells, warped cells, and non-orthogonal cells near boundaries.
5) Observation is needed for any specific requirements on mesh expansion ratios.
6) Use a finer and more regular mesh in regions of interest with high flow gradients or with large changes.
7) Make use of a grid dependency study to analyze the suitability of the mesh in order to obtain an estimate of the numerical error in the simulation for each class of problem.

COST (Franke et al., 2007) suggests that grid stretching should be small in regions of high gradients, keeping the truncation error small. The term for grid stretching which clusters the nodes of the computational grid within the regions of steep gradients without an increase in the total number of grid nodes (Liseikin, 2010). The expansion ratio between two consecutive cells

should be below 1.3 within regions and a value of 1.2 for the maximum expansion ratio (Franke et al., 2007).

The shape of the grids can be categorized as either an unstructured or structured mesh. COST (Franke et al., 2007) consider hexahedral cells to be preferable to tetrahedral cells because hexahedral cells produce smaller truncation errors and provide better iterative convergence. They also note that when using tetrahedral cells, prismatic cells must be used at the wall and tetrahedral cells away from the wall since the grid lines should be perpendicular to the wall. Tominaga et al. (2008) also indicate that it is important to arrange that prismatic cells are parallel to walls and ground surfaces when using tetrahedral cells.

Thus, both hexahedral and tetrahedral mesh can be used for CFD applications for wind flow around buildings. In addition, at least 10 cells per cube root of building volume are recommended for the initial grid resolution.

3.2.4. Boundary conditions

The definition of the boundary conditions determines at what point the surroundings are deemed to no longer have a significant effect on the computational domain, so it is important to choose proper boundary conditions since these decide to a large extent the solution in the computational domain (Franke et al., 2007). As mentioned in Appendix, there are two types of boundary conditions and combinations of these can be used. The Dirichlet condition defines the distribution of a physical quantity over the boundary at a given time step and the Neumann condition specified the distribution of its first derivative (Casey & Wintergerste, 2000). Casey & Wintergerste also suggest guidelines for selecting boundary conditions: 1) Ensure that proper conditions are available for the case being considered and 2) check whether the CFD code allows inflow for open boundary conditions.

When setting the inflow boundary conditions, the mean velocity profile and information about the turbulence quantities is needed to create an equilibrium boundary layer (Franke et al., 2007).

This means that the velocity profile can be achieved either from the logarithmic profile corresponding to the upwind terrain via the roughness length z_0 or from the profiles of the wind tunnel simulations. In the case of steady RANS simulations, the mean velocity profile and information about the turbulence quantities is needed and suitable profiles can be achieved from the assumption of an equilibrium boundary layer. When wind tunnel data for turbulent kinetic energy are available, these should be employed to describe the profile. Franke et al. also suggest that an analysis should be conducted to ascertain whether the chosen grid and boundary conditions are consistent before simulating flow over obstacles. In this instance, an empty computational domain with the same grid and periodic boundary conditions can be used for the analysis to obtain consistent profiles that match the velocity measurements at the meteorological station.

For the top and lateral boundaries, Tominaga et al. (2008) suggest that the inviscid wall condition can be used since these boundaries do not affect the calculated results around the target building. Franke et al. (2007) disagree, however, instead recommending symmetry conditions for these boundaries.

For the outflow boundary conditions, open boundary conditions are used at the boundary behind the obstacles and outflow or constant static pressure conditions are frequently used for the open boundary conditions in CFD codes. In addition, this outflow boundary condition has to be far enough away from the region of interest (Franke et al., 2007; Tominaga et al., 2008; Casey & Wintergerste, 2000).

Therefore, the mean velocity profile prescribed by logarithmic law and information about turbulence quantities is required for inlet. For outlet boundary condition, constant pressure conditions are recommended. In addition, symmetry conditions are used for the top and lateral boundaries.

3.2.5. Turbulence models

Turbulent flow in urban or industrial environments is modeled by the Navier-Stokes equations and it is important to decide whether the application needs a steady or an unsteady treatment (Franke et al., 2007). According to Casey & Wintergerste (2000), there is no universally valid general turbulence model for all classes of flows, so validation and calibration with experimental data are necessary for all applications. They also note that examination of the effect and sensitivity of results to the turbulence model is necessary, which requires changing the models being used, and a thorough review of the published literature regarding the known weakness of the model is needed in order to use a particular turbulence model.

Generally, a steady-state RANS simulation is used for many simulations, which provides an average flow field. In the case of wind tunnel experiments, RANS equations can represent the wind tunnel's reality (Franke et al., 2007) but it is difficult to reproduce the separation and reverse flow at the roof top of a building using RANS equation approaches such as the standard k-ε model (Tominaga et al., 2008). Due to the drawbacks of the RANS approach, the LES approach has also been used to predict and represent wind loads on buildings (Tamura et al., 2008). However, although LES can provide more information about the flow field than the RANS approach, it requires substantially greater computing resources (Franke et al., 2007).

Therefore, both LES and the RANS turbulence models can be used to reproduce wind flow around a building.

3.2.6. Convergence criteria

Generally, CFD codes employ iterative methods to calculate the algebraic system of equations and the termination criterion is subject to the residuals of the corresponding equations (Franke et al., 2007). The termination criterion must move from one to zero and the residuals are scaled iteratively and Franke et al. recommend a termination criterion of 0.001 for industrial applications. Tominaga et al. (2008) take an alternative approach, suggesting that it is better to

check the solution directly using different convergence criteria such as the relaxation coefficient or periodic fluctuations than to simply use a yardstick of four orders of magnitude for the residuals. Thus, it is recommended that the scaled residuals are terminated at 0.001.

3.3. Summary of the best practice guidelines

Since CFD simulations have been developed based on numerical methods and algorithms, it was considered preferable to summarize the characteristics of the computational parameters rather than provide explanations of the equations for non-CFD experts. Thus, several widely used best practice guidelines were reviewed for this study.

In general, the best CFD practice guidelines have been developed over the past decade to support the proper use of CFD simulations. They were considered necessary due to CFD's complexity and the potentially serious effects of computational errors or uncertainties and many researchers have now used these guidelines for a wide range of applications. For this study, three best practice guidelines were selected and reviewed that focused primarily on CFD applications related to wind flow around buildings. Based on the computational parameters described in the CFD fundamentals outlined in Appendix, specific recommendations regarding the need to consider the size of the computational domain, geometrical representation, grid generation, the selection of boundaries, the selection of turbulence models, and convergence criteria were discussed:

1) What level of detail in the geometrical representation of the buildings is needed?

- The central region of interest (the area of a radius 1 -2 H from the building of interest) is reproduced as accurately as possible.
- At least one additional street block in each direction around the central region of interest is represented.
- Buildings located away from the region of interest are represented by simple blocks.

2) What is the proper size of the computational domain?

- 5H for the top and 10H for the lateral boundary are recommended in both the case of a single building and urban areas with multiple buildings when H is the height of the tallest building.
- 5H and 15H can be used for the upstream and the downstream length respectively.

3) What is the appropriate the type of computational grid and grid resolution?

- Both hexahedral and tetrahedral mesh can be used for CFD applications for wind flow around buildings.
- At least 10 cells per cube root of building volume are recommended for the initial grid resolution.

4) What is the appropriate boundary conditions including inlet, outlet and the top and sides?

- The mean velocity profile prescribed by logarithmic law and information about turbulence quantities is required for inlet boundary condition.
- For outlet boundary condition, constant pressure conditions are recommended.
- Symmetry conditions are used for the top and lateral boundaries.

5) What is the proper turbulence model?

- In order to reproduce wind flow around a building, both LES model and turbulence models based on the RANS approach can be used.

6) What is the proper range for the iterative convergence criteria?

- The scaled residuals are terminated at 0.001

The main purpose of this study was to obtain a rich description of the CFD process by validating the results obtained by comparison with experimental results. The recommendations provided by the best practice guidelines were used to specify the computational conditions, but it is important to note that it is not sufficient to perform CFD simulations based solely on these conditions. Thus, more specific information regarding appropriate computational parameters will be obtained through an analysis of four journal papers, as described in the next chapter.

4. THE TEN ITERATIVE STEPS APPROACH

4.1. Introduction

Generally, the output of CFD simulations is highly sensitive to a wide range of computational parameters that are chosen by the user (Blocken & Gualtieri, 2012). In order to achieve successful CFD simulations, best practice guidelines have been proposed to reduce computational errors or uncertainties caused by the users. As mentioned in the previous chapter, the existing CFD best practice guidelines have mainly dealt with target variables, the extent of model, time intervals, the choice of turbulence models, boundary conditions, convergence criteria and initialization. However, these alone are not sufficient to ensure the credibility, acceptance and impact of CFD results, and Blocken and Gualtieri (2012) therefore employed the ten iterative steps approach to construct a comprehensive framework for CFD models.

The ten iterative steps approach was originally introduced in a position paper by Jakeman et al. (2006). This approach develops purposeful, credible models from data and prior knowledge, working closely with the end-users and with every stage open to critical review and revision (Jakeman et al., 2006). Their paper was intended to provide more general guidelines covering a wide range of model types including empirical, data-based, statistical models, specific theory-based or process-based models such as CFD, conceptual models based on assumed structural similarities to the system, agent-based models, and rule-based models. For this study, four journal articles were selected and analyzed using the ten iterative steps approach. Through the journal analysis, lessens-learned were gathered focusing on the CFD application for wind flow around buildings.

4.2. The characteristics of the ten iterative steps approach

In presenting the ten steps approach, Jakeman et al. stated “Whatever the type of modeling problem, certain common steps must be considered if the goals are credible results and knowledge acquisition, for the immediate purpose of the exercise and for the wider community

and the longer term" (2006, p.606). As shown in Figure 4.1, this approach is largely composed of a series of iterative steps, thus including trial and error for pursuing good practice in model development and application (Jakeman et al., 2006). The following ten steps were defined by Jakeman et al. (2006):

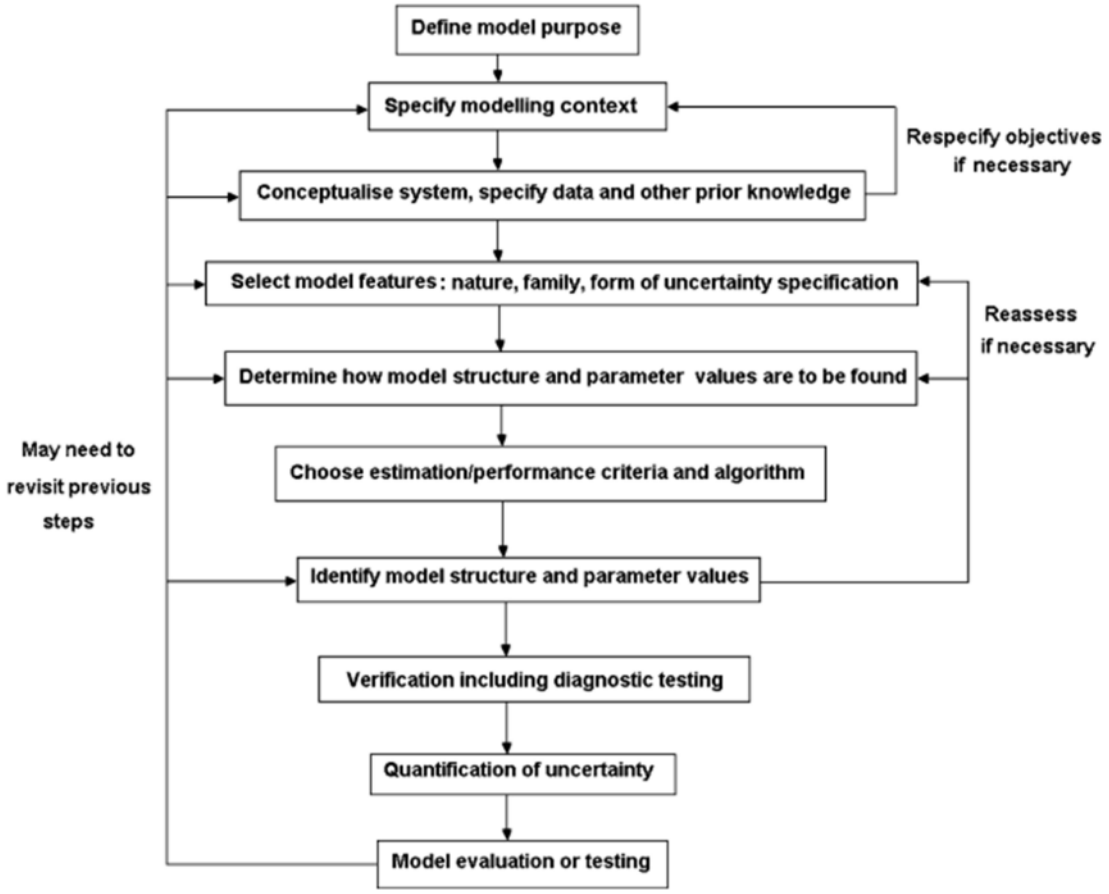

Figure 4.1 - Iterative relationship between model building steps. (Jakeman et al., 2006)

4.2.1. Definition of the purposes for modeling

In general, it is often difficult to be clear about the precise purpose of any modeling process as different stakeholders will have different degrees of interest in the possible purposes of the end product. Thus, the modeler should establish the purposes and priorities of the model that is to be

produced because these choices can have a profound effect on the model development, particularly during the later stages (Jakeman et al, 2006).

4.2.2. Specification of the modeling context: scope and resources

This step identifies the specific questions and issues to be addressed by the model, the required output, the forcing variables, temporal and spatial scope, scale and resolution, the available resources and the model flexibility (Jakeman et al., 2006).

4.2.3. Conceptualization of the system, specification of data and other prior knowledge

Jakeman et al. (2006) define conceptualization as the basic premises governing the working of the system being modeled. In this step, the data, prior knowledge and assumptions about processes are defined.

4.2.4. Selection of model features and families

Any modeling approach needs to choose model features such as the types of variables and the nature of their treatment based on the preceding three steps. The links between system components and processes are specified by the model structure, which includes the functional form of the interactions between the components and processes, the data structures or measures used to specify links, and the spatial and temporal scales of the processes and their interactions (Jakeman et al, 2006).

4.2.5. Choice of how model structure and parameter values are to be found

Prior science-based theoretical knowledge is generally sufficient to suggest the form of the relations between the variables in the model (Jakeman et al, 2006).

4.2.6. Choice of estimation performance criteria and technique

The parameter estimation criteria reflect the desired properties of the estimates and the parameter estimation technique must be:

- Computationally as simple as possible to minimize the chance of coding error;
- Robust in the face of outliers and deviations from assumptions (e.g. about noise distribution);
- As close to statistically efficient as feasible (as reflected by the amount of data required for the estimates to converge);
- Numerically well-conditioned and reliable in finding the optimum;
- Able to quantify uncertainty in the results (not at all easy, as the underlying theory is likely to be dubious when the uncertainty is large); and
- Accompanied by a test for over-parameterisation. (Jakeman et al., 2006, p.610)

4.2.7. Identification of model structure and parameters

In this step, the iterative process of finding a suitable model structure and parameter values are addressed, which involves hypothesis testing of alternative model structures. According to the results of the model testing through steps 5.2.8 – 5.2.10, the complexity of interactions proposed for the model may be increased or reduced (Jakeman et al., 2006).

4.2.8. Conditional verification including diagnostic checking

The eighth step is very important because not only it checks the model's believability, but also it builds the client's confidence in the model. Jakeman et al. explained the process involved as follows:

Once identified, the model must be 'conditionally' verified and tested to ensure it is sufficiently robust, i.e. insensitive to possible but practically insignificant changes in the data and to possible deviations of the data and system from the idealizing assumptions made (e.g. of Gaussian distribution of measurement errors, or of linearity of a relation within the model). It is also

necessary to verify that the interactions and outcomes of the model are feasible and defensible, given the objectives and the prior knowledge. (2006, p.611)

This step should include as wide a range of quantitative and qualitative criteria as circumstances allow. For quantitative verification this could encompass a wide range of criteria, including goodness of fit and tests on residuals or errors, particularly for relatively simple empirical models. In the case of qualitative verification, this generally involves knowledgeable data suppliers or model users who are not modelers (Jakeman et al, 2006).

4.2.9. Quantification of uncertainty

Jakeman et al. noted that "Uncertainty must be considered in developing any model, but is particularly important, and usually difficult to deal with, in large, integrated models" (2006, p.612). They also stressed that model uncertainty should be considered in the context of the purposes of the model.

4.2.10. Model evaluation or testing (other models, algorithms, comparisons with alternatives)

The model should be evaluated in the light of its specific objectives (Jakeman et al., 2006). Blocken and Gualtieri developed this further by adding questions originally posed by Robson et al.:

- How well does the model reproduce an independent data set?
- How well does the model perform under unusual conditions?
- Is the complex model better than a simpler one?
- Can the model be used to improve understanding of underlying system function?
- Finally, and most importantly, does the model help to answer questions about the system function and can it be used to make predictions about the future? (Robson et al., 2008, as quoted in Blocken and Gualtieri, 2012, p.612)

4.3. Selection of journal papers

Four articles published in refereed journals related to CFD investigations of wind flow around a building were selected for further analysis. As computer technology has advanced considerably in recent years, it was possible to choose a range of computational conditions and/or parameters. For example, the number of grids that can be generated has increased and more turbulence models have become available. Thus, only papers published since 2010 were chosen for this analysis.

Table 4.1 - Selected journal papers

Authors	Title	Journal
Tominaga & Stathopoulos (2010)	Numerical simulation of dispersion around an isolated cubic building: Model evaluation of RANS and LES	*Building & Environment*
Montazeri & Blocken (2013)	CFD simulation of wind-induced pressure coefficients on buildings with and without balconies: Validation and sensitivity analysis	*Building & Environment*
Abohela et al. (2013)	Effect of roof shape, wind direction, building height and urban configuration on the energy yield and positioning of roof mounted wind turbines	*Renewable Energy*
Chavez et al. (2011)	Near-field pollutant dispersion in the built environment by CFD and wind tunnel simulations	*Journal of Wind Engineering & Industrial Aerodynamics*

Tominaga and Stathopoulos (2010) utilized CFD to predict dispersion around buildings based on a RANS model. They also employed an LES model in order to obtain a more accurate prediction. The performance of the two types of turbulence models was compared in order to identify the most suitable numerical method for this purpose.

To gain information regarding the pressure distribution on building walls, Montazeri and Blocken (2013) conducted a CFD analysis to investigate mean wind pressures on the windward

and leeward surfaces of a medium rise building with and without balconies using a 3D RANS approach. They also performed a grid sensitivity analysis.

Abohela et al.'s (2013) study examined the effect of different roof shapes, building heights and urban configurations using CFD in order to identify the optimum placement for roof mounted wind turbines based on the predicted energy yield.

Finally, Chavez et al. (2011) investigated pollutant dispersion for three cases, namely an isolated low-rise building, a taller building placed upwind of the source and taller buildings placed upwind and downwind of the source using CFD with a RANS approach.

The articles selected all provided highly detailed descriptions of the studies performed; the purpose of this analysis was not to fully describe the CFD models, schemes, algorithms and conclusions reached from the numerical results, but rather to explore the application of the ten-iterative steps approach to this journal analysis (Blocken & Gualtieri, 2012).

4.4. Lessons-learned from the journal article one: Numerical simulation of dispersion around an isolated cubic building: Model evaluation of RANS and LES (Tominaga & Stathopoulos, 2010)

4.4.1. Definition of the purposes for modeling

Plume dispersion near buildings is an important factor in the design of exhaust vents and air intakes in order to avoid adverse air quality impacts. In this paper, the CFD method was applied to predict dispersion around buildings based on a RANS (Reynolds Averaged Navier Stokes equations) model. However, the authors reported that the RANS approach under-predicted the horizontal concentration diffusion. To achieve more accurate results, LES (Large Eddy Simulation) was then used to take into account the fluctuations that were causing the problem. Although LES has become a widely used tool for dealing with more complicated practical problems of turbulent flow, this approach does incur higher computational costs. Thus, although

the factors that should be considered when selecting a suitable numerical method for its purpose need to be clarified, very few studies have compared the basic performance of LES for dispersion fields with a simple configuration with the results obtained for the same scenario using the RANS model.

For this case study, the performance of the RANS and LES approaches was investigated for flow and concentration fields around a cubic building with a flush bent at the rooftop placed within the neutral surface boundary layer. The specific purposes of this study were to confirm the accuracy of LES in modeling dispersion near and around a simple building and to clarify the mechanism of the discrepancy in relation to the RANS computation.

4.4.2. Specification of the modeling context: scope and resources

4.4.2.1. Available resources

In order to validate the CFD prediction accuracy for a velocity field, two sets of wind velocity data measured in a wind tunnel were used. The first wind tunnel measurements were carried out by the authors (Tominaga & Stathopoulos, 2010) and the other wind tunnel measurements were conducted by Li and Meroney (1983). Tominaga and Stathopoulos recorded wind tunnel measurements of velocity around a cubic model without vent emission, with wind velocity being measured by a split fiber. The wind tunnel measurements by Li and Meroney investigated wind velocity around a cubic building with vent emission. The other available resource from these two measurements was the turbulence intensity.

4.4.2.2. Forcing variables and required outputs

This study used two numerical methods, RANS and LES. For RANS, the RNG k-ε model utilized a turbulent Schmidt number of 0.7 and the QUICK scheme was used. At the inlet, inflow type boundaries were applied with a generalized log-law profile (Launder & Spalding, 1974). The vertical distributions of U, k and ε at the inflow boundaries were based on the results of the

wind tunnel tests. The details of the boundary conditions are provided in Tominaga and Stathopoulos (2009).

For LES, the standard Smagorinsky model with an empirical constant C_s of -0.12 was used for the sub-grid scale eddy viscosity model. The sub-grid scale Schmidt number was 0.5 and a second-order centered difference scheme was used. The inflow boundary condition was that proposed by Kataoka and Mizuno (2002). For the boundary condition at the solid walls, a linear or 1/7 power-law distribution of instantaneous velocity was assumed (Werner & Wengle, 1993).

The required outputs were the parameters of the averaged flow field, such as pressure and velocity components, and the parameters of the averaged concentration field, such as turbulent fluxes and concentration.

4.4.2.3. Spatial and temporal scope, scale and resolution

The computational domain for both RANS and LES is presented in Figure 4.2. The domain was discretized into 86 (x1) × 76 (x2) × 46 (x3) grids with structured rectangular girds. The minimum grid width was $0.0045H_b$.

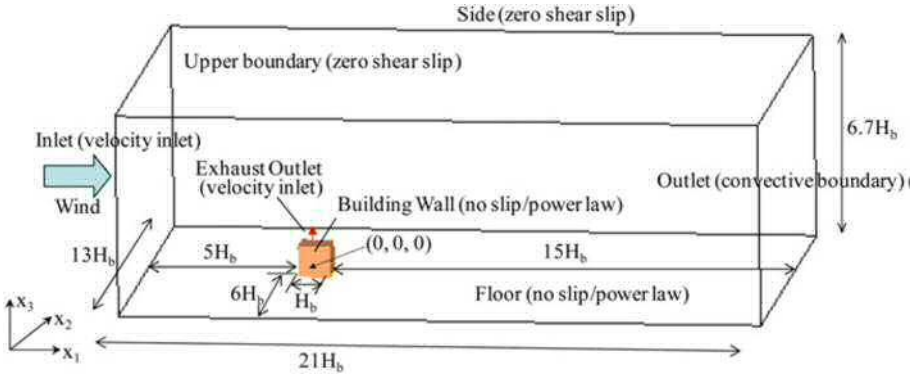

Figure 4.2 - Computational domain and boundary conditions of LES (Tominaga & Stathopoulos, 2010)

4.4.2.4. Users of the model and model flexibility

The choice of input parameters of the wind tunnel measurements for computational conditions is best made by a CFD expert. Understanding the difference between RANS and LES in the application for the dispersion around simple cubic model was a primary goal of this study. Thus, results such as those obtained for the fluctuating instantaneous values could be applied to understand the management of the model, which could include a gas that contains toxic, flammable or odorous components.

Generally, the time required to generate the high-resolution computational mesh constitutes the largest part (85 - 90%) of the computational time needed for the total modeling effort. Thus, flexibility in generating additional meshes for the mesh sensitivity analysis and additional geometries is essential (Blocken & Gualtieri, 2012). With regard to model flexibility, it should be noted that it would be easy to change the location of the vent on the wall of the geometric model.

4.4.3. Conceptualization of the system, specification of data and other prior knowledge

Conceptualization of the system refers to the relationship between the prediction accuracy of the velocity fields and the concentration distributions among the different turbulence models. Generally, air pollutants being emitted from or near a building can cause much higher than allowable concentrations in the atmosphere, which can adversely affect people's health or disposition. In this study, two numerical approaches were used in order to reproduce the flow field around a single building placed at a surface boundary layer. On each surface of the building, the concentration obtained is caused by a process of separation and recirculation. This concentration, which governs the dispersion of the pollutants, is displayed as a time-averaged value.

Prior knowledge for this system includes the fundamental physical principles of CFD such as conservation of mass, Newton's second law and conservation of energy.

4.4.4. Selection of model features and families

Traditionally, the prediction of plume dispersion has been studied using models of buildings in wind tunnels or water tunnels. The task of constructing a series of scale-model experiments to explore systematically the general "model space" of a collection of buildings is laborious because of the multiplicity of configurations that must be investigated. Furthermore, wind-tunnel experiments require resources of time and expertise which are often not directly available to architects and planners. The results of these methods provide little information on dispersion, such as an expected minimum dilution factor or a recommended stack height, and are also difficult to apply to more complex building geometries. In contrast, CFD techniques can provide flow properties around buildings with complex geometric shapes at every point simultaneously. The relative performance of various turbulence models for flow fields around buildings has been examined in several studies (Murakami, 1993; Tominaga et al., 2008). CFD is expected to be a particularly powerful tool for designing exhaust stacks and the air intakes of buildings because it can provide three-dimensional maps of concentration distributions around individual buildings by solving the relevant transport equations. Several studies have sought to validate the CFD method for dispersion around buildings (Zhang et al., 1996; Li & Stathopoulos, 1997; Meroney et al., 1999), but although the prediction accuracy of these phenomena has been questioned, applications of CFD have now been extended to dispersion in street canyons and urban geometry (Li et al., 2006).

For the present study, CFD was deemed the best choice, primarily due to the comparisons between the results of the experiment and the two numerical methods. As mentioned above, CFD provides whole-flow field data, which allows the prediction accuracy between two numerical methods to be determined and compared.

4.4.5. Choice of how model structure and parameter values are found

This section addresses the definition of the structure of the model, including the form of the relations between the variables in the model (Jakeman et al., 2006). The variables of interest are

the velocity components and the parameters of the averaged concentration field, such as turbulent fluxes and concentration. The relations between the variables are derived from the physical laws of the conservation of mass, Newton's second law and the conservation of energy, all of which are prescribed by partial differential equations that can be simplified by both RANS and LES. The use of both these approaches in the study are based on a literature review and on past experience by the authors (Tominaga & Stathopoulos, 2010), who used their own CFD code in this research. The default turbulence model parameters were based on experimental data. The value of the Schmidt number for the RANS approach with RNG k-ε was set to 0.7 based on the findings of an earlier study (Tominaga & Stathopoulos, 2007) and 0.5 was set for the LES approach (Antonopoulos, 1981). The inlet profiles, wall functions and wall function roughness were extracted from the scientific literature (Tominaga & Stathopoulos, 2009; Launder & Spalding, 1974; Kataoka & Mizuno, 2002; Ono et al., 2008; Werner & Wengle, 1993). The experimental data were also taken from previous studies (Li & Meroney, 1983).

4.4.6. Choice of performance criteria

According to Robson et al. (2008), the performance criteria for environmental models must reflect the overall aims and specific objectives of the modeling activity.

The first purpose of this study was to confirm the accuracy of LES in modeling dispersion near and around a simple building model. This could be deemed to be performing well if it could reproduce the wind velocity and instantaneous fluctuations of concentration at the building surfaces. The simulation results of the RANS and LES models were compared with experimental data collected by Li and Meroney (1983) and in the authors' own wind tunnel tests. Therefore, the wind velocity and instantaneous fluctuations of concentration were considered to be the performance criteria. The second objective was to clarify the mechanism of the discrepancy in relation to the RANS computation. Since it can be difficult to compare the mechanism between two numerical methods due to the different convergence criteria applied, the CPU time could be considered as the performance criterion.

4.4.7. Identification of model structure and parameters

Whereas steps 5 and 6 discussed the choice of appropriate methods for identifying the model structure and parameters and the criteria and techniques for estimating model performance, respectively, the present step addresses the iterative process of finding a suitable model structure and parameter values (Jakeman et al., 2006).

This study addressed both RANS and LES methods. For the RANS approach, the authors selected the RNG k-ε model rather than one of the other four types of turbulence models used in a previous study (Tominaga & Stathopoulos, 2009) because of its superior agreement with the experimental results. The generalized log-law approximation was employed for the solid boundary (Launder & Spalding, 1974). For LES, the standard Smagorinsky model was chosen for the sub-grid scale eddy viscosity model. However a dynamic model has been used in recent LES computations, as the standard model has exhibited some numerical instability and required large computation times (Murakami, 1993; Tominaga et al., 1997). A power-law distribution for the instantaneous velocity was therefore used for the boundary condition at the solid walls (Wener & Wengle, 1993).

4.4.8. Conditional verification including diagnostic checking

According to Jakeman et al. (2006), quantitative verification of a model may be attempted using different criteria, most of which are based on a comparison between the model results and observed data. Qualitative verification preferably involves knowledgeable data suppliers or model users who are not modelers themselves.

In this study, both quantitative and qualitative verifications were made. The comparison with measured data could be categorized as quantitative verification; this will be addressed in Sections 4.4.9 and 4.4.10, respectively. The model results for the contours can be considered as qualitative verification. In the contour distribution, the feasibility of the calculated wind flow can be confirmed by non-CFD experts.

4.4.9. Quantification of uncertainty

According to Blocken and Gualtieri (2012), uncertainty in CFD modeling can be seen in a very wide range of sources. These can include the simplification of model geometry, the mesh resolution, the choice of RANS versus LES, boundary conditions, and so on. They contended that a substantial reduction in uncertainty can be achieved by carefully following the CFD best practice guidelines. The main purpose of these guidelines is to reduce as far as possible both the errors and uncertainty in CFD simulations. In the present case study, CFD best practice guidelines were applied for the size of the computational domain.

4.4.10. Model evaluation or testing (other models, algorithms, comparisons with alternatives)

The final step in the process is the evaluation of the model considering its objectives. The first purpose of this study was to investigate the accuracy of LES in modeling dispersion near and around a cubic model. As the first step of model evaluation, various comparisons among the experimental data and that obtained from the RNG and LES approaches were carried out. As table 4.2 shows, the reattachment lengths on the roof (X_R) values of both computations showed good agreement with the experimental values. However, the value obtained by RNG is slightly larger than the experimental value.

Table 4.2 - Comparison of reattachment lengths on roof and behind cube (Tominaga & Stathopoulos, 2010)

	X_R	X_F
RNG	$0.64H_b$	$1.33H_b$
LES	$0.64H_b$	$1.33H_b$
Experiment	$0.64H_b$	$1.33H_b$

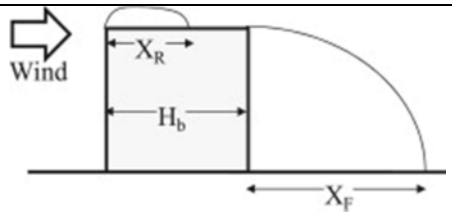

Figure 4.3 compares the contours of the time-averaged dimensionless concentration, (K), on the roof and wall surfaces provided by the RNG and LES calculations, as well as the experimental

results measured by Li and Meroney (1983). The high concentration region on the roof suggested by RNG was larger than either of the other two values. In the case of LES, the concentration was widely spread in the horizontal direction.

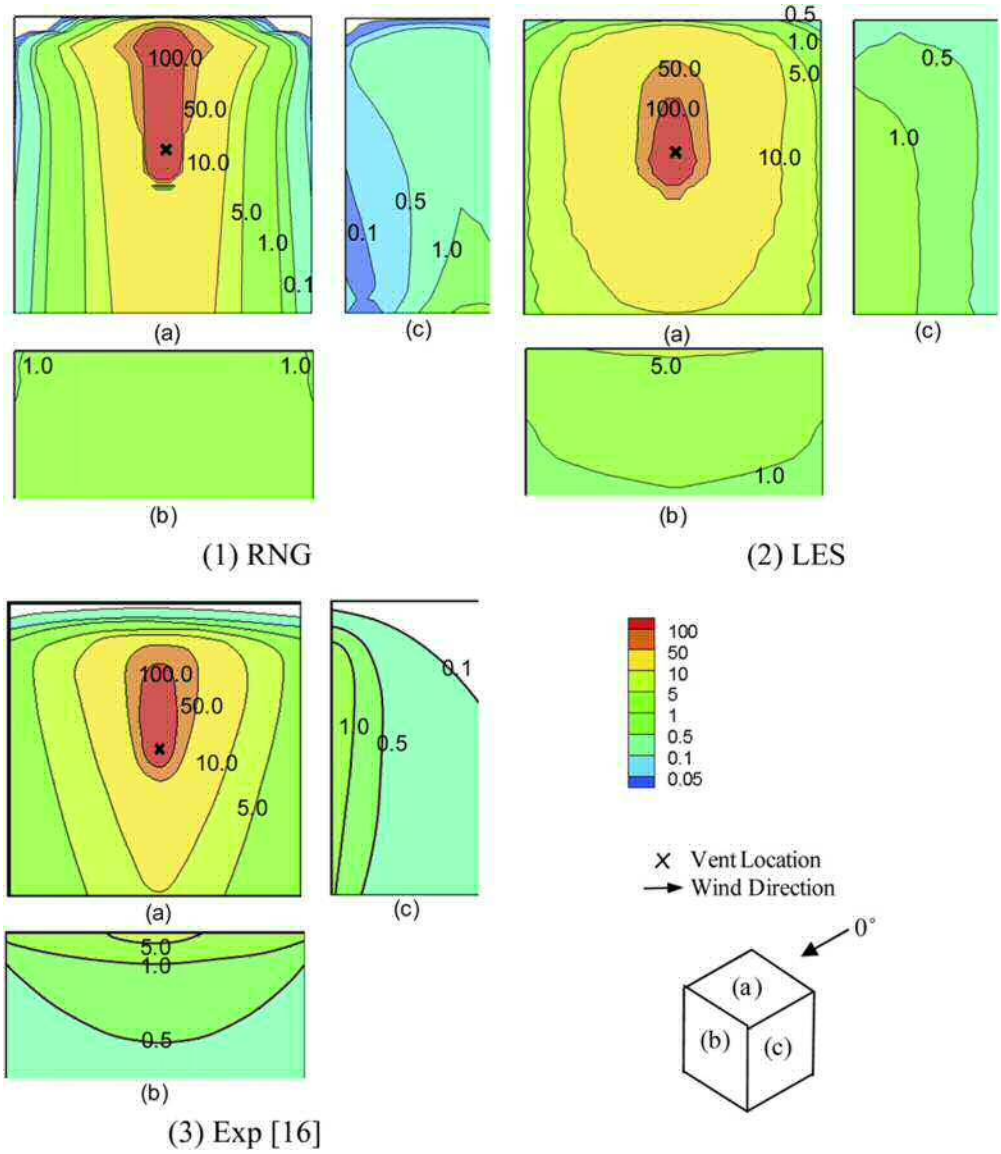

Figure 4.3 - Distribution of time-averaged dimensionless concentration (K) on roof and wall surfaces (Tominaga & Stathopoulos, 2010)

Another useful point of comparison is the distribution of K on the centerline of the roof and walls (Figure 4.4). Comparing the results of LES and RNG with Saathoff et al. (1995)'s

experiments, the values of K in LES were smaller than the values according to RNG in the streamwise direction, but the LES values were much higher than those from RNG in the lateral direction.

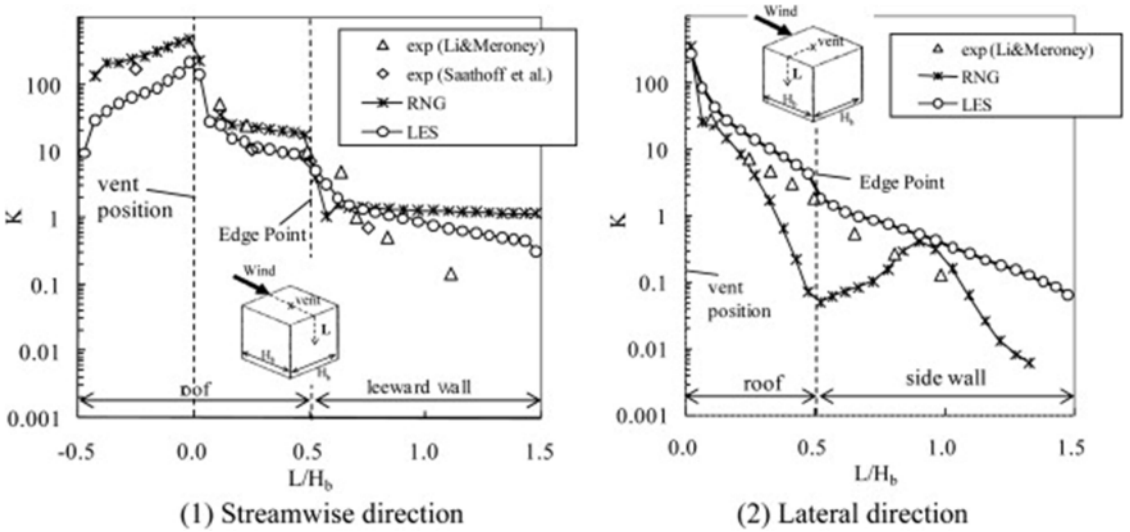

Figure 4.4 - Distribution of time-averaged dimensionless concentration (K) on the centerline of the roof and leeward and side walls (Tominaga & Stathopoulos, 2010).

Concerning the predictions of LES and RNG, other comparisons were also analyzed in this paper. Comparing the distributions of K, LES showed very good agreement with the experimental data. Based on these results, the authors concluded that the simple LES method showed better results than conventional RNG modeling of the distribution of concentration. RNG underestimated the turbulence diffusion near the cube model in comparison with LES.

The second purpose of this study was to elucidate the mechanism of the difference between LES and RANS computations. Note that a direct comparison between RNG and LES is difficult due to different convergence criteria. The authors of this study pointed out that the CPU time required to achieve statistically significant values of LES was about 25 times longer than for the RNG case.

Overall, this study concluded that the LES method can yield important information on instantaneous fluctuations of concentration that cannot be achieved by RANS approaches.

4.5. Lessons-learned from the journal article two: Wind-induced pressure coefficients on buildings with and without balconies (Montazeri & Blocken, 2013)

4.5.1. Definition of the purposes for modeling

Knowledge of the pressure distribution on building walls is important for evaluating wind-induced natural ventilation and assessing wind loads on building walls and building components. A wide range of factors such as approach-flow conditions, urban surroundings, building geometry and wind direction all have an effect on the pressure distribution on a building's walls. In particular, building facade details such as balconies and other protrusions can have a major effect on the peak and mean surface pressure distributions on buildings' walls and roofs.

The study in this paper conducted CFD simulations to predict mean wind pressure distributions on building facades. The specific purpose of this study was to evaluate a 3D RANS CFD approach for predicting pressure distributions on a building with and without balconies for both normal and oblique approach-flow conditions based on a grid-sensitivity analysis and on validation with wind-tunnel measurements. An additional purpose was to investigate the impact of several computational parameters, namely the resolution of the computational grid, the reference static pressure and the turbulence model.

4.5.2. Specification of the modeling context: scope and resources

4.5.2.1. Available resources

This study investigated mean wind pressure distributions on building facades with and without balconies utilizing CFD methods. In order to evaluate the CFD simulations, wind data measured by wind tunnel experiments conducted by Chand et al. (1998) were utilized. In these experiments,

a scaled model 0.60 m in length and 0.25 m wide, with a height of 0.50 m, was installed in an open –circuit wind tunnel 16 m long with a cross-section area of 2.5 × 1.8 m^2. The upstream wind velocity was 7.1 m/s at the building height, yielding a building Reynolds number of 250,000. Thus, the first available resource was the specific building plan needed to reproduce the 3D building geometry for CFD simulations. The second resource was the measured wind profile, which was used for CFD accuracy. The last resource was the commercial CFD code Fluent 6.3.26, which was used to perform the simulations. In this study, the 3D steady RANS equations were applied in combination with the realizable k-ε turbulence model proposed by Shih et al. (1995). The SIMPLE algorithm was used for pressure-velocity coupling, pressure interpolation was second order and second-order discretization schemes were employed for both the convection terms and the viscous terms of the governing equations. When all the scaled residuals leveled off and reached a minimum of 10^{-6} for x, y momentum, 10^{-5} for y momentum and 10^{-4} for k, ε and continuity, convergence was assumed.

4.5.2.2. Forcing variables and required outputs

In the simulations, the inlet boundary conditions were applied with the measured vertical wind profile and inlet turbulent intensity and roughness length were assigned. The longitudinal turbulence intensity ranged from 13% near ground level to 3% at gradient height. The upstream wind velocity at building height was 7.1 m/s, so the roughness length was derived using the log-low equation to be 0.008 m. For the ground surface, the standard wall functions with roughness modification were used. The standard wall functions were also used at the surfaces of the building of interest. Zero static pressure was applied at the outlet domain. Symmetry conditions, i.e. zero normal velocity and zero normal gradients of all variables, were used at the top and lateral sides of the domain.

The required outputs included the parameters of the averaged flow field, such as the pressure coefficient and velocity components.

4.5.2.3. Spatial and temporal scope, scale and resolution

The reduced-scale building model used in the wind-tunnel measurements was selected as a computational model in this study. The building, at scale 1:30, had dimensions width × depth × height of 0.60 × 0.25 × 0.50 m^3, corresponding to full-scale dimensions 18 × 7.5 × 15 m^3. For the evaluation of the effect of balconies, three balconies with width 0.15 m, depth 0.05 m and height 0.03 m were evenly spaced across the width of each of the five floors except for the ground floor (Figure 4.5).

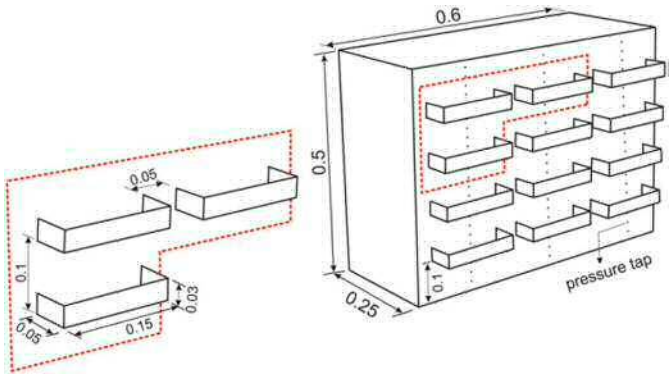

Figure 4.5 - Geometry of building model and balconies (unit:mm) (Montazeri & Blocken, 2013)

For the size of the computational domain, the best practice guidelines recommended by Franke et al. (2007) and Tominaga et al. (2008) were employed. The upstream domain length was 5H (2.5 m). The resulting dimensions of the domain were W × D × H (10.6 × 10.25 × 3 m^3), which corresponds to 318 × 307.5 × 90 m^3 in full scale. The resulting domain is shown in Figure 4.6.

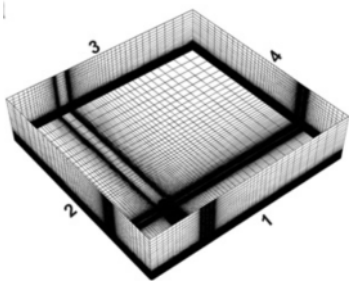

a. Grid at bottom and side faces of computational domain

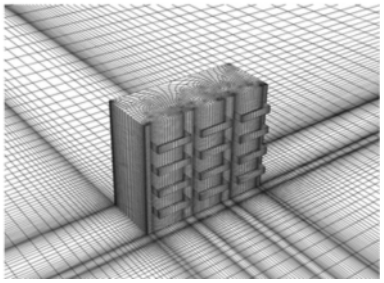

b. Grid at building surfaces and ground surface

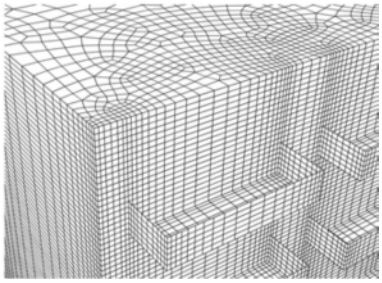

c. Detail of grid near balconies

Figure 4.6 - Computational grid (Montazeri & Blocken, 2013)

For the computational grid, the surface-grid extrusion technique presented by van Hooff and Blocken (2010) was used. The result was a hybrid grid with 2,102,250 prismatic and hexahedral cells. The computational domain allowed two different wind directions, which corresponded to those used in the wind tunnel experiments (Figure 4.6 - a).

For the resolution, an additional two grid resolutions were utilized for the grid sensitivity analysis in order to reduce both discretization errors and computational times. Figure 4.7 shows the coarse grid, basic grid and fine grid tested. The minimum and maximum cell volumes in the domain were approximately 5×10^{-8} m^3 and 7.5×10^{-2} m^3, respectively. The coarse grid consisted of 720,937 cells, while the fine grid had 6,755,370 cells.

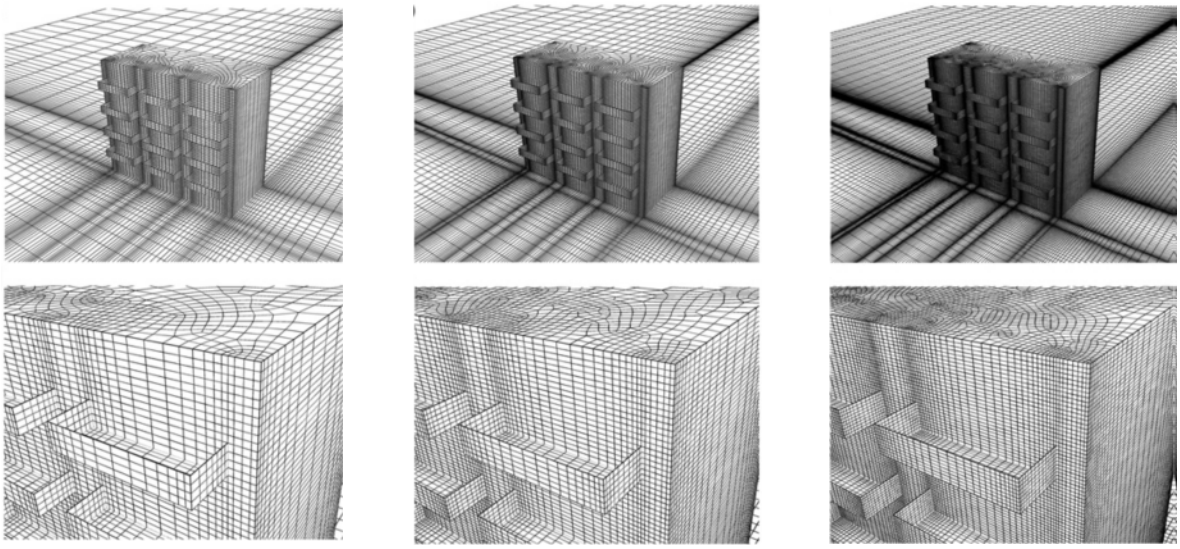

a. Coarse grid b. Basic grid c. Fine grid

Figure 4.7 - Computational grids for grid-sensitivity analysis (Montazeri & Blocken, 2013)

4.5.2.4. Users of the model and model flexibility

This study conducted a systematic evaluation of CFD simulations for the prediction of the mean pressure distributions on building surfaces. The CFD method was validated using the results of wind tunnel tests. Thus, the choices of input parameters for the CFD simulation and the sensitivity analyses should be made by CFD experts. The selection of input parameters such as aerodynamics, which was derived from the wind tunnel measurements, the computational physical models and the results of the sensitivity analyses for the grid selection were all very important in order to reduce discretization errors and computational costs and thus provide an accurate interpretation of the CFD results (Blocken & Gualtieri, 2012).

As mentioned for the first paper analyzed, the model flexibility is very important for CFD applications. In this study, the basic mesh had 2,102,250 prismatic and hexahedral cells and a coarser grid and a finer grid were created for the mesh-sensitivity analysis. The coarse grid had 720,937 cells, while the fine grid had 6,755,370 cells. The three grids are shown in Figure 4.7.

4.5.3. Conceptualization of the system, specification of data and other prior knowledge

In this case, conceptualization of the system refers to the systematic evaluation of CFD for the prediction of the mean wind pressure coefficients on building facades with balconies. In this paper, the evaluation was based on validation with the wind tunnel tests and on a grid-sensitivity analysis. In the wind tunnel experiment, an isolated building with balconies was considered. The building at scale 1:30 had dimensions width × depth × height (0.60 × 0.25 × 0.50 m^3), which resulted in a blockage ratio of about 6.6%. The measurements were conducted for a building with three evenly spaced balconies of width 0.15 m, depth 0.05 m and height 0.03 m, which were positioned across the width at each of the five floors except for the ground floor. The data from the wind tunnel measurements were compared with the CFD results of pressure coefficients along the vertical measurement lines at the building façade. In order to conduct the sensitivity analyses for the various geometrical and computational parameters, systematic changes were made to the reference case which was then validated with the wind tunnel tests. One of the geometrical or computational parameters was varied, while all others were kept identical to those in the reference case for the sensitivity analyses.

Prior knowledge on this system includes the fundamental physical principles of CFD such as the conservation of mass, Newton's second law and the conservation of energy.

4.5.4. Selection of model features and families

Generally, pressure coefficients can be investigated using full-scale on-site measurements (Levitan et al., 1991), reduced-scale wind-tunnel measurements or numerical simulation with CFD (Stathopoulos, 1997). Full-scale measurements provide an advantage in that the real situation and the full complexity of the problem can be considered. However, full-scale measurements are usually only conducted over a limited number of points in space and there is no or only limited control over the boundary conditions (Reinhold, 1982). On the other hand, wind-tunnel measurements can offer a strong degree of control over the boundary conditions but are also limited to a few points in space (Stathopoulos, 1997). Unlike full-scale or wind tunnel

measurements, CFD offers data on the relevant parameters at all points of the computational domain (Chen, 2009; Blocken & Gualtieri, 2012; Blocken et al., 2012). Moreover, CFD does not impact potentially incompatible similarity requirements because CFD can be performed at full scale and CFD simulations can easily perform parametric studies to evaluate alternative design configurations (Hooff & Blocken, 2010). Currently, CFD is increasingly used to investigate a wide range of atmospheric and environmental processes.

Therefore, CFD is the best choice in this case study due to (1) the ability to perform sensitivity analyses with geometrical changes and (2) the detailed flow over the building facades. In order to perform an accurate assessment of those purposes, a CFD approach is needed.

4.5.5. Choice of how model structure and parameter values are found

The variables of interest here were the pressure coefficient and k-ε turbulence parameters. The relations between these parameters are provided by the classical conservation laws for mass and momentum and are expressed in the form of partial differential equations. For the pressure coefficient, this can be computed as $C_p = (P - P_0) / (0.5\rho U^2_{ref})$, where P is the static pressure at the surface, P_0 is the reference static pressure, ρ 1.225kg/m^3 is the air density and U_{ref} is the reference wind speed at building height. In order to deal with turbulent flow, the RANS approach was selected in this study. The turbulence model parameters were based on extensive fitting to experimental data obtained from wind tunnel experiments.

4.5.6. Choice of performance criteria

The first objective was to evaluate a 3D RANS CFD approach for predicting pressure distributions on a building with and without balconies for both normal and oblique approach-flow conditions based on a grid-sensitivity analysis and on validation with wind-tunnel measurements. This was assessed as performing well if it reproduced wind pressure distributions across building facades with balconies with the RANS approach and obtained good agreement between the CFD results and wind tunnel measurements. Another purpose was to investigate the

impact of computational parameters such as the resolution of the computational grid, the reference static pressure and the turbulence model. The assessment criterion in this case was the ability to analyze the sensitivity of the selected parameters.

4.5.7. Identification of model structure and parameters

In this study, the authors (Montazeri & Blocken, 2013) chose the 3D RANS approach because LES is considerably more computationally expensive than RANS. The 3D RANS simulations were made in combination with the realizable k-ε turbulence model (Shih et al., 1995). The SIMPLE algorithm was employed for pressure-velocity coupling, pressure interpolation was second order and second-order discretization schemes were used for both the convection terms and the viscous terms of the governing equations.

4.5.8. Conditional verification including diagnostic checking

Grid-sensitivity analysis and comparisons with data of wind tunnel measurements can be considered as quantitative verification. In addition, a qualitative verification was performed. The results, including pressure coefficient distributions or velocity vector fields across the building facades, could provide information for building scientists who were not CFD experts, enabling them to determine the wind flow and pressure distribution through building geometries.

4.5.9. Quantification of uncertainty

In this study, CFD best practice guidelines were applied for the size of the computational domain, the choice of the input parameters for turbulence kinetic energy and dissipation rate, the choice of turbulence model and the discretization schemes. Grid independence of the results was confirmed by a grid-sensitivity analysis based on three different grid sizes: coarse, basic and fine.

4.5.10. Model evaluation or testing (other models, algorithms, comparisons with alternatives)

The final step is the evaluation of the model considering its objectives. The study only utilized steady RANS CFD simulations and its main purpose was to study how well the RANS approach reproduced wind pressure distributions across building facades with balconies. Despite the well-known incompleteness and other deficiencies of the steady RANS method, a good agreement was achieved between the CFD simulations and the wind-tunnel measurements for the windward facade both with and without balconies. There was also good agreement for the leeward facade and for perpendicular wind. Figure 4.8 compares the simulated distribution of C_p across the entire windward façade for the case with and without balconies. However, the RANS method did produce large discrepancies with the wind tunnel tests in the case of an oblique wind flow. Thus, 3D steady RANS CFD was acceptable for the prediction of wind-induced mean pressures on windward building facades and on the leeward wall for the case of a perpendicular approach flow with and without balconies.

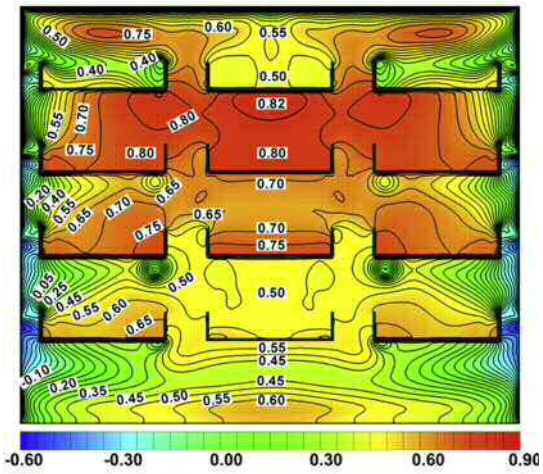

a. Pressure coefficient across windward façade of building with balconies

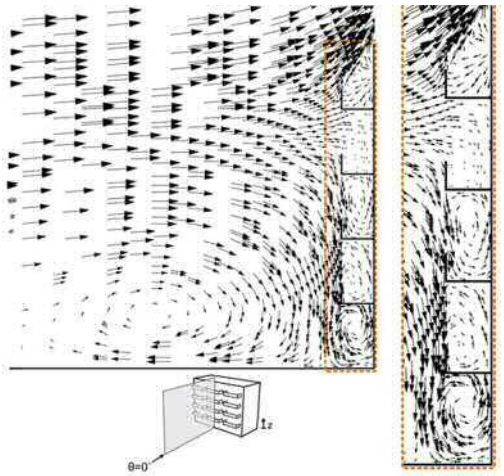

b. Velocity vector field in cross-section of building with balconies

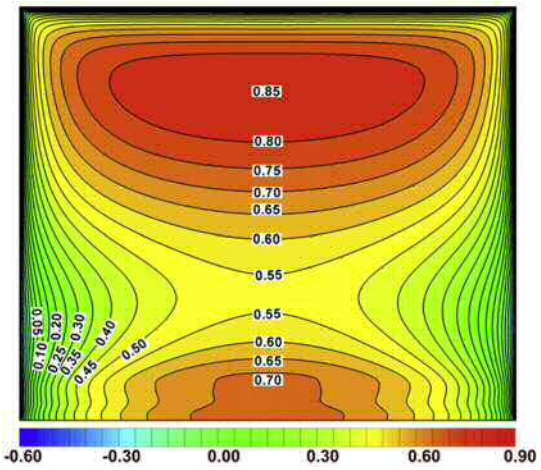

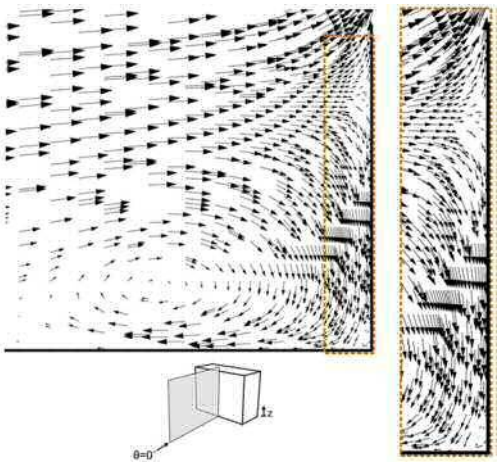

c. Pressure coefficient across windward façade of building without balconies

d. Velocity vector field in cross-section of building without balconies

Figure 4.8 - The results of pressure coefficient distribution and velocity vector field (Montazeri & Blocken, 2013)

A detailed sensitivity study of important computational parameters such as computational grid, turbulence model, and wind direction was also conducted. Figure 4.9 shows the grid sensitivity analysis for three different grids. The results of this analysis revealed that a careful selection of these parameters was very important for accurate and reliable results.

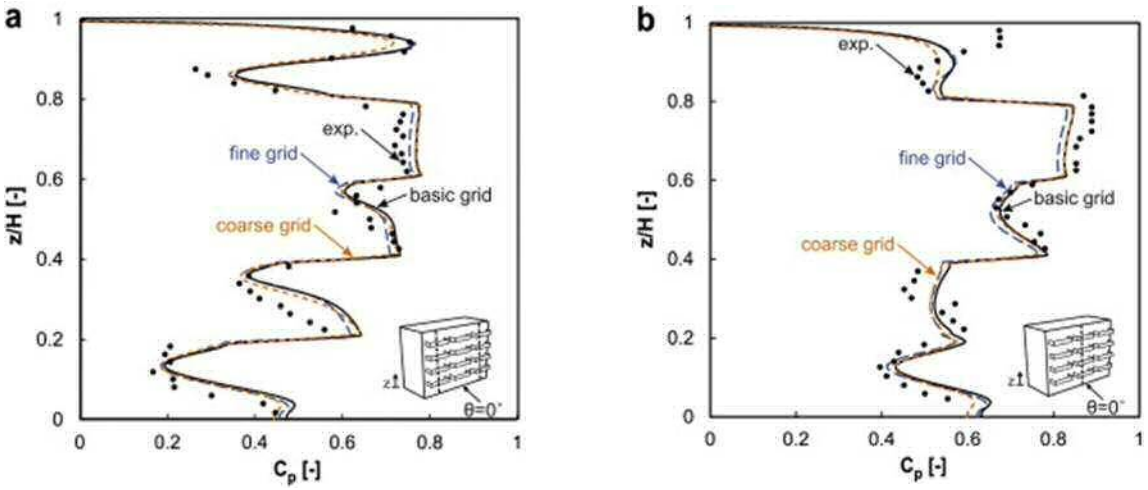

a. Pressure coefficient along edge line

b. Pressure coefficient along center line

Figure 4.9 - Results for grid-sensitivity analysis with three different grids (Montazeri & Blocken, 2013)

4.6. Lessons-learned from the journal article three: Effect of roof shape, wind direction, building height and urban configuration on the energy yield and positioning of roof mounted wind turbines (Abohela et al., 2013)

4.6.1. Definition of the purposes for modeling

Roof mounted wind turbines have a high potential for integration within the built environment but there is some uncertainty regarding their feasibility as a result of uninformed decisions about positioning and locating the wind turbines. The factors that affect the installation of wind turbines are wind directions, roof shapes, building heights and urban configurations.

This paper presented an investigation of air flow over a range of building roof shapes in order to determine the most productive location in terms of power generated for a wind turbine using CFD methods. The specific purpose of this study was to investigate the effect of different roof shapes, wind direction, building height and urban configurations by examining the flow characteristics in terms of wind flow patterns, turbulence intensities and streamwise velocities.

4.6.2. Specification of the modeling context: scope and resources

4.6.2.1. Available resources

The study was intended to reproduce wind flow around buildings based on changes in several parameters (roof shapes, wind directions, building heights and urban configurations). Thus, the first resources were the modeled parameters. All roof shapes were designed to cover a building with a square cross section of 6 m × 6 m and a height of 6 m. For the roof shape, the authors (Abohela et al., 2013) used six different roof shapes: flat, domed, gabled, pyramidal, barrel vaulted and wedged (Figure 4.10). For the wind directions, simulations were conducted with five wind directions (0°, 45°, 90°, 135° and 180°). To understand the effect of building height on wind flow above the building, three different heights were considered (6 m, 12 m, and 24 m). Finally, two urban configurations were considered a street canyon and a staggered street.

The other resource was the commercial CFD software package and postprocessor Fluent 12.1. This commercial code was applied over a wide range of options to examine the wind flow around buildings. When the scaled residuals reached the range of $10^4 – 10^6$, the simulations were terminated.

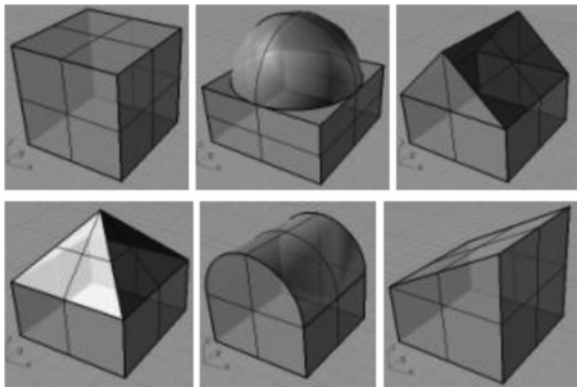

Figure 4.10 - Roof shapes, from top left:
flat, domed, gabled, pyramidal, barrel vaulted and wedged (Abohela et al., 2013)

4.6.2.2. Forcing variables and required outputs

In the simulations the inlet boundary conditions were specified using a user defined function for the log law ABL profile. For the ground surface, the standard wall functions for a rough wall were used. The standard wall functions were also used for the surfaces of the building of interest. Zero static pressure was applied at the outlet domain. Symmetry conditions, i.e. zero normal velocity and zero normal gradients for all variables, were used at the top and lateral sides of the domain. The realizable k- ε turbulence model was employed for the closure of the transport equations and the SIMPLE algorithm scheme was used for the pressure-velocity coupling. Pressure interpolation was second order and second-order discretization schemes were employed for both the convection and the viscous terms of the governing equations.

The required outputs of the model were the values of the reattachment length on top of the roof through variables such as roof shape, building height, wind direction and urban configuration. In this paper, all flow features around a roof mounted cube in a turbulent channel flow were

captured including streamwise velocity pathlines and the pressure distribution passing through the vertical central plane was as shown in Figure 4.11.

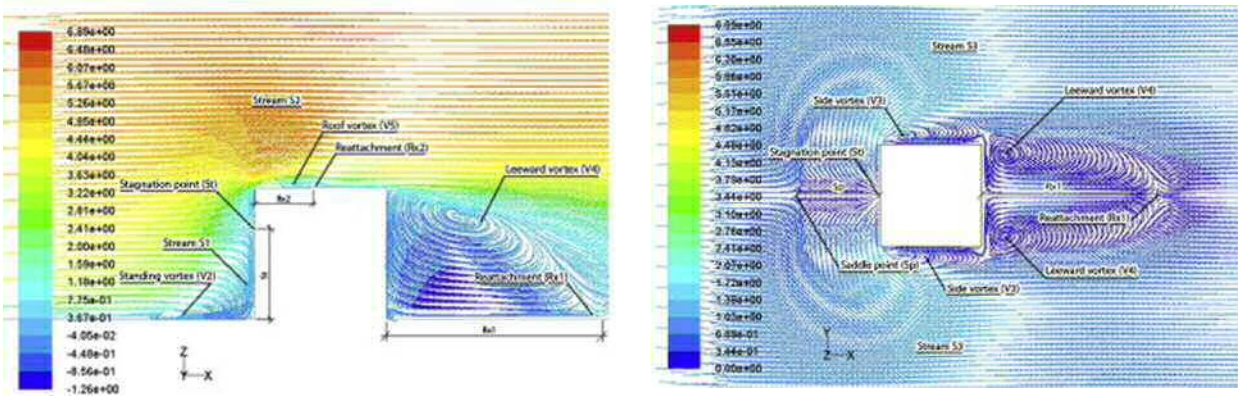

a. Stremwise velocity pathlines through the vertical central plan

b. Streamwise velocity pathlines at ground level

Figure 4.11 - The results of straemwise velocity pathlines and the pressure distribution (Abohela et al., 2013)

4.6.2.3. Spatial and temporal scope, scale and resolution

For the computational domain, 2H + building width was utilized for the lateral dimension, 20H + building dimension for the flow direction, and 6H for the vertical direction, where H is the height of the building. Thus, a 126 m × 36 m × 36 m structured mesh was constructed, giving 1,306,368 hexahedral cells and maintaining a blockage ratio below 3%. Three mesh sizes were compared in order to determine the dependence of the flow field on the refinement of the mesh. As a result, a resolution of 0.3 m around the cube and 0.8 m throughout the rest of the computational domain was established (Figure 4.12)

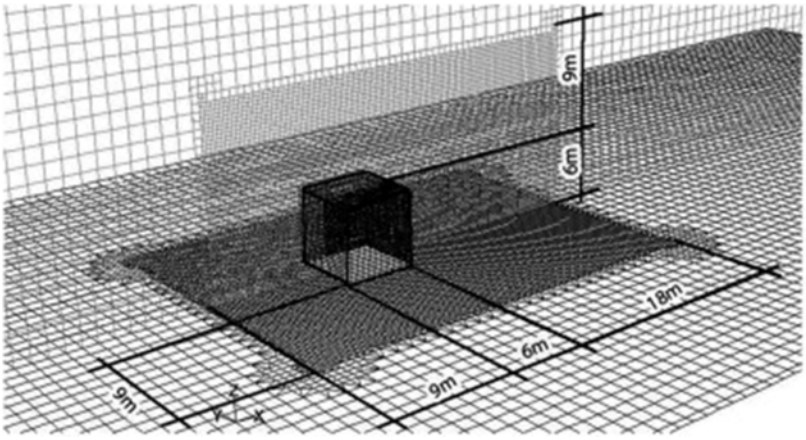

Figure 4.12 - Mesh refinement areas around the cube (Abohela et al., 2013)

4.6.2.4. Users of the model and model flexibility

This study investigated the effects of a large number of input parameters and conducted sensitivity tests for the model results in order to help users make appropriate choices using the commercial CFD code Fluent 12.1. However, the model in this study should still be applied by CFD experts. Although there are CFD best practice guidelines that can assist non-CFD experts, a knowledge of the physical models, potential computational errors or uncertainties should be determined by CFD experts to ensure the correct application of the CFD model.

Generally, the process of generating additional meshes for mesh sensitivity analyses, the representation of various models or additional geometries is very time consuming. For this study, model flexibility was very important. The authors selected simple geometries that could easily be made with structured mesh and once the proper mesh size was identified through a mesh independence study, this was then applied to generate the meshes for all the parameters in this study.

4.6.3. Conceptualization of the system, specification of data and other prior knowledge

Conceptualization of the system refers to the processes that plot streamwise velocity pathlines along the central plane on the roofs parallel to the wind direction for the most productive location

for a micro turbine. In the case of a building-integrated micro wind turbine and its location, it is important when designing this structure to consider fully all aspects related to safety, structural building integrity and turbine performance in order to achieve the maximum wind speed within the built environment. Both the wind flow and turbulence intensity depend strongly on the roof shape. Employing a CFD approach enables the air flow to be represented over a range of common building roof shapes to achieve the most efficient location in terms of power production.

Prior knowledge for the system in this study includes the basic principles of physics in CFD such as the conservation of mass, Newton's second law and the conservation of energy and a familiarity with the CFD best practice guidelines.

4.6.4. Selection of model features and families

4.6.4.1. Modeling approach

The CFD approach adopted for this study was the best choice. The main reason is that four factors affecting the location of the roof mounted wind turbines (six roof shapes, five different wind directions, three building heights, and urban configuration) were modeled and flow patterns visualized along the vertical streamwise central plane. Although this type of investigation has generally been performed in a wind tunnel, the CFD approach is cost- effective and produces more information than wind tunnel testing.

4.6.4.2. Conceptual model

As mentioned in Blocken and Gualtieri (2012), it is not efficient to attempt to include all the physical processes involved and to encompass all possible combinations of meteorological conditions. The model in this study therefore surveyed the scientific literature to identify substantial simplifications. For the set of parameters to represent wind flows around buildings, CFD best practice guidelines were adopted to achieve consistent results. Regarding the physical processes and boundary conditions, the equilibrium ABL profile was modeled for the wind flow.

4.6.5. Choice of how model structure and parameter values are found

The variables of interest in this study are the streamwise velocity and the turbulence intensity. From the streamwise velocity along the vertical central plane on the roof, the maximum acceleration location can be determined. The relations between parameters can be expressed in the form of partial differential equations. Generally, these equations can be solved using different approaches (Blocken & Gualtieri, 2012); here, these equations were solved using the RANS approach. The realizable k-ε turbulence model was used for the turbulence closure.

4.6.6. Choice of performance criteria

The purpose of this case study was to analyze wind flow over a range of common building roof shapes to identify the most power productive location for building-integrated micro-wind turbines. The authors addressed four main factors, namely roof shape, wind direction, building height and urban configuration, that affect the installation of roof mounted wind turbines. The model would be deemed successful if it was found to be capable of plotting the streamwise velocity and the turbulence intensity along the central plane of the roof. Thus, the performance criteria were the streamwise velocity and the turbulence intensity.

4.6.7. Identification of model structure and parameters

The knowledge gained from the literature and the CFD best practice guidelines was employed to identify models and parameters. The authors selected the 3D RANS approach with the realizable k-ε turbulence model for the closure of the transport equations due to its good performance for the resolution of wind flows around buildings. The SIMPLE algorithm scheme was employed for the pressure-velocity coupling. The pressure interpolation was second order and second-order discretization schemes were used for both the convection and the viscous terms of the governing equations (Blocken et al., 2010; Franke et al., 2007; Zhai & Chen, 2004).

4.6.8. Conditional verification including diagnostic checking

For quantitative verification, comparisons of the pressure coefficient distribution along the centerline of the windward, leeward façade and roof were conducted for data gathered from 15 wind tunnel tests, full-scale measurements and the CFD results. In this study, no qualitative verification was conducted but its results could be presented to roof designers or scientists who study renewable energy.

4.6.9. Quantification of uncertainty

In order to reduce computational errors or uncertainties from model geometry, the mesh generation, the choice of turbulence models, boundary conditions, and other factors, this case study employed the CFD best practice guidelines. Hence, a range of 10^{-4} – 10^{-6} was applied for the scaled residuals, and the choice of 3D RANS approach and the realizable k-ε turbulence model, the computational domain size, the choice of the boundary conditions, the horizontal homogeneity of the ABL profile, and so on were all based on the guideline recommendations. Mesh independence analysis was conducted based on three different mesh sizes.

4.6.10. Model evaluation or testing (other models, algorithms, comparisons with alternatives)

The purpose of this study was to investigate the effect of the roof shape, wind direction, building height and surrounding urban configurations on the wind flow above the roof to identify the optimum location where the accelerating effect occurs on top of the roof to maximize the energy generation performance of a wind turbine. For the evaluation of the model, a qualitative analysis of the streamwise velocities for the effects of different roof shapes was investigated (Figure 4.13). In addition, comparisons of the turbulence intensities and velocities were carried out quantitatively and quantitatively for the effects of building height and urban configuration (Figure 4.14).

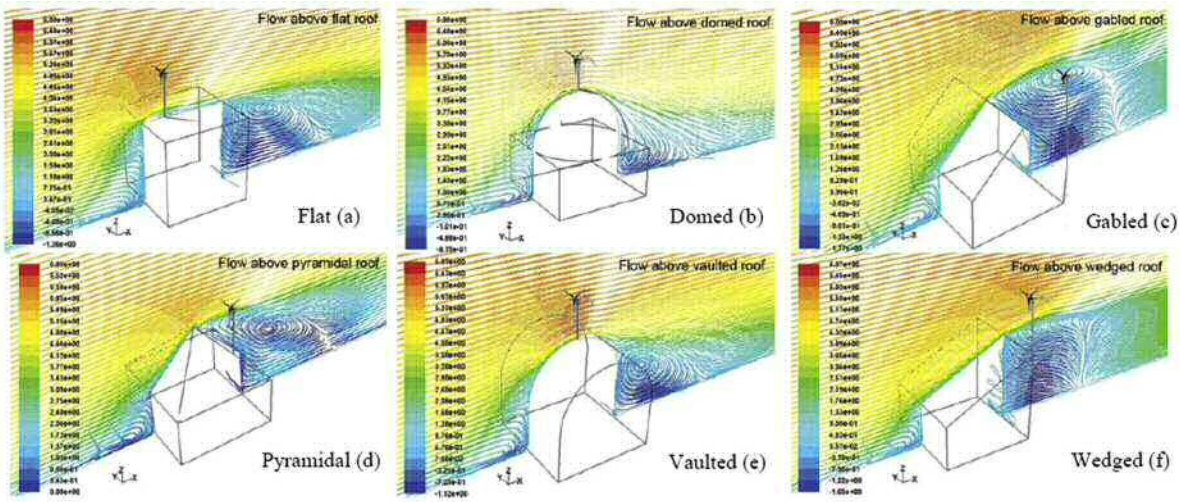

Figure 4.13 - Optimum mounting location for different investigated roof shapes under 0 wind direction (Abohela et al., 2013)

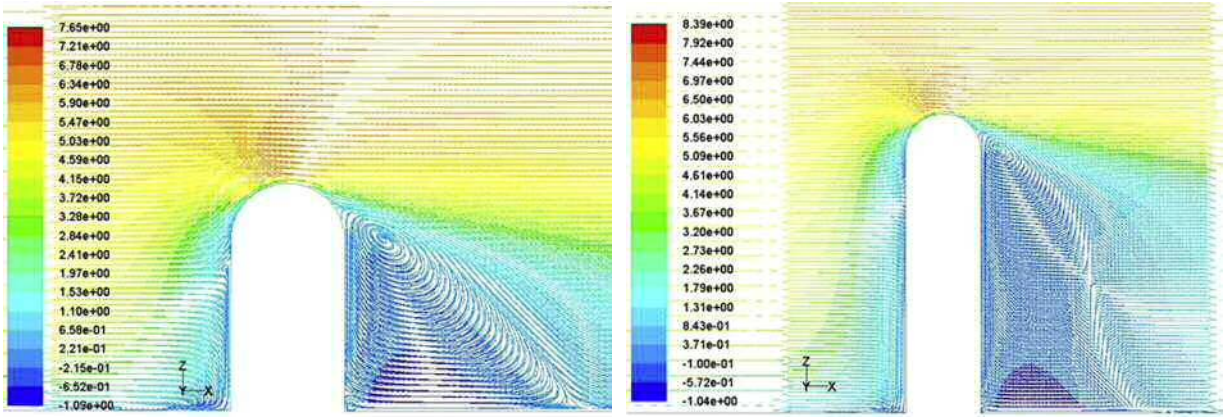

a. Streamlines velocity pathlines along the central vertical axis for the 12 m vaulted building

b. Streamlines velocity pathlines along the central vertical axis for the 24 m vaulted building

Figure 4.14 - The results of streamlines velocity pathlines for the 12 and 24 m vaulted building (Abohela et al., 2013)

Model simplifications were adopted for this study due to the complexity of the built environment. All the variables were fixed except for the variable being investigated and all the measured flow

variables were normalized against the values of the flow variables at the same locations under the same flow conditions in an empty domain to identify the accelerating effect of the roof shape.

In sum, this study concluded that the positioning of a roof mounted wind turbine requires careful assessment of wind flow in order to maximize the energy extracted. The analyses carried out for the study also increased our understanding of the accelerating effects of different variables on wind flow across a roof.

4.7. Lessons-learned from the journal article four: Near-field pollutant dispersion in the built environment by CFD and wind tunnel simulations (Chavez et al., 2011)

4.7.1. Definition of the purposes for modeling

It is important to be able to assess pollutant concentrations in the built environment due to the complexity of airflows around a multiple building configuration. When pollutants from roof stacks become trapped in recirculation zones, this polluted air may re-enter the source building as well as affecting adjacent buildings located downwind or upwind of the emitting building. Although this re-entering polluted air is recognized to constitute a risk to human health, previous studies have not provided appropriate design criteria to avoid this problem occurring in new or existing buildings.

In this study, numerical simulations were conducted to reproduce pollutant dispersion within a multiple building configuration. Specifically, this study investigated near field dispersion for three different building configurations using CFD. The three different building configurations were 1) a low-rise isolated building (emitting building); 2) a taller building placed upstream of the emitting building; and 3) tall buildings placed upstream and downstream of the emitting building. For the validation, the simulations results were compared with experimental results. Another purpose of this study was to investigate the effect of different turbulence Schmidt numbers on pollutant dispersion using CFD analysis.

4.7.2. Specification of the modeling context: scope and resources

4.7.2.1. Available resources

For the investigations of pollutant dispersion, three resources were available for this study. The first consisted of detailed building models for three different cases and the second was a set of wind tunnel results (Stathopoulos et al., 2008) for comparison with the numerical results. The other available resource was the commercial CFD code Fluent 6.1. For the building detail, three cases were considered; the dimensions of the buildings are shown in Figure 4.15 and Table 4.3. For all cases, it was assumed that the pollutant was released at the roof of B1.

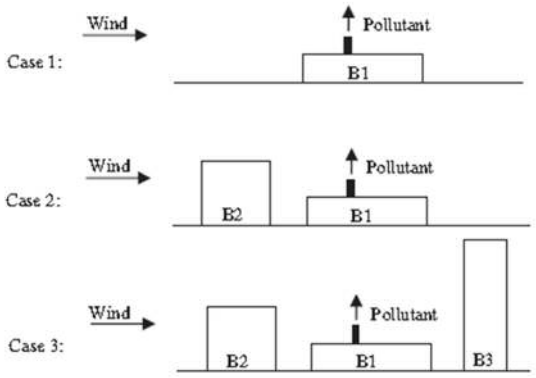

Figure 4.15 - Three cases for CFD simulation (Chavez et al., 2011)

Table 4.3 - Building models for CFD and wind tunnel experiments (Chavez et al., 2011)

Building	Height (m)	Width (m)	Length (m)
B1	0.075(15)	0.25(50)	0.25(50)
B2	0.15(30)	0.25(50)	0.15(30)
B3	0.27(54)	0.22(44)	0.075(15)

The wind tunnel experiments were conducted in the open circuit variable height boundary layer wind tunnel of Concordia University by Stathopoulos et al. (2008). The dimensions of the wind tunnel were 1.8 m × 1.8 m in section and 12.2 m in length and model buildings at a scale of 1:200 were used. A mixture of SF_6 and nitrogen with a concentration of 10 ppm was released.

Concentration levels were measured using receptors located on the roof of B1 (Figure 4.16). Each case utilized 10 receptors (4 upwind and 6 downwind from the stack) and these receptors were located 0.125 m from the lateral edges and spaced 0.025 m apart. For case 3, 10 receptors were located centrally at the windward wall of B3, starting at 0.004 m from the edge.

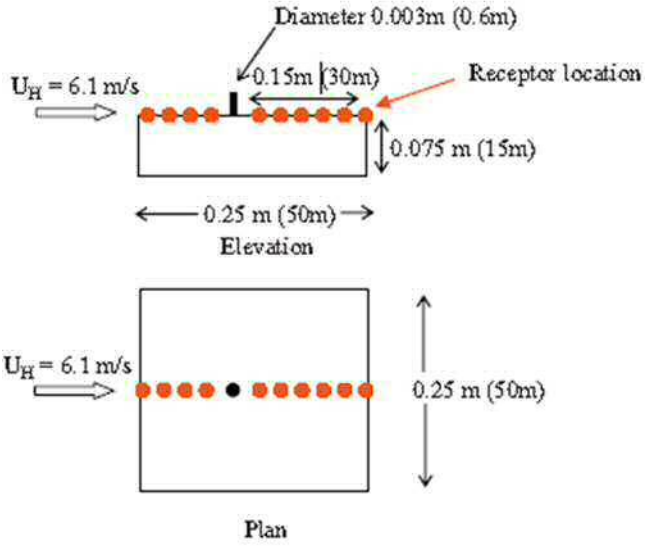

Figure 4.16 - Plan view and elevation (Chavez et al., 2011)

For the CFD code, Fluent 6.1 was used. This study employed the realizable k-ε turbulence model and modified the turbulence Schmidt number (Sc_t) to solve the transport mass equation. In this application, values of 0.1, 0.3 and 0.7 were used for Sc_t and the convergence criterion for all residuals was fixed at $10e^{-5}$.

4.7.2.2. Forcing variables and required outputs

In the simulations, the inlet boundary conditions were specified using a power law exponent of 0.33, which corresponds to a light urban terrain such as the one used in the experiment. The velocity at the roof of B1 was 6.1 m/s. In the case of the top and lateral boundaries, slip walls were modeled. For the outlet boundary, a zero gradient condition was specified. For walls, the standard wall function was used because y* i.e. dimensionless wall distance was in a large number of cells. Figure 4.17 shows the boundary conditions used for the CFD model.

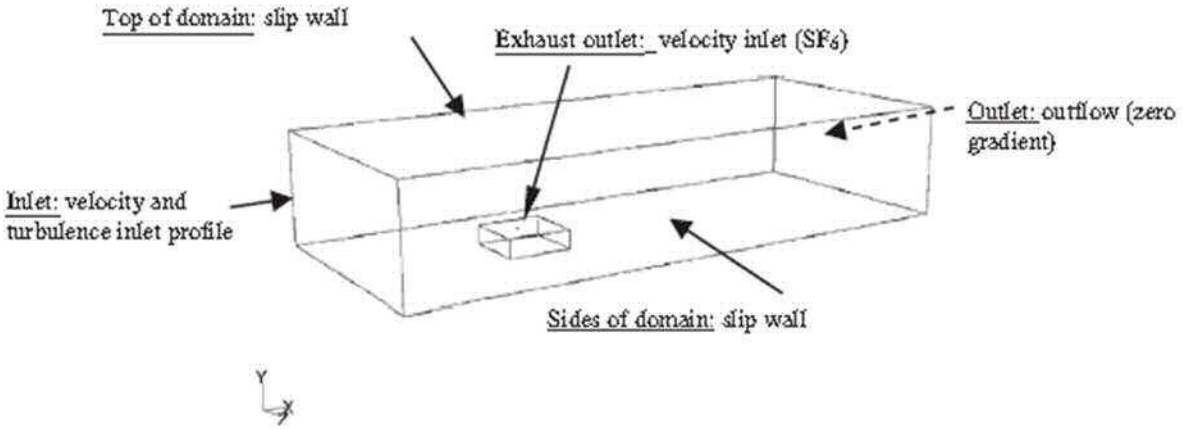

Figure 4.17 - Boundary conditions used for the CFD model (Chavez et al., 2011)

The required outputs for the model were the velocity and the dilution field. For the general view of the results, the mean velocity magnitude of the vertical plane and the streamlines for the middle vertical cross section and plane were presented to highlight differences in the velocity field behavior. Contour lines for the dilution field were also presented to reveal the plume behavior. Another required output was the normalized dilution for different values of Sc_t. The authors expected to be able to predict pollutant dispersion based on the value of Sct for CFD investigations.

4.7.2.3. Spatial and temporal scope, scale and resolution

The present study employed established CFD best practice guidelines for the computational domain. For example, taking H as the building height of B1 (Case 1), the lateral and top boundaries were 5 H away from building B1 and the outlet boundary was 20 H downwind. For Cases 2 and 3, H was considered to be the building height of the tallest building. In order to minimize the development of a streamwise gradient, a distance of 3 H away from the inlet to the target building was employed. The dimension of this computational domain maintained the blockage at 1.5 % in order to avoid any influence due to the lateral walls on the region of interest, as recommended by the CFD best practice guidelines.

The computational model was constructed using a structured hexahedral mesh and the total number of cells in the meshes ranged between 0.9×10^6 and 1.5×10^6 for Cases 1 to 3. The expansion ratio between two consecutive cells was limited to 1.25. Figure 4.18 shows the mesh for building B1.

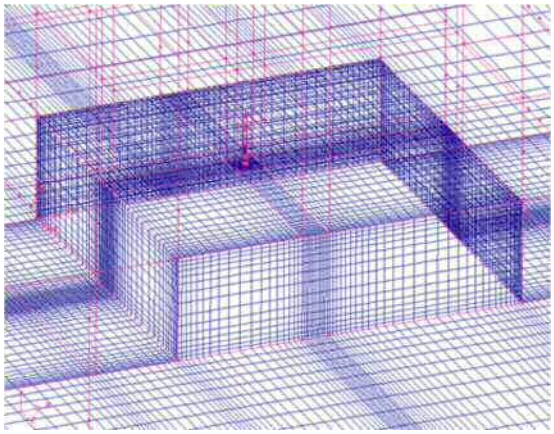

Figure 4.18 - Perspective view of the mesh of isolated building case B1 (Chavez et al., 2011)

4.7.2.4. Users of the model and model flexibility

Although the commercial code, Fluent 6.1, provides a user-friendly interface for users, the numerical model in this study needs to be handled carefully by the users. A knowledge of aerodynamics, computational inputs for CFD analysis and the uncertainties of physical numerical modeling, as well as an analysis of the grid sensitivity, were all required to obtain a correct numerical modeling solution. Due to these requirements, this type of numerical study should be carefully conducted by CFD experts.

The mesh sensitivity analysis examined three meshes: fine, medium and coarse. As the comparison of normalized dilution in a specific point in the space showed very similar values for the medium and fine meshes, the medium mesh was chosen by the authors. Regarding model flexibility, this study only considered three different cases with up to three buildings. The stack location was fixed on the roof of building B1 and the other buildings were just simple blocks. Therefore, adding or removing meshes could be easily performed.

4.7.3. Conceptualization of the system, specification of data and other prior knowledge

Conceptualization of the system in this study refers to the processes that affect pollutant dispersion. In urban areas, effluents released from stacks located on the roof of a building can be trapped in recirculation zones and may impact sensitive zones by re-entering the same building or affecting an adjacent building. This can cause potentially serious health problems for the occupants of the buildings.

Since previous studies showed that the turbulence Schmidt number (Sct) has a strong impact on determining pollutant dispersion in the case of an isolated building. An assessment of the value of Sct was therefore deemed important for the prediction of pollutant dispersion using CFD. Sct is defined as the ratio of turbulent momentum diffusivity to mass diffusivity. Here, Sct values of 0.1, 0.3 and 0.7 were chosen based on the findings of previous studies (Blocken et al., 2008).

Prior knowledge for this system includes the fundamental physical principles of CFD such as the conservation of mass, Newton's second law and the conservation of energy.

4.7.4. Selection of model features and families

4.7.4.1. Modeling approach

In order to assess pollutant concentration, a wide range of methods have been applied including wind tunnel tests, field measurements, CFD and other semi-empirical models. However, most available semi-empirical models are unable to solve near-field pollutant dispersion problems, and wind tunnel and field measurements suffer from time and financial constraints. Thus, CFD analysis was chosen in this case study. CFD has been widely used in studies of turbulent flow and pollutant dispersion around buildings. It is expected to achieve whole flow data in order to visualize flow and plume behaviors for qualitative analysis. Furthermore, it can easily provide numerical data to permit the determination of Sct and hence analyze the effect of Sct on pollutant dispersion.

4.7.4.2. Conceptual model

Based on a knowledge of the literature and considering wind tunnel measurements, substantial simplifications were employed for this numerical study. For the model geometry, only three simple block type buildings were considered and a single wind direction perpendicular to the building was adopted. For the assessment of pollutant dispersion, ten receptors were placed centrally along the windward wall of the rooftop.

4.7.4.3. Spatial and temporal scales

As mentioned earlier, this case study investigated pollutant dispersion in an urban area. For the numerical model, structured hexahedral meshes were constructed except for the stack. Because the stack had a circular cross-section, an unstructured wedge grid was used in this area. Within the computational domain, a distinction can be made in spatial zones such as boundary conditions.

4.7.5. Choice of how model structure and parameter values are found

The variables of interest in this study were the velocity and normalized dilution. The mean velocity magnitude and streamlines for the three cases permit the flow behaviors to be visualized. For normalized dilution, this can represent plume behavior such as that used for pollutant modeling as well as comparing the effects of different values of Sct. The velocity can be determined based on the physical laws of the conservation of mass, Newton's second law and the conservation of energy, all of which were established using partial differential equations. These equations can be simplified using the RANS or LES approaches (Blocken & Gualtieri, 2012). The value of Sct was based on previous studies (Blocken et al., 2008).

4.7.6. Choice of performance criteria

The main objective of this study was to reproduce the pollutant dispersion within a multiple building configuration using a numerical approach such as CFD. Another objective was to assess the effect of different values of Sct on pollutant dispersion. For the assessment of these objectives, tracer concentrations from the CFD simulation results were used to obtain the normalized dilution. This normalized dilution was also compared with wind tunnel results by the authors and literature field results from Stathopoulos et al. (2008). It was also observed that dilution was affected by the value of Sct, so the normalized dilution can be considered as a performance criterion. Another criterion could be a qualitative comparison of the mean velocity magnitude and the streamlines from the simulation results among the three cases.

4.7.7. Identification of model structure and parameters

According to Jakeman et al. (2006), this step is generally an iterative process of finding a suitable model structure and parameter values. In this study, a 3D RANS approach was employed rather than LES models. Although LES has been shown to provide a better agreement with experimental results in pollutant dispersion, this requires computational resources about 100 times greater than those needed by steady RANS models. Among the RANS models, the realizable k-ε turbulence model was selected because the value of Sct can be modified in this model and it also exhibits much better agreement with experimental results than other steady RANS turbulence models.

4.7.8. Conditional verification including diagnostic checking

In this study, both qualitative and quantitative verifications were conducted. In the case of qualitative verification, the mean velocity magnitude and contour lines of the dilution field for all three cases were examined. For the quantitative verification, a comparison with measured data was conducted in order to assess the effect of the value of Sct and the mesh sensitivity was also analyzed.

4.7.9. Quantification of uncertainty

Uncertainty in CFD modeling can arise from a very wide range of sources including the simplification of model geometry, the mesh generation, the choice of turbulence models, boundary conditions, and so on (Blocken & Guartieri, 2012). In order to reduce or avoid uncertainties, this study employed the CFD best practice guidelines concerning the size of the computational domain. The mesh sensitivity test was conducted based on three different meshes.

4.7.10. Model evaluation or testing (other models, algorithms, comparisons with alternatives)

For the final step, the objectives of the model were evaluated. The main objective of this case study was to reproduce near field pollutant dispersion for three different building configurations using the CFD technique. For the model evaluation, a qualitative analysis was conducted. Among the three cases, the mean velocity magnitude, the streamlines of the vertical cross-section and the plan view, and the contours of normalized dilution were presented. For example, Figure 4.19 shows the concentration of the dilution for the three cases. This qualitative comparison shows how the vortices interact with the surroundings and provide a better understanding of pollutant dispersion within an urban area.

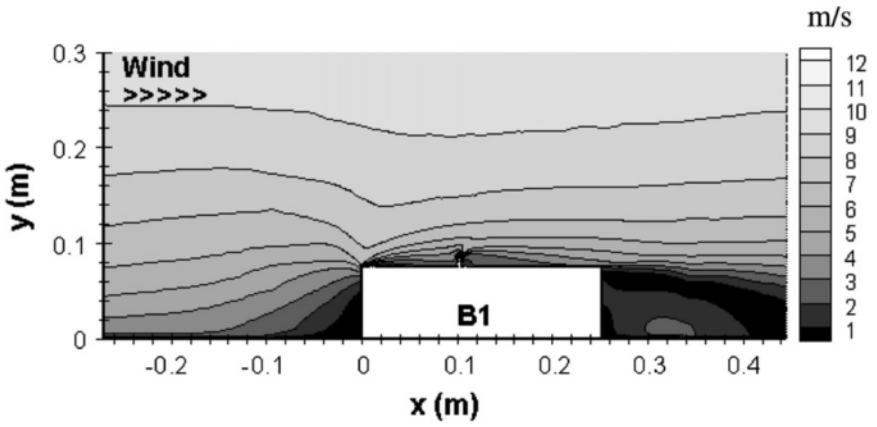

a. Case 1

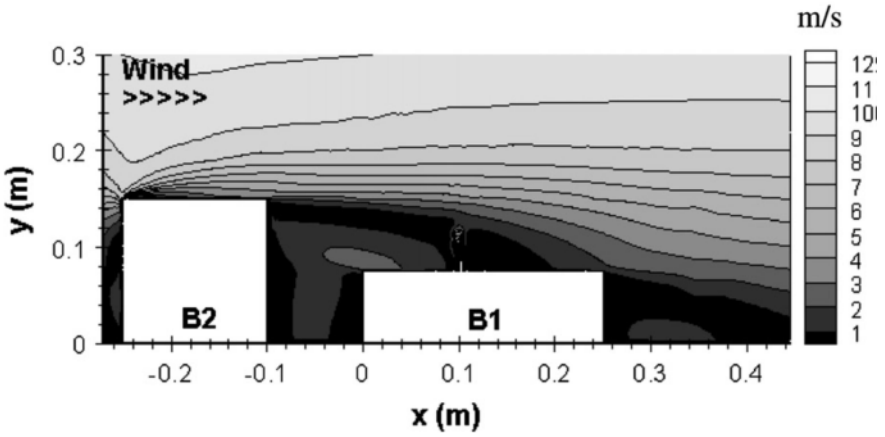

b. Case 2

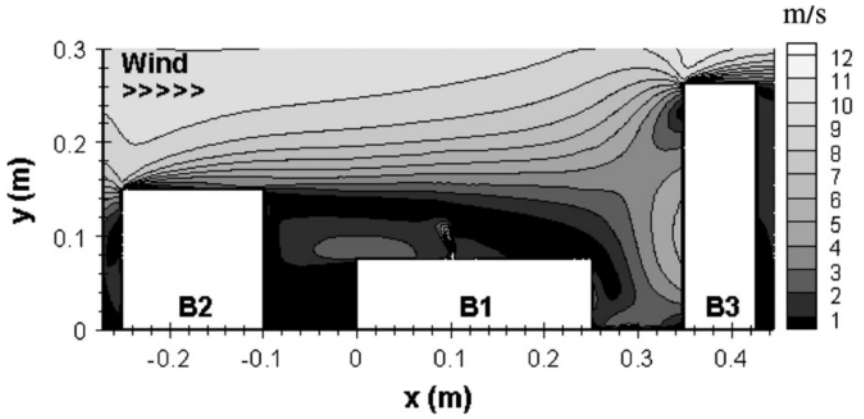

c. Case 3

Figure 4.19 - Contours of mean velocity magnitude (m/s) for stack height h - 1 m and exhaust momentum M – 3 (Chavez et al., 2011)

Another objective of the study was to investigate the effect of the value of the turbulence Schmidt number, Sct. The numerical results were compared with the experimental data using results obtained from wind tunnel tests, CFD for different values of Sct and data provided in ASHRAE-2007. This comparison revealed that pollutant dispersion from a rooftop stack on an isolated building was greatly affected by the value of Sct. However, changing the value of Sct had far less of an impact on the plume dilutions in Cases 2 and 3.

4.8. Summary of lessons-learned from the journal analysis

Four journals were analyzed using the ten-iterative steps approach focusing on wind flow around buildings in order to achieve the practical guidelines of CFD. Through the analysis, a rich description of the CFD processes and lessons-learned were gathered:

Journal articles 1 and 4 used CFD to predict dispersion around an isolated building. While paper 1 was interested in comparing the RANS and LES models to obtain more credible results, paper 4 focused primarily on pollutant dispersion within multiple building configurations. In addition, paper 2 investigated the pressure coefficients on buildings using CFD, while paper 3 conducted a CFD analysis to understand the effect of various configurations in order to determine the optimum position for roof mounted wind turbines.

Three of the papers (1, 2 and 4) reported conducting wind tunnel tests and using the data collected to evaluate the CFD results. The specific size of the wind tunnel facility and the velocity or pressure data measured in the wind tunnel, along with the boundary conditions, were therefore available for the CFD simulations. In the case of paper 3, the specific conditions utilized were those from earlier studies.

For the computational domain, all the studies created the domain recommended by the CFD best practice guidelines (Franke et al., 2007; Tominaga et al., 2008). When H is the height of the building of interest, the length of the upwind distance was 5H from the inlet domain and the downwind length was 15H from the outlet boundary condition. For the vertical and lateral dimensions, 6H was used for the height of the domain and 10H+w (where w is the building width) was the lateral length. In the case of paper 4, distances of 3H for the upstream length and 20H for the downstream length were used.

All studies utilized structured hexahedral meshes except paper 2, which generated a hybrid mesh composed of both hexahedral and prismatic cells. All four studies performed the grid sensitivity

analysis with three different grid densities in order to identify the proper mesh size. Three meshes, namely fine, medium and coarse, were generated for each analysis.

For the boundary conditions, the commonly measured vertical wind profile from the experiments was applied as the inlet boundary condition. In order to specify the velocity profile of the atmospheric boundary layer at the inlet, two kinds of expression are used. One is a log-law and another is a power law (Huang et al., 2007). Between these two expressions, the power-law velocity profile has been generally used when the experimental data is not available (Ai & Mak, 2013). While papers 2 and 3 employed a log-law, paper 4 used a power-law for the inlet condition, and paper 1, used both log-law and power-law for their RANS and LES approaches, respectively. For the top and lateral boundary conditions, papers 2 and 3 used symmetry conditions while paper 1 used no-slip conditions and paper 4 used slip wall conditions for the top and lateral sides of the domain. In the case of the outlet boundary conditions, most of the studies assumed a zero static pressure condition. For the ground surface, the standard wall functions as a rough wall were applied by all the studies.

For all four sets of researchers, the velocity components were the common variable of interest. This parameter can be expressed in the form of partial differential equations (see Chapter 2). Generally, these equations can be solved using either the RANS or LES approaches. Papers 2, 3, and 4 employed the RANS approach with the realizable k-ε turbulence model for the closure while paper 1 employed both the RANS with the RNG k-ε turbulence model and LES approaches in order to compare the accuracy of the results of these models.

In papers 2 and 3, the SIMPLE algorithm was employed for the pressure-velocity coupling, the pressure interpolation was second order and second-order discretization schemes were employed for both the convection terms and the viscous terms of the governing equations. In addition, most of the studies assumed that convergence was obtained when all the scaled residuals leveled off within the range of $10^4 – 10^{6.}$

After convergence had been obtained, the outputs for all the articles consisted of all the parameters of the average flow field around the building of interest. The velocity or pressure

field and other simulations results were generally represented through the research purpose. In the case of paper 1, the wind velocity and instantaneous fluctuations of concentration at the building surfaces were the criteria and these criteria were validated with wind tunnel data in order to identify the preferred turbulence model between the RANS and LES methods. The purpose of paper 2 was to predict the pressure distribution on a building with and without balconies using a 3D RANS approach. Thus, the target criteria of this paper consisted of the pressure distributions on the building surface, which were also validated with experimental data and then used to investigate the impact of computational parameters. For paper 3, the streamwise velocity and turbulence intensity were used to investigate various options for roof shape, wind direction, building height and urban configuration in order to identify the most productive location for power generation by building-integrated wind turbines. Finally, paper 4 conducted CFD simulations to predict pollutant dispersion within buildings. The results of this study were expressed in terms of the mean velocity magnitude and the streamlines.

The final step was to evaluate the objectives of each journal article. For paper 1, the main objective was to investigate the accuracy of LES for the reproduction of dispersion around a building. Through the various comparisons, LES showed better agreement with experimental data and provided more important information than the RANS approach that was also tested. However, this came at a cost; the computation time for LES was significantly longer than that of the RNG k-ε model. The objective of paper 2 was to reproduce wind pressure distributions across building facades with balconies. Here, only a steady RANS approach with the realizable k-ε turbulence model was employed and the results compared with wind tunnel data. Good agreement was obtained between CFD and wind tunnel tests and the sensitivities of computational parameters such as grids, turbulence models and wind direction were analyzed. The authors concluded that the careful selection of computational parameters was very important to ensure the accuracy and reliability of the results. In the case of paper 3, the objective was to investigate the effect of roof shape, wind direction, building height and surrounding urban configurations on the wind flow above the roof. Employing the RANS approach with the realizable k-ε turbulence model, the streamwise velocities for the effects of different roofs shapes were analyzed qualitatively and comparisons of the turbulence intensities and velocities were

conducted quantitatively to examine the effects of different building heights and urban configurations. Finally, the objective of paper 4 was to reproduce near field pollutant dispersion within three different building configurations using the RANS approach with the realizable k-ε turbulence model. The mean velocity magnitude and the streamlines were presented for qualitative analysis and the numerical results of the concentration were compared with wind tunnel data.

As described above, the description of the CFD process and lessons-learned were obtained through the journal analysis. These findings can be helpful to assist designers and architects to utilize CFD in the architectural design process. By considering these findings, the practical computational parameters for wind flow around buildings were achieved and summarized in table 4.4.

Table 4.4 - A summary of lessons-learned: the computational parameters for wind flow around buildings

The computational domain size	- 5H and 15H for the length of upwind and downwind length respectively (when H is the height of the building of interest) - 6H for the vertical extension -10H+W (where, w is the building width) is for the lateral length
Grid type and resolutions	- Hexahedral meshes were used. - Three different grids were constructed.
Boundary conditions	- The experimental data were specified at the inlet using power law and logarithmic law. - A zero static pressure condition was imposed at the outlet - For the sides and tops, symmetry conditions were used. - The standard wall functions were used for wall boundaries.
Turbulence models	- Two RANS approaches (the Realizable k-ε and the RNG k-ε). - LES model was also considered for the accuracy.
Algorithm and scheme	- The SIMPLE algorithm and second-order discretization schemes
Convergence criteria	- All the scaled residuals leveled off within the range of 10^4 – 10^6.

5. WIND TUNNEL TESTING

In general, wind tunnels have been used to study the flow of air over objects of interest, the forces acting on them and their interaction with the flow. Nowadays, wind tunnels are employed to verify aerodynamic studies in a wide range of applications, including in the automotive industry, architecture, environment, and education. While the use of numerical approaches such as CFD has increased, wind tunnel tests are still important for developing new aircraft, wind turbines or other designs that involve complex interactions with the flow (Hernández et al., 2013). In the case of architecture, the effects of aerodynamic forces on buildings and structures must also be considered for structural stability (English, 2007).

5.1. Architectural applications of wind tunnel testing

Wind tunnels have been used to determine the aerodynamic characteristics of buildings for a number of years (Zhang & Gu, 2008). In recent examples, Yasui et al. (2002) performed wind tunnel tests, full-scale observation and CFD to investigate wind pressures on tower-like structures, while Lo et al. (2013) conducted a combined approach with CFD and wind tunnel testing for indoor airflow prediction of wind-driven cross ventilation. To predict dispersion in a street canyon with tree planting, Gromke et al. (2008) conducted both wind tunnel tests and numerical investigations and Wong and Heryanto (2004) investigated an active stack effect for improving natural ventilation by means of wind tunnel and CFD simulations. Recently, the use of wind tunnel studies has been increasingly applied for building applications (Cochran & Derickson, 2011).

5.2. Overview of wind tunnel testing at IBHS

Wind tunnel tests were performed to characterize the innovative vent system developed by Virginia Tech and Acrylife Inc. at the wind facility belonging to the Institute for Business and Home Safety (IBHS) in Richburg, SC. This wind tunnel testing was assisted by Acrylife and Radco Construction. Pressures were measured under the roof membrane and initial tests without

the membrane were conducted to gather baseline data on pressure magnitudes and distributions on the roof surface. After the initial measurements, tests were performed with up to two roof vents, a parapet vent system, and parapet walls. Wind speed data from a reference anemometer at an elevation of 13 ft and pressure readings recorded at each of the roof pressure taps were stored at the IBHS (Morrison et al., 2012b).

5.2.1. The IBHS wind facility

The Insurance Center for Building Safety Research (ICBSR) was created by the Institute for Business & Home Safety (IBHS) to provide a unique research center that can test low-rise buildings subjected to a variety of natural hazards as well as other types of losses. The main facility is a large open-jet wind tunnel that can subject full-scale one or two-story buildings to high winds accompanied by wind-driven rain, hail and even fire. Testing in the facility includes the ability to rotate building orientation relative to the wind direction, change vanes to generate lateral turbulence, introduce rain drops with prescribed distributions of droplet sizes and rainfall rates, inject burning embers of various sizes, and simulate hailstones. The research conducted at the IBHS improves our understanding of the interaction between extreme winds and buildings. Moreover, it provides information on the weaknesses of residential buildings and building systems subjected to natural storms as well as offering opportunities to improve construction techniques and building component design and manufacturing. It also influences public policy such as building code development (Liu et al., 2009).

a. Aerial photograph of the IBHS Research Center

b. 105 fans of the Inlet

Figure 5.1 - IBHS Research Center in Richburg, SC (Morrison et al., 2012a)

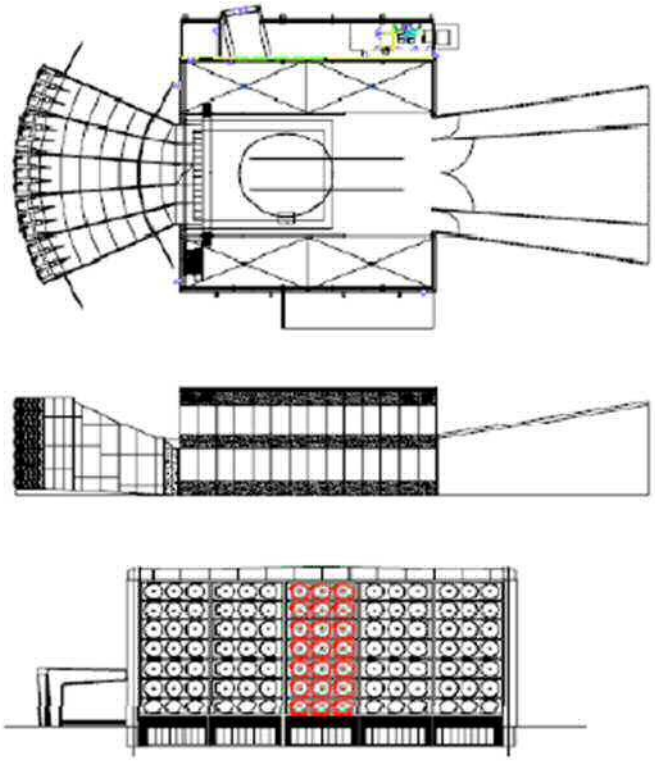

Figure 5.2 - Plan view and elevation views of the IBHS facility (Liu et al., 2009).

5.2.2. Facility details of the IBHS

The test chamber in the wind tunnel is 145’ (44.2 m) wide × 145’ (44.2 m) long, with a clear interior height of 60’ (18.3 m). Since the length is relatively short, this facility cannot reproduce the mean and turbulence characteristics of the atmospheric boundary layer. Due to this limitation, this facility uses both active and passive control elements. One hundred and five 5.5’ (1.68 m) diameter vane-axial fans with 350 horse power medium voltage electric motors are used to produce the wind flow. The array for these fans is divided into 15 cells placed in a grid 5 cells across and 3 cells high. As shown in Figures 5.3 and 5.4, the contraction from the fans to the inlet is approximately 2:1 and the size of the inlet has dimensions of 65’ (19.8 m) × 30’ (9.1 m). The speed of each fan cell is independently operated by a programmable logic controller (PLC) capable of updating the running speed of the fans at a maximum frequency of 4 Hz. The directional wind vanes and spires can also be used to control the fan speed to develop appropriate flow characteristics to reproduce the ABL. There are 16 wind vanes extending the entire height of the inlet. These vanes are divided into five groups capable of rotating independently of each other at angles of between -15° to +15°, with 0° representing the streamwise direction. The movement of the wind vanes produces large-scale flow fluctuations in the lateral direction. In order to produce turbulence at higher frequencies than are possible by modulation the fan speeds alone, spires are used to alter the mean flow profile within the lower and middle cells. A 55ft diameter turntable within the test chamber can be used to rotate the structural test specimens remotely (Morrison et al., 2012a).

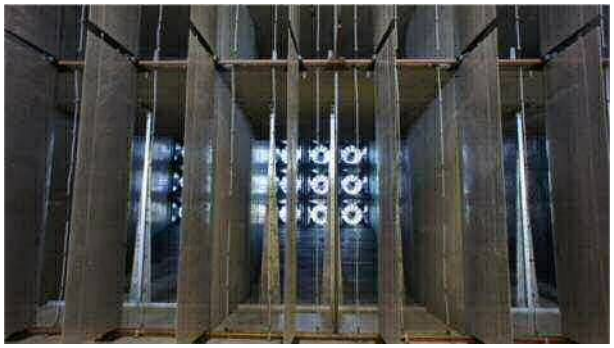

Figure 5.3 - Wind vanes at the inlet of the IBHS wind facility

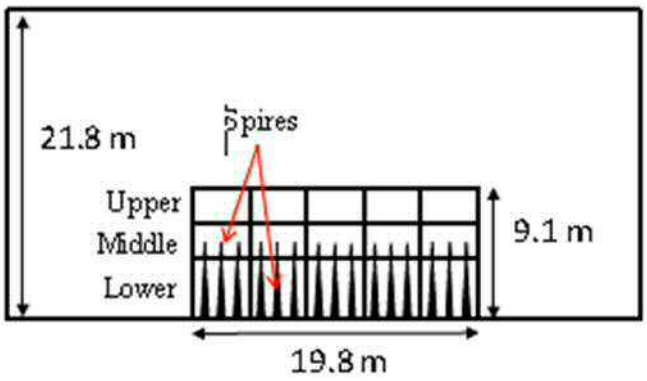

Figure 5.4 - Layout of the IBHS Research Center test chamber and inlet from the fans (Morrison et al., 2012a)

5.3. Experimental configuration

The data used in the current study were acquired during experiments performed at the IBHS wind tunnel facility. The overall view of the test building is shown in Figure 5.5. The test building was 30ft × 40ft in size, with a height of 13ft, and located 26ft downstream from the inlet. The test building was furnished with 158 pressure taps. The pressure scanning system used in the experiment measured all the pressures almost instantaneously. The pressure taps were located on the left windward quadrant of the roof, as shown on the plan view of the instrumented module sketched in Figure 5.6. These tap locations were developed as part of IBHS testing of root top equipment (Morrison et al., 2012b). The density of pressure taps was higher close to the windward sides of the roof, where larger pressure variations were expected and the tap line closest to the roof edge was at y/H = 0.038. In the tests, a 900 s sample with 100 Hz sampling rate was recorded as a time series for every tap at 6 approaching wind angles: 0°, 15°, 30°, 45°, 60° and 90°.

a. Test building

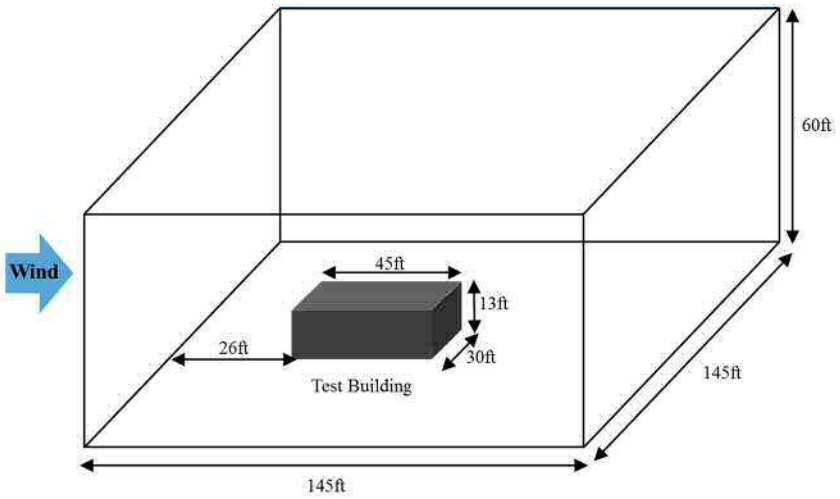

b. Layout of the test building and the chamber

Figure 5.5 - The overall view of the wind tunnel facility

The reference velocity was monitored using a RM Young anemometer at roof height. The obtained surface pressure data were converted to the non-dimensional pressure coefficient Cp [1] using:

[1] Pressure coefficient (Cp) is defined as the non-dimensional ratio which describes the relative pressures throughout a flow field.

$$\mathrm{Cp} = \frac{P - P_{\infty}}{0.5\rho V^2}$$ Equation 5.1 – Calculation of the pressure coefficient

where P is the average pressure measured on each tap on the surface, P∞ is the static pressure within the test chamber and V is the 15 minute mean velocity at roof height (Morrison et al., 2012a).

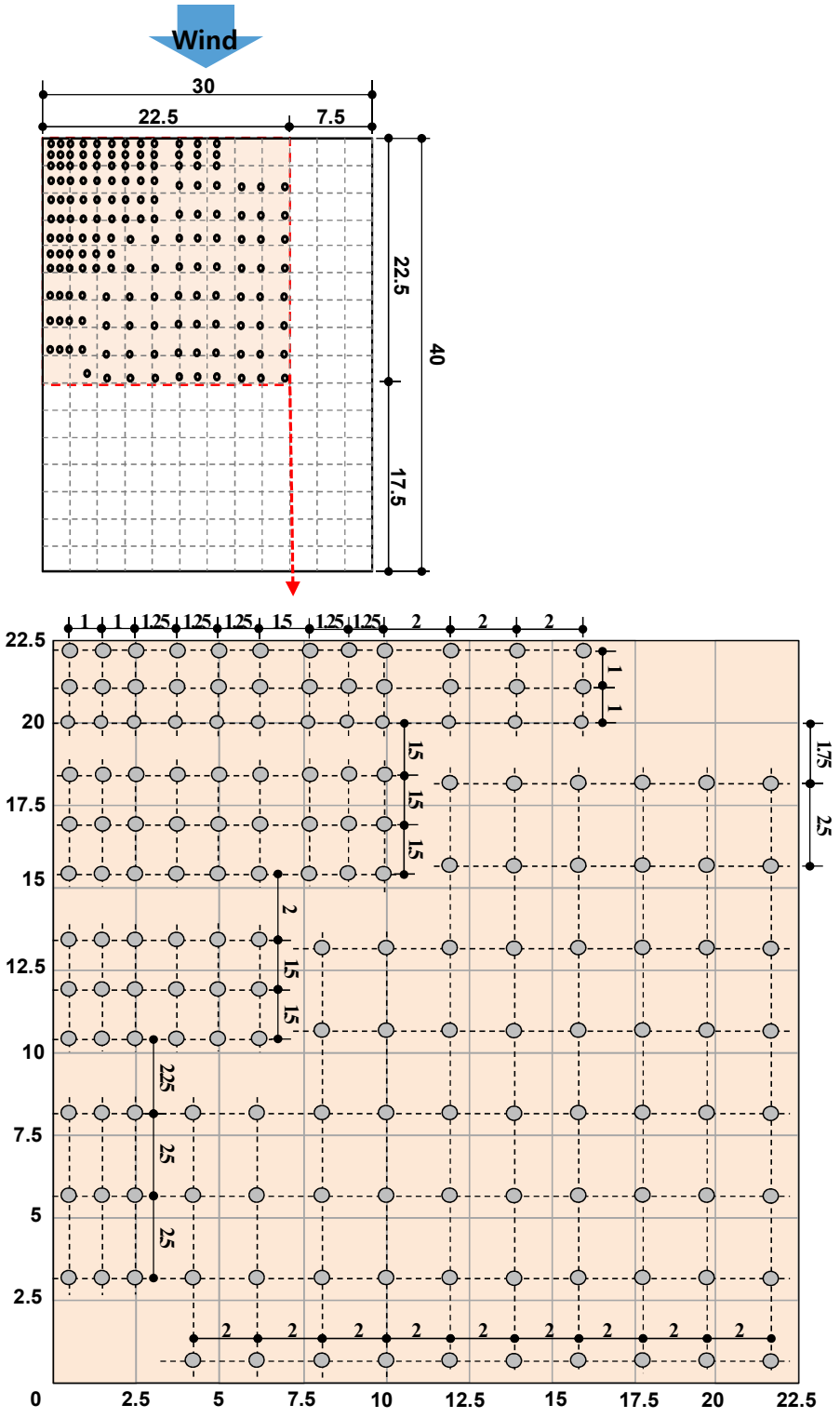

Figure 5.6 - The location of the pressure taps on the roof of the test building

In addition, the mean wind velocity profile and the longitudinal intensity profiles (Iu) were provided for this study. These measurements were previously conducted in order to provide realistic predictions of the performance of full-scale structures at the IBHS facility. The data obtained were compared with field data provided by Texas Tech University. According to the report by Morrison et al. (2012a), the mean velocity profile and the longitudinal and lateral turbulence intensity profiles showed good agreement with both field measurements and theoretical profiles. Among the data obtained, the mean velocity and longitudinal turbulence intensity profiles were used to determine the turbulent kinetic energy and turbulent dissipation rate for the CFD modeling (Figure 5.7).

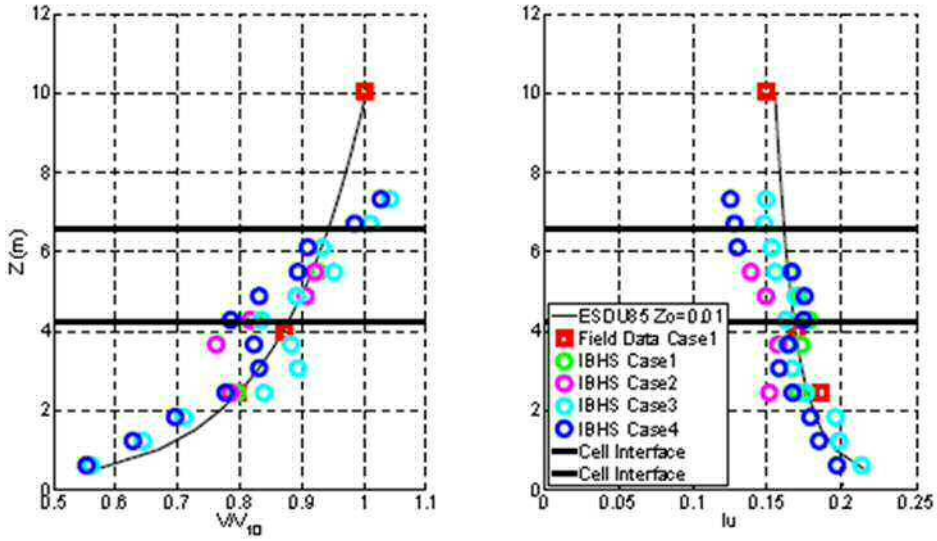

Figure 5.7 - Mean velocity (left) and longitudinal turbulence intensity (Iu) (right) profiles (Morrison et al., 2012a)

For the evaluation of roof vent performance, pressures on the roof surface were measured. First, tests were conducted with no membrane on the roof surface at various wind angles. Second, measurements were performed with the membrane in place. After investigating the pressures with and without the membrane, two roof vent systems were installed at two locations and the effect of a parapet vent system was also investigated.

5.4. Results

A number of different experimental configurations were investigated at the IBHS wind facility. All pressure data were acquired and analyzed by IBHS staff (Morrison et al., 2012b), who provided the results as contour plots of non-dimensional pressure coefficients. While experiments with various configurations were conducted, pressure data measured on the roof surface without the membrane were selected for this study. Since one of the purposes of this study was to gather a rich description of the CFD process that can be achieved by validation with experimental data, a simple geometry was used when performing CFD simulation in an attempt to avoid numerical errors or uncertainties. Thus, the mean surface pressures on the roof deck without the membrane at a wind angle of 0 degrees were chosen for the validation with CFD.

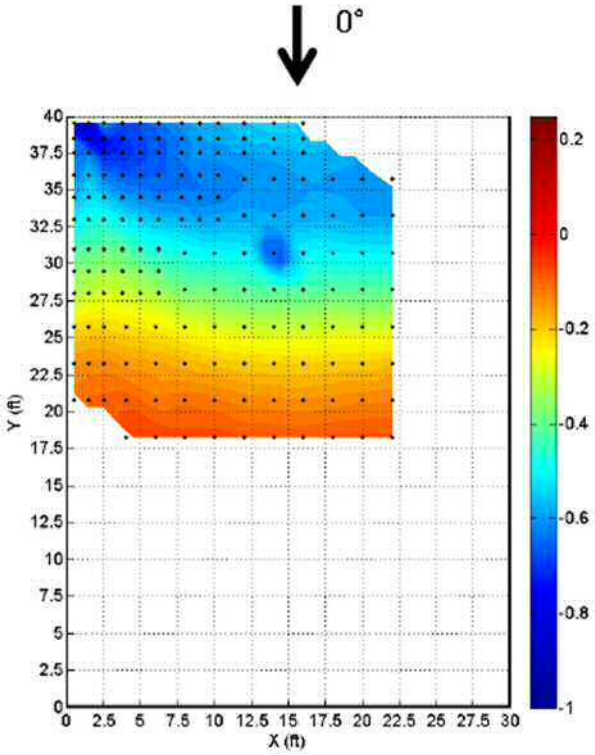

Figure 5.8 - Pressure coefficient distribution on the roof surface (Morrison et al., 2012b)

Figure 5.8 shows the distribution of the non-dimensional pressure coefficients on the roof surface without a membrane. The reference wind speed at the building height was 46.2 mph (20.69 m/s). According to Figure 5.9, the mean pressure coefficients near the edge of the roof were relatively lower and the pressure coefficients generally increased along the centerline of the roof surface. This indicates that the highest suction occurred near the edge, decreasing as it progressed along the centerline.

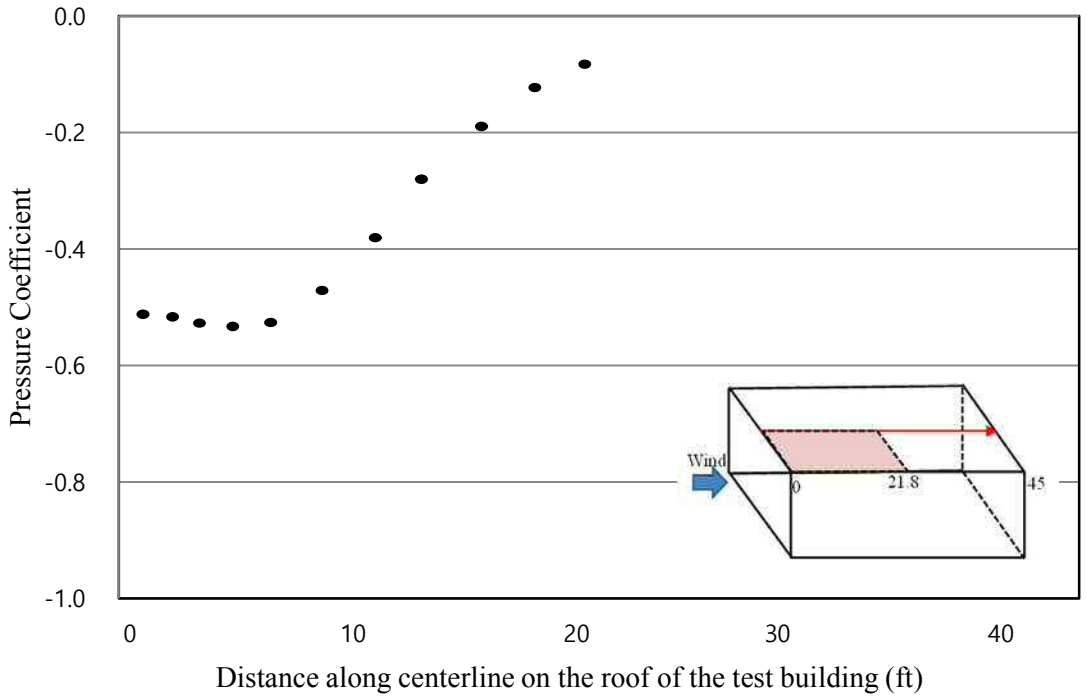

Figure 5.9 - Pressure coefficient distribution along the centerline on the roof surface

For the CFD analysis, the geometry of the building of interest was employed to create a computational domain. The wind tunnel data for the rooftop sensors was used for grid sensitivity tests and the validation. The detailed comparison with the CFD results will be presented in Chapter 7.

6. THE SENSITIVITY ANALYSIS

6.1. Introduction

Based on the document analysis described in Chapter 3 and 4, several computational parameters were chosen. The selected computational parameters and their influence on CFD analysis are described in this chapter through the sensitivity analysis. The sensitivity of three computational parameters including the computational domain size, the grid size and turbulence model was tested and all the sensitivity analyses employ the same geometry as the wind tunnel testing at the IBHS.

6.2. Context of the wind tunnel tests at the IBHS

For the sensitivity analysis, the wind tunnel tests with a full-scale building at the IBHS wind facility were reproduced using the CFD simulation. The purpose of the wind tunnel tests and the details of the wind facility and the experimental configurations were described in Chapter 5.

The dimensions of the wind tunnel facility are 145 ft long by 145 ft wide, with a height of 60ft. Although this facility cannot reproduce the mean and turbulent characteristics of the atmospheric boundary layer due to its short length, the speed of each of its 105 350 horse power fans can be adjusted by a programmable logic controller to reproduce the conditions typically experienced in the atmospheric boundary layer.

Inside the chamber, a 30 ft by 40 ft, 13 ft tall, test building was placed 26 ft downstream from the inlet. The test building was furnished with 163 pressure taps on the left windward quadrant of the roof. Various experimental configurations were investigated and pressure data obtained using the pressure taps. During these tests, a 15-min mean speed of the order of 40 - 45 mph was achieved. In addition, the mean velocity and longitudinal turbulence intensity profiles measured for the previous experiments were employed to obtain the turbulent kinetic energy and turbulent dissipation rate for the inlet boundary condition.

Among the various configurations tested in the original wind tunnel experiments, wind flow on the roof surface without a membrane was selected for the CFD modeling. Since this test had the simplest geometry, with no extraneous features such as parapet walls, membranes, or vents, this configuration was selected in order to facilitate the CFD simulation. The obtained pressure data were used to investigate the impact of computational parameters.

6.3. Other computational parameters

Although the sensitivity analysis investigates the impact of the computational domain size, the grid density and the selection of turbulence model, respectively, it is necessary to clarify a number of other computational parameters including initial conditions, discretization methods, boundary conditions, solution algorithms, and convergence criteria in order to perform the CFD analysis. According to the guidelines laid out by Casey & Wintergerste (2000), the parameters for the control of convergence of the solution algorithm, including the relaxation factor, damping factors or time steps as recommended by the commercial CFD code, can be used. In addition, the commercial code provides useful parameters or conditions for non-experts to help them conduct a successful CFD analysis, the default settings of the commercial code were employed for this study (Bakker et al., 2001). Other computational parameters of best practice guidelines and the analysis of journal articles (Chapter 3 & 4) were used.

6.4. Investigations of wind flow on a roof with three different computational domain sizes

6.4.1. Problem statement

To maximize the accuracy of the CFD simulation, it is important to determine the size of the entire computational domain in the vertical, lateral and in/out flow directions. In general, the recommendations of the best practice guidelines by Franke et al. (2007) and Tominaga et al. (2008) were employed to create the computational domain. However, the upstream length of the wind tunnel was only 2H, which was smaller than the recommendations of the best practice

guidelines, where H is the height of the building of interest. In addition, Ramponi and Blocken (2012) observed that the blockage ratio also influences the results of CFD.

For this study, the sensitivity of three different computational domain sizes was investigated. For the reference model, 5H for the upstream length and 15H for the downstream length were employed. For the lateral and vertical domain lengths, the height and width of the wind tunnel were used. As mentioned previously, 2H was the upstream length for the first test model. Other conditions were the same as the reference model. For the second test model, an increased blockage ratio was employed to compare the effect of the blockage ratio.

6.4.2. Computational domain

As described above, a full-scale building in a wind tunnel was modeled explicitly, satisfying the best CFD practice guidelines requirements for upstream and downstream length as a reference model. In addition, two other computational domain sizes were also constructed. For all computational domains, the upstream length was kept as short and the length of downstream was set long enough to allow the development of the wake region behind the building and thus support the convergence of the simulations (Blocken et al., 2012). For the reference model, the domain dimensions were L × W × H – 307 ft × 145 ft × 60 ft (93.7 m × 44.2 m × 18.3 m). In the wind tunnel tests at the IBHS, the upstream length from the inlet boundary to the test building was 2H (26 ft) and the blockage ratio was 4.5 %. In order to investigate the impact of upstream length on the results of CFD, an upstream length of 2H was also applied for the first model; the dimensions L × W × H – 268 ft × 145 ft × 60 ft (81.7 m × 44.2 m × 18.3 m) were applied. Franke et al. (2007) recommended a maximum blockage of 3% but used the same cross-section of the wind tunnel for the computational domain. Thus, the blockage ratio of the reference model was 4.5%. In order to compare the effect of the blockage ratio, a blockage of 6.8 % was applied to the second model. When the height of the building is H, H_d is the height of the computational domain and this can be expressed as $H_d – H + d$. For the lateral extension, W is the test building's width and W_d is the width of the computational domain. W_d can be expressed as $W_d – W + 2d$. While 5H was used for the vertical and lateral extension in order to avoid any interference of the

domain size on the numerical results (Ramponi & Blocken, 2012), 3H was employed with a blockage ratio of 6.8% in order to investigate the impact of the blockage ratio, thus reducing the computational domain size. The dimensions of the second model were L × W × H – 307 ft × 109 ft × 52 ft (93.7 m × 33.2 m × 15.8 m). The three domains are presented in Figure 6.1.

6.4.3. Computational grid

The grid was constructed based on the recommendations made by Franke et al. (2007) and Tominaga et al. (2008). The grid for the three cases consisted solely of hexahedral cells. While a considerable effort was required to generate a hexahedral mesh, this type of grid avoids the well-known convergence problems associated with hybrid grids that include tetrahedral cells (Blocken et al., 2012). For this grid, a second-order discretization scheme was used, as recommended by Franke et al. (2007). This option is set as the default in the commercial code STAR-CCM+8.04 and this scheme is considered the most accurate for steady-state calculations (STAR-CCM+ UserGuide 8.04).

For the reference model, 682,380 cells were created using the generating mesh tool in STAR-CCM+ 8.04. For the first model for the evaluation of effect of the upwind length, 606,008 cells were constructed. The final model for the investigation of the effect of the blockage ratio consisted of 393,456 cells.

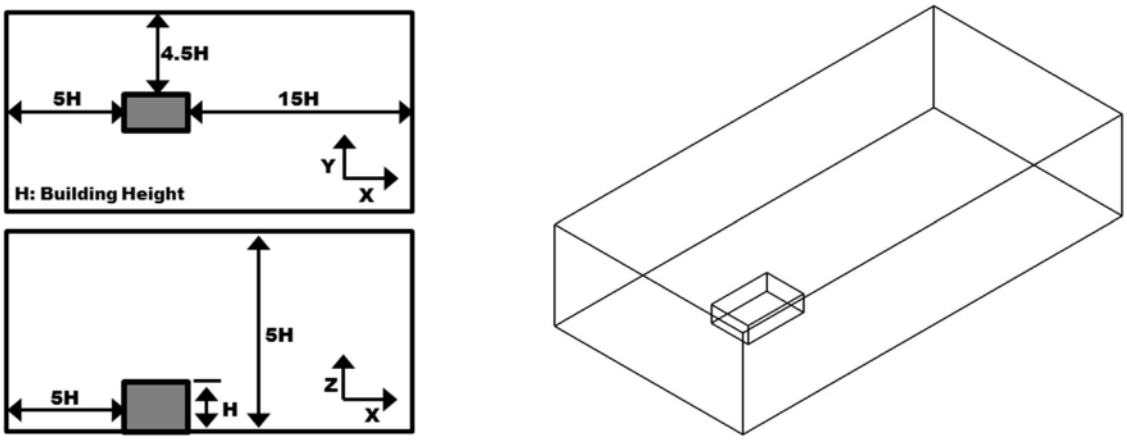

a. Computational domains for the reference model

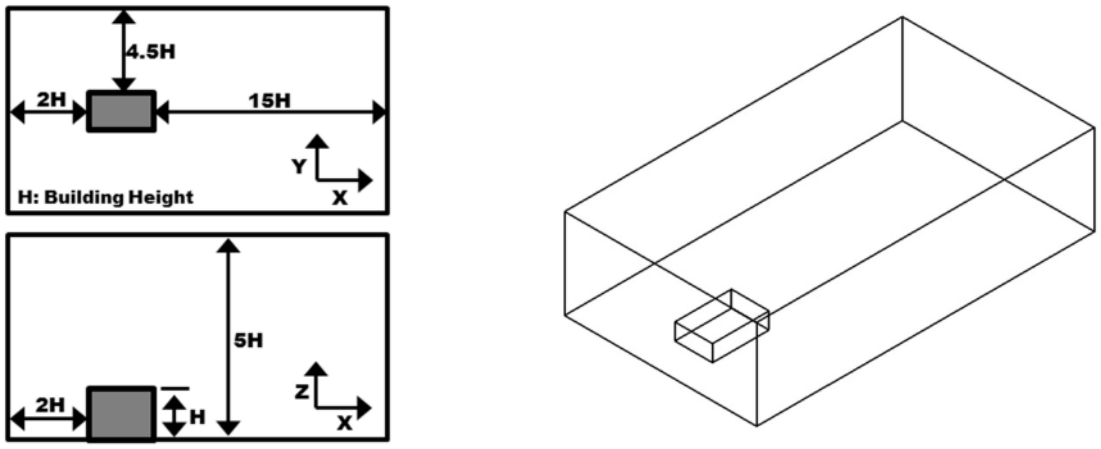

b. Computational domains for the model with 2H of the upstream length

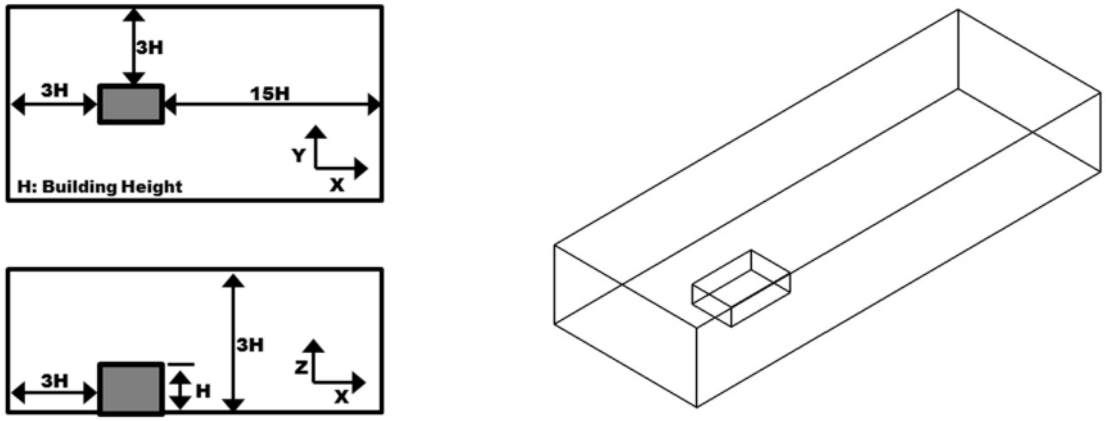

c. Computational domains for the increased blockage ratio model

Figure 6.1 - Three different computational domains

6.4.4. Boundary conditions

In order to obtain a better agreement between the experimental and numerical results, the boundary conditions adopted in the CFD simulation should be the same as those measurements, especially for inflow boundary conditions (Huang et al., 2007). For this study, the atmospheric boundary layer inflow was created at the inlet. The inlet boundary conditions, including the mean velocity, turbulent kinetic energy and turbulence dissipation rate, were based on the measured incident vertical profiles of mean wind speed and longitudinal turbulence intensity. The mean wind speed profile was prescribed by the power law with an exponent of 0.143, which corresponds to an open land surface. The velocity at the test building height was 20.69 m/s (46.3 mph). The estimated turbulence intensity, the inlet value of turbulence kinetic energy, k, and the turbulence dissipation rate, ε are given by Equations. 6.1 and 6.2:

$$\mathrm{k} = \frac{3}{2}(U_{avg} I)^2$$ Equation 6.1 – Calculation of the turbulence kinetic energy

$$\varepsilon = {C_\mu}^{3/4} \frac{k^{3/2}}{l}$$ Equation 6.2 – Calculation of the turbulence dissipation rate

where U_{avg} is the mean velocity at the inlet, I is the turbulence intensity, C_μ is an empirical constant specified in the turbulence model (~ 0.09), and *l* is the turbulence integral length scale. These values are presented in Figure 6.2. These values can be specified at the inlet in order to obtain a better agreement between experiments and CFD.

Based on reports in the literature (Blocken et al., 2012), symmetry boundary conditions were applied for the sides and the top of the computational domain that assumed zero normal velocity and gradients. For the outlet condition, a static pressure of zero was defined. Within the computational domain, no-slip wall boundary conditions were applied for the surfaces of the test building.

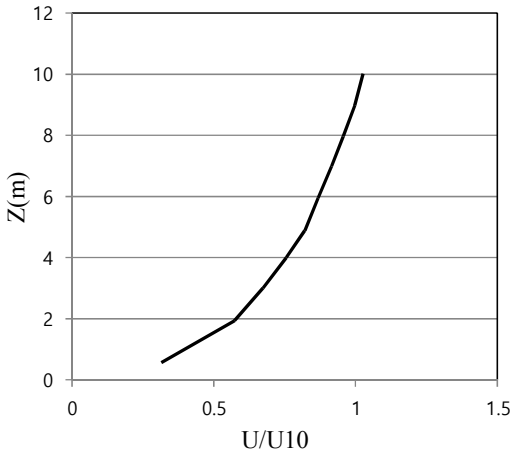

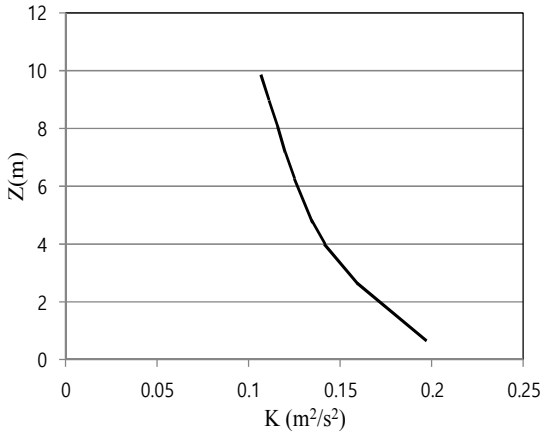

a. The mean wind speed profile by power law b. Turbulence kinetic energy k

Figure 6.2 - The inlet boundary conditions

6.4.5. Other computational conditions

The commercial code STAR-CCM+ 8.04 was employed for this CFD simulation with the 3D RANS equations. The realizable k-ε turbulence model was used for the analysis of wind flow around a building and the choice for this turbulence model was based on earlier successful validation studies for wind around a building (Blocken et al., 2012; Montazeri et al., 2013; Janssen et al., 2013). Steady state calculations were performed using the SIMPLE algorithm with a second-order discretization scheme for convection terms and viscous terms of the governing equations. When the residuals reached 10^5 for the velocities of x, y, and z, 10^5 for k and ε, and 10^5 for continuity, the iteration process ended.

6.4.6. CFD simulation results

6.4.6.1 Qualitative comparisons

First, the results of the computations in terms of velocity were analyzed for all three models. Figure 6.3 shows a comparison of the predicted mean velocity magnitude for the middle vertical plane. According to this comparative view of the results, the wind flow patterns in three cases are

similar. Although the upwind flow of the second case is stronger than that in two other cases, a large difference among three cases is not observed.

As shown in Figure 6.4 and Figure 6.5, contours of mean velocity magnitudes and pressure coefficients distribution on the roof surface of each case are presented. Similar to the comparisons in Fig 7.3, the result of the reference model shows the similar patterns with the two other cases. Overall, the effect of the shorter upstream length and the increased blockage ratio on both the velocity and pressure field is small.

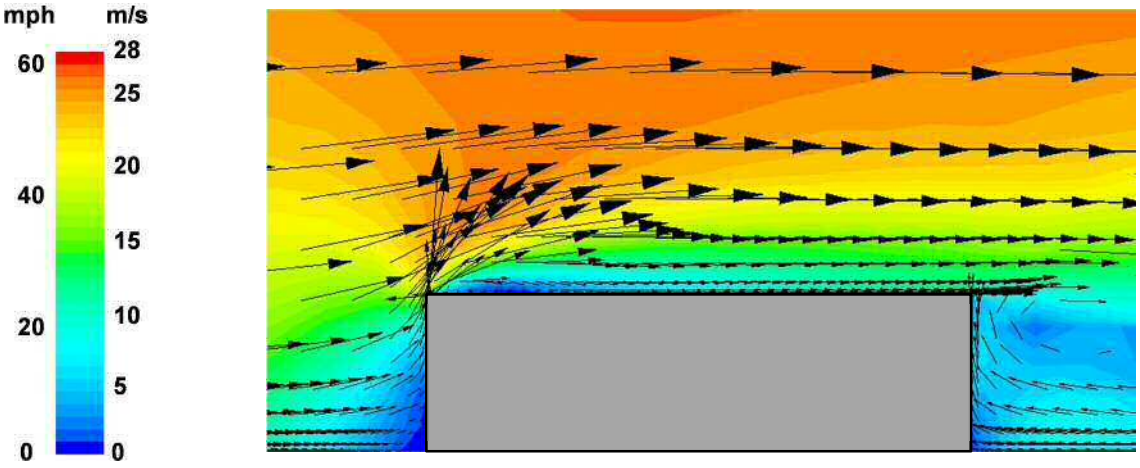

a. The reference model

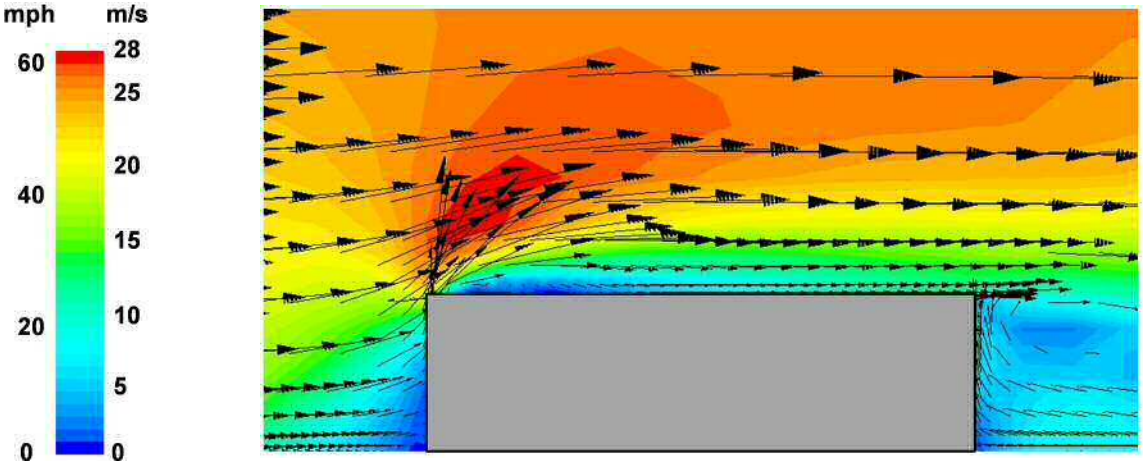

b. 2H of upstream length

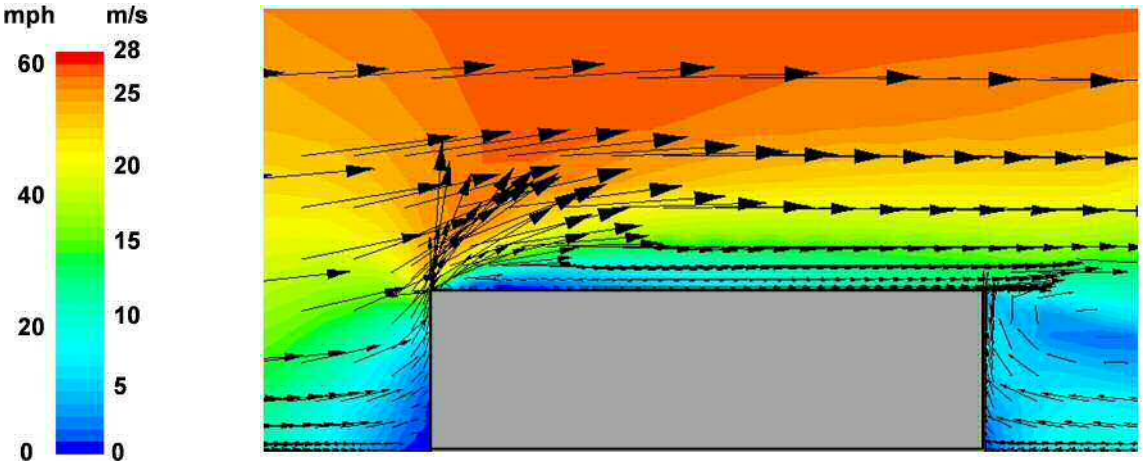

c. The increased blockage ratio

Figure 6.3 - Contours and vectors of mean velocity magnitude for the middle vertical plan

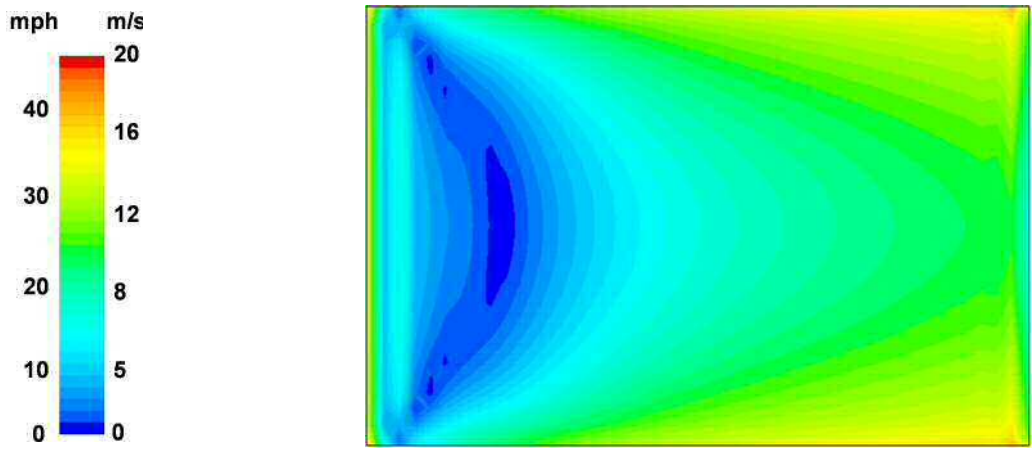

a. The reference model

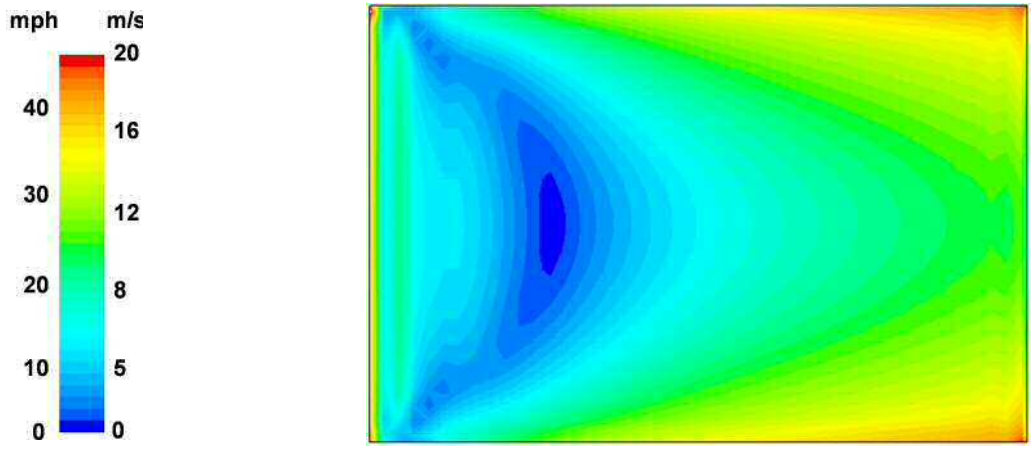

b. 2H of upstream length

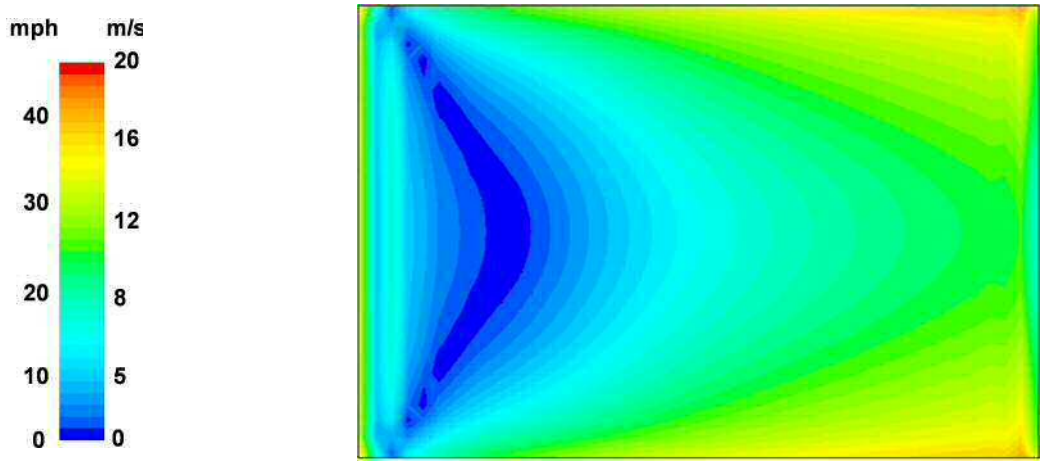

c. The increased blockage ratio

Figure 6.4 - Contours of mean velocity magnitude on the roof surface

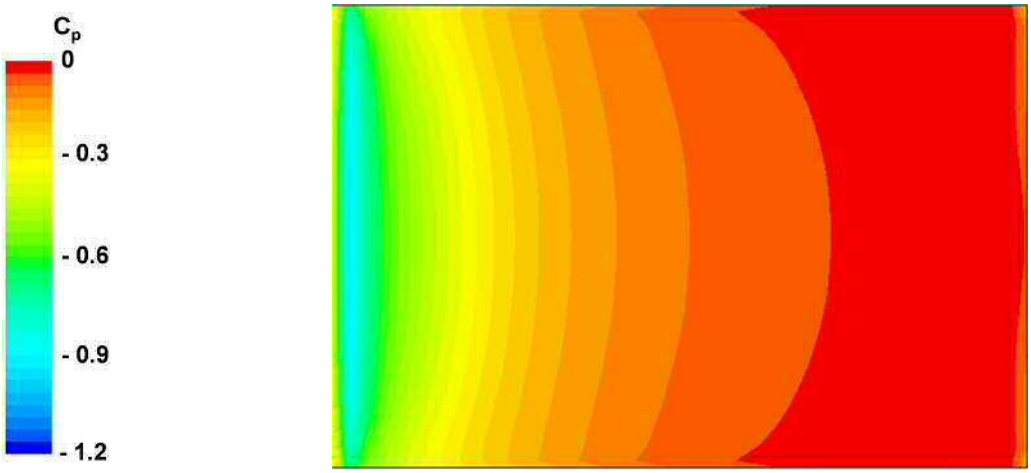

a. The reference model

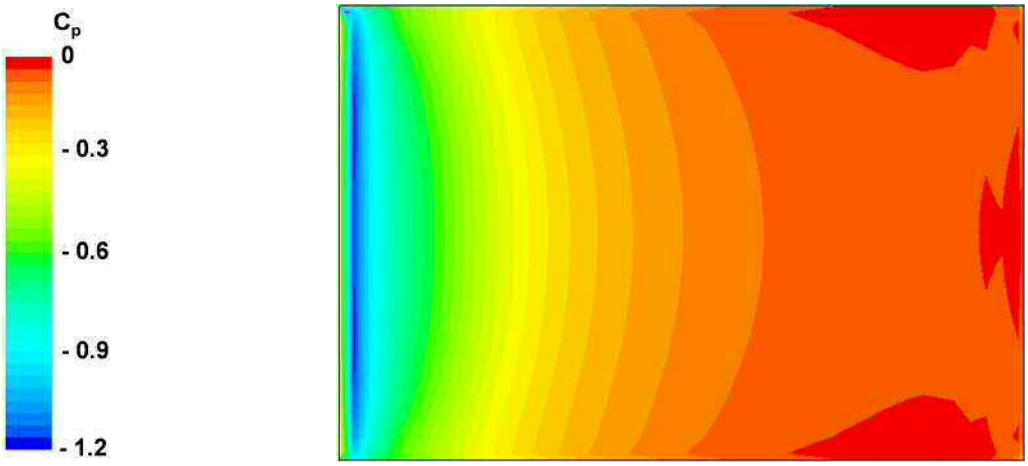

b. 2H of upstream length

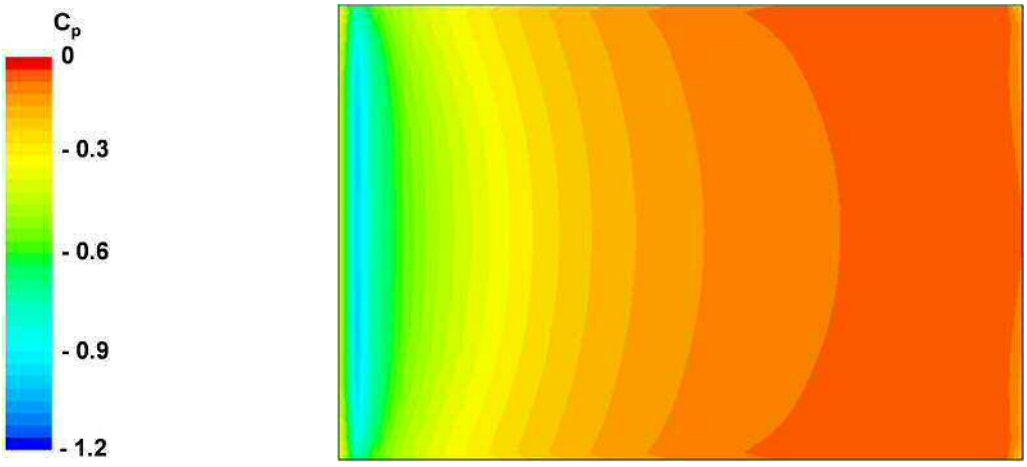

c. The increased blockage ratio

Figure 6.5 - Contours of pressure coefficients distribution on the roof surface

6.4.6.2 Comparisons of pressure coefficient on the roof surface of the three models

As shown in Figure 6.6, the CFD results for the reference model were compared with the results of the wind tunnel measurements. Extremely high suction values were observed near the edge, decreasing rapidly for both cases. While the highest suction for the CFD simulation was observed at the edge, the suction for the experimental roof were highest 4 – 6 ft from the edge. Both Cp values were the same at the middle of the roof surface. Concerning these results, the agreement between the experiments and the CFD results of the reference model could not be determined because of the limited data available from the experiment.

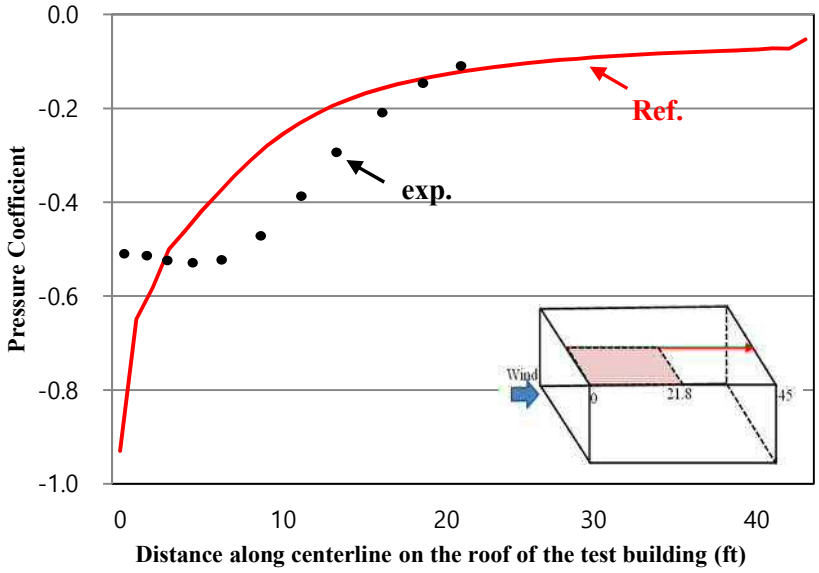

Figure 6.6 - Comparison of pressure coefficient from CFD simulation results and wind tunnel measurements along the roof surface centerline

Figure 6.7 shows the results obtained for three different computational domains. The average absolute deviation between the CFD results and the measurements for the center lines is 0.063, 0.067 and 0.062 for the reference, upstream length: 2H and blockage ratio: 3H respectively. Along the centerline on the roof surface, the results of the two cases showed similar trends to the reference case. Although the pressure coefficient distribution of the domain with the shorter

upstream length was lower than the other cases, the results of all three cases showed a small change in pressure distribution.

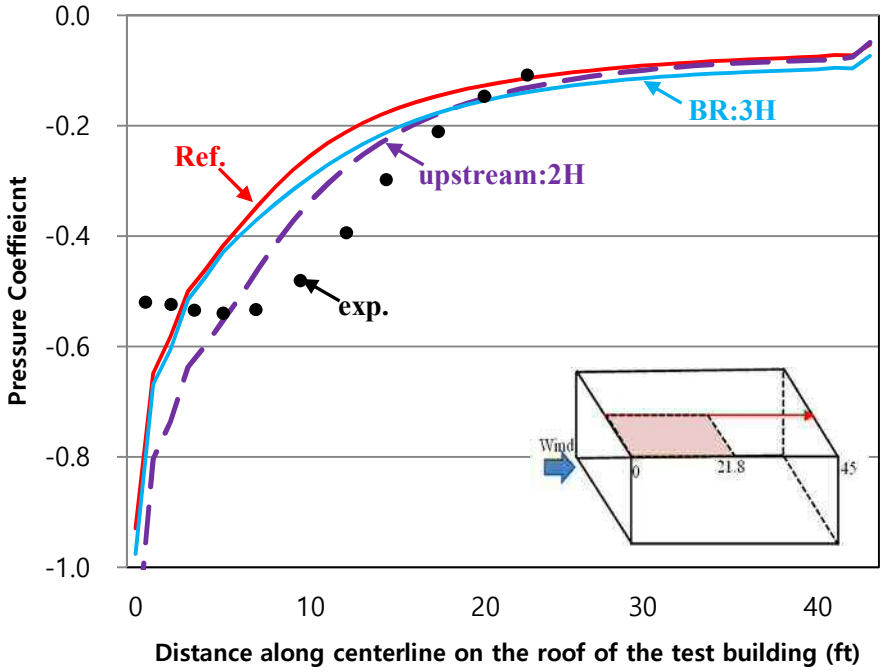

Figure 6.7 - Impact of the computational domain size on CFD simulation results for the pressure coefficient along the roof surface centerline

6.4.7. Discussion

This study focused on the validation of the results between CFD and wind tunnel tests, specifically investigations of CFD simulations of wind flow on the roof surface and the impact of three different computational domain sizes. The main conclusions can be summarized as follows.

First, the results of the CFD simulation were compared with the wind tunnel tests. Both cases showed that high suction occurred near the edge. However there was a discrepancy in the Cp values of both cases near the edge, probably because of the characteristics of the RANS turbulence model. For this study, the realizable k-ε turbulence model was employed, based on reports in the literature. According to the study by Abohela et al. (2013), a comparison of

pressure coefficients of published in-situ measurements, wind tunnel tests and validated CFD simulations (Figure 6.8) revealed similar patterns for both CFD and wind tunnel tests. Thus, the discrepancy in the results of the current study was likely caused by the RANS turbulence model and it is thus necessary to examine the impact of different turbulence models.

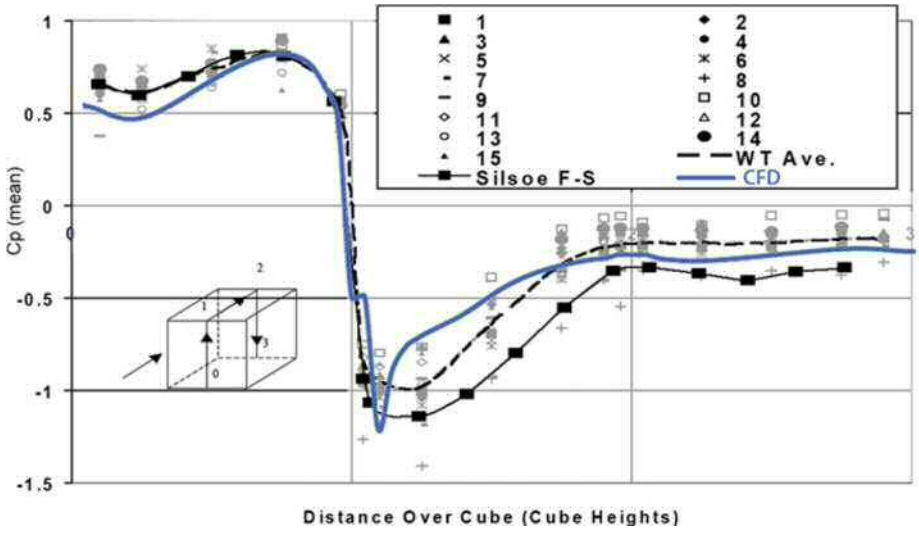

Figure 6.8 - Comparison of pressure coefficients along the centerline of the windward façade, roof and leeward façade with the average of the 15 wind tunnel tests, the Silsoe 6 m cube full scale measurement and CFD simulation (Abohela et al., 2013)

The results of the examination of the impact of different computational domain sizes confirmed that the wind flow behavior was indeed affected by the size of the computational domain. Compared with the reference model, the impact of the shorter upstream length was more significant than the increased blockage ratio. However, all three cases showed only a small change in the Cp values. This seems to indicate that the different computational domains were not highly sensitive to the results of CFD simulation.

6.5. The sensitivity analysis of the impact of the computational grid resolution

6.5.1. Problem statement

With regard to the generation of the computational grid, the discretization method must be specified to ensure that the grid is created in such a manner that it does not cause errors that are too large. This means that its resolution has to be fine enough to capture important physical phenomena such as shear layers and vortices with sufficient resolution (Franke et al., 2007). As mentioned earlier, as the number of cells increases, the accuracy of the simulation also increases but at the cost of extremely high computer memory requirements. Therefore, it is important to determine the optimum size of mesh. Casey & Wintergerste (2000) suggested the analysis of grid sensitivity to ensure the suitability of the mesh in CFD simulations.

Three different discretization methods may be used: the Finite Volume, Finite Difference and Finite Element methods. Among these, the Finite Volume method was selected for this study because it has been widely used in commercial codes and micro-scale obstacle accommodating meteorological models (Franke et al., 2007). With the Finite Volume method, three significantly different grid resolutions were generated for the grid sensitivity analysis in an attempt to reduce both discretization errors and computation time. For the reference model used in the first case study, 682,380 cells were created for the reference model, along with a coarser grid and a finer grid. The grid sensitivity analysis was performed in order to determine how grid density influences the results of the CFD simulation and the impact on the accuracy of the CFD.

6.5.2. Computational domain

As in the first sensitivity test in Section 6.4, a full-scale building in the wind tunnel was modeled. Satisfying the best CFD practice guidelines, the upstream length was 5H and the downstream length was set as 15H, with H as the height of the test building. The vertical and lateral distance from the test building were the same as the wind tunnel. Thus, the domain dimensions of the reference model were L × W × H – 307 ft × 145 ft × 60 ft (93.7 m × 44.2 m × 18.3 m), with a

blockage ratio of 4.5%. In the computational domain, the building of interest was located 26 ft from the inlet boundary.

6.5.3. Computational grid

The grid was created following the recommendations made by Franke et al. (2007) and Tominaga et al. (2008). In addition, the second-order discretization scheme recommended by Franke et al. (2007) was utilized. The grids for the reference, coarser and finer models were constructed entirely of hexahedral cells. The three grids are illustrated in Figure 6.9. The three grids were constructed by increasing the resolution by about a factor of 2 (Ramponi & Blocken, 2012). The grid for the reference model consisted of 682,380 cells, the coarse grid had 98,510 cells, and the fine grid had 1,590,548 cells.

6.5.4. Boundary conditions

The same boundary conditions as used in the first sensitivity test were also applied for the second. At the inlet boundary condition, the measured vertical velocity profile was applied and the turbulence kinetic energy k, and dissipation rate ε were specified. For the outlet boundary conditions, zero static pressure was defined. Symmetry boundary conditions were applied for the sides and the top of the computational domain, which again assumed zero normal velocity and gradients. No-slip wall boundary conditions were applied for the surfaces of the test building in the computational domain.

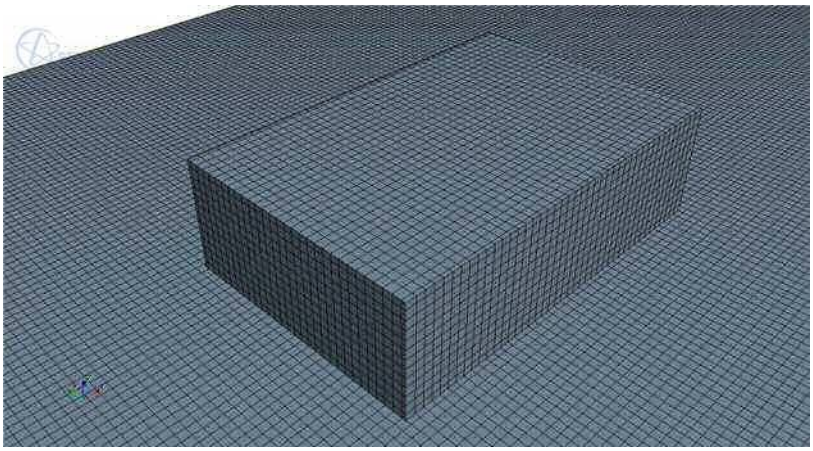

a. The reference model: 682,380 cells

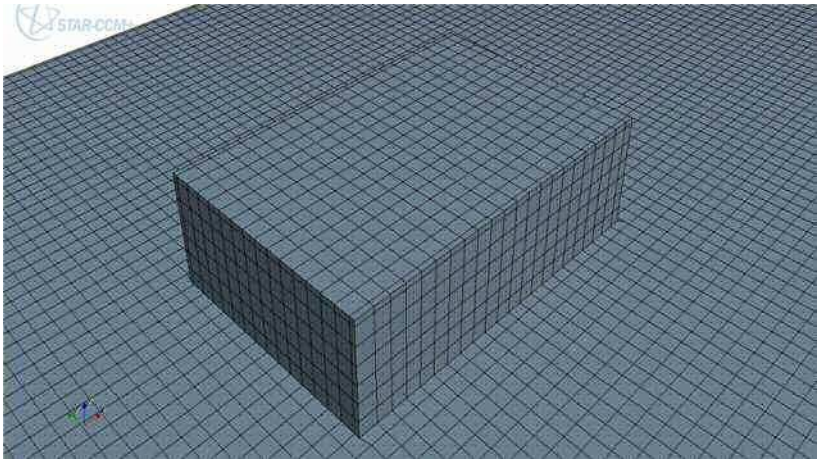

b. The coarse grids: 98,510 cells

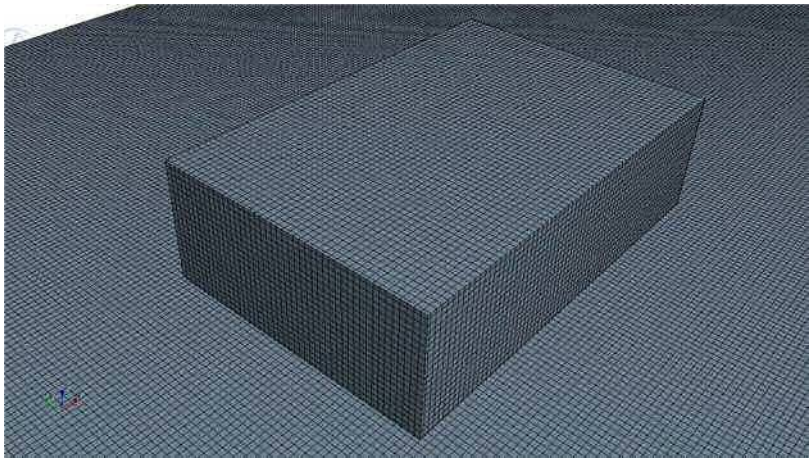

c. The fine grids: 1,590,548 cells

Figure 6.9 - Three different computational grids for grid-sensitivity analysis

6.5.5. Other computational conditions

The commercial code STAR-CCM+ 8.04 was employed for this CFD simulation, along with the 3D RANS equations. The realizable k-ε turbulence model was used for the analysis of wind flow around the building. Steady state calculations were performed using the SIMPLE algorithm with a second-order discretization scheme for convection terms and viscous terms of the governing equations. Convergence was obtained when the scaled residuals reached a minimum of 10^5 for the velocities of x, y, and z, 10^5 for k and ε, and 10^5 for continuity.

6.5.6. CFD simulation results

6.5.6.1 Qualitative comparisons

First, a view of the computations in terms of velocity was analyzed for three grid types. Figure 6.10 compares the mean velocity magnitudes of their vertical cross-sections. This comparative view of the results shows the differences in the velocity field behavior of the three difference grids. In three grids, the wind flow patterns are similar and a large difference was not observed.

Figure 6.11 presents contours of mean velocity magnitudes on the roof surface of each grid. The results of the reference model and fine grid show very similar trends in the velocity field. However, the wind pattern at the upwind region in the coarse grid is different with other cases. In addition to Figure 6.12, the contours of pressure coefficients on the roof surface are compared. Due to the coarsen grid density, the distribution patterns of pressure coefficients are different with the reference and the fine grid.

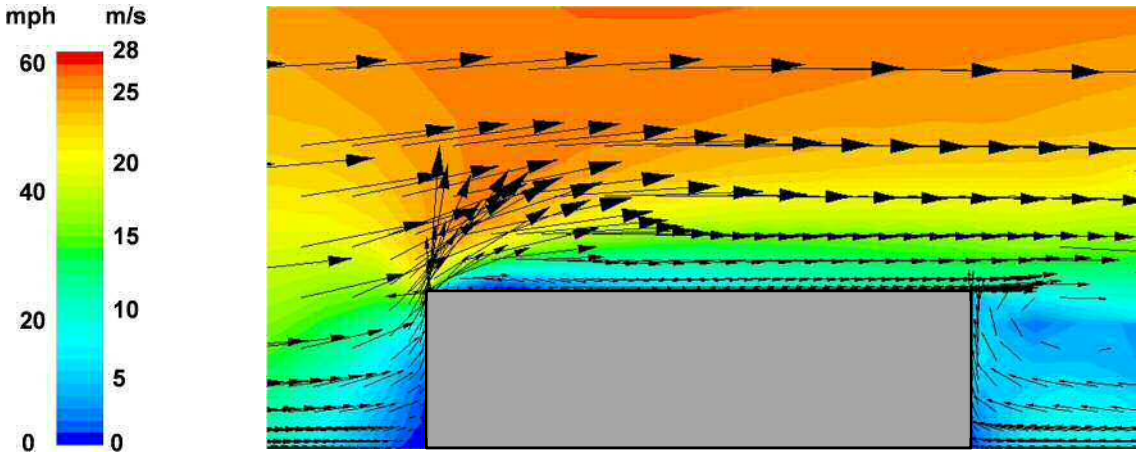

a. The reference model

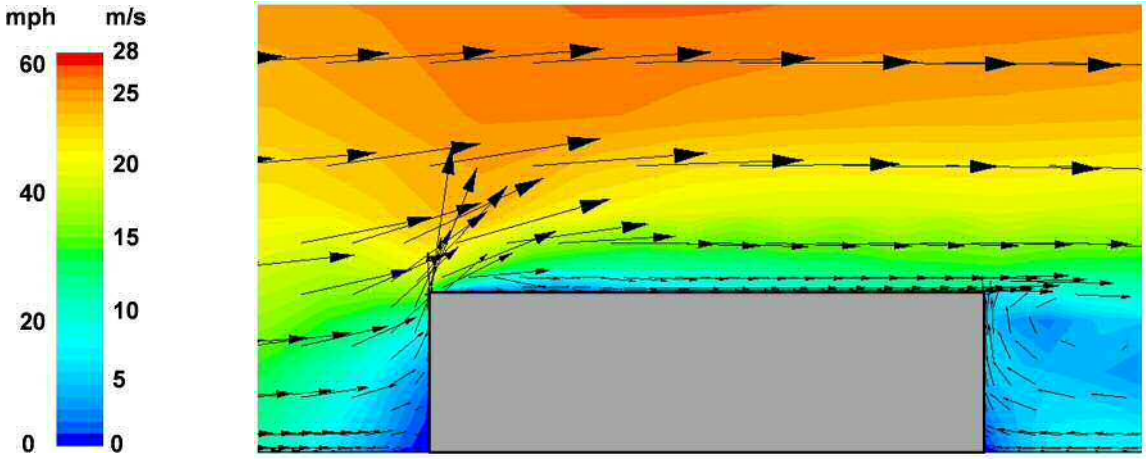

b. The coarse grids

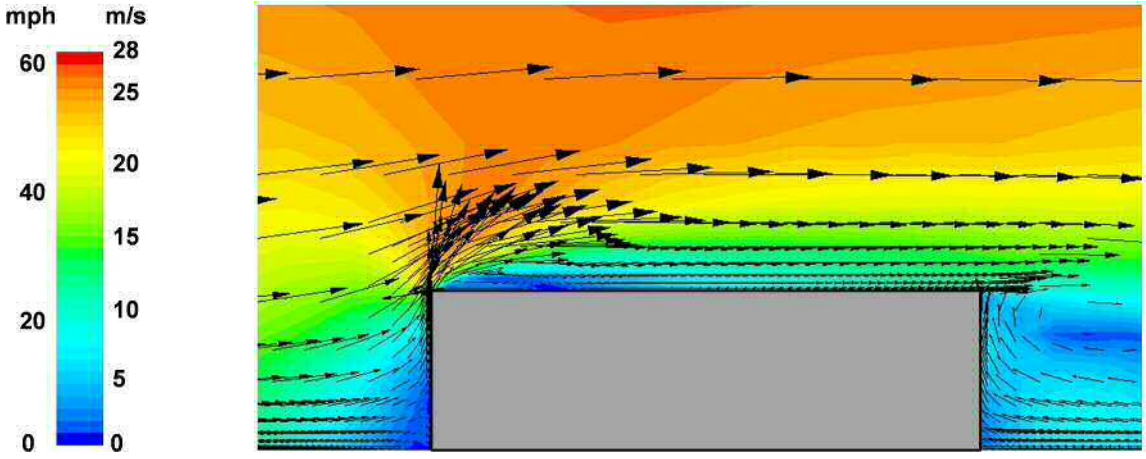

c. The find grids

Figure 6.10 - Contours and vectors of mean velocity magnitude for the middle vertical plan

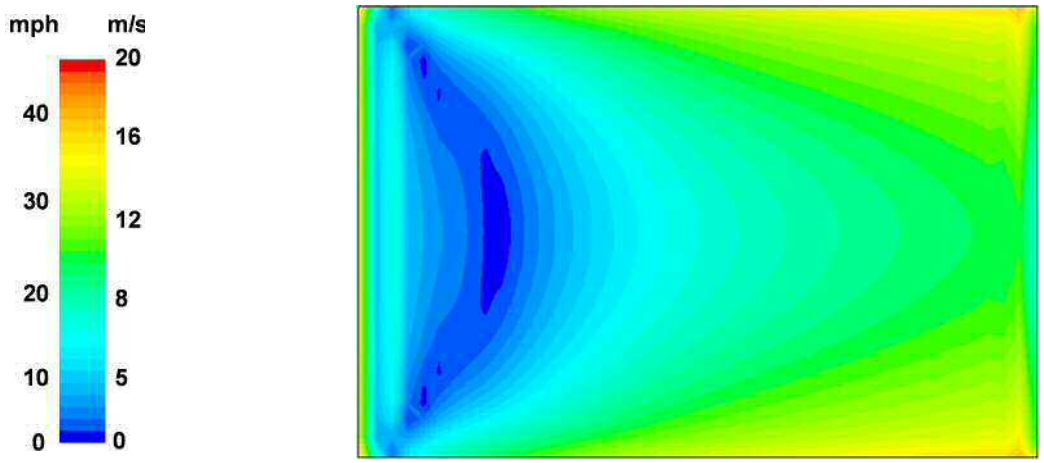

a. The reference model

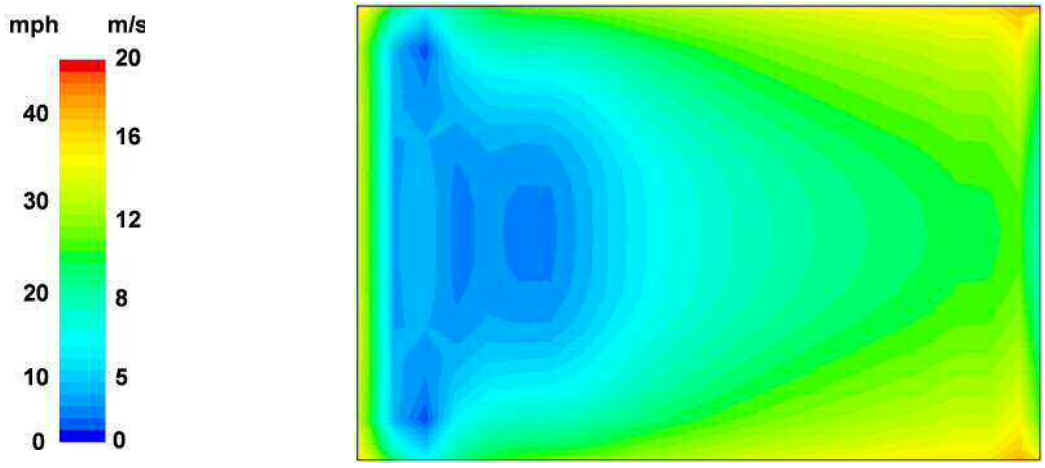

b. The coarse grids

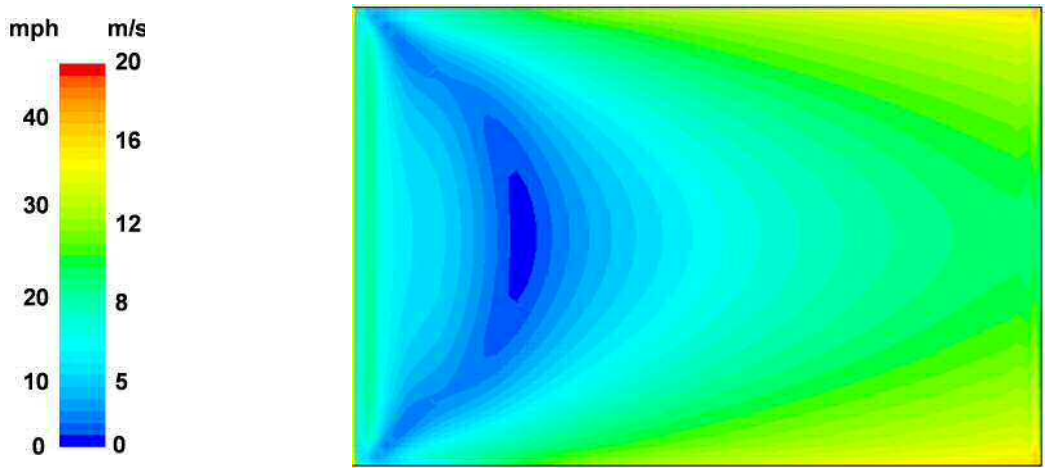

c. The find grids

Figure 6.11 - Contours of mean velocity magnitude on the roof surface

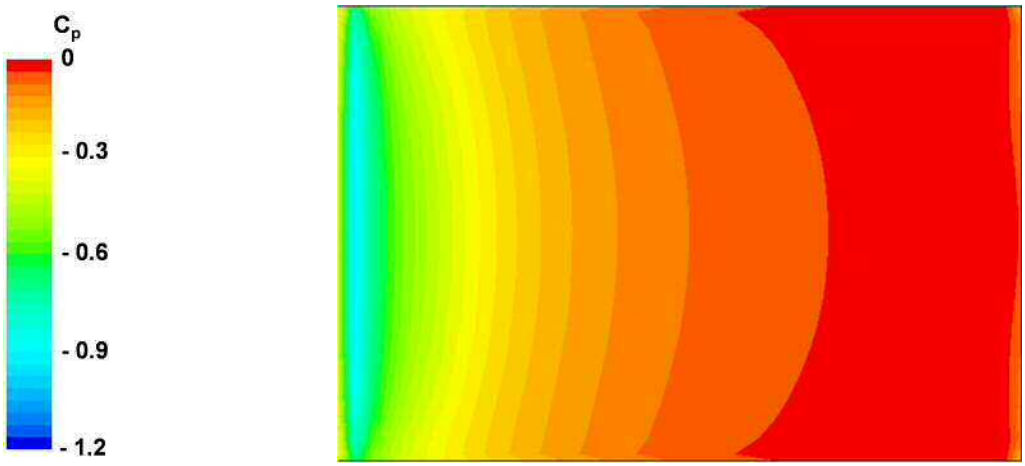

a. The reference model

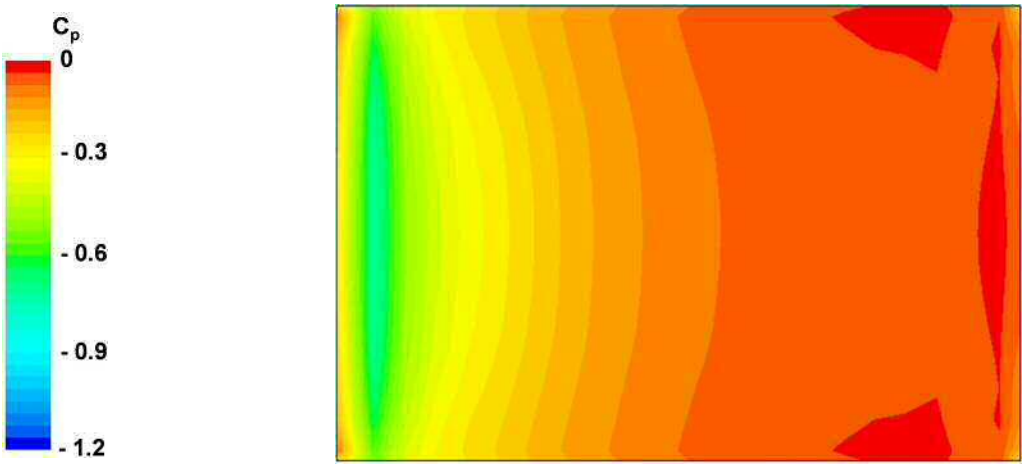

b. The coarse grids

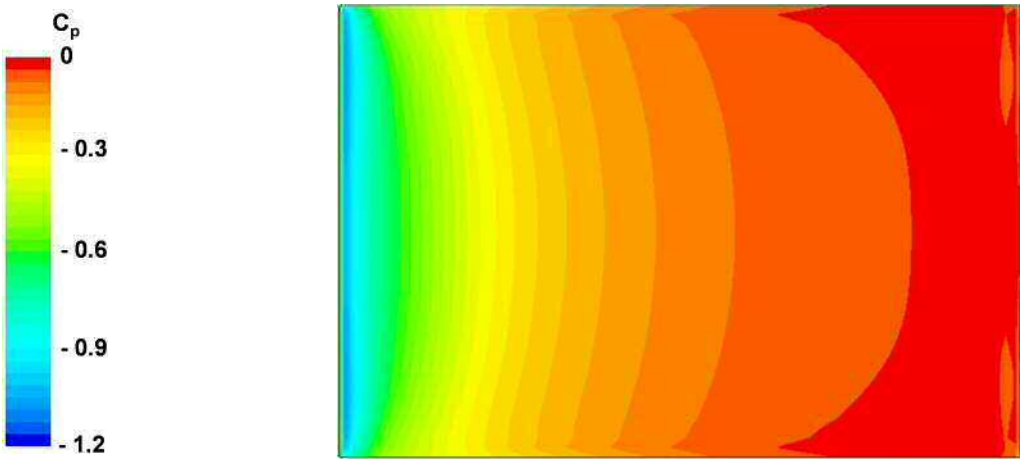

c. The find grids

Figure 6.12 - Contours of pressure coefficients distribution on the roof surface

6.5.6.2 Comparison of the pressure coefficient distributions on the roof surfaces for the three grids

Figure 6.13 compares the pressure coefficient distribution along the centerline of the roof surface obtained from the CFD for the three different grids. The average absolute deviation between the CFD results and the measurements for the center lines is 0.063, 0.15 and 0.062 for the reference, coarse and find grids respectively. Near the edge, the pressure coefficient in the coarse grid was markedly higher than either of the other two. The pressure distribution predicted by the fine grid was very similar to that of the reference grid.

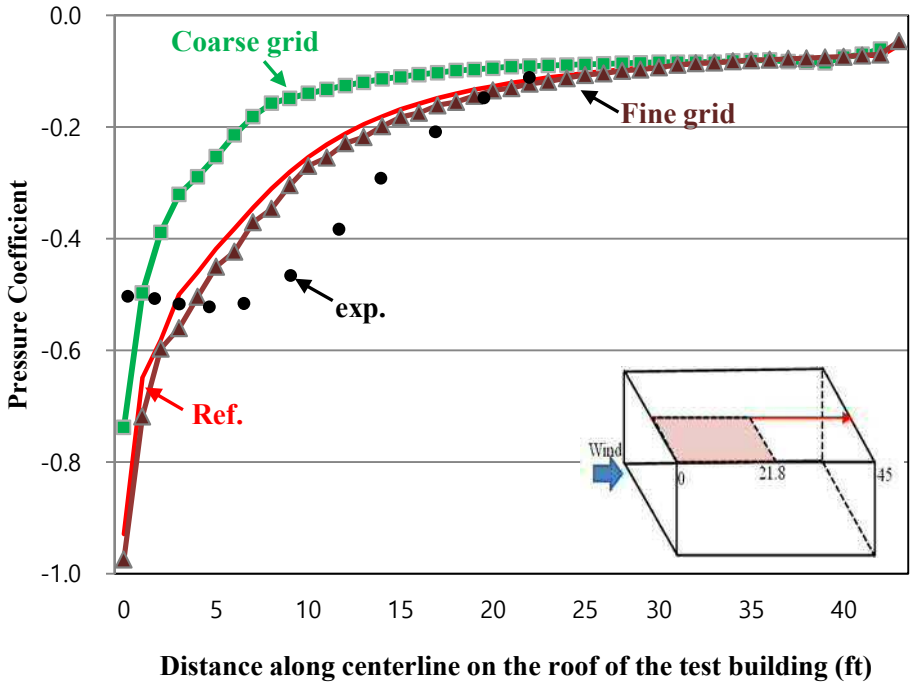

Figure 6.13 - Results of the grid sensitivity analysis: pressure coefficient along the centerline of the roof surface

6.5.7. Discussion

This study focused on an analysis of three grid sensitivities, namely the reference (basic) mesh and a coarser and finer mesh, in order to provide information on how the grid sensitivity influences the CFD results and the choice of an optimum mesh size for CFD simulations. The results showed that the reference and fine mesh were in generally good agreement with the wind tunnel data but the coarse mesh was substantially different. The pressure coefficient distribution for the coarse mesh produced noticeably higher values than either of the others. Although the results for the reference and fine mesh were very similar, the running time for the fine mesh was twice that for the reference grid. Thus, the reference grid was deemed most suitable based on the results of this study.

Predicted wind flow behaviors are clearly influenced by the grid density and special care should therefore be taken to choose a suitable mesh size that will balance computational accuracy and computational cost. Furthermore, it is imperative to perform a grid sensitivity analysis for successful CFD simulations.

6.6. The sensitivity analysis of the impact of turbulence model

6.6.1. Problem statement

Another challenge facing the user of a CFD method is to choose the optimal turbulence model for the application at hand from the various models available. However, it is not possible to specify which model will offer the highest accuracy in advance. In addition, considerable attention should be given to the numerical modeling approach and the required computer power. For example, more complex models are less robust and require many times more computing power than the additional number of equations would indicate. It is not common to provide general rules and recommendations for the selection and use of turbulence models for complex applications (Menter et al., 2002). Casey and Wintergerste (2000) therefore recommended that validation and calibration of the turbulence model with experimental data should be carried out

for all applications and it is also important to consult the published literature regarding the advantages and disadvantages of the model selected.

Considering the statements above, it is necessary to investigate the sensitivity of turbulence models for successful CFD modeling. For this study, three turbulence models including two RANS turbulence models and one LES model were examined and the impact of each investigated. The results of these investigations were analyzed qualitatively using the visualization of mean wind velocity and compared with the pressure coefficient data measured in the wind tunnel experiments. These analyses demonstrated how the different turbulence models influenced the results of the CFD and how they were determined.

6.6.2. The selection of turbulence models

According to Tominaga and Stathopoulos (2010), the selection of the turbulence model has a significant effect on the reproduction of the flow structure around buildings. Many studies have investigated wind flow around a building using the CFD technique. Among these, Tominaga and Stathopoulos (2010) investigated the relationship between the prediction accuracy of the velocity fields around a cubic building for four types of turbulence models: the standard k–ε model, the RNG k–ε model, the k–ε model with Launder and Kato modification and the Realizable k–ε model. They concluded that the RNG k–ε model was the most suitable turbulence model tested, providing results that were in general agreement with the experimental data. Gousseau et al. (2011) employed LES and the RANS standard k–ε turbulence model in their investigation of pollutant dispersion around a building. Through the validation of the two CFD results with wind tunnel measurements, they reported that LES demonstrated a better agreement with the experimental results. In recent studies, Montazeri and Blocken (2013), Blocken et al. (2012), Chavez et al. (2011) and Montazeri et al. (2013) all employed the Realizable k-ε turbulence model in order to predict wind flow or dispersion around a building.

For this sensitivity test, two types of RANS approaches, the standard k–ε model and the Realizable k–ε model, and one LES model were selected. The standard k–ε model was selected because this has been widely used to predict industrial flow problems, while the RNG and the Realizable k-ε models have shown much better agreement with the experimental data (Gousseau et al., 2011; Chavez et al., 2011). Although the RNG k–ε model has shown similar results to the realizable k–ε model, it was not chosen for inclusion in this study because STAR-CCM+ 8.04 does not provide this model (Chavez et al., 2011).

6.6.3. Computational domain

The RANS models and LES model used the same size of the computational domain. Based on the COST Action 732 guidelines (Franke et al., 2007), the domain dimensions were L × W × H – 307 ft × 145 ft × 60 ft (93.7 m × 44.2 m × 18.3 m) and its blockage ratio was 4.5%.

6.6.4. Computational grid

In the present study, the computational grids consisted solely of hexahedral cells, as recommended by Franke et al. (2007) and Tominaga et al. (2008). RANS and LES were applied on the same computational grid. As in the first and second studies, the grid was composed of 682,380 cells.

6.6.5. Boundary conditions

For both RANS and LES, the profiles of mean velocity, turbulent kinetic energy, and turbulent energy dissipation rate were prescribed at the inlet boundary condition based on the wind tunnel experiments. A 1/7 power-law was assumed for the profiles of mean velocity at the inlet of the domain and a turbulent kinetic energy k and turbulent energy dissipation rate ε were specified. Symmetry boundary conditions were used at the top and lateral boundaries. At the outlet of the domain, zero static pressure was applied. All building surfaces were specified as smooth, no-slip walls.

6.6.5.1. Parameters for LES

In LES, it is important to determine a suitable time step size and this is limited by the dimensions of the smallest cells. In this sense, the large dimensions of the domain need a long averaging time to obtain a statistically-steady solution. Several "flow-through" time units were therefore used: T – L / U_{ref}, where L is the domain dimension in the streamwise direction and U_{ref} is the reference velocity (Gousseau et al., 2011).

The LES calculations were initialized with the solution from the standard k-ε simulations. In order to achieve the initial conditions, the steady state calculation was first performed using the standard k-ε model. Once sufficient convergence was obtained, the turbulence model was changed to LES and the unsteady calculation started (Kobayashi et al., 2013). For this study, the time interval was 2.0×10^{-4} s, calculated for 35,000 time steps in total.

6.6.6. Other computational conditions

The commercial code STAR-CCM+ 8.04 was also employed for this CFD simulation with the 3D RANS models and LES. Both the RANS and LES models were performed using the SIMPLE algorithm. For discretization schemes, a second-order discretization scheme for convection terms and viscous terms of the governing equations was applied for the RANS model, while a central differencing scheme was used for LES. In addition, the Dynamic Smagorinsky Subgrid Scale model was employed to calculate the subgrid scale in the LES model. In the case of the two RANS models, with the standard k-ε and the realizable k-ε, convergence was obtained when the scaled residuals reached a minimum of 10^5 for velocities of x, y, and z, 10^5 for k and ε, and 10^5 for continuity. For LES, all the scaled residuals reached a minimum of 10^5, after which the calculation was terminated.

6.6.7. CFD simulation results

6.6.7.1 Qualitative comparisons

The results are shown in Figures 6.14 - 6.16. In Figure 6.14, the mean velocity magnitudes of vertical cross-section for each turbulence model are presented. As opposed to the two RANS model, the reversed flows on the roof at upwind region were observed in LES model.

In addition, contours of pressure coefficients distribution and mean velocity on the roof surface were shown in Figure 6.15 and Figure 6.16. While the velocity field of two RANS models including the realizable k-ε model and the standard k-ε model showed very similar trends, the LES model exhibited completely different patterns in both velocity and pressure field.

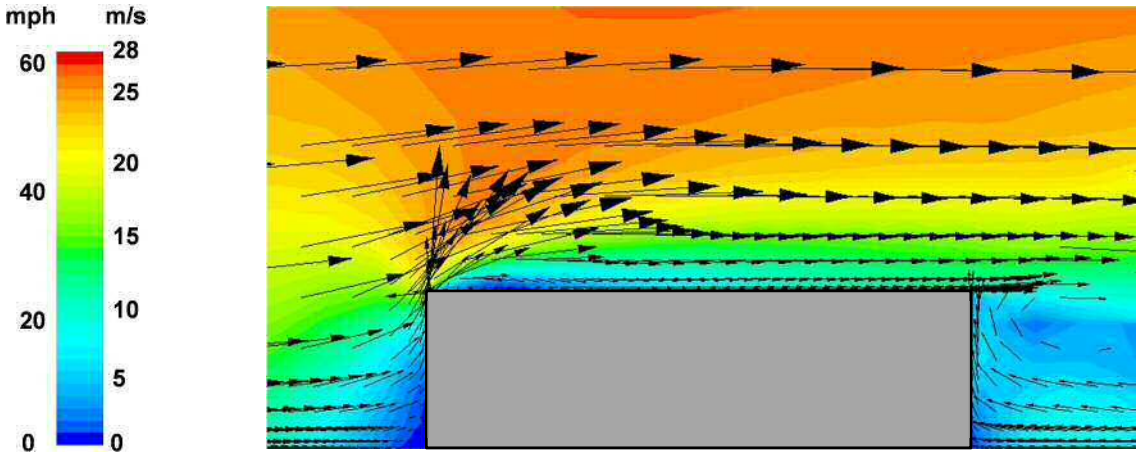

a. The reference model: the Realizable k-ε turbulence model

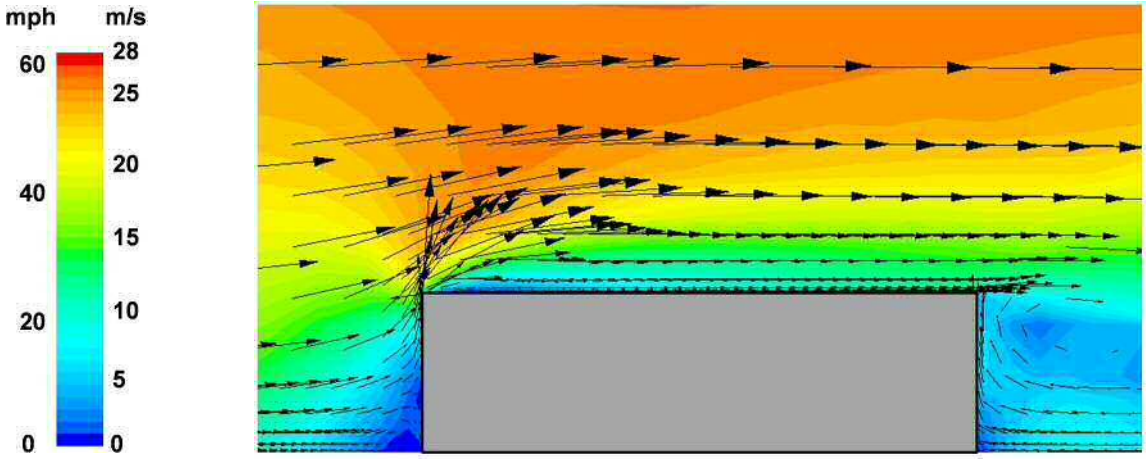

b. The Standard k-ε turbulence model

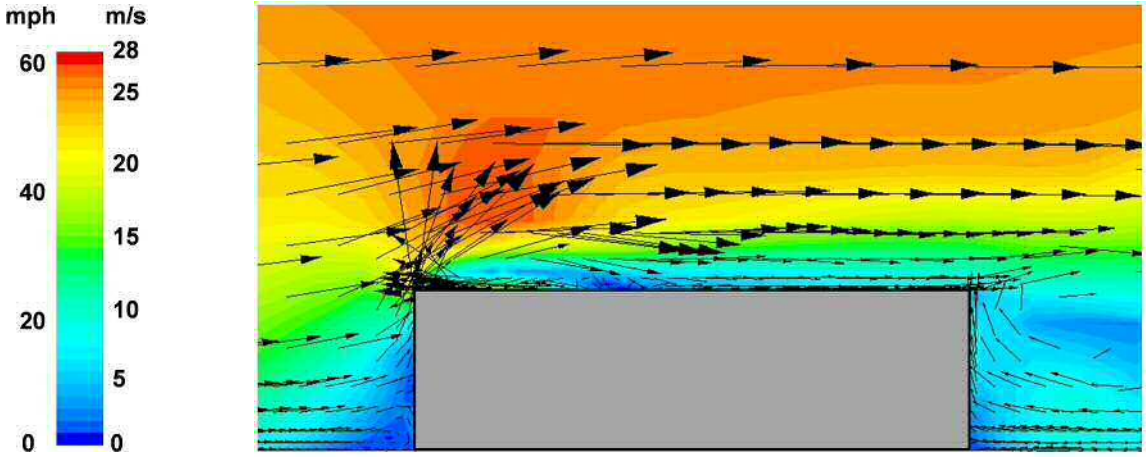

c. The LES model

Figure 6.14 - Contours and vectors of mean velocity magnitude for the middle vertical plan

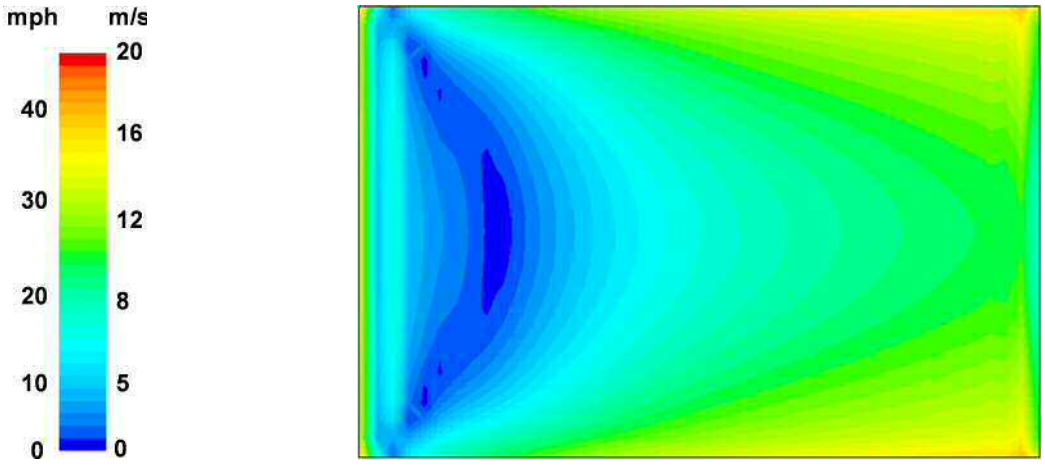

a. The reference model: The Realizable k-ε turbulence model

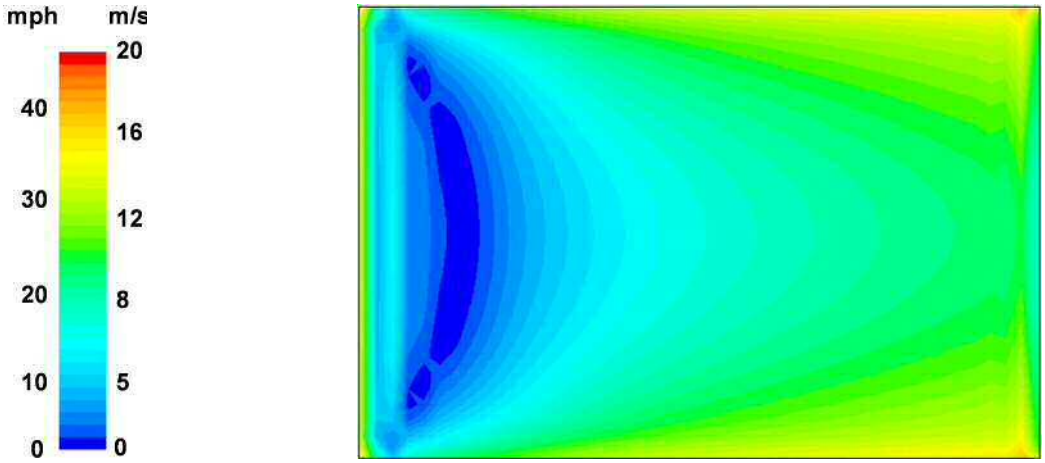

b. The Standard k-ε turbulence model

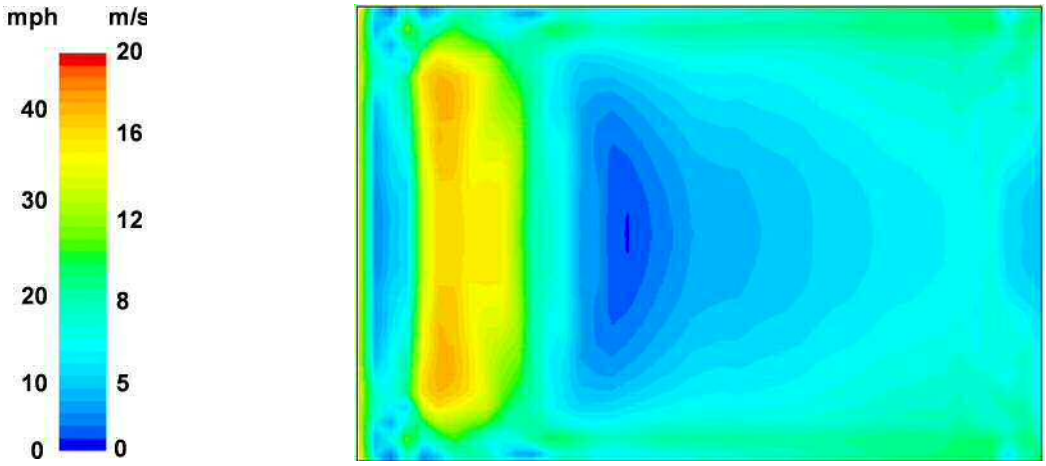

c. The LES model

Figure 6.15 - Contours of mean velocity magnitude on the roof surface

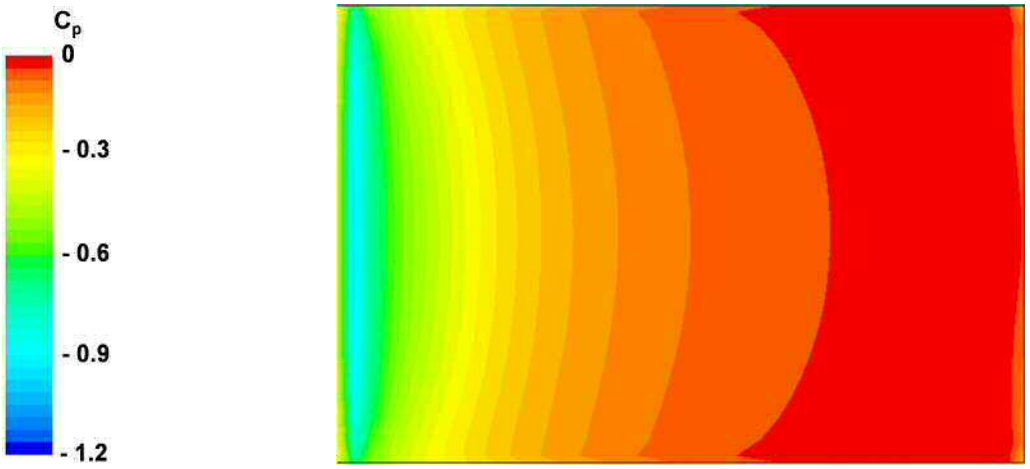

a. The reference model: The Realizable k-ε turbulence model

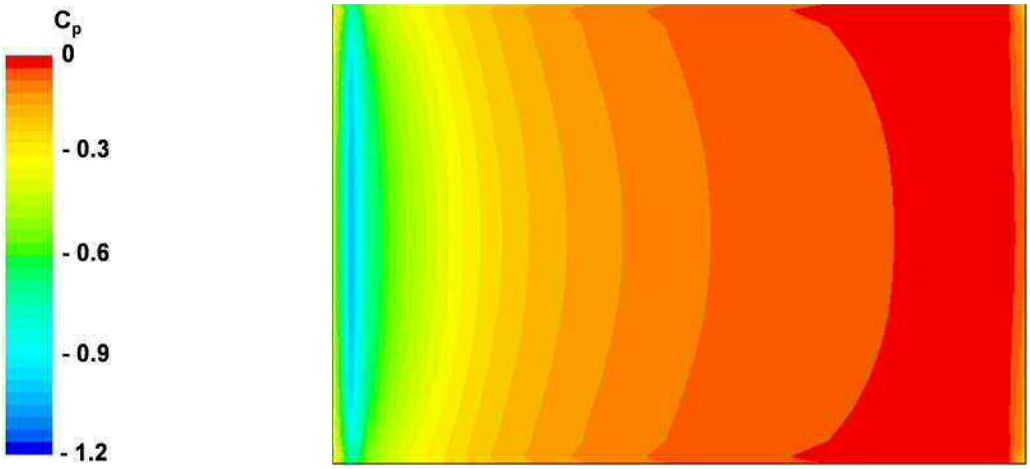

b. The Standard k-ε turbulence model

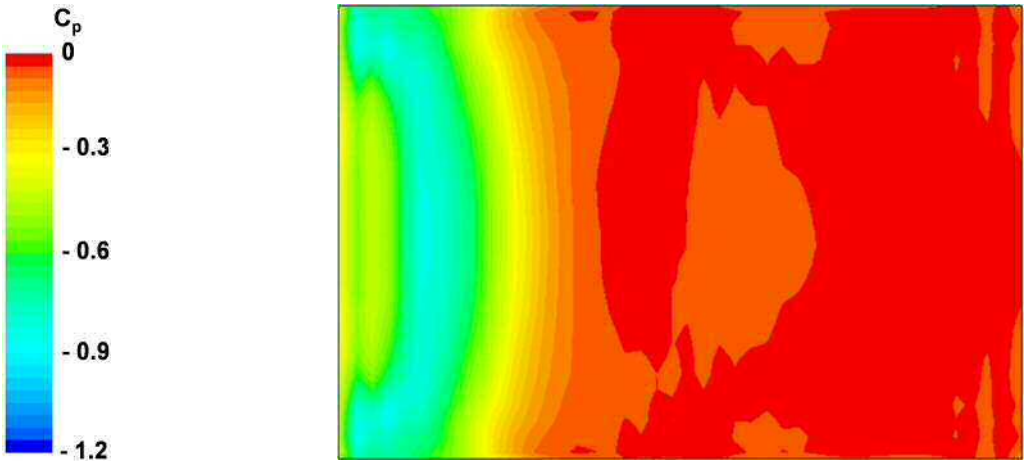

c. The LES model

Figure 6.16 - Contours of pressure coefficients distribution on the roof surface

6.6.7.2 Comparisons of pressure coefficients on the roof surface for the three turbulence models

Figure 6.17 compares the pressure coefficients along the centerline of the roof surface for the three turbulence models. The average absolute deviation between the CFD results and the measurements for the center lines is 0.063, 0.076 and 0.036 for the reference, standard k-ε and LES respectively. While LES showed somewhat higher values for the pressure coefficients near the edge than the experimental data, it still showed the best overall agreement with the experimental results among the three turbulence models tested in this case study. As in the first sensitivity tests in Section 6.3., the realizable k-ε turbulence model tended to overestimate the pressures near the edge and the standard k-ε turbulence models showed similar results.

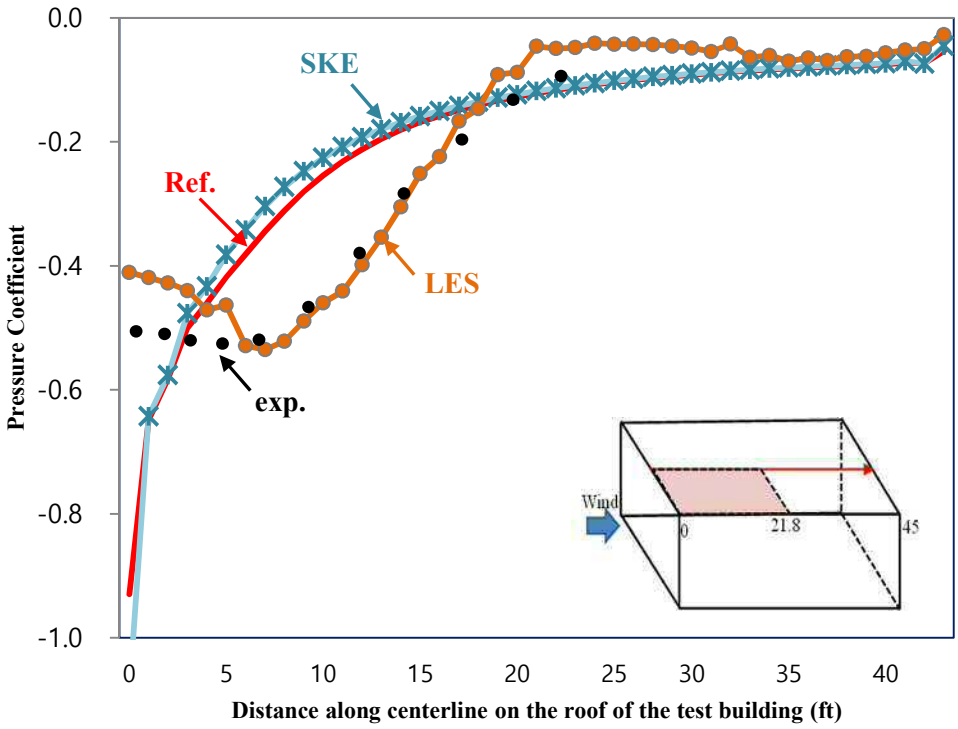

Figure 6.17 - CFD simulation results: Impact of turbulence models on the pressure coefficients along the centerline of the roof surface

6.6.8. Discussion

CFD simulations for wind flow around a building were conducted with three different turbulence models: two RANS models, standard k-ε and realizable k-ε, and one LES model that used the dynamic Smagorinsky SGS model to calculate the subgrid scale. This study focused on the wind flow field on the roof surface for the three different turbulence models.

LES gave better results than either of the two RANS turbulence models but was approximately 40 times more demanding in terms of computational cost than the RANS models when PC with 64bit, 8GB RAM and CPU 2.5GHz was applied. The same grid was used for all three.

6.7. Summary of the sensitivity analysis

The three sensitivity tests described above investigated the impact of computational parameters on the CFD modeling process. The CFD modeling conducted for each study reproduced experiments conducted at the wind tunnel test facility at the IBHS to investigate the sensitivities of three parameters: the size of the computational domain, the grid density and the selection of turbulence models. The findings of the three studies were as follows:

1) The computational domain
- The computational domain was created using recommendation by the best practice guidelines (Franke et al., 2007; Tominaga et al., 2008).
- The pressure distribution of the reference case was found to more closely replicate the experimental results than either of the other two domain sizes tested. The results for the domain with the decreased upstream length showed a better agreement with the experimental data than the domain with the decreased blockage ratio.

2) Grid generation
- Based on the recommendations in the best practice guidelines, the grids constructed consisted entirely of hexahedral cells.

- The grid sensitivity analysis revealed that the difference between the results obtained for the fine and reference meshes was only about 10%. Given that the fine grid required considerably more computing resources, the reference grid was therefore selected.

3) Turbulence model

- As a result of the analysis of the impact of three different turbulence models, the LES model showed a better agreement with the experimental results than either of the two RANS approaches tested. However, it also required considerably more computing time and resources.
- Among the RANS approaches, the results of two RANS models including the realizable k-ε model and the standard k-ε model showed very similar but the standard k-ε model more overestimated wind flow near the edge than the realizable k-ε model. Thus, the realizable k-ε turbulence model is preferred to predict wind flow around a building.

6.8. Computational parameters for wind flow around building through research process

As mentioned in Chapter 1, CFD process is complex and various calculation conditions must be set by the user. Thus, careful consideration must be given to the selection of computational parameters. For this present study, the design objective is the CFD analysis of wind flows around buildings. In the early design stage, computational parameters were specified through the review of best practice guidelines, the analysis of journal articles and the sensitivity analysis. The computational parameters are summarized in table 6.1.

Table 6.1 - A summary of computational parameters for wind flow around buildings through the research process

What level of detail in the geometrical representation of the buildings is needed?	- The central region of interest is reproduced as accurately as possible (the area of a radius 1 -2 H from the building of interest, when H is the height of the tallest building) - Buildings located away from the region of interest are represented by simple blocks. - At least one additional street block in each direction around the central region of interest is represented.
What is the proper size of the computational domain?	- 5H and 15H are recommended for the upstream and downstream length respectively - 5H for the height of the domain - 10H+w (where w is the building width) for the lateral length
What is the appropriate the type of computational grid and grid resolution?	- Hexahedral meshes are generally used but a tetrahedral mesh can be used in a case of urban environments. - At least 10 cells per cube root of building volume can be used as the minimum grid resolution.
What is the appropriate boundary conditions including inlet, outlet and the top and sides?	- For the inlet, the mean velocity profile by logarithmic law or power law and turbulence information is needed. - For the outlet, a zero static pressure condition is used. - For the sides and tops, symmetry conditions can be used. - The standard wall functions are imposed at wall boundaries.
What is the proper turbulence model?	- The LES showed the most accurate result. - The RANS turbulence models can be also used.
What is the proper range for the convergence criteria?	- All the scaled residuals leveled off within the range of $10^4 – 10^6$.
What other parameters are considered?	- For algorithm and scheme, the SIMPLE algorithm and second-order discretization schemes can be used.

7. IMMERSIVE CASE STUDY

7.1. Introduction

Generally, wind flow around buildings creates both negative and positive fluctuations over a roofing system and these pressures are dynamic. In addition, the pressures can be separated into static and fluctuating components. Due to vortex flow and separations, the wind pressure distribution varies spatially over a roof and it can cause high suction at the corner and perimeter. These high intermittent suctions could make the roofs susceptible to uplift and detachment. Thus, the roof design must account for these situations that could occur from high winds (Baskaran et al., 2007).

In an effort to resist wind fluctuation that can cause roof uplift failures, the roof vent system was developed by Dr. Demetri Telionis, Dr. Jim Jones and Dr. Elizabeth Grant of Virginia Tech and marketed by Acrylife®. For this roof vent system, it can eliminate the pressure variation that causes the upward suction during high wind conditions creating a negative pressure zone underneath the roof membrane. In addition, the performance of the roof vent system is highly affected by its position. (Dockins & Tankersley, 2009). In order to determine layout of the roof vent system, it is important to understand pressure and velocity on the roof surface.

Figure 7.1- Prototype of the roof vent system (Grant, 2003, p. 35)

The case studies reported in this chapter investigated the effect of design parameters such as building height, aspect ratio and parapet height on the wind flow over the roof of a low-rise building. While wind flow over the roof of a low-rise building has been generally tested using wind tunnel testing and it provides reliable results, the cost is relatively high when compared to numerical simulations and the number of parameters that can be tested is limited. In this study, CFD was employed to investigate the effects of several different building configurations in order to inform the design of low-rise buildings and to provide information such as the length of the wind reattachment for roof vent systems.

Based on best practice guidelines, an analysis of journal articles and the sensitivity analysis, a set of computational parameters were chosen for this study of wind flow around buildings. For the case study, these computational parameters were reselected for the investigation of wind flow over the roof because detailed information on both velocities and pressures are needed. All case studies were designed to respond to the design parameters, specifically building height, building aspect ratio, and parapet heights. In describing the scope of each case, the researcher immersed himself into each case study and observed the entire CFD modeling process for wind flow over the roof of a low-rise building.

7.2. Preparation for input computational parameters

As mentioned in Chapter 1, CFD simulation is a powerful tool in the development of building design. However the simulation process is still very challenging. Thus, it is important to select the right simulation models carefully. Moreover, the computational parameters should be assessed iteratively in order to achieve the maximum results. This section presented preparation for the selection of the computational conditions for case studies.

7.2.1. The selection of the turbulence model

During CFD processes, one of the most important steps is to select the proper turbulence model. As mentioned in Chapter 6, the turbulence models based on the RANS approach can be generally

applied to the prediction of wind flow around building and the LES model can provide more accurate result than the RANS turbulence models.

For the case study, the impact of design parameters such as building height, aspect ratio and parapet height was investigated in order to provide information for the proper layout of the roof vent systems. While the turbulence models based on the RANS approach provide easier approach, their results provide overestimated wind flow on the roof. In order to compare the differences between the LES model and the turbulence model based on the RANS approach, these two turbulence models were applied to a building with height 36 ft, aspect ratio 1:2 and parapet wall height 42 inch. Figure 7.2 showed the result of contours and vectors of the mean velocity magnitude for the middle vertical plane of a building when the turbulence model based on the RANS approach was applied. As mentioned in Chapter 6, the turbulence model based on the RANS approach cannot reproduce the wind flow near the edge. Thus, the LES model was recommended for this case study.

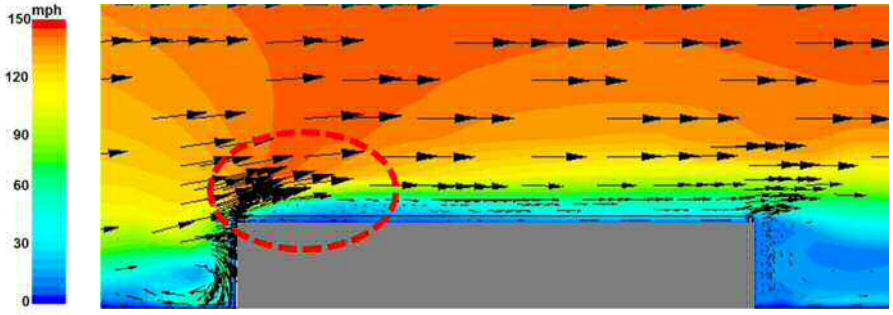

Figure 7.2 - The result of contours and vectors of the mean velocity magnitude for the middle vertical plane of a building when the RANS turbulence model was applied

7.2.2. The selection of the geometry

For the geometry, two different roof surface areas were suggested: 50,000 ft^2 and 150,000 ft^2. These two roof surface areas with a low rise building with height 36 ft, aspect ratio 1:2 and parapet wall height 42 inch were applied into the computational domain using the recommendations described in Chapter 6. The grid for these two models consisted of hexahedral

meshes with a grid resolution of 723,580 cells for the roof surface area 50,000 ft^2 and 1,870,000 cells for the others. As described in Section 6.5, as the number of cells increases, the cost of high computing resources are required. For calculating time, approximately 350 hours were required for the case with the roof surface area 50,000 ft^2. In the other case with the roof surface area 150,000 ft^2, the calculation took approximately 500 hours but the result was not sufficiently accurate. As shown in Figure 7.3, the result of the roof surface area 150,000 ft^2 showed that the wind flow in flow direction was not fully calculated. Considering the computer resources and run-time of the simulation, the geometry of the roof surface area 50,000 ft^2 was applied for the case study.

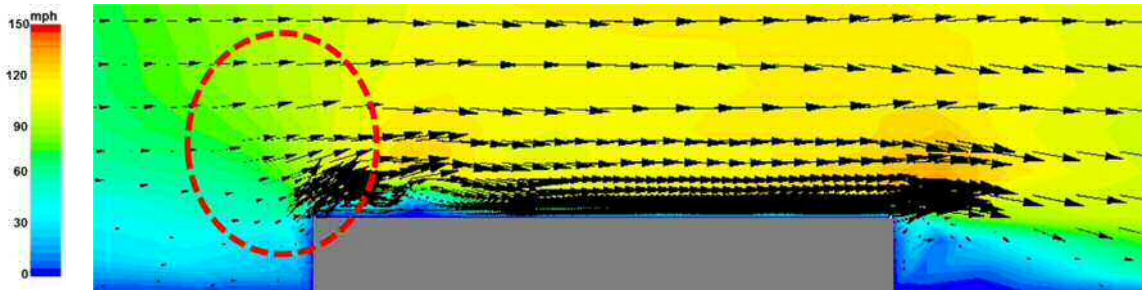

Figure 7.3 - The result of contours and vectors of the mean velocity magnitude for the middle vertical plane of a building with the roof surface area 150,000 ft^2

7.2.3. Other computational parameters

Other computational parameters such as boundary conditions utilized the benchmark data provided by the wind tunnel tests at the IBHS (Chapter 5) and the sensitivity analysis (Chapter 6). For example, the velocity profile for the inlet boundary condition was specified using power law with an exponent of 0.143, which corresponds to an open land surface. In addition, the wind speed was 60 mph which was the same conditions as the wind tunnel testing at the IBHS. For case studie, a wind angle of 0 degrees was considered because of the large cost of the required LES model. Once cases with the wind angle of 0 degrees are completed, the various wind angles of 30 degrees, 45 degrees, 60 degrees will be tested for further research.

7.3. Case study A: An investigation of wind flow over a flat roof for two different building heights

7.3.1. Introduction and context

For this case study, wind flow over the roof of a low-rise building with two different building heights was investigated. As shown in Figure 7.4, the reference building with a height of 36 ft and the other building with a height of 12 ft were created. For both buildings, the flat roof surface area was 50,000 ft^2 and the building aspect ratio which is the ratio of width to length was 1:2. In addition, a parapet wall with a height of 42 inch was considered for both buildings. A wind speed of 60 mph was used for the inflow condition in the CFD simulations.

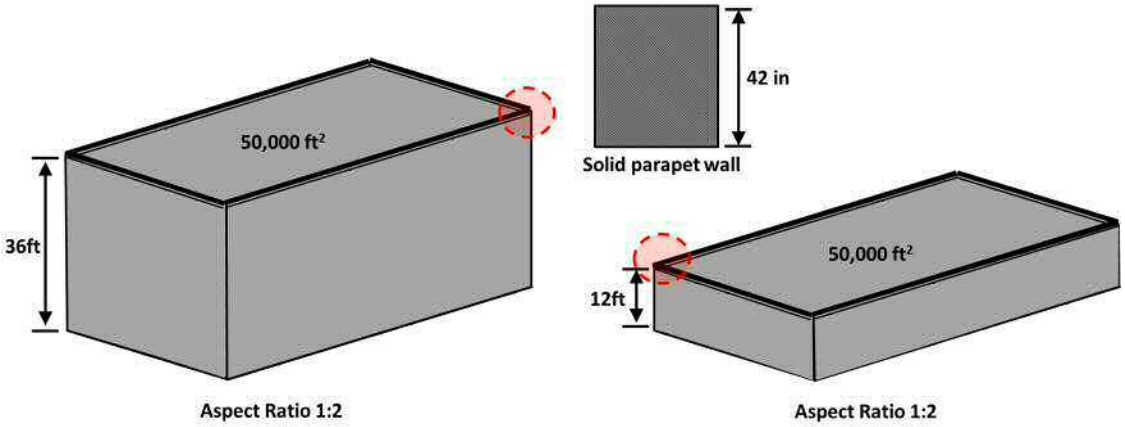

a. Reference model: Height=36 ft b. Building with height=12 ft

Figure 7.4 - Two different building height

7.3.2. Computational domain

For this case study, two computational domains were created using the recommendations obtained through the research. The dimensions of the two computational domains are described in Figure 7.5. For the reference model, the domain dimensions were L × W × H – 880 ft × 676 ft × 180 ft and the blockage ratio was 9%. The computational domain size for the other building with the height 12 ft was L × W × H – 636 ft × 676 ft × 60 ft. For this building, the ratio of the

lateral extension of the computational domain to its height was assumed to be similar to the corresponding ratio of the building because the lateral direction was much larger than the height (Franke et al., 2007).

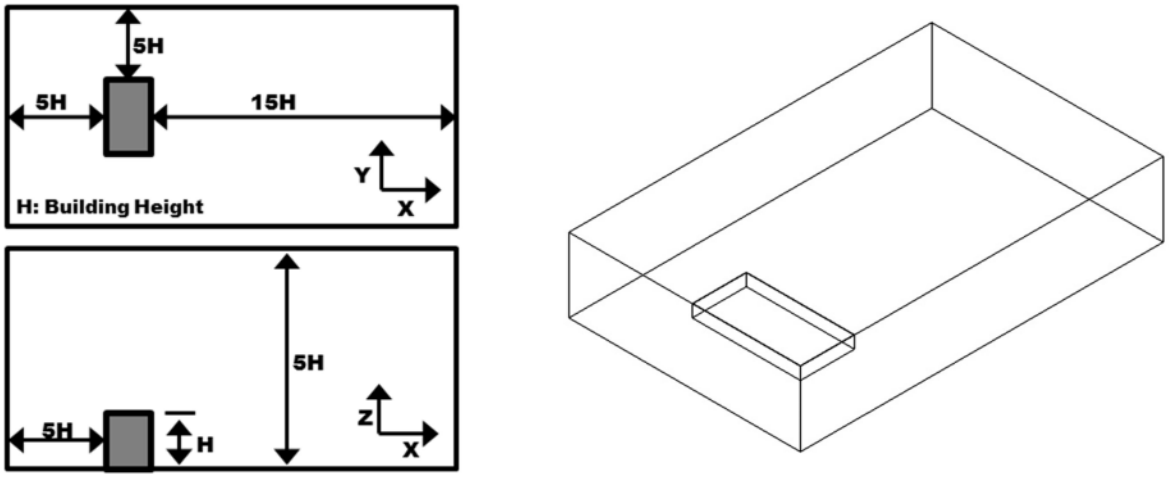

a. Reference model (building height: 36 ft)

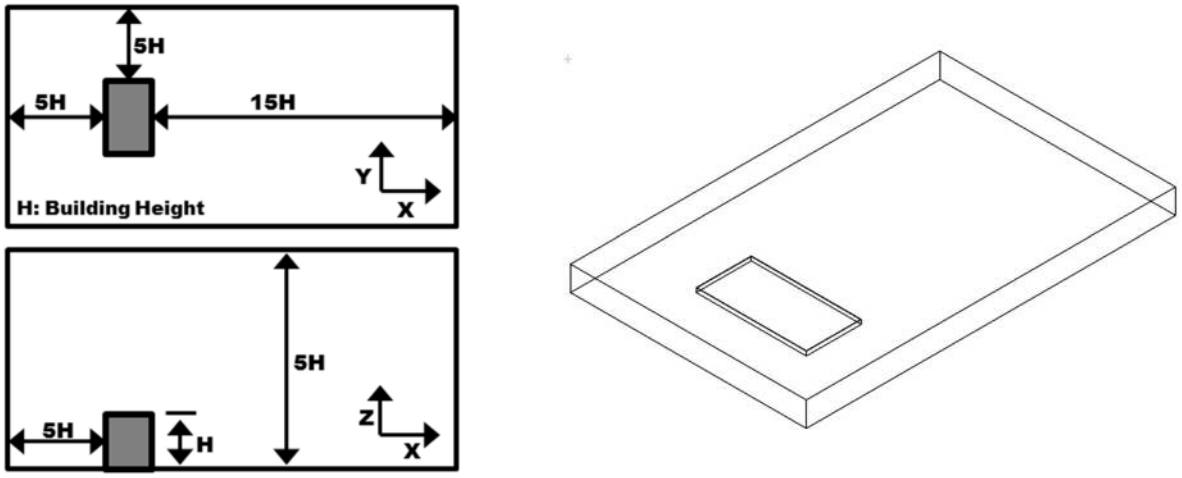

b. The 12 ft high building

Figure 7.5 - The two different computational domains

7.3.3. Computational grid

The grid for these two cases consisted solely of hexahedral meshes, as shown in Figure 7.6. Since significant information regarding the details of turbulent flow over the roof surface is needed, hexahedral grids were employed. For the gird resolution, the base size of the grid was based on the smallest length scale of the building. For both models, the base size for grid generation was based on the parapet wall height. As described in Section 6.5, coarser and finer grids were constructed. However, more than 1,000,000 grids required considerably higher computing resources (See Section 7.2). Thus, a grid resolution of 723,580 cells for the reference model and 842,940 cells for the other was selected.

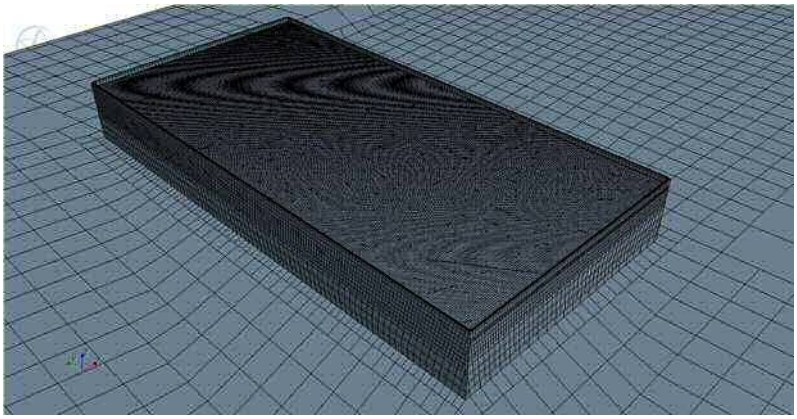

a. Computational grids for the reference model

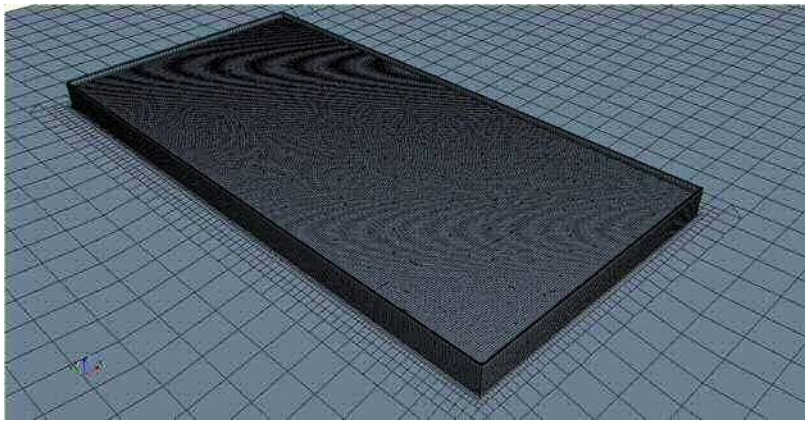

b. Computational grids for the 12 ft high building

Figure 7.6 - The computational grids

7.3.4. Boundary conditions

As mentioned previously, the experimental data should be specified for the inlet boundary conditions. However, the measurement data was not available for this case study so the inlet velocity profile was defined using the power law with an exponent of 0.143, which corresponds to an open land surface. The velocity at a height of 33 ft was 60 mph.

For other boundary conditions such as the top, sides and outlet condition, the same boundary conditions as those used in Chapter 6 were applied because the simulation settings of the case study was similar to those of CFD modeling in Chapter 6. Symmetry boundary conditions were applied for the sides and the top of the computational domain. For the outlet condition, a static pressure of zero was defined. Within the computational domain, no-slip wall boundary conditions were applied for the surfaces of the building.

7.3.5. Other computational parameters

The commercial code STAR-CCM+ 8.04 was employed for this CFD simulation with the 3D RANS equations. The LES model was used for this analysis because it offers a useful way to predict wind flow distributions over the roof surface. As described in Chapter 6, the same conditions for the LES model were applied. The SIMPLE algorithm with a central differencing scheme was employed. In order to calculate the subgrid scale in the LES model, the Dynamic Smagorinsky Subgrid Scale model was used. The LES calculations were initialized with the solution from the standard k-ε simulations. For the initial conditions, the steady state calculation was first performed using the standard k-ε model. Once sufficient convergence was obtained, the turbulence model was changed to the LES model and the unsteady calculation started (Kobayashi et al., 2013). For this study, the time interval was 2.0×10^{-4} s, calculated for 50,000 time steps in total. When all the scaled residuals reached a minimum of 10^{5}, convergence for the LES model was obtained.

7.3.6. CFD simulation results

7.3.6.1 Qualitative comparisons

First, the results of the computations in terms of velocity were analyzed for two cases. Figure 7.7 shows a comparison of the predicted mean velocity magnitude for the middle vertical plane and on the roof surface. According to this comparative view of the results, the wind flow patterns in the two cases are similar. For the reference model, the upwind flow near the edge is stronger and the length of the wind reattachment is shorter than for the other case.

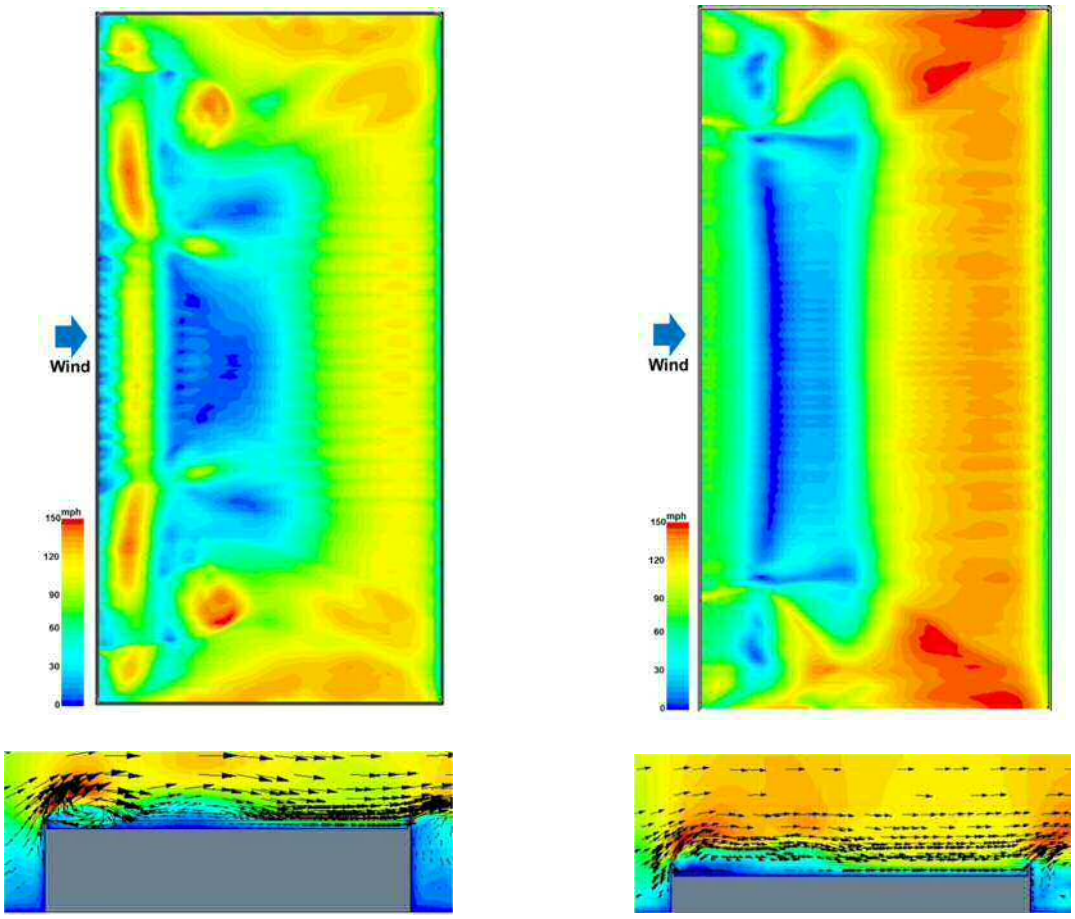

a. The reference model b. The 12 ft high building

Figure 7.7 - Contours and vectors of mean velocity magnitude on the roof and for the middle vertical plane

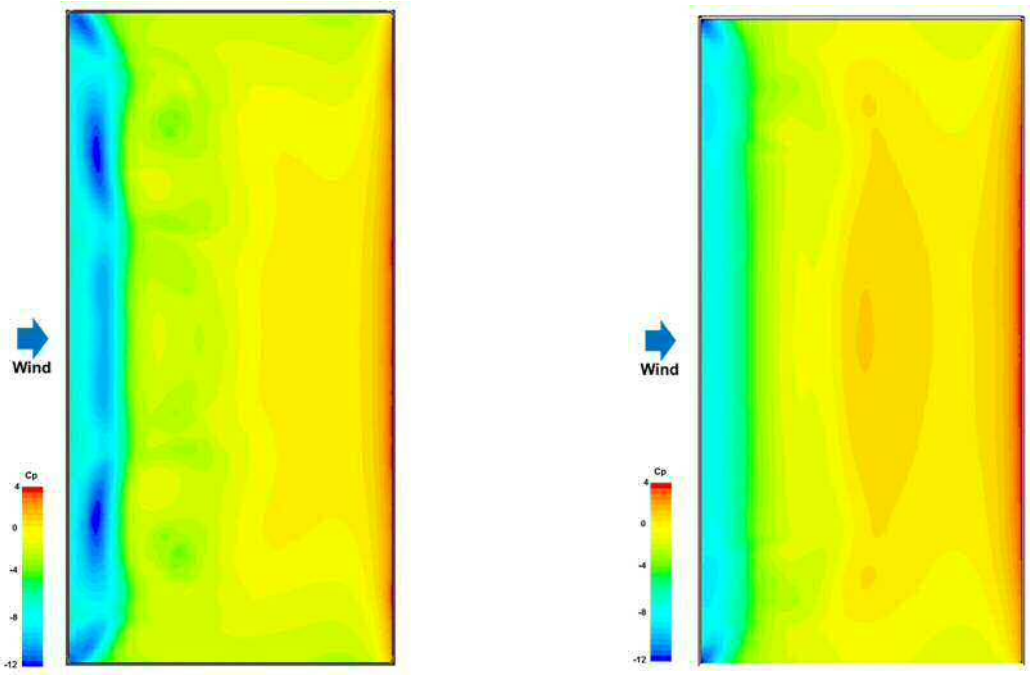

a. The reference model b. The 12 ft high building

Figure 7.8 - Contours of pressure coefficients on the roof

Figure 7.8 shows the contours of the pressure coefficient distribution on the roof surface for each case. Similar to the comparisons in Figure 7.7, the results for the reference model predict lower pressure coefficients near the edge than for the other case.

7.3.6.2. Comparisons of pressure coefficient distributions on the roof surfaces

As shown in Figure 7.9, the CFD results for the reference model were compared with the results for the building with a height of 12ft. For both cases, high suction values were observed near the edge, decreasing rapidly as it progressed along the centerline. While the highest suction for the reference model was observed 62 ft in from the edge, the suction for the other case was highest 32 ft from the edge. Both Cp values were the same at the middle of the roof surface. These results clearly indicate that differences in building height influenced the wind flow over the roof surface.

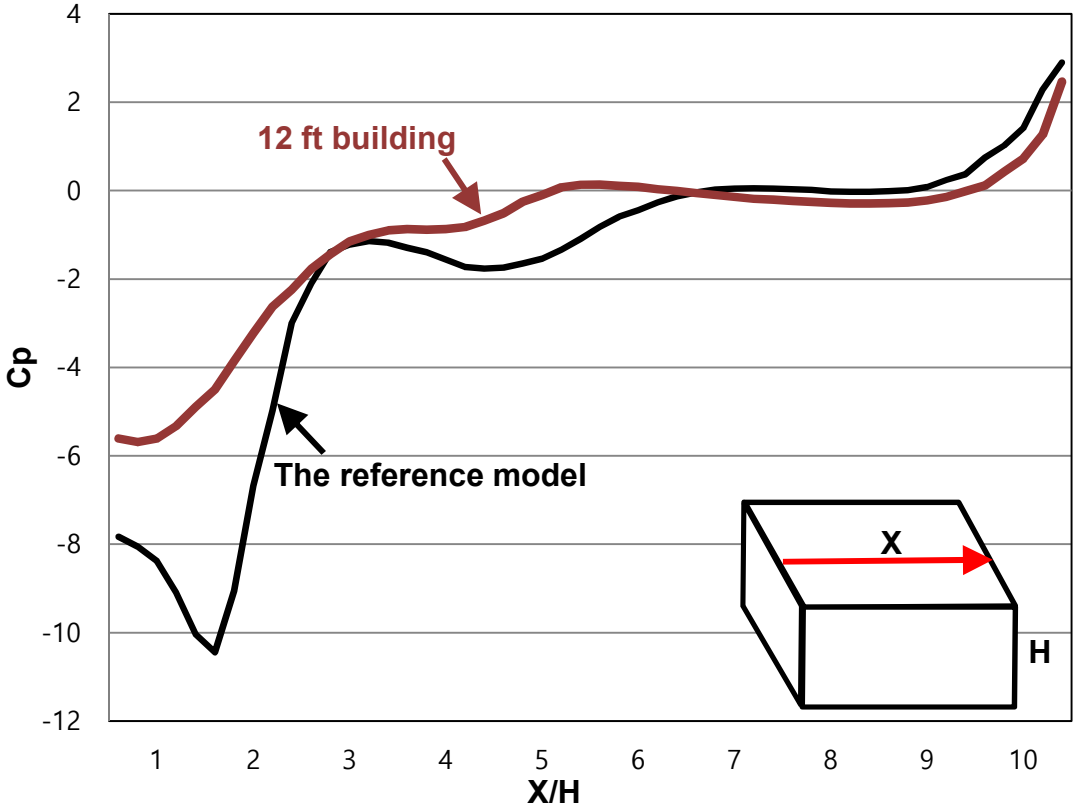

Figure 7.9 - CFD simulation results for the pressure coefficient along the centerline of the roof surface for the two structures

7.3.7. Discussion

This case study focused on investigating CFD simulations of wind flow over a roof surface and the impact of different building heights. The study's discussions for the CFD process can be summarized as follows.

1) For the size of the computational domain, while the computational domain for the reference model was constructed using the recommendations obtained through Chapter 3 to 6, the computational domain for the building with the height 12 ft was created using best practice guidelines (Franke et al., 2007). For this case, it was difficult to generate the wind profile using the same recommendations as those used for the reference model because the lateral

direction was much larger than the height of the building. Thus, the ratio of the lateral extension of the computational domain to its height was assumed to be similar to the corresponding ratio of the building in order for the sufficient distance for the wind profile at the inlet.

2) For the grid generation, the same base size of the grid was applied for both cases. Based on the base size, the coarser and finer grids were constructed. In the case of the coarse grid, it caused computational errors in representing the parapet wall. While the fine grids represented the parapet wall, more than 1,000,000 grids were generated. Thus, a grid resolution of 723,580 cells for the reference model and 842,940 cells for the other were applied for this case study.

7.4. Case Study B: A comparisons of wind flow over a flat roof surface with two different building aspect ratios

7.4.1. Introduction and context

For the second case study, the wind flow over the flat roofs of two low-rise buildings with different building aspect ratios was investigated. As shown in Figure 7.10, two different building aspect ratios were created: 1:2 for the reference building and 1:1 for the other. For both buildings, the roof surface area was 50,000 ft^2 and the building height was 36 ft. A parapet wall with a height of 42 inch was used for both cases. 60 mph was used for the inflow condition in the CFD simulations.

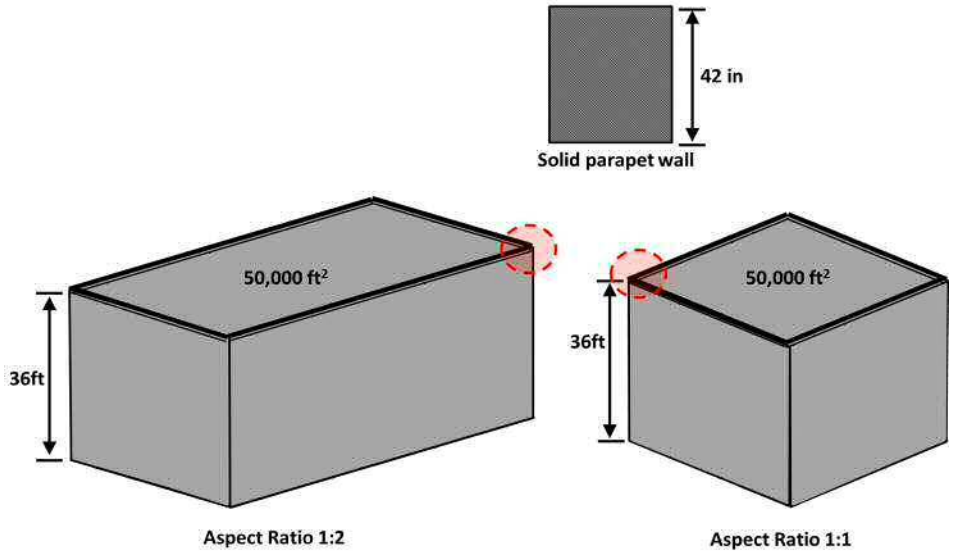

a. Reference model: Aspect ratio 1:2 b. Test building: aspect ratio 1:1

Figure 7.10 - Two different building aspect ratios

7.4.2. Computational domain

For this case study, two computational domains were created. The dimensions of these computational domains were as described in Figure 7.11. For the reference model, the same computational domain as that used in the first case study was applied. The computational domain size for the other building with the building aspect ratio 1:1 was L × W × H – 944 ft × 584 ft × 180 ft.

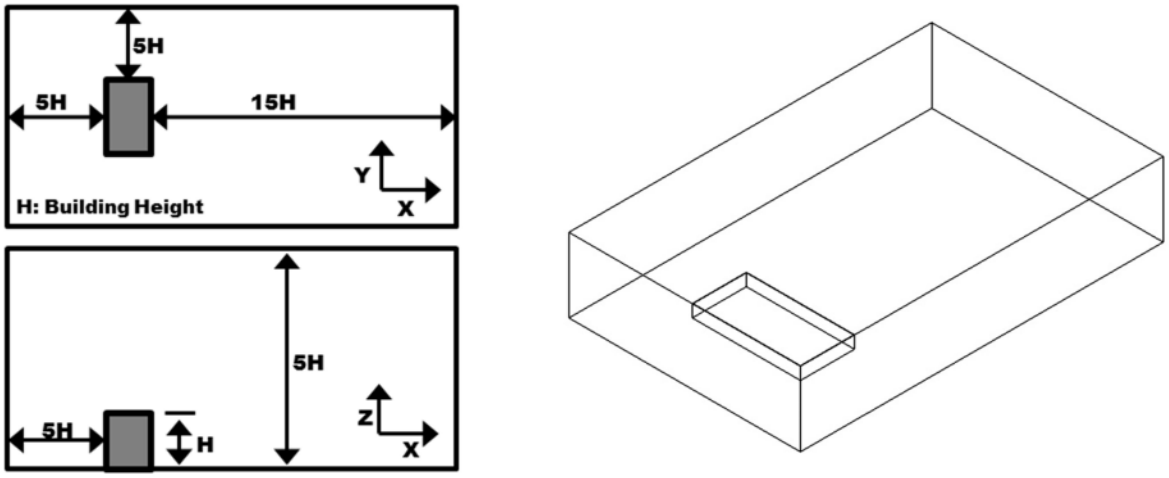

a. Reference model with the building aspect ratio 1:2

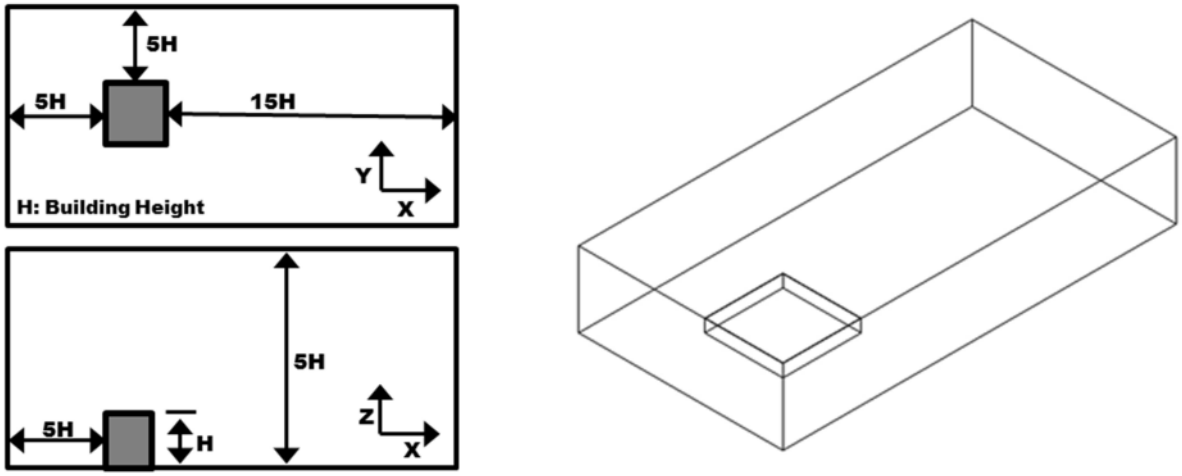

b. Test building with the building aspect ratio 1:1

Figure 7.11 - Two different computational domain

7.4.3. Computational grid

As described in the first case study in Section 7.3.3, the grid for these two cases consisted solely of hexahedral meshes, as shown in Figure 7.12. For the grid resolution, 723,580 cells were generated for the reference model. For the building with the aspect ratio 1:1, the grid consisted of 687,430 cells.

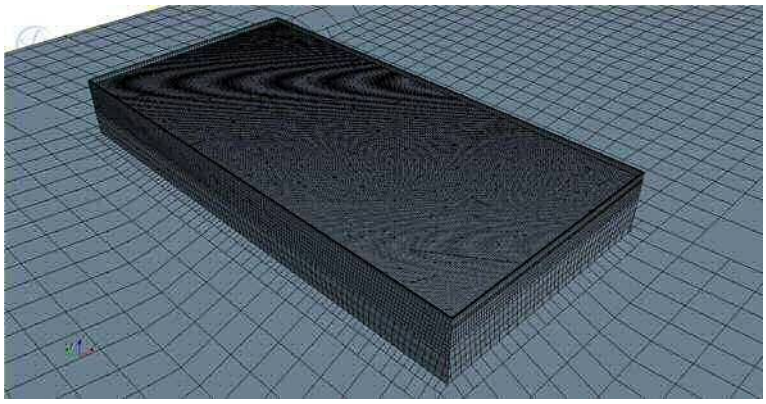

a. Computational grids for the reference model with a building aspect ratio 1:2

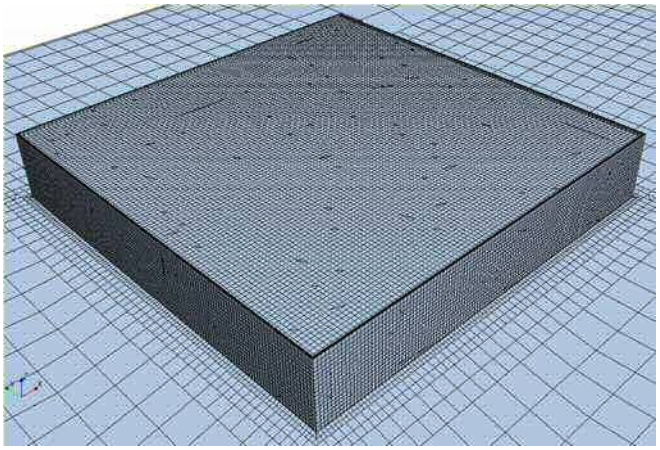

b. Computational grids for the building with a building aspect ratio 1:1

Figure 7.12 - The computational grids

7.4.4. Boundary conditions

As described in the first case study in Section 7.3, the velocity profile was specified at the inlet boundary condition using a power law with an exponent of 0.143, which corresponds to an open land surface. The velocity 33 ft above the ground was 60 mph. For the sides and the top of the computational domain, symmetrical boundary conditions were applied. For the outlet condition, a static pressure of zero was defined. Within the computational domain, no-slip wall boundary conditions were applied for the surfaces of the building in the computational domain.

7.4.5. Other computational parameters

The commercial code STAR-CCM+ 8.04 was employed for this CFD simulation with the 3D RANS equations. The LES model was used for this analysis because it offers a useful way to predict wind flow distributions over a flat roof surface. In addition, the SIMPLE algorithm with a central differencing scheme was employed. In order to calculate the subgrid scale in the LES model, the Dynamic Smagorinsky Subgrid Scale model was used.

The LES calculations were initialized with the solution from the standard k-ε simulations. For the initial conditions, the steady state calculation was first performed using the standard k-ε model. Once sufficient convergence was obtained, the turbulence model was changed to the LES model and the unsteady calculation started (Kobayashi et al., 2013). For this study, the time interval was 2.0×10^{-4} s, calculated for 50,000 time steps in total. When all the scaled residuals reached a minimum of 10^5, convergence for the LES model was obtained.

7.4.6. CFD simulation results

7.4.6.1. Qualitative comparisons

Contours and vectors of the mean velocity magnitude for both cases are compared in Figure 7.13. This comparative view of the results clearly shows the differences in the velocity field behavior for the two cases. In this case, the wind flow patterns were similar and a large difference was not observed.

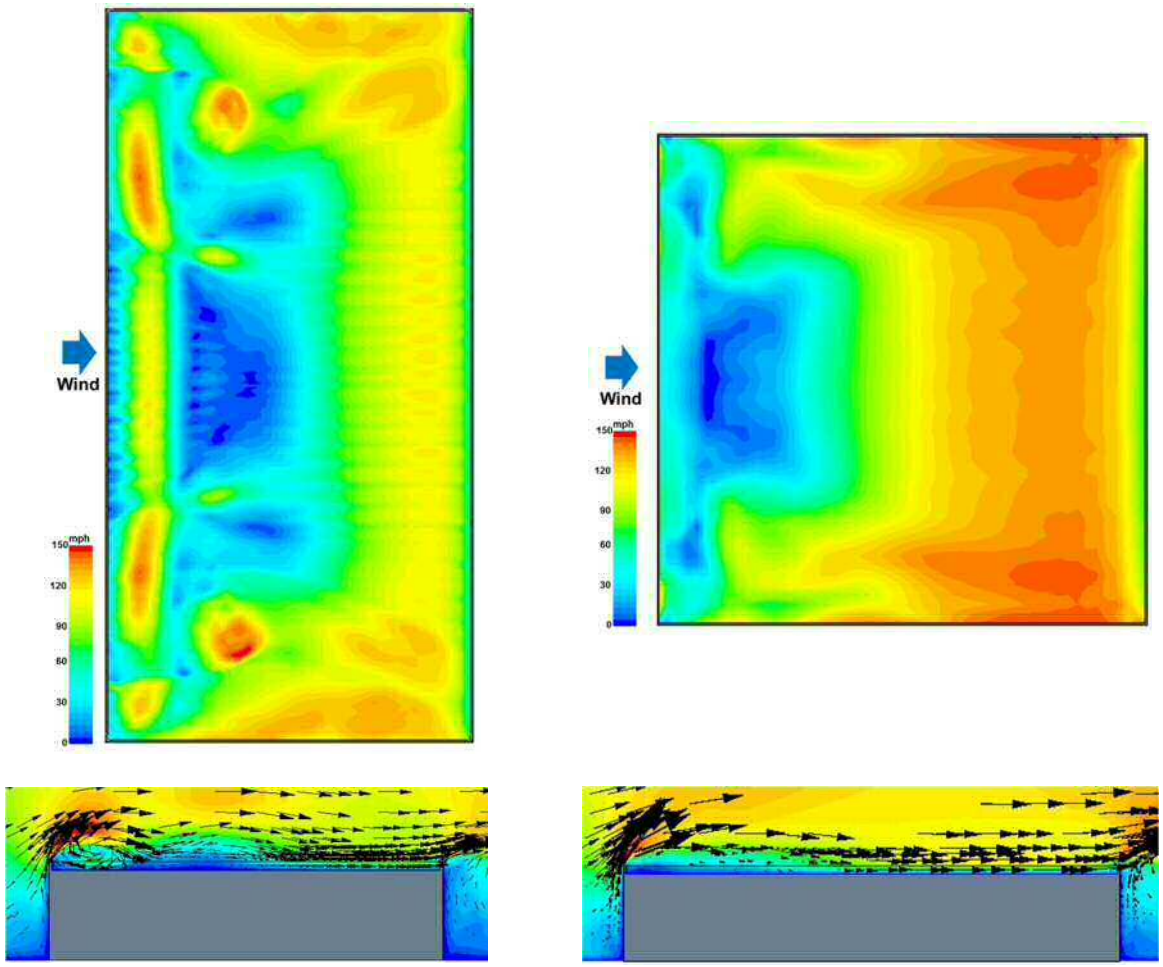

a. The reference model: Aspect ratio 1:2 b. The building with aspect ratio 1:1

Figure 7.13 - Contours and vectors of mean velocity magnitude on the roof and for the middle vertical plane

Figure 7.14 presents the contours of the pressure coefficients on the roof surface. As for the comparison of mean velocity magnitude, the results for both cases revealed similar trends, although somewhat lower values in pressure coefficients for the reference model were observed near the edge.

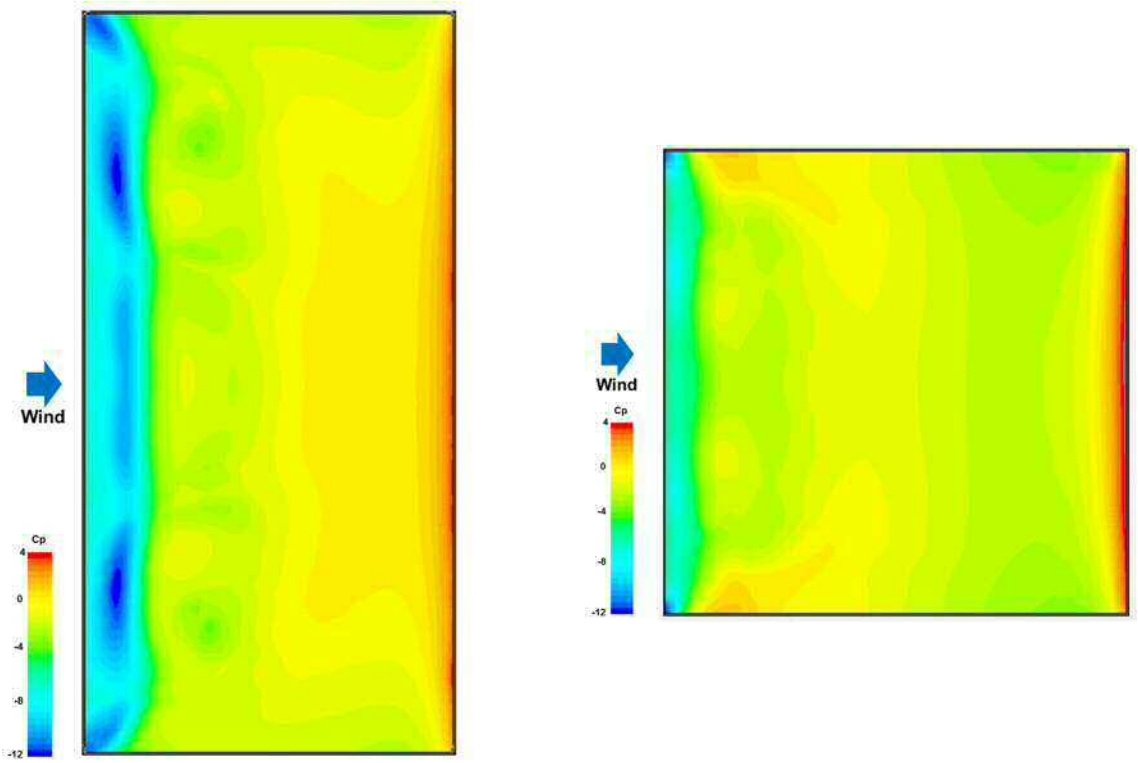

a. The reference model b. Test building with a height of 12 ft

Figure 7.14 - Contours of pressure coefficients on the roof

7.4.6.2. Comparison of the pressure coefficient distributions on the roof surfaces for the three grids

Figure 7.15 compares the pressure coefficient distribution along the centerline of the roof surface obtained from CFD for both cases. Near the edge, the pressure coefficient in the reference model was somewhat lower than for the other case. The highest suction was observed at 62 ft and 20 ft from the edge for the reference building and the other building, respectively.

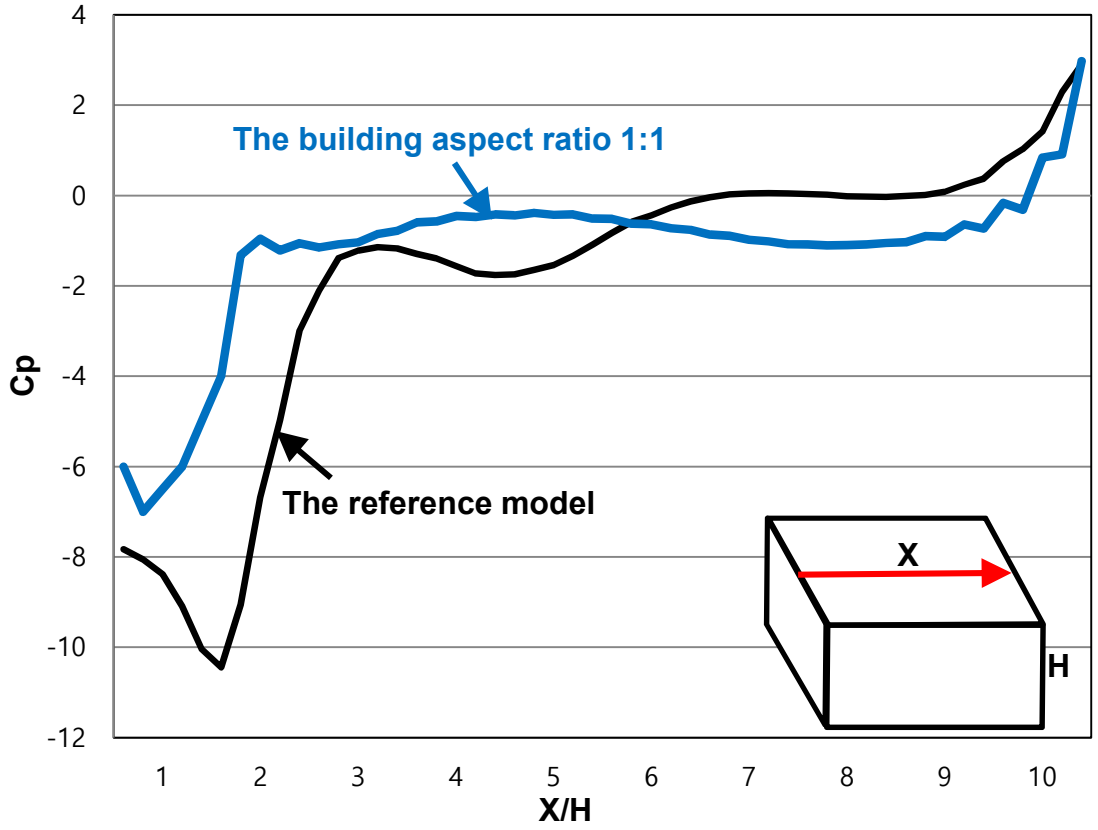

Figure 7.15 - Results of pressure coefficients along the centerline of the roof surface

7.4.7. Discussion

This case study focused on an analysis of wind flow over the flat roof surface of a low-rise building with two different building aspect ratios.

For the CFD process, the size of the computational domain for the model with building aspect ratio 1:1 was created using the recommendations in Chapter 6. In addition, the same base size of the grid as used for the reference model was applied for this model. For boundary conditions, the same conditions used for the sensitivity analysis (Chapter 6) were applied because the geometry and the simulation settings were similar.

7.5. Case Study C: A comparisons of wind flow over the flat roof surface of a low-rise building with three different parapet walls

7.5.1. Introduction and context

For this case study, wind flow over the flat roof of a low-rise building with three different parapet walls was investigated. As shown in Figure 7.16, three different parapet walls were defined. For these parapet walls, heights of curb edge (3 inch), 24 inch and 42 inch were applied to the reference building. The building height and aspect ratio used for the reference building in the first and second case studies, respectively, was applied. A wind speed of 60 mph was used for the inflow condition in the CFD simulations.

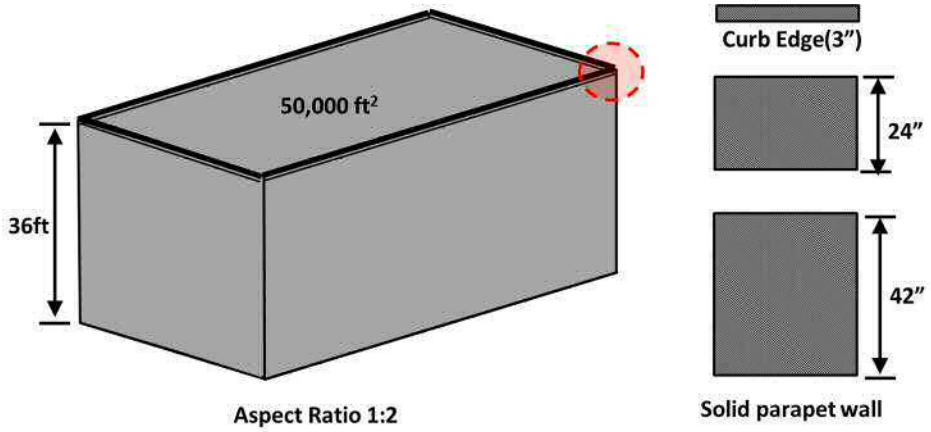

Figure 7.16 - The reference building with three different parapet walls

7.5.2. Computational domain

For this study, the same computational domain used for the reference model in the first and second case studies was applied. The dimensions were L × W × H – 880 ft × 676 ft × 180 ft and the blockage ratio was 9%. This is shown in Figure 7.17.

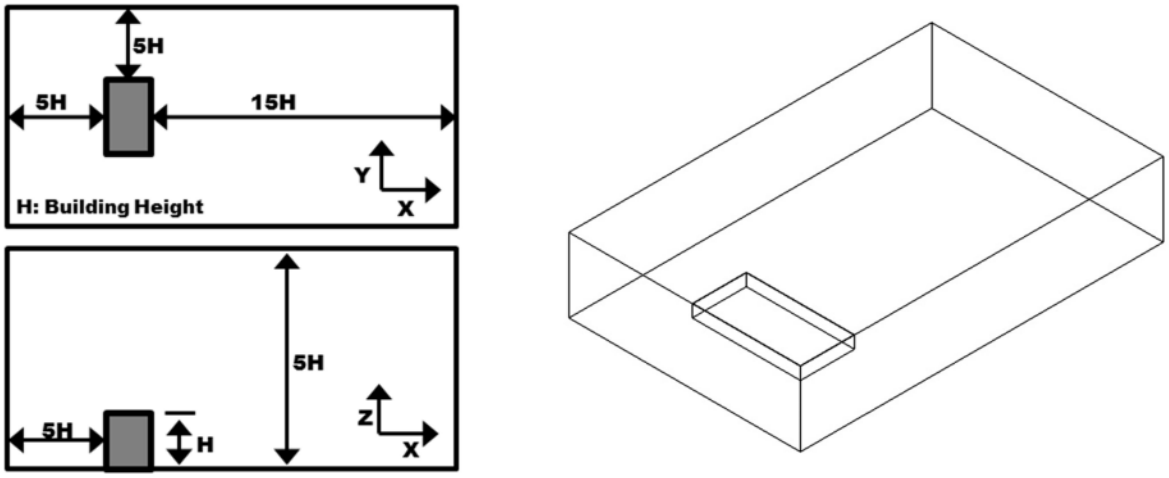

Figure 7.17 - The computational domain for the reference model

7.5.3. Computational grid

For this case study, three grids were generated using hexahedral meshes. As shown in Figure 7.18, 723,580 cells were generated for the reference model with a 42 inch parapet wall, the building with a 24 inch parapet wall utilized 791,250 cells, and 833,920 cells were generated for the building with a 3 inch curb edge.

7.5.4. Boundary conditions

As described in the first and second case study, the velocity profile was specified at the inlet boundary condition using a power law with an exponent of 0.143, which corresponds to an open land surface. The velocity 33 ft above the ground was 60 mph.

For the sides and the top of the computational domain, symmetrical boundary conditions were applied. For the outlet condition, a static pressure of zero was defined. Within the computational domain, no-slip wall boundary conditions were applied for the surfaces of the building in the computational domain.

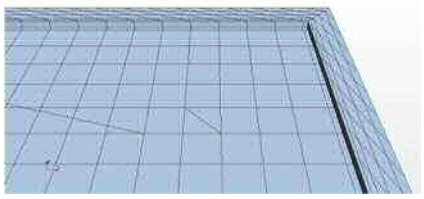

a. Computational grids for the reference building with the 3 inch curb edge

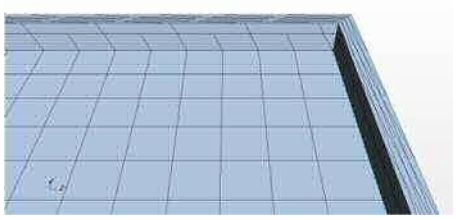

b. Computational grids for the reference building with 24 inch parapet wall

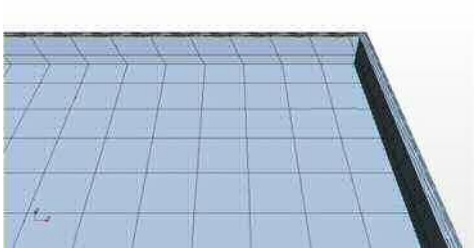

c. Computational grids for the building with 42 inch parapet wall

Figure 7.18 - The computational grids for the three different parapet walls

7.5.5. Other computational parameters

The commercial code STAR-CCM+ 8.04 was employed for this CFD simulation with the 3D RANS equations. The LES model was used for this analysis because it is a good way to predict wind flow distributions over a flat roof surface. In addition, the SIMPLE algorithm with a central differencing scheme was employed. In order to calculate the subgrid scale in the LES model, the Dynamic Smagorinsky Subgrid Scale model was used.

The LES calculations were initialized with the solution from the standard k-ε simulations. For the initial conditions, the steady state calculation was first performed using the standard k-ε model. Once sufficient convergence was obtained, the turbulence model was changed to the LES

model and the unsteady calculation started (Kobayashi et al., 2013). For this study, the time interval was 2.0×10^{-4} s, calculated for 50,000 time steps in total. When all the scaled residuals reached a minimum of 10^{5}, convergence for the LES model was obtained.

7.5.6. CFD simulation results

7.5.6.1. Qualitative comparisons

In Figure 7.19, the mean velocity magnitudes of vertical cross-section for each turbulence model are presented. The wind flow patterns for three cases were similar but the wind reattachment region migrated closer to the edge as the parapet wall height diminished.

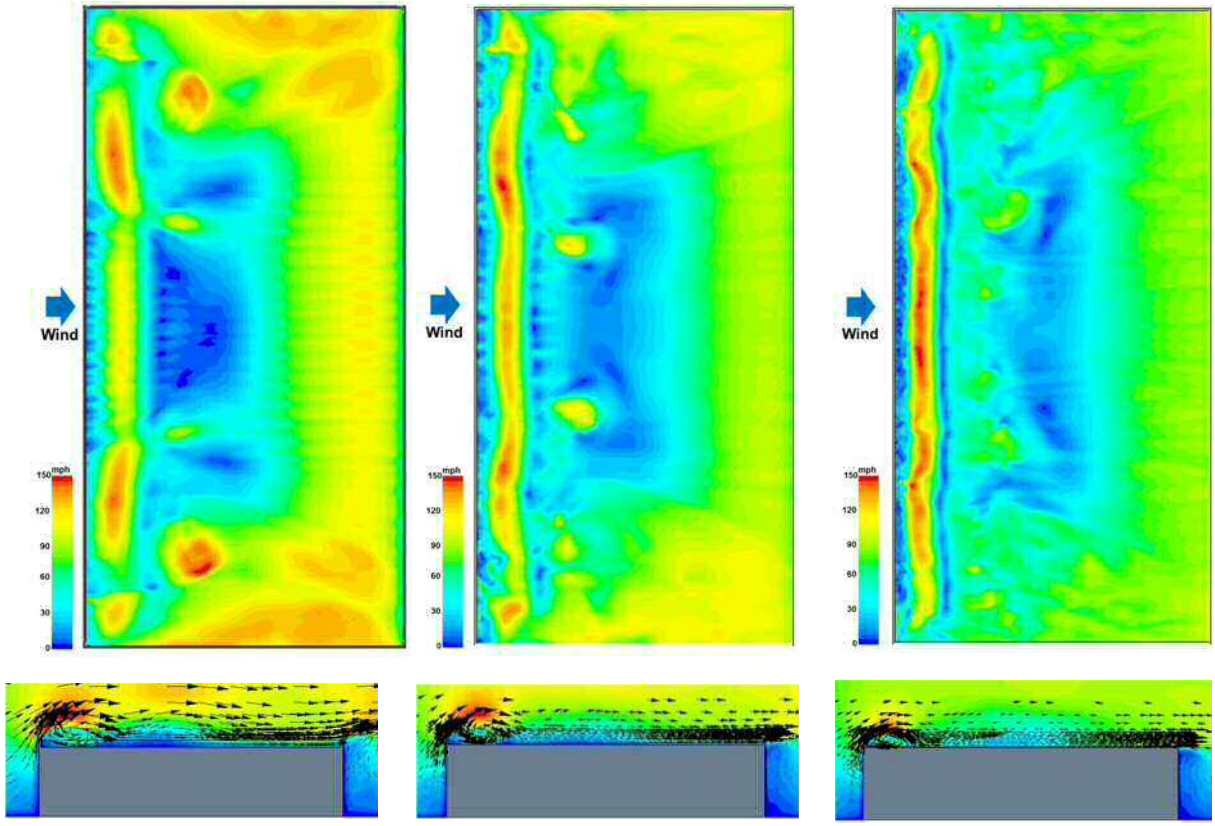

a. The reference model with the parapet height 42 inch

b. The building with the parapet height 24 inch

c. The building with the curb edge

Figure 7.19 - Contours and vectors of mean velocity magnitude on the roof and for the middle vertical plane

For the comparisons of contours of pressure coefficients distribution on the roof surface shown in Figure 7.20, the three cases showed similar patterns in the pressure field. For the third case of the building with the curb edge, the highest suction was closer to the edge than either of the other two cases.

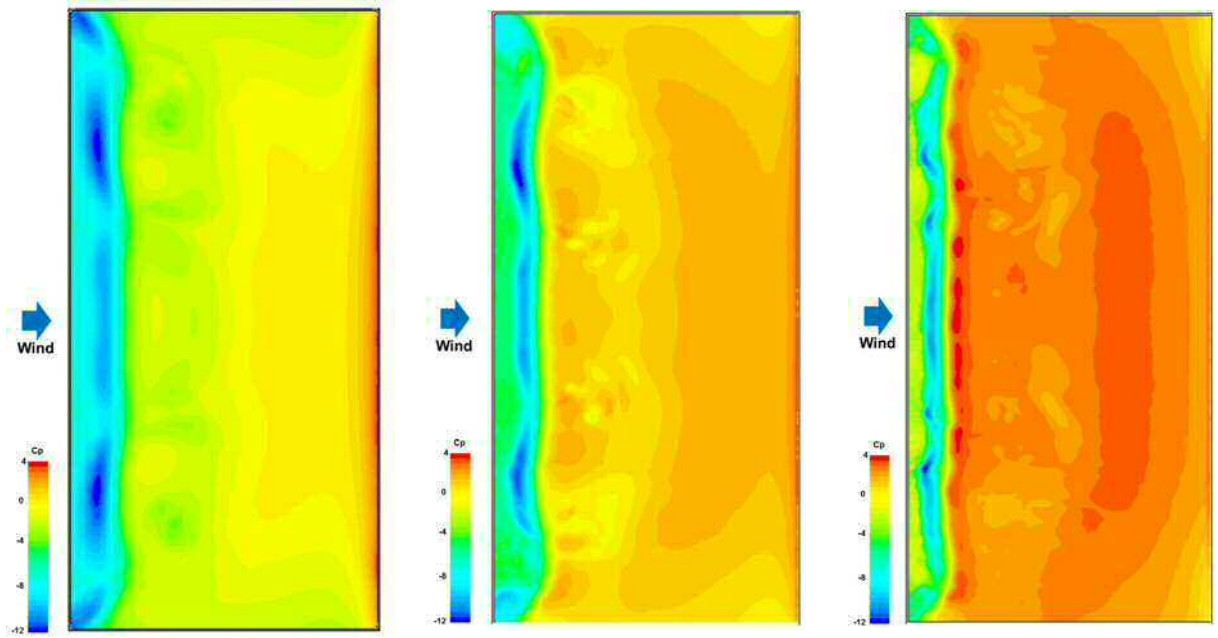

a. The reference model with the parapet height 42 inch

b. The building with the parapet height 24 inch

c. The building with the curb edge

Figure 7.20 - Contours of pressure coefficient on the roof

7.5.6.2. Comparisons of pressure coefficients on the roof surface for the three parapet walls

Figure 7.21 compares the pressure coefficients along the centerline of the roof surface for the three parapet walls. The pressure coefficient distributions for the reference model with the 42 inch parapet wall and the building with the 24 inch parapet wall showed similar results. The region of highest suction was 43 ft from the edge for the building with the curb edge, while the two other cases exhibited the highest suction 62 ft from the edge.

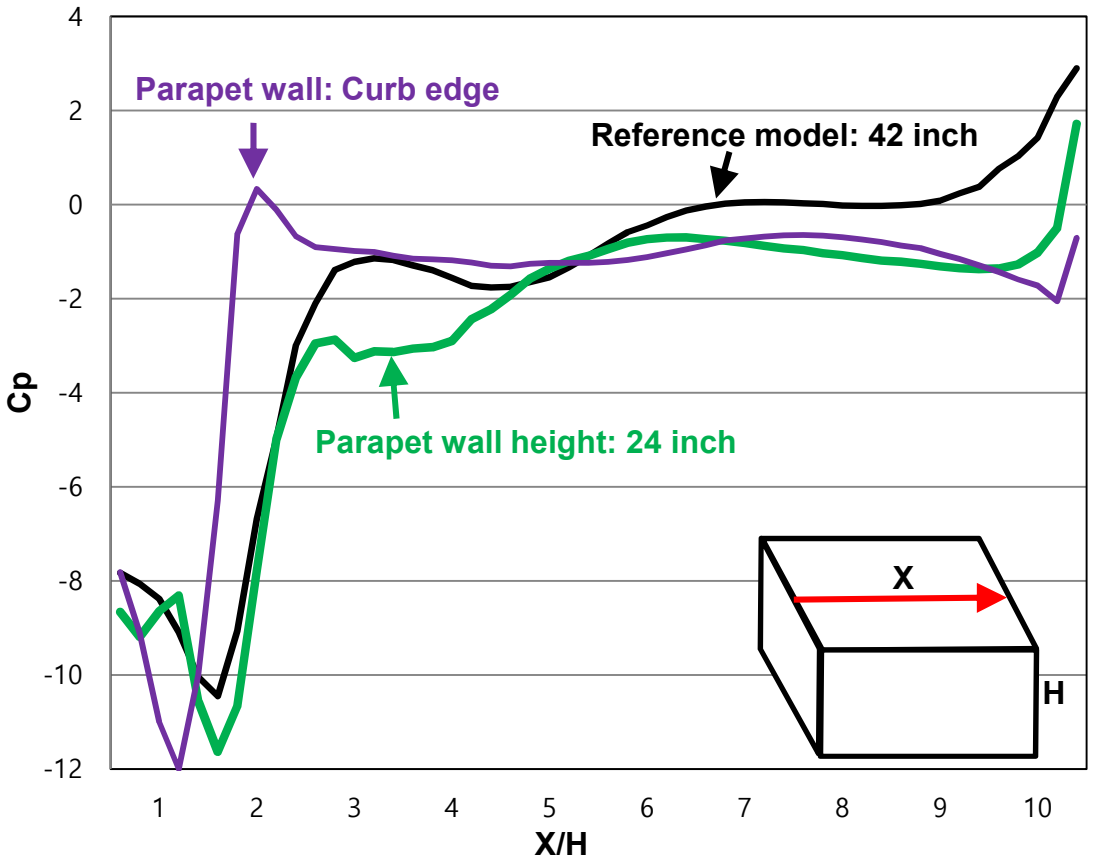

Figure 7.21 - CFD simulation results: Impact of turbulence models on the pressure coefficients along the centerline of the roof surface

7.5.7. Discussion

CFD simulations for the wind flow around a building with three different parapet wall heights were compared. The parapet wall heights tested were: curb edge (3 inch), 24 inch and 42 inch. The discussions for the CFD process are summarized as follows.

1) For the third case study, the same computational domain was used for the three cases. Only three different parapet wall heights were considered.
2) During the CFD process, the grid generation was a very time consuming because of the large difference in length scale between the parapet heights and the computational domain. As

mentioned above, very large discretization errors were occurred when representing two small parapet wall heights of the curb edge (3 inch) and 24 inch. Thus, the different base size of the grid was applied for the two cases in order to avoid the computational errors.

7.6. Summary of case studies

The three case studies described above investigated the impact of different building configurations including the building height, aspect ratio and parapet wall heights. The CFD modeling conducted for each case study employed the computational parameters identified through the document analysis and the sensitivity analysis reported in Chapters 3 to 6. The findings of the three case studies can be summarized as follows:

1) Wind flow over the flat roof surface of a low-rise building for three different building configurations was examined using CFD simulations and the mean velocity magnitude and pressure coefficient distributions calculated. Among these building configurations, the building height significantly influenced wind flow over the roof surface. As the building height increases, lower values of the pressure coefficient can be achieved.
2) The parapet wall also affected the wind flow behavior over the roof surface. Wind flow and pressure field were not highly influenced by increasing the height of the parapet wall between the heights 24 inch and 42 inch. However, the comparison between the curb edge and the other parapet walls showed a significant difference in the pressure coefficients near the edge. As the parapet wall height decreased, the region of wind reattachment migrated closer to the edge.
3) While somewhat lower values of pressure coefficients were observed for the reference model, the building aspect ratio did not substantially influence wind flow over the roof surface.

7.7. Discussion of the computational parameters through case studies

For the case studies, CFD simulations were employed to investigate the wind flow behaviors over the flat roof surface of a low-rise building for several building configurations. Computational parameters for wind flow around buildings were obtained through document analysis and sensitivity analysis. However, several parameters such as turbulence model and grid type were reselected to better reproduce the wind flow over the building.

In order to represent the wind flow behaviors on the roof surface, the LES model was applied. As mentioned in Chapters 3 to 6, this turbulence model requires substantial calculating time and computational resources. Since the k-ε turbulence models based on the RANS equations cannot adequately represent wind flow over a roof surface, the LES model was used for this case study. For calculating time, approximately 350 hours were required to achieve the results presented here.

For the grid type, a hexahedral grid was used rather than a tetrahedral grid because of its convenience for achieving numerical values and improving accuracy. Although a tetrahedral grid is generally preferred to represent the air flow patterns around buildings in urban areas, it is difficult to plot the resulting numerical data. For this case study, it was necessary to compare numerical values such as pressure coefficients in order to examine the impact of several building configurations. Thus, a hexahedral grid was employed.

The other computational parameters, including the computational size, grid resolution, boundary conditions, and convergence criteria, were obtained using the procedures described in Chapters 3 to 6 for this case study.

8. CFD AS A DESIGN ASSITANCE TOOL IN SCHEMATIC DESIGN STAGE

Computational parameters were analyzed and specified for wind flow around buildings through the research process. Based on the results, the CFD process for specific computational parameters was obtained. This chapter presents the findings of this study based on a sensitivity analysis and supported by the reviewed documents. The findings will now be considered in terms of the two themes that emerged from the data:

1) Which computational parameters maximize the accuracy of the CFD modeling? and,
2) Which computational parameters facilitate the effective use of CFD as a design assistance tool regarding time efficiency and ease of use?

Considering the above two themes, the data presented in the following sections focus on the researcher's observations regarding collecting and analyzing data related to the computational parameters in the context of CFD simulations of wind flow around a building. Within the CFD process, the pre-processing steps that consist of selecting the commercial code, preparation of geometry, the size of computational domain, grid generation, selecting boundary condition and turbulence model were the primary considerations.

8.1. Selecting the commercial code

Many commercial codes have been employed to simulate flow problems. Among these, the code FLUENT has been most widely applied; all the journal articles in Chapter 5 used FLUENT for their studies, for example. As mentioned in Chapter 2, FLUENT has three major components: 1) GAMBIT (the mesh generator), 2) FLUENT Solvers and 3) the FLUENT post-processor (ANSYS FLUENT, 12.0). In the case of the code STAR-CCM+, it provides a single integrated software environment from CAD creation to post-processing that automates simulation workflow and performs iterative design studies with minimal user interaction. In addition, the CAD-embedded environment of STAR-CCM+ does not require detailed knowledge of a specialist simulation package (http://www.cd-adapco.com/products/ comprehensive-simulations).

Although FLUENT has been widely used and its accuracy and reliability has been verified, it does suffer from difficulties when creating models and meshes from other tools. Moreover, the user-friendly interface and a single integrated environment of STAR-CCM+ provide an easier approach to solving time consuming tasks such as repeated simulations on design variables for designers and analysts than those offered by FLUENT. The accuracy and credibility of STAR-CCM+ have been confirmed by a number of recent publications (Lo et al, 2013; Pieterse & Harms, 2013; Norton et al., 2010; Zeng et al., 2012).

In addition, STAR-CCM+ was used for the sensitivity analysis and the case studies for this study. As mentioned above, this approach reduced the time required for repeated CFD simulations such as those utilized for these analyses.

Table 8.1 shows a comparison of the characteristics of the two commercial codes. Considering the advantages and disadvantages of both, the code STAR-CCM+ is recommended for predicting wind flow around buildings in the architectural design process.

Table 8.1 - Comparison between the characteristics of FLUENT and STAR-CCM+

CFD Code	Accuracy	Effective use of CFD	
		Time efficiency	Ease of use
FLUENT	✓		
STAR-CCM+	✓	✓	✓

8.2. Preparing the geometry

One of the most difficult and time consuming processes is the preparation of the geometry. As mentioned in Chapter 4, the area of a radius 1-2 H from the building of interest must be reproduced as accurately as possible, where H is the height of the tallest building in the region of interest. In addition, at least one additional street block in each direction around the region of interest must also be clearly reproduced, with buildings located away from the central region being represented by simple blocks. For example, Hooff & Blocken (2010) investigated urban

wind flow and natural ventilation for the Amsterdam ArenA stadium using CFD techniques. As indicated in Figures 8.1 and 8.2, they modeled the ArenA stadium in great detail but the buildings situated within a radius of 500 m from the stadium were reproduced by only their main shape.

Figure 8.1 - Aerial view of the area north of the Amsterdam ArenA football stadium and its surroundings (Hooff & Blocken, 2010)

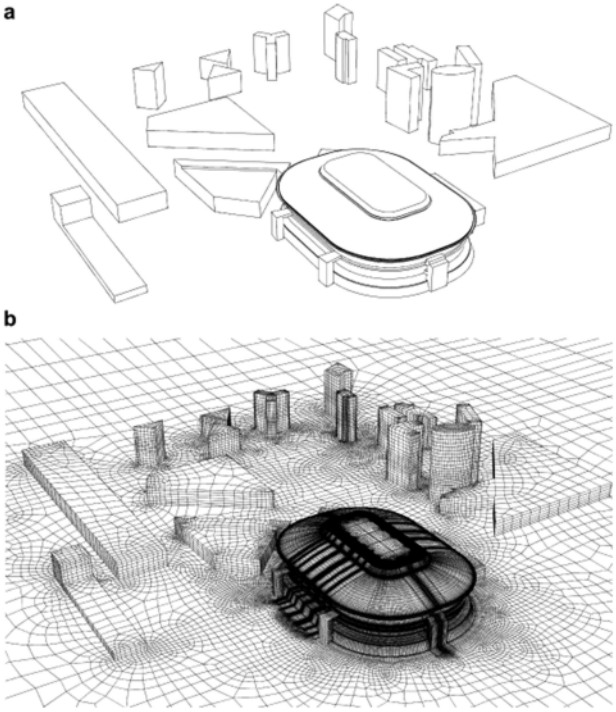

Figure 8.2 - Grid generation for the Amsterdam ArenA football stadium and surroundings: (a) Computational model geometry, view from northeast; (b) computational grid for the building surfaces and part of the ground surface (Hooff & Blocken, 2010)

8.3. The computational domain size

Once the geometry has been cleaned up and represented, it is transferred into the computational domain. Generally a rectangular computational domain is used in urban-scale studies in which wind is simulated with a constant profile, entering from upstream, encountering buildings of interest, and exiting the domain downstream (Gousseau et al., 2011; Mirzaei, & Carmeliet, 2012; Tominaga & Stathopoulos, 2011). Depending on the wind flow analysis through wind rose and Climate Consultant, the inflow direction of the computational domain is determined and the magnitude of the approaching wind is simplified according to the existing prevailing and frequent winds on the area of interest (Mirzaei, & Carmeliet, 2012). For example, the wind statistics for the location of the Eindhoven university campus were illustrated by means of wind rose in Figure 8.3. This wind rose was divided into twelve directions with frequency distribution of the hourly mean wind speed. According to the wind analysis through the wind rose, twelve different computational domains have to be created in order to cover twelve different wind directions. However, this would be an idealistic assumption because it is not easy to consider all approaching winds in the architectural design process. Thus, the wind from one or two prevailing directions obtained through wind rose or Climate Consultant can be used to determine the inflow direction in the computational domain. However, if no one or two wind directions are dominant form the wind rose analysis, then a decision must be made concerning multiple analyses for a range of wind directions and simulation domain orientations.

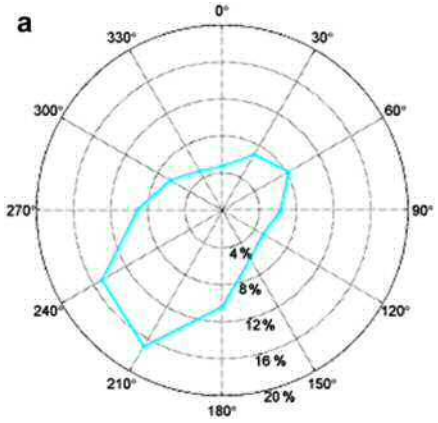

Figure 8.3 – Standard wind rose with frequency distribution of the hourly mean wind speed for Eindhoven University campus (Janssen et al., 2013)

Through the inflow direction of the computational domain, 5H and 15H are used for the upstream and downstream length respectively, where H is the height of the tallest building. In addition, 5H is used for the vertical extension and 10H+w is used for the lateral extension, where w is the built area that surrounds the region of interest. Figures 8.3 and 8.4 show examples representing the computational domain of a single building and its urban environment, respectively. In Figure 8.3, a single building tested at the wind tunnel at the IBHS is represented in the computational domain, applying 5H for the upstream length and 15H for the downstream length. The height and width of the wind tunnel were used for the lateral and vertical domain lengths. In Figure 8.4, the park tower and its urban surroundings in Antwerp are represented in the computational domain. Here, the computational domain consists of the basic domain and an additional downstream subdomain for wind directions 180°–270° because the prevailing wind direction is 210°. The explicitly modeled buildings are the park tower and the surrounding buildings for a rectangle of 1037 by 632 m^2 around the tower, when the height of the park tower is 78.18 m. The tower is reproduced in detail, while the surrounding buildings are represented by only their main shape (Montazeri et al. 2013). For this computational domain, the distance from the building to the side, to the inlet and to the top of the domain is at least five times the height of the building and the distance from the building to the outlet is fifteen times the height.

As can be seen in Figures 8.4 and 8.5, these are consistent with best practice guidelines. Therefore, the size of the computational domain recommended by best practice guidelines can be employed.

a. Test building in the wind tunnel at the IBHS

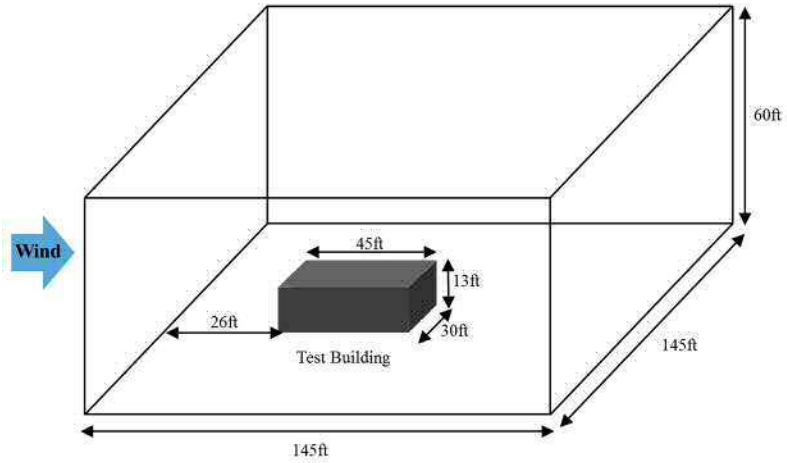

b. Layout of the test building and the chamber

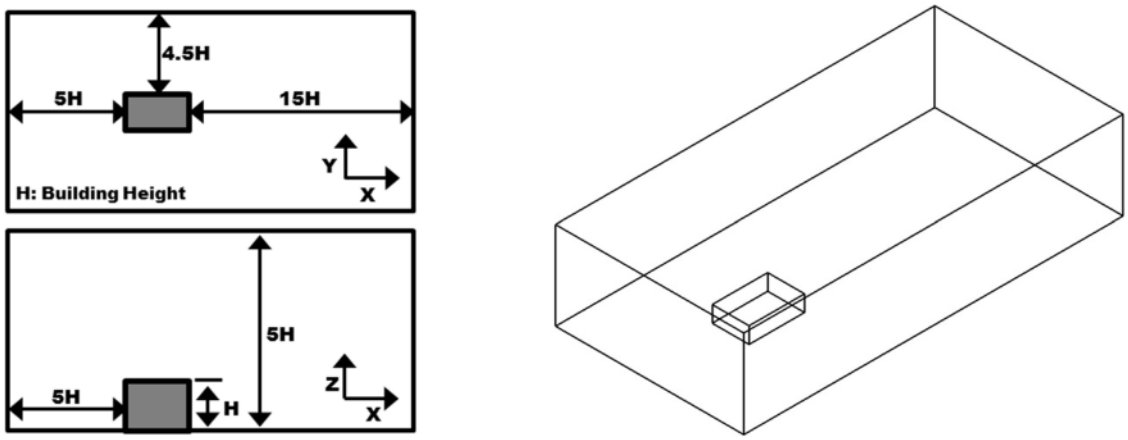

c. The test building in the computational domain

Figure 8.4 - A single building in the computational domain

a. Aerial view of the Park Tower (red) and surrounding buildings

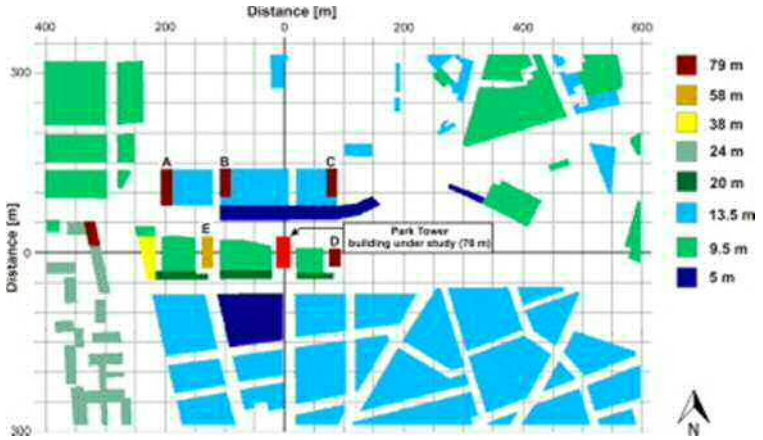

b. Top view of Park Tower and wider surroundings in a rectangular area of 630–1000 m^2 with an indication of building heights

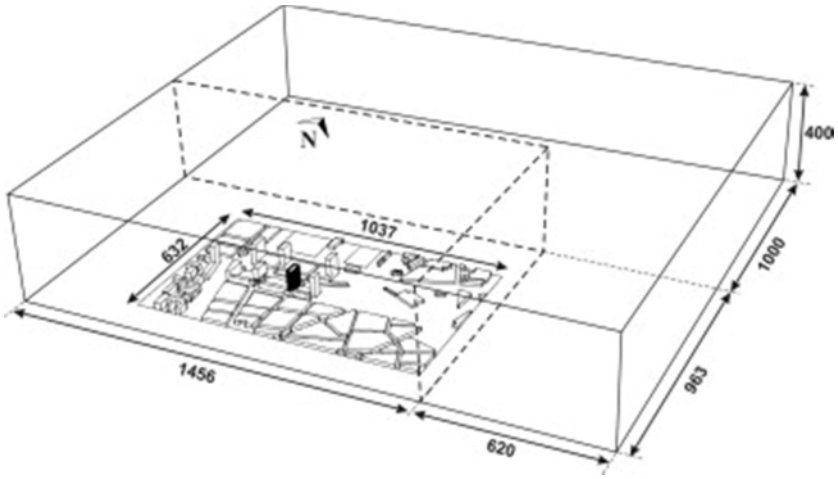

c. Computational domain for wind directions 180°–270°, consisting of a basic domain and an additional downstream domain

Figure 8.5 - The computational domain of an urban area in Antwerp (Montazeri et al. 2013)

8.4. Grid generation

Once the computational domain size has been determined, this domain must be discretized using grids that provided an adequate resolution of the geometry and expected flow fields (Casey & Wintergerste, 2000). Two types of grid topologies are generally used to capture the geometrical details of domains: structured grids and unstructured grids. For structured grids, the connectivity is straight-forward and employs a hexahedral shape. In the case of unstructured grids, a tetrahedral shape is utilized. According to Franke et al. (2007), hexahedral grids are to be preferred as they lead to smaller truncation errors and better iterative convergence than tetrahedral grids. However, a tetrahedral mesh generally provides a better fit for complicated domains and offers more convenient mesh adaptivity (Oliveira et al., 2008). According to a study by Hefny & Ooka (2009), generating hexahedral grids follows the structured grid constraint of having continuous gridlines on all faces, which requires the domain to be subdivided into blocks. Since the gridlines must remain continuous throughout the geometry, these blocks are difficult to develop. By contrast, tetrahedral grids can be generated automatically using commercial grid generation software packages (Hefny & Ooka 2009). When it comes to accuracy, it is commonly accepted that hexahedral grids provide more accurate results than tetrahedral grids at similar densities. Tetrahedral grids also require 4–10 times more elements than a hexahedral grid to obtain the same level of accuracy (Hefny & Ooka 2009; Shepherd & Johnson, 2007).

Table 8.2 - Comparison between the characteristics of hexahedral and tetrahedral grids

Grid type	Accuracy	Effective use of CFD	
		Time efficiency	Ease of use
Hexahedral grids	✓		
Tetrahedral grids			✓

Table 8.2 shows a comparison of the characteristics of the two types of grids. As described above, it is normally recommended that hexahedral grids be used for accuracy. For example, a hexahedral grid was used for the sensitivity analysis in Chapter 6. The geometry of the test building in the wind tunnel test at the IBHS consists of a simple block. For this geometry, a

hexahedral grid was used and the detailed information of velocities or pressures was easily achieved for the analysis. However, it is often difficult to reproduce urban flow situations using hexahedral grids, while tetrahedral grids are created automatically by the software. Hexahedral grids may also cause computational errors during grid generation. When considering time efficiency, correcting the computational errors created by hexahedral grids may take longer than the computational resources required when using tetrahedral grids to achieve the same level of accuracy. Thus, hexahedral grids are preferred for a simple geometry such as wind tunnel testing, while tetrahedral grids are preferred for the representation of urban wind flows regarding the time efficiency.

Considering the aspects of ease of use and time efficiency, it is thus recommended that a tetrahedral grid be used for the representation of urban wind flow situations. However, a hexahedral grid can be used for a simple geometry such as wind tunnel testing and when highly detailed information is required.

8.5. Turbulence model

Of the many ways of treating turbulent flows, the RANS equations have been most widely used for CFD simulations of industrial flows. These equations are derived by time or ensemble averaging the Navier-Stokes equations, reducing the resolution requirements by many orders of magnitude. However, because of the averaging procedure involved, information about the turbulence is lost. In the RANS equations, many different turbulence closures have been provided, including different versions such as the k-ε model, the k-ω model, and so on. These two-equation models are the mainstay of CFD simulations and provide a good compromise between complexity, accuracy and robustness. In order to achieve significant information regarding the details of turbulent flow, LES methods can be used that are based on the numerical resolution of the large turbulence scales and the modeling of the small scales. Due to the large cost of the required unsteady simulations, this approach is not employed routinely in industrial flow simulations (Menter et al., 2002), although as computer technology continues to develop,

the use of the LES approach is becoming feasible and it is now beginning to be used to analyze industrial flow.

According to the journal articles related to the representation of urban wind flow discussed in Chapter 4, the RANS approach with the realizable k-ε model, the RNG k-ε model and standard k-ε model have been most popular because they are easier to use than the LES model and less time consuming. Considering the results of the sensitivity analysis for the turbulence model presented in Chapter 6, the RANS approaches generally took 6 to 8 hours to achieve convergence, while the LES took 40 times longer than either of the RANS models to do so.

Table 8.3 - Comparison of the characteristics of the RANS approach and the LES model

Turbulence model	Accuracy	Effective use of CFD	
		Time efficiency	Ease of use
The RANS approach		✓	✓
LES model	✓		

Table 8.3 compares the RANS approach and the LES model. In the architectural design process, CFD has been generally used to modify design problems related to air flow in and around buildings. For this process, it is difficult to use the LES model because it requires more computational resources and time than those needed for the RANS turbulence model. Also, additional computational parameters such as time step and time interval must be set for the LES model.

Considering time efficiency and ease of use, RANS approaches such as the realizable k-ε model are recommended for studying wind flow around buildings in the architectural design process. In the case of the LES model, it can be used for the accurate information of velocities and pressures such as wind uplift on the roof surface (Chapter 6 and 7).

8.6. Boundary conditions

The boundary conditions reproduce the influence of the surroundings when cut off by the computational domain (Franke et al., 2007). In general, it is difficult to define some of the boundary conditions at the inlet and outlet of the computational domain at the level of detail that is required for an accurate simulation (Casey & Wintergerste, 2000). Significant care is therefore required when specifying the boundary conditions.

For the inlet boundary conditions, the data from experiments, including the turbulent kinetic energy k and dissipation rate ε, are needed to prescribe the profiles. Most of the studies discussed in Chapter 4 determined the velocity profile at the inlet using the measured wind profile from experiments and it was specified using logarithmic or power laws. In the case of the use of CFD in the architectural design process, the information pertaining to wind data and turbulence from measurements are not generally available because a design concept at the schematic design stage does not yet exist. In order to specify the mean velocity profile at the inlet, the information obtained from previous studies related to similar issues or the weather condition at the site can be used. When deciding between the use of a logarithmic law or a power law to create wind speed profiles, the following equations apply. For a log law, the wind profile is given by:

$$\mathrm{U}\,(\mathrm{z}) = \frac{U_*}{k} ln\left(\frac{z-d}{z_0}\right)$$ Equation 8.1 – A log-law for the wind profile

where u_* is the surface friction velocity, k is von Karman's constant (0.4), d is the zero plane displacement and z_0 is the surface roughness length (Drew et al., 2013).

In the case of a power law, the mean velocity profile is given by

$$\mathrm{U}\,(\mathrm{z}_1) = \mathrm{U}(z_2)\left(\frac{z_1}{z_2}\right)^{\alpha}$$ Equation 8.2 – A power law for the mean velocity profile

where $U(Z_1)$ and $U(Z_2)$ are the mean wind speeds at heights of Z_1 and Z_2, respectively, and α is the magnitude of the exponent (Drew et al., 2013). Values for the terrain dependent parameters are typically those shown in Table 8.4. Using these equations, the mean wind profile can be specified at the inlet boundary condition.

Table 8.4 - Values for typical terrain dependent parameters in the UK (Cook, 1997, as quoted in Drew et al., 2013)

Description	Typical rural	Suburban	City
Roughness length, Z_0 (m)	0.03	0.3	0.8
ABL Height (m)	2550	3000	3250
Exponent α	0.16	0.24	0.32

For the outlet boundary conditions, zero static pressure can be imposed and symmetrical boundary conditions employed for the top and sides of the domain.

8.7. Numerical schemes and the algorithm

In general, higher order approximations such as second-order methods are recommended for dealing with this type of problem (Franke et al., 2007). For the RANS approach, the SIMPLE algorithm is employed for pressure-velocity coupling, pressure interpolation is second order and second-order discretization schemes are used for both the convection terms and the viscous terms of the governing equations.

8.8. Convergence criterion

As Franke et al. (2007) explain, CFD simulations employ iterative methods to solve the algebraic system of equations. The termination criterion is usually based on the residuals of the corresponding equations and a typical termination criterion of 0.001 is used in industrial

applications. For example, one of the studies examined in Chapter 4 used termination criteria of 10^6 for the x, y and z momentum, and 10^5 for k, ε and continuity (Montazeri & Blocken, 2013) and Abohela et al. (2013) also set their scaled residuals in the range of 10^4 – 10^6. Hence, convergence is assumed to obtain when all scaled residuals are reached in the range of 10^4 – 10^6.

8.9. Conclusions regarding the CFD simulation process for wind flow around buildings in the schematic design stage

Concerning the data gathered from the analysis of documents, the sensitivity analysis, and observations, the optimal CFD modeling process for wind flow around buildings can be summarized as follows:

8.9.1. Pre-processing

1) The commercial CFD code: STAR-CCM+
2) Prepare the geometry:
- The central region of interest (the area of a radius 1-2 H from the building of interest) is reproduced as accurately as possible.
- One additional street block in each direction around the region of interest is also clearly reproduced.
- Buildings located away from the region of interest are represented by simple blocks.

3) Transfer the AutoCAD file: Stereo lithography file (.stl), IGES (.iges and .igs), etc. of AutoCAD file formats
4) The computational domain size:
- With H being the height of the building of interest, upstream and downstream lengths of 5H and 15H, respectively
- 5H for the height of the domain
- 10H+W (the width of built area) for the lateral extension

5) Grid design:

- Tetrahedral grids
- At least 10 cells per cube roof of building volume for grid resolution

6) Turbulence model: the RANS equations with the realizable k-ε turbulence model

7) Boundary conditions:

- The inlet: the mean vertical velocity profile is specified using a power law or log law.
- The outlet: zero static pressure condition
- Top and sides of the domain: symmetry boundary conditions

8) Numerical schemes and the algorithm:

- The SIMPLE algorithm for pressure-velocity coupling, second order for pressure interpolation and second-order discretization schemes are used in the RANS approach.

9) Convergence criterion: the scaled residuals were set in the range of $10^4 – 10^6$.

8.9.2. Solving

1) The solution can be calculated using the solvers of STAR-CCM+ 8.04, with continuous monitoring of the scaled residuals.

8.9.3. Post-processing

1) Visualization: the CFD results may conveniently be visualized as contour and vector plots of velocity and pressure.

The computational parameters for wind flows around buildings can be presented via the CFD process. Since the results of CFD simulations are very sensitive to a number of computational parameters and these parameters are chosen by the user, a number of parameters were reviewed and analyzed based on the findings of previous studies. Among the selected computational parameters, conditions of the preparation of the geometry, the computational domain size, and boundary conditions were developed using the recommendations. Other computational parameters including turbulence models and grid generation were established through an analysis

of journal articles published since 2011, because the recent rapid developments in computing power make it possible to incorporate more computational parameters. The selected computational parameters can be used for the CFD analysis of wind flow around buildings. The results of CFD will provide information regarding the air flow around building to architects and designers to assist their design development in the schematic design stage.

9. LESSONS-LEARNED

9.1. Introduction

The research was designed to provide a better understanding of the CFD simulation process by adopting a combined qualitative and quantitative approach. Through the case study research method, the researcher described how the CFD modeling process can be conducted in the context of wind flow around buildings in order to improve our understanding of the application of CFD for building design.

By identifying computational parameters based on document analysis and observations during a case study, lessons-learned were gathered. These lessons will be shared with others planning to use CFD as a design assistance tool in order to help them use it more effectively and avoid computational errors in the schematic design stage.

9.2. Consider influential factors in the urban area including vegetation and surface characteristics when preparing the geometry

When commencing any project related to CFD, it is important to determine what must be included and what can safely be ignored regarding the geometry of the target objects when preparing the geometry. Generally the distribution of buildings is the major factor that influences wind flow patterns, while secondary influencing factors in the urban area are vegetation and surface characteristics such as roads, grass and sand (Franke et al., 2007).

In the case of CFD analysis for wind comfort, trees, grass, road and sand are generally neglected, although vegetation has sometimes been considered in the planning process for the wind energy industry. As the examples in Sections 8.2 and 8.3 demonstrate, surface characteristics are generally not reproduced in the computational domain. Whether the details of the geometry are included or excluded may significantly influence the number of grid cells. As noted earlier, increasing the number of grid cells greatly increases the computing resources required and the

running time. The optimum balance to be struck is normally based on the user's experience, previous studies and the best practice guidelines.

9.3. Clean up and reproduce the initial design of the building of interest and surroundings in the native AutoCAD file as much as possible before importing them into the computational domain

After the appropriate level of detail in the geometrical representation has been determined, the initial design of the building of interest and surroundings are reproduced and cleaned up in order for them to be imported into the computational domain. Generally, the buildings in the native AutoCAD file format are made of surfaces. When the AutoCAD file is imported into the commercial CFD code, this may produce computational surface errors such as pierced faces, free edges, non-manifold edges, etc. These computational surface errors may create substantial computational volume errors which then go on to produce incorrect results in the CFD simulation. In the case of the wind tunnel tests at the IBHS used for the sensitivity analysis (Chapter 6), the test building in the wind tunnel was reproduced as solid object in the AutoCAD and imported into the computational domain in order to avoid computational errors. Thus, it is important to clean up and reproduce the initial design of the building of interest and its surroundings in the AutoCAD file format. While the commercial CFD code provides a tool for correcting computational errors, it is typically easier and faster for architects and designers to clean up and reproduce them in the AutoCAD file format than to correct computational surface errors in the commercial code. As mentioned above, the building of interest and its surroundings should be represented as solid objects in order to be read into the commercial code.

9.4. Choose the proper grid type for various applications of building design

As mentioned in Section 8.4, it is important to choose the proper grid type associated with various building design objectives including building site design, pedestrian wind comfort, natural ventilation, pollutant dispersion around buildings, wind uplift on the roof, etc. Generally, hexahedral grids are used for simple geometries, while tetrahedral grids are preferred for the

investigation of overall wind flow patterns in urban area and complex geometries. In order to achieve results that satisfy a particular purpose, the grid type should be carefully selected.

A hexahedral grid is generally used to produce detailed information on velocity and pressure. For natural ventilation as a design objective, a hexahedral grid is employed to calculate the air exchange rate in a building and for the prediction of pollutant dispersion around buildings. A hexahedral grid is used for the calculation of how the pollutant dispersion is influenced by surrounding buildings. In addition, this type of grid can be used to produce detailed information such as the velocity and pressure on the roof for the investigation of wind uplift. For example, a hexahedral grid was used for both the sensitivity analysis in Chapter 6 and the case studies in Chapter 8 because detailed information on turbulence quantities was required. While the geometry of the wind tunnel tests in Chapter 5 consisted of a simple block, the geometry for the case studies in Chapter 7 employed large differences in geometrical length scales between the computational domain and the parapet wall. However, although it caused computational errors when a hexahedral grid was applied for the geometries in Chapter 8, this grid was deemed to be more useful overall because of its accuracy and convenience as a way of achieving numerical values for velocities and pressures.

A tetrahedral grid is generally employed to inform the design of building site planning and wind comfort studies because of its mesh adaptivity for complex geometries. For example, a tetrahedral grid is generally used to predict the distributions of air velocity around buildings. Table 9.1 summarizes the recommendations for the selection of the proper grid type in the light of various building design objectives.

Table 9.1 - Recommendations for the selection of a suitable grid type for various applications

Building design	Computational grids	
	Hexahedral grids	Tetrahedral grids
A study of natural ventilation design	✓	
Building site planning		✓
An assessment of pedestrian wind comfort		✓
Prediction of pollutant dispersion	✓	
Investigation of wind uplift on the roof	✓	

9.5. Consider the smallest length scale of the building of interest when determining the base size of grids and check for computational errors after grid generation

The most time-consuming and difficult task in the CFD process is the grid generation. To achieve accurate results, it is important to understand the influence of the mesh size. However, issues concerning a suitable mesh density to achieve the desired accuracy for a specific problem still remain. Although commercial CFD codes can automatically generate grids, it is important to have proper initial values for the base grid size.

When generating grids, the base size should be set up as approximately 5% to 10% of the length of the building of interest. Considering the smallest length scale of the building of interest, the value for the base grid size can be varied in order to produce accurate results. In the case of the sensitivity analysis in Chapter 6, the base size of grids was approximately 10% of the length of the test building in the wind tunnel and the results of the computational model showed good agreement with the finer grids. This comparison is shown in Figure 6.13. In addition, the smallest length scale was focused on the parapet wall of the building in the case studies in Chapter 7. After the grids have been generated, it is strongly recommended to check whether computational errors are created at the building of interest.

9.6. Choose the proper turbulence model for applications of building design, namely either LES or the RANS turbulence model

The selection of the turbulence model depends on considerations such as the physics encompassed in the flow situation, the objectives for a specific problem, and the amount of time available for the simulation. For the architectural design process, it is important to choose the most appropriate turbulence model for various objectives of building design including the study of natural ventilation, a prediction of pollutant dispersion around buildings, an assessment of pedestrian wind comfort, building site planning and an investigation of wind uplift on the roof.

As mentioned in Chapter 6, the LES model provides more accurate information about turbulence quantities such as velocity and pressures. In addition, the sensitivity analysis showed that LES gave better results than either of the two RANS turbulence models at the perimeter of the roof (Chapter 6). The LES model was therefore used for the investigation of wind uplift on the roof surface described in Chapter 7 as it provided more detailed information regarding wind loads on the roof. Moreover, the LES model when used for the prediction of the pollutant dispersion did not underestimate the turbulence kinetic energy at the recirculation zone on the roof (Gousseau et al., 2011) as the RANS models did. In the case of an investigation of roof detachment in hurricane prone areas, the LES model would be more reliable.

Because the modeling process is easier and simulations take much less time, the RANS turbulence models are generally employed for the study of natural ventilation, an assessment of pedestrian wind comfort and building site planning.

Although LES can predict wind loads on the roof and pollutant dispersions around buildings, the calculating time required is much longer than that for the RANS turbulence models. For example, approximately 350 hours were needed to achieve the results when the LES model was applied for the case studies in Chapter 7. Thus, the use of LES for the architectural design process should be carefully considered. For most architectural design objectives that involve CFD, the RANS

turbulence models can be used to assist design development. Table 9.2 summarizes the recommendations for the selection of the turbulence model for various building design objectives.

Table 9.2 - Recommendations for the selection of turbulence model for various applications

Building design	Turbulence model	
	The RANS models	LES model
A study of natural ventilation design	✓	
Building site planning	✓	
An assessment of pedestrian wind comfort	✓	
Prediction of pollutant dispersion		✓
Investigation of wind uplift on the roof		✓

9.7. Use the default values provided for turbulence quantities in the commercial code for the inlet boundary condition when experimental data is not available

In order to reproduce the mean velocity profile at the inlet of the computational domain, the profiles of mean wind speed, turbulent kinetic energy and turbulence dissipation rate must be prescribed at the inlet. The best way to establish values for the inlet turbulence quantities is to analyze experimental data such as that from a wind tunnel or from in-situ monitoring at the site. As indicated in Chapter 6, the values of the turbulence quantities are calculated using equations such as power-laws. When the experimental data is applied for the inlet boundary condition, the velocity profile of the CFD can reproduce very similar flow behavior to that observed experimentally. However, the experimental data is not generally available when CFD is applied for small scale projects or for the early stages of design development. In addition, it is difficult for non-CFD experts or designers to calculate turbulence quantities for the inlet boundary condition even if the measurement data is available.

When experimental data is not available, the default values for turbulence quantities such as turbulence kinetic energy and turbulence dissipation rate provided by the commercial codes can be used to specify the velocity profile for the inlet boundary condition in order to predict the air flow patterns in and around buildings because the default values of the commercial code are generally adequate for most applications. In addition, the mean wind speed can be employed using the weather conditions at the site. As described in Chapter 7, the default values of turbulence quantities provided by the commercial code "STAR-CCM+ were applied to the case studies because of the measurement data were not available. Although the use of default values for the inlet boundary condition cannot typically reproduce accurate flow profiles when compared with experimental data, its predictions of the air flow patterns are generally acceptable.

9.8. Monitor the residuals and visualization of the results while calculating the solutions

After defining the boundary conditions, the computational parameters are applied to the solvers. Even though all the conditions have been defined completely, errors may occur. When calculating the solution, these errors may be revealed by monitoring the residuals and visualizing the velocities or pressures during the calculation process. For example, if some computational parameters are missed, the rate of change of residuals such as continuity, x, y and z momentum, energy, and turbulence dissipation rate and kinematic energy could either stagnate or diverge. Figure 9.1 and 9.2 show the residuals, the vector and contour plots during calculation of the sensitivity analysis (Chapter 6). Thus, it is recommended that users should monitor the residuals or visualization of the results, including the vector or contour plots, during calculations.

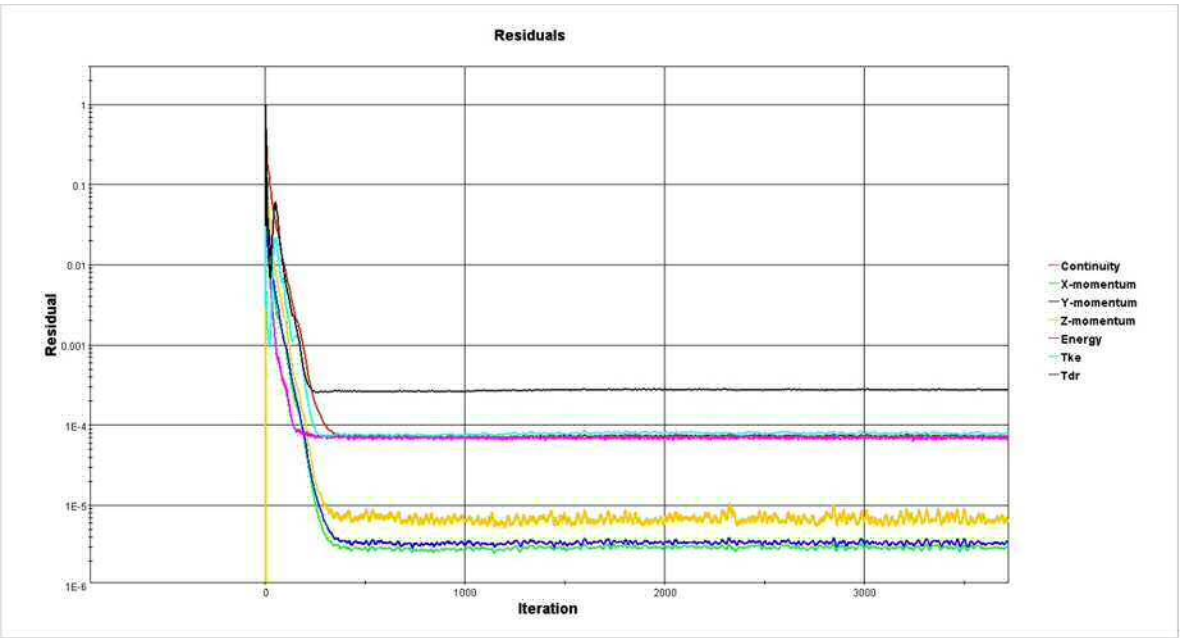

Figure 9.1 - An example of the residuals during calculation of the sensitivity analysis in Chapter 6.

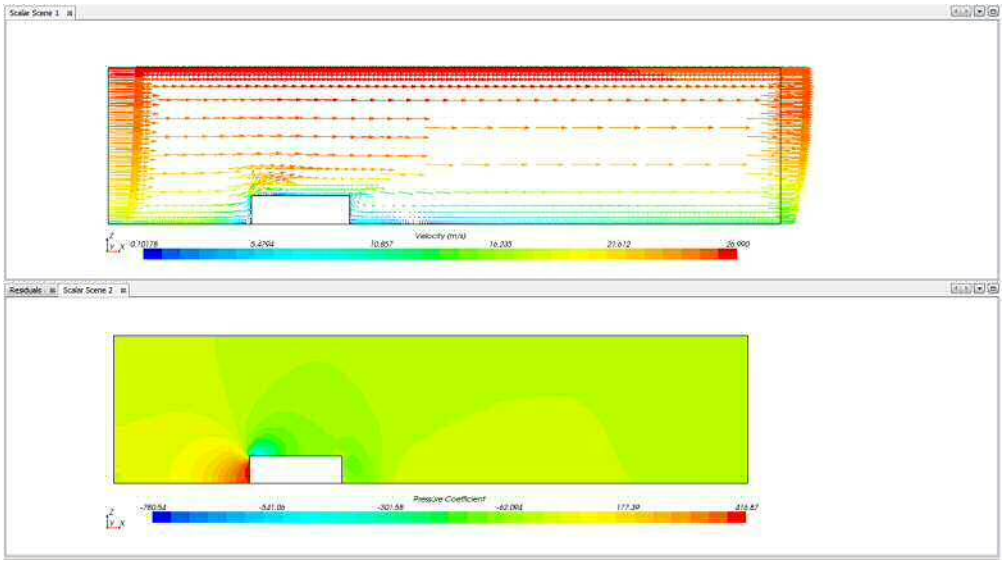

Figure 9.2 - Monitoring the vector and contour plots of mean velocity during calculation of the sensitivity analysis in Chapter 6.

9.9. Practice an effective visualization of the results

Unlike other building simulation tools, one of the advantages of CFD is its ability to visualize the results. After the results have been calculated, they are presented to the user using the visualization tool provided in the commercial code. In general, vector and contour plots for velocities and pressures are visualized. Figure 9.3 shows an example of the visualization of velocities using vector and contour plots used in the sensitivity analysis in Chapter 6. At this point, the user must decide on what and how results will be represented in order to effectively understand and present them to others. There is no preferred approach to visualizing CFD results. Whatever the graphic tools used, an effective visualization can be obtained through practice. In addition, some familiarity with the literature or with similar projects can assist the user to create an effective visualization of the results.

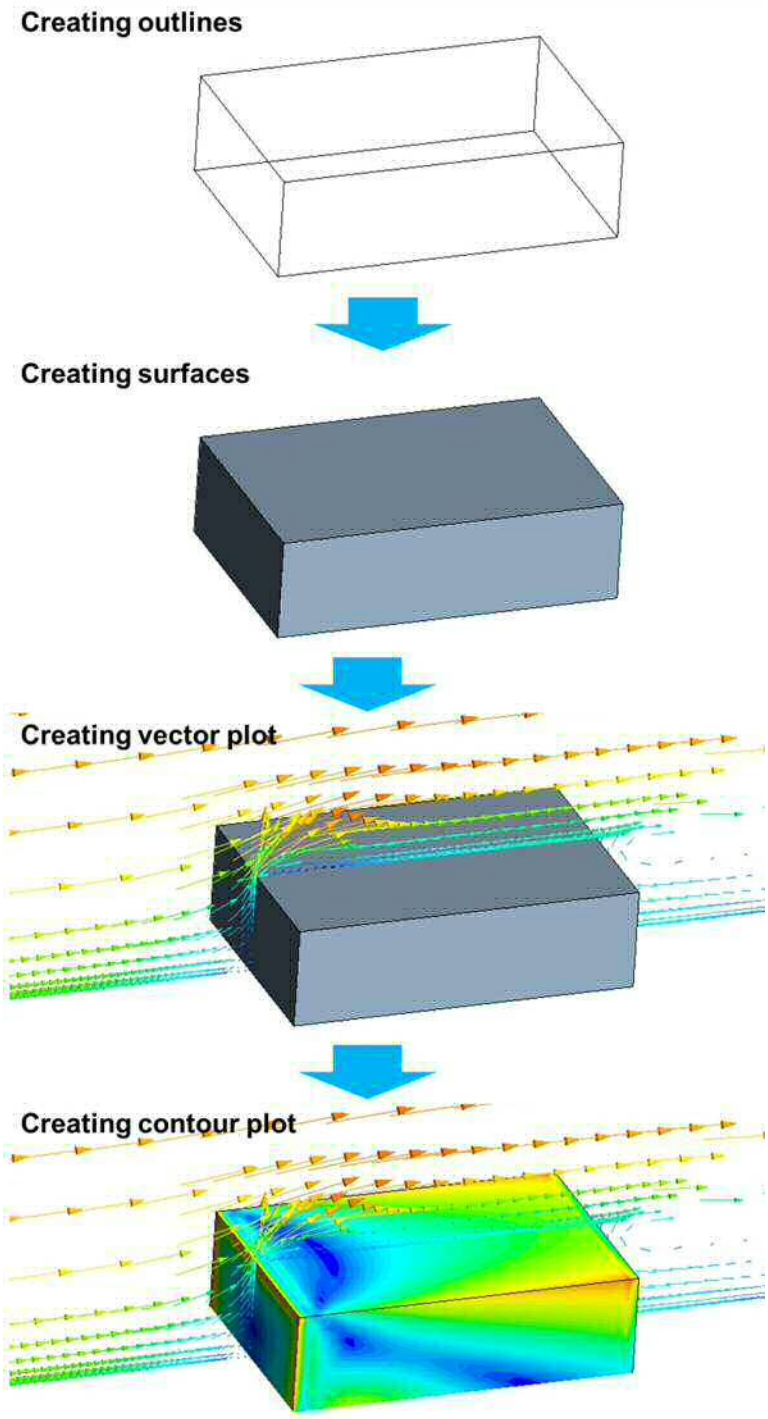

Figure 9.3 - An example of the visualization of CFD results

10. CONCLUSIONS

10.1. Introduction

CFD analysis is now being applied over a wide range of fields and applications. With the development of more powerful computer technology and the increasing frequency of applications such as building design, CFD software is available for both non-experts and designers. Many architects have begun to take advantage of CFD techniques as a design assistance tool because CFD analysis generates detailed information throughout all design stages, providing a flexible and interactive design environment for design decision making. For example, when an architect creates a design, an engineer simulates it using CFD in order to calculate air flows in and around buildings. Through the CFD results, the design can be modified. Thus, a strong collaboration between engineers and architects is needed to improve the quality of buildings.

However, the CFD process is relatively complex and a good understanding of the model on which the numerical method is based is required. In addition, values for various computational conditions must be assigned. Although much of the research published on the use of CFD for predicting building performance has focused on the quantitative aspects of the problem, far fewer studies have involved qualitative investigations into the effectiveness of adopting CFD as a design assistance tool.

The purpose of this research was to improve our understanding of the procedures involved in the implementation of CFD for building design in order to utilize CFD effectively as a design assistance tool and to minimize inaccuracies in its application for building design. Research was conducted through a combined qualitative and quantitative investigation, with the researcher immersing himself in a case study approach to analyze the wind effects around a building. Through this research process, the computational parameters and conditions involved in CFD analyses of wind flow on buildings were identified while focusing on addressing the study's research questions:

1) What computational parameters are used in the context of the CFD analysis of wind flow around a building?
2) How has the wind tunnel testing informed the CFD modeling process?
3) How are the credibility and reliability of the CFD results determined?
4) What CFD tool is most appropriate to support architectural design decision making? and
5) How can CFD modeling be integrated with the architectural design process?

This chapter summarizes the research findings of this study. During the process of conducting this research, many valuable lessons were learned. These lessons are presented here to describe the CFD simulation process and provide recommendations for the effective use of CFD.

10.2. Methodology

The research was designed to provide a better understanding of the CFD simulation process for wind flow around a building through the case study research method. For data collection, the detailed description and analysis of computational parameters and conditions involved in the early design process is presented in Chapters 3 through 7. Chapter 3 reviewed several best practice guidelines for CFD simulations to identify the most important computational parameters concerning wind flow around buildings. Chapter 4 presented an analysis of four recent journal articles using the ten-iterative steps approach to achieve more generic and purposeful CFD guidelines focused on wind flow around a building. Chapter 5 presented the results of wind tunnel tests conducted at the IBHS facility to examine wind flow patterns on a roof surface and in Chapter 6 three sensitivity analyses were conducted to investigate the impact of the selected computational parameters. The computational parameters identified in Chapters 3 to 6 were then applied to the case studies. Through three case studies, the computational parameters were specified in Chapter 7.

The data collected from the early design stage were categorized in the schematic design stage in terms of the two themes that emerged from the data, namely 1) Which computational parameters maximize the accuracy of the CFD modeling? and 2) Which computational parameters facilitate

the effective use of CFD as a design assistance tool regarding time required and ease of use? These two themes are discussed below in the context of CFD investigations of wind flow around buildings.

10.3. Research findings

10.3.1. Selecting the commercial code

Generally, the code FLUENT has been most widely applied to solve flow problems. All the journal articles in Chapter 4 used FLUENT for their studies. As mentioned in Appendix, FLUENT has an additional tool for mesh generation called GAMBIT, while STAR-CCM+ provides a single integrated software environment from CAD creation to post-processing that can decrease the time associated with repairing CAD problems and repeating simulations on design variables easily. In addition, the interactive graphical interface of STAR-CCM+ allows non-experts to use a step-by-step approach for specific tasks. Moreover, the cost of the FLUENT license is prohibitively expensive for researchers, while STAR-CCM+ provides an academic license and professional training without charge. For the sensitivity analysis and case studies in this study, the approaches offered by STAR-CCM+ performed the repeated simulations more easily and faster. Considering these advantages, STAR-CCM+ is preferred to assist design development in the architectural design process.

10.3.2. Preparing the geometry

Generally, it is very important to determine how best to prepare the geometry in a format such as an AutoCAD file before importing it to the computational domain. This is a very time consuming process. Thus, the recommendations made by best practice guidelines are generally employed. As described in Chapter 3, the area of a radius 1-2 H from the building of interest should be reproduced as accurately as possible, where H is the height of the tallest building in the region of interest. In addition, at least one additional street block in each direction around the region of interest is also clearly reproduced, then buildings located away from the central region can be

represented by simple blocks. Considering the analysis in Chapter 8, wind flow in the urban area can be adequately represented using the recommendations made by best practice guidelines.

10.3.3. Importing the geometry

After determining the level of detail to be included in the geometrical representation, the next consideration is to import the geometry into the computational domain. In general, most architectural geometry is created in a native AutoCAD file format. The surface data of the AutoCAD file can be imported into the commercial code after the AutoCAD file has been thoroughly checked.

10.3.4. Creating the computational domain

The computational domain size is generally determined by the recommendations provided by best practice guidelines. The analysis of the effect of different domain sizes conducted for this study highlight the need for care when setting the size of the computational domain in order to reproduce the flow field around the building of interest as accurately as possible. As described in Chapters 6 and 7, the recommendations made by best practice guidelines for the computational domain size can be employed in most CFD investigations for building design.

10.3.5. Generating grids

Generally, two types of grids can be used to generate the mesh. When selecting a grid type, this may depend on the details of the geometry. Both the literature and personal experience suggest that a hexahedral mesh is to be preferred because it can provide more accurate results than a tetrahedral mesh. However, it is not easy to create a complex geometry using a hexahedral mesh. When using a hexahedral mesh for a complex geometry, there are several possible approaches but grid refinement is recommended. However, it is not easy to learn how to perform grid refinement. Although the commercial code does provide an easier way to refine the meshes, it may cause computational errors. Although a tetrahedral mesh provides less accurate results than

a hexahedral mesh, it is automatically generated. Thus, tetrahedral meshes are recommended for use in modeling wind flow around buildings rather than hexahedral meshes.

Concerning the number of cells, at least 10 cells per cube root of the building volume of interest should be used, as suggested by the best practice guidelines. Although more cells can be generated in order to achieve more accurate results, this would require three or four times longer running times. In order to reduce running time and at the same time avoid errors, recommendations from the best practice guidelines can be used for grid resolutions.

10.3.6. Selecting a turbulence model

Before considering which turbulence model to use, a choice must be made between the steady-state and unsteady approach. If the steady-state approach is selected, then RANS equations with various k-ε turbulence models have been used successfully in many studies because of the easier access and shorter running time compared to the LES model. When CFD simulations began to be widely used a decade ago, the basic model, namely the standard k-ε turbulence model, was used for building analysis. However, the advent of more powerful computers has allowed other models such as the realizable k-ε model and the RNG k-ε model, among others, to be used more frequently than the standard k-ε model.

In the case of the unsteady approach, the LES model can be employed. As computer technology continues to develop, time-dependent turbulence models will become feasible for many industrial applications. Generally LES provides more accurate and detailed information about the flow field than the RANS model. However, it also requires considerably higher computing power than RANS. Depending on the capacity of the computers available, LES may become more widely used. Where more detailed information regarding the turbulence in and around buildings is required, the LES model is preferred.

For most architectural design problems, the RANS approach is thus more useful than LES in terms of time-efficiency and ease of use. In the future, more turbulence models based on RANS

are likely to be developed, and these are likely to maintain their advantage with regard to the computer resources required.

10.3.7. Boundary conditions

For an accurate simulation, it is important to reproduce the influence of the surroundings as accurately as possible in the computational domain. Significant care is therefore required when specifying the boundary conditions including the inlet, outlet, top and sides boundary conditions.

In general, the data from experiments, including the turbulent kinetic energy k and dissipation rate ε, are needed to prescribe the profiles for the inlet boundary conditions. The velocity profile at the inlet can be achieved using logarithmic or power laws. However, the information pertaining to wind data and turbulence from measurements are not generally available because a design concept at the schematic design stage does not yet exist and it is time consuming and costly. In order to specify the mean velocity profile at the inlet, the information obtained from previous studies related to similar issues or the weather condition at the site can be employed. For the outlet boundary conditions, zero static pressure can be imposed. In addition, symmetrical boundary conditions can be employed for the top and sides of the domain.

10.3.8. Numerical schemes and the algorithm

For the steady state simulation, the SIMPLE algorithm is employed for pressure-velocity coupling, pressure interpolation is second order and second-order discretization schemes are used for both the convection terms and the viscous terms of the governing equations. In the case of unsteady simulation, the SIMPLE algorithm with the central-differencing scheme can be used.

10.3.9. Convergence criterion

CFD simulations employ iterative methods to solve the algebraic system of equations. The termination criterion is usually based on the residuals of the corresponding equations. The convergence is assumed to obtain when all scaled residuals are in the range of $10^4 – 10^6$.

10.4. Recommendations for the computational parameters for various building design objectives

Adopting a combined qualitative and quantitative investigation, a comprehensive set of recommendations for the computational parameters to guide the use of CFD for building design were achieved. These recommendations for various building design objectives are summarized in Table 10.1.

Table 10.1 - Recommendations for the computational parameters for various building design objectives

Computational parameters		Natural ventilation design	Building site planning	Pedestrian wind comfort	Pollutant dispersion	Wind uplift on the roof
CFD Codes	STAR-CCM+	✓	✓	✓	✓	✓
	FLUENT					
Preparation of the geometry by Best Practice Guidelines		✓	✓	✓	✓	✓
The Computational domain size by Best Practice Guidelines		✓	✓	✓	✓	✓
Grid design	Hexahedral grids	✓			✓	✓
	Tetrahedral grids		✓	✓		
Turbulence models	The RANS models	✓	✓	✓		
	The LES model				✓	✓
Boundary conditions	The inlet: Power law	✓	✓	✓	✓	✓
	The inlet: Logarithmic law					
	The outlet, top and sides by Best Practice Guidelines	✓	✓	✓	✓	✓
Numerical algorithm	The SIMPLE	✓	✓	✓	✓	✓
Numerical scheme	Second order	✓	✓	✓		
	Central differencing				✓	✓
Time steps and intervals						✓

10.5. Lessons-learned through the research process

Based on the data collected through document analysis and participant observations, a set of useful lessons-leaned for CFD modeling was achieved. Among the lessons-learned through the research, most were related to the pre-processing because this phase includes the preparation of the geometry, grid generation and the selection of turbulence models. Designers and architects who want to utilize CFD as a design assistance tool need to carefully consider the selection of the computational parameters in the pre-processing phase.

Although these lessons are insufficient for the CFD modeling, it could be a starting point to allow architects and designers to consider the use of CFD in their design development. In addition, I hope that these lessons can be used to assist architecture students to develop various design alternatives at the early design stage using CFD simulations.

10.6. Suggestions for further research

CFD is being increasingly used by many industries to provide an insight into existing technologies or products. However, few studies for the use of CFD in the architectural design process have been conducted, specifically in the early design stages when many critical decisions are made, including those pertaining to the building performance (Kaijima et al., 2013). The main purpose of this research was not to extend knowledge in the field of CFD but to improve our understanding of CFD simulations in order to facilitate their more effective use during the architectural design stage. The outcomes of this research suggest several possibilities for further research:

Generally, the application of CFD has been limited to the schematic design phase. CFD simulations are seldom used for the generation of design, probably due to mathematical issues and the complexities of computational parameters. In addition, CFD tools are not routinely employed to support different design alternatives at the early design phase. In the case of the example of the Bishopsgate tower, CFD contributed to the form development of the aerodynamic shape of the building. The tower designed by architects Kohn Pedersen Fox Associates is the tallest building in London and it is nearly 300 m tall (Hesselgren et al., 2007). Due to wind loading problems, its double skin of partially overlapping glazing panels introduced "Snake-Skin" design which is a singly and doubly curved façade (Hanna et al., 2010). For the façade design, CFD was used to improve the performance of natural ventilation while taking advantage of the prevailing winds (Hesselgren et al., 2007). In addition, CFD was used to predict wind effects on pedestrian areas at the ground level because of the possible impact that could be adversely affected by winds redirected and amplified by the building's extreme size (Hanna et al., 2010). As a result, the vertical surfaces of the glazed tower expanded outward to form a canopy and redirect wind flow at the ground level for pedestrian wind comfort (Hanna et al., 2010). Although the CFD modeling in this example was performed by engineers, it showed that CFD can contribute to the early design stage in the architectural design process. Future work could investigate the connection between design variables at the early design phase and the computational parameters needed in order to utilize CFD for form development in the

architectural design process. In addition, it is expected that CFD will become an integrated component of the design process.

Moreover, CFD simulations have been conducted by engineers and experts to test both macro and micro levels of performance in the example of the Bishopsgate tower. Although CFD simulations performed by engineers and experts can be applied to all design stages, the main benefits of CFD cannot yet be realized by architects. In addition, large amounts of input data are required. To facilitate the effective use of CFD by architects, this research could serve as the first step for utilizing CFD in their design development, although it will still require some knowledge of computational parameters. In the future, it would be beneficial to identify and define computational parameters focused on design-oriented applications to enable architects to make full use of CFD.

While this research discussed the application of CFD to model wind flows around buildings, it would be very helpful to investigate computational parameters for air flow in indoor environments such as natural ventilation strategies and HVAC system design. In the case of the San Francisco Federal Building designed by Morphosis architects, the design concept of the building maximizes natural airflow for cooling and ventilation in order to provide a comfortable interior environment using CFD simulation (Mayne, 2008). According to various space conditioning strategies applied for the building, the first five levels are fully air-conditioned because of high concentrations of people and equipment, while the windows automatically adjust to allow fresh air directly into the building for natural ventilation and free cooling above the fifth floor (Mayne, 2008). As can be seen in this example, CFD can contribute to the climate control in order to improve indoor environmental quality.

In addition, the example of the San Francisco Federal building presented the phenomenological concepts in the architectural design process looking at the relationship between a person and space. For the phenomenological approach, there are two roles of architecture: one is to make us aware of our presence in the space and the other is to make us aware of our place in the outside world. According to the example above, breezes can pass the space controlled of our own

identifying ourselves in the space. Moreover, breezes coming from the outside allow the building to be connected to the outside world through the windows. In this sense, CFD can contribute the two roles in phenomenology. Visualizing the results, CFD allows us to see air flow in the space and to make us to design the openings in the space. It can also help architecture students to understand indoor environmental issues in their design development.

Through the present study, pre-processing including problem thinking, meshing and generation of the computational model is still the most time-consuming and difficult process for architects in order to utilize CFD in the architectural design process. During the early design stage, multiple geometries can be generally created for a particular building design. It means that multiple generations of the computational model such as the computational domain and grids are needed for the design development. Although architects require visual accuracy and speed rather than qualities of the results from analysis in the early design stage to compare multiple geometries, a significant amount of pre-processing should be repetitive for the results at the current state of technology (Kaijima et al., 2013).

However, in the future, CFD software can be integrated with CAD systems from the graphical interface to model preparation to easy meshing in order to avoid the repetitive pre-processing processes in the early design stage. In addition, the computational time and resources will be decreased with the advent of more powerful computers. It can offer more available computational parameters such as turbulence models for making fast and accurate comparisons of various building designs.

The present study showed that CFD modeling can be effectively extended into the design process in architecture. Although the present study cannot give exact answers, I believe that it can help architects and designers to facilitate CFD as a design assistance tool and assist to make fact-assisted design decisions through the visualization of the airflow in and around buildings. In addition, this research will be of assistance to architectural students seeking to use CFD for building design, especially its use for issues related to environmental design.

Through the researcher's roles as architect and CFD simulator, he will continue to seek new ways of bridging the gap between architecture and engineering in order to facilitate the use of CFD simulations in the architectural design process.

REFERENCES

Abohela, I., Hamza, N., & Dudek, S. (2013). Effect of roof shape, wind direction, building height and urban configuration on the energy yield and positioning of roof mounted wind turbines. *Renewable Energy*, 50, 1106-1118.
ISSN 0960-1481, http://dx.doi.org/10.1016/j.renene.2012.08.068.

Ai, Z.T., & Mak, C.M. (2013). CFD simulation of flow and dispersion around an isolated building: Effect of inhomogeneous ABL and near-wall treatment. *Atmospheric Environment*, 77, 568-578.
ISSN 1352-2310, http://dx.doi.org/10.1016/j.atmosenv.2013.05.034.

ANSYS FLUENT 12.0 User's Guide

Antonopoulos, D.M. (1981). Large eddy simulation of a passive scalar inisotropic turbulence. *Journal of Fluid Mechanics*, 104, 55-79.

Alexander, D, Jenkins, H., & Jones, P. (1997). A comparison of wind tunnel and CFD methods applied to natural ventilation design. *Proceedings of Building Simulation '97*, pp. 321-326.

Anderson, J. (1995). *Computational Fluid Dynamics: The basics with applications*. New York, NY: McGraw-Hill, Inc.

Bakker, A., Haidari, A.H., Oshinowo, L.M. (2001). Realize Greater Benefits from CFD, CEP magazine, 45-53. Retrieved from http://www.bakker.org/cfmbook/030145.pdf

Balocco, C. & Lio, P. (2011). Assessing ventilation system performance in isolation rooms. *Energy and Buildings*, 43(1), 246-252.
ISSN 0378-7788, http://dx.doi.org/10.1016/j.enbuild.2010.09.020.

Balogh, M., Parente, A., & Benocci, C. (2012). RANS simulation of ABL flow over complex terrains applying an Enhanced k-ε model and wall function formulation: Implementation and comparison for fluent and OpenFOAM. *Journal of Wind Engineering and Industrial Aerodynamics*, 104–106, 360-368.
ISSN 0167-6105, http://dx.doi.org/10.1016/j.jweia.2012.02.023.

Bangalee, M.Z.I., Lin, S.Y., & Miau, J.J. (2012). Wind driven natural ventilation through multiple windows of a building: A computational approach. *Energy and Buildings*, 45, 317-325. ISSN 0378-7788, http://dx.doi.org/10.1016/j.enbuild.2011.11.025.

Baskaran, B., Murty, B., & Wu, J. (2009). Calculating roof membrane deformation under simulated moderate wind uplift pressures. *Engineering Structures*, 31 (3), 642-650. ISSN 0141-0296, http://dx.doi.org/10.1016/j.engstruct.2008.10.013.

Bern, M., & Plassmann, P. (2000).Chapter 6 - Mesh Generation, In Handbook of Computational Geometry, edited by J.-R. Sack and J. Urrutia, North-Holland, Amsterdam, 291-332, ISBN 9780444825377, http://dx.doi.org/10.1016/B978-044482537-7/50007-3.

Blessing, C., Chowdhury, A., Lin, J., & Huang, P. (2009). Full-scale validation of vortex suppression techniques for mitigation of roof uplift. *Engineering Structures*, 31 (12) 2936-2946. ISSN 0141-0296, http://dx.doi.org/10.1016/j.engstruct.2009.07.021

Blocken, B., Defraeye, T., Derome, D., & Carmeliet, J. (2009). High-resolution CFD simulations for forced convective heat transfer coefficients at the facade of a low-rise building. *Building and Environment*, 44(12), 2396-2412. ISSN 0360-1323, http://dx.doi.org/10.1016/j.buildenv.2009.04.004.

Blocken, B., & Gualtieri, C. (2012). Ten iterative steps for model development and evaluation applied to Computational Fluid Dynamics for Environmental Fluid Mechanics. *Environmental Modelling & Software*, 33, 1-22. ISSN 1364-8152, http://dx.doi.org/10.1016/j.envsoft.2012.02.001.

Blocken, B., Janssen, W.D., & Hooff, T.V. (2012). CFD simulation for pedestrian wind comfort and wind safety in urban areas: General decision framework and case study for the Eindhoven University campus. *Environmental Modelling & Software*, 30, 15-34. ISSN 1364-8152, http://dx.doi.org/10.1016/j.envsoft.2011.11.009

Blocken, B., & Persoon, J. (2009). Pedestrian wind comfort around a large football stadium in an urban environment: CFD simulation, validation and application of the new Dutch wind nuisance standard. *Journal of Wind Engineering and Industrial Aerodynamics*, 97 (5–6), 255-270. ISSN 0167-6105, http://dx.doi.org/10.1016/j.jweia.2009.06.007.

Blocken, B., Stathopoulos, T., Saathoff, P., & Wang, X. (2008). Numerical evaluation of pollutant dispersion in the built environment: Comparisons between models and experiments. *Journal of Wind Engineering and Industrial Aerodynamics*, 96 (10–11), 1817-1831. ISSN 0167-6105, http://dx.doi.org/10.1016/j.jweia.2008.02.049.

Blocken, B., Stathopoulos, T., Carmeliet, J., & Hensen, J.L.M. (2011). Application of computational fluid dynamics in building performance simulation for the outdoor environment: an overview. *Journal of Building Performance Simulation*, 4 (2), 157-184.

Bosbach, J., Pennecot, J., Wagner, C., Raffel, M., Lerche, T., & Repp, S. (2006). Experimental and numerical simulations of turbulent ventilation in aircraft cabins. *Energy*, 31 (5), 694-705. ISSN 0360-5442, http://dx.doi.org/10.1016/j.energy.2005.04.015.

Casey, M., & Wintergerste, T. (2000). Best Practice Guidelines, ERCOFTAC Special Interest Group on Quality and Trust in Industrial CFD. ERCOFTAC, Brussels.

Castro I.P., & Robins, A.G. (1977). The flow around a surface-mounted cube in uniform and turbulent streams. J Fluid Mech 1977;79:307e35.

Chand, I., Bhargava, P.K., & Krishak, N.L.V. (1998). Effect of balconies on ventilation inducing aeromotive force on low-rise buildings. *Build Environment*, 33, 385-396. ISSN 0360-1323, http://dx.doi.org/10.1016/S0360-1323(97)00054-1.

Chavez, M., Hajra, B., Stathopoulos, T., & Bahloul, A. (2011). Near-field pollutant dispersion in the built environment by CFD and wind tunnel simulations. *Journal of Wind Engineering and Industrial Aerodynamics*, 99(4), 330-339. ISSN 0167-6105, http://dx.doi.org/10.1016/j.jweia.2011.01.003.

Chavez, M., Hajra, B., Stathopoulos, T., & Bahloul, A. (2012). Assessment of near-field pollutant dispersion: Effect of upstream buildings. *Journal of Wind Engineering and Industrial Aerodynamics*, 104–106, 509-515. http://dx.doi.org/10.1016/j.jweia.2012.02.019.

Chen, Q. (2009). Ventilation performance prediction for buildings: A method overview and recent applications. *Building and Environment*, 44 (4), 848-858. ISSN 0360-1323, http://dx.doi.org/10.1016/j.buildenv.2008.05.025.

Chen, X., & Zhou, N. (2007). Equivalent static wind loads on low-rise buildings based on full-scale pressure measurements. *Engineering Structures*, 29(10), 2563-2575.
ISSN 0141-0296, http://dx.doi.org/10.1016/j.engstruct.2007.01.007.

Cheung, J.O.P., & Liu, C.H. (2011). CFD simulations of natural ventilation behaviour in high-rise buildings in regular and staggered arrangements at various spacings. *Energy and Buildings*, 43(5), 1149-1158.
ISSN 0378-7788, http://dx.doi.org/10.1016/j.enbuild.2010.11.024.

Chiang, W. H., Wang, C.Y., & Huang, J. S. (2012). Evaluation of cooling ceiling and mechanical ventilation systems on thermal comfort using CFD study in an office for subtropical region. *Building and Environment*, 48, 113-127.
ISSN 0360-1323, http://dx.doi.org/10.1016/j.buildenv.2011.09.002.

Chung, T. (2002). *Computational fluid dynamics*. Newyork, NY: Cambridge University Press.

Cresswell, J.W. (2009). *Research design: Qualitative, Quantitative, and Mixed Methods Approaches*. Sage Publications, Inc. London, United Kingdom.

Cochran, L., & Derickson, R. (2011). A physical modeler's view of Computational Wind Engineering. *Journal of Wind Engineering and Industrial Aerodynamics*, 99 (4) 139-153.
ISSN 0167-6105, http://dx.doi.org/10.1016/j.jweia.2011.01.015.

Drew, D.R., Barlow, J.F., & Lane, S.E. (2013). Observations of wind speed profiles over Greater London, UK, using a Doppler lidar. *Journal of Wind Engineering and Industrial Aerodynamics*, 121, 98-105.
ISSN 0167-6105, http://dx.doi.org/10.1016/j.jweia.2013.07.019.

Elsharawy, M., Stathopoulos, T., & Galal, K. (2012). Wind-induced torsional loads on low buildings. *Journal of Wind Engineering and Industrial Aerodynamics*, 104–106, 40-48.
ISSN 0167-6105, http://dx.doi.org/10.1016/j.jweia.2012.03.011.

English, T.G. (2007). Application of experimental design of efficient wind tunnel testing: the Tandem wing MAC case (Master's thesis). Retrieved from
http:// http://diginole.lib.fsu.edu/cgi/viewcontent.cgi?article=1423&context=etd

Ferziger, J. H. (1990). Approaches to turbulent flow computation: Applications to flow over obstacles. *Journal of Wind Engineering and Industrial Aerodynamics*, 35, 1-19. ISSN 0167-6105, http://dx.doi.org/10.1016/0167-6105(90)90208-T.

Franke, J., Hellsten, A., Schlünzen, H., & Carissimo, B. (2007). Best Practice Guideline for the CFD Simulation of Flows in the Urban Environment. COST 732: Quality Assurance and Improvement of Microscale Meteorological Models. COST Office Brussels, ISBN 3-00-018312-4.

Franke, J., Hirsch, C., Jensen, A.G., Krüs, H.W., Schatzmann, M., Westbury, P.S., Miles, S.D., Wisse, J.A., & Wright, N.G. (2004). Recommendations on the use of CFD in wind engineering. Proc. Int. Conf. Urban Wind Engineering and Building Aerodynamics. In: van Beeck, J.P.A.J. (Ed.), COST Action C14, Impact of Wind and Storm on City Life Built Environment. von Karman Institute, Sint-Genesius- Rode, Belgium. 5-7 May 2004.

Glicksman, L., & Lin, J. (Eds.). (2006). *Sustainable Urban Housing in China*. Alliance for Global Sustainability Bookseries Volume 9. ISBN: 978-1-4020-4785-5 (Print) 978-1-4020-4786-2 (Online). Springer, Netherlands.

Gousseau, P., Blocken, B., Stathopoulos, T. & Heijst, G.J.F.V. (2011). CFD simulation of near-field pollutant dispersion on a high-resolution grid: A case study by LES and RANS for a building group in downtown Montreal, *Atmospheric Environment*, 45 (2), 428-438. ISSN 1352-2310, http://dx.doi.org/10.1016/j.atmosenv.2010.09.065.

Grant, E.J. (2003). Design and implementation of a pressure-equalizing vent system for low-slope roofs (Master's thesis).

Graumann, A., Houston, T., Lawrimore, J., Levinson, D., Lott, N., McCown, S., Stephens, S., & Wuertz, D. (2005). *Hurricane Katrina A Climatological Perspective-Preliminary Report*, NOAA's Natioanal Climatic Data Center. Retrieved Jan, 2005, from http://www.ncdc.noaa.gov/

Groat, L. & Wang, D. (2002). *Architectural research methods*. New York: John Wiley & Sons, Inc.

Gromke, C., Buccolieri, R., Sabatino, S.D., & Ruck, B. (2008). Dispersion study in a street canyon with tree planting by means of wind tunnel and numerical investigations – Evaluation of CFD data with experimental data. *Atmospheric Environment*, 42 (37), 8640-8650.
ISSN 1352-2310, http://dx.doi.org/10.1016/j.atmosenv.2008.08.019.

Hanna, S., Hesselgren, L., Gonzalez, V., & Vargas, I. (2010). Beyond simulation: designing for uncertainty and robust solutions. *In: Proceedings of the 2010 Spring Simulation Multiconference* (SpringSim '10), 182.
DOI10.1145/1878537.1878727

Hefny, M.M. & Ooka, R. (2009). CFD analysis of pollutant dispersion around buildings: Effect of cell geometry. *Building and Environment*, 44 (8), 1699-1706.
ISSN 0360-1323, http://dx.doi.org/10.1016/j.buildenv.2008.11.010.

Hernández, M. A. G., López, A. I. M., Jarzabek, A., Perales, J. M. P., Wu, Y., & Xiaoxiao, S. (2013). Design Methodology for a Quick and Low-Cost Wind Tunnel, Wind Tunnel Designs and Their Diverse Engineering Applications, Dr. Noor Ahmed (Ed.). ISBN: 978-953-51-1047-7, InTech, DOI: 10.5772/54169. Retrieved from: http://www.intechopen.com/books/wind-tunnel-designs-and-their-diverse-engineering-applications/design-methodology-for-a-quick-and-low-cost-wind-tunnel

Hertwig, D., Efthimiou, G.C., Bartzis, J.G., & Leitl, B. (2012). CFD-RANS model validation of turbulent flow in a semi-idealized urban canopy. *Journal of Wind Engineering and Industrial Aerodynamics*, 111, 61-72.
ISSN 0167-6105, http://dx.doi.org/10.1016/j.jweia.2012.09.003.

Hesselgren, L., Charitou, R., & Dritsas, S. (2007). The Bishopsgate Tower Case Study. *Journal International Journal of Architectural Computing,* 5(1), 62-81.
ISSN 1478-0771, DOI 10.1260/147807707780912912.

Hirsch, C. (2006). The Development of a Framework for CFD Validation and Best Practice: The QNET-CFD Knowledge Base. *Chinese Journal of Aeronautics*, 19(2), 105-113.
ISSN 1000-9361, http://dx.doi.org/10.1016/S1000-9361(11)60290-2.

Ho, T., Surry, D., Morrish, D., & Kopp, G. (2005). The UWO contribution to the NIST aerodynamic database for wind loads on low buildings: Part 1. Archiving format and basic aerodynamic data. *Journal of Wind Engineering and Industrial Aerodynamics*, 93(1) 1-30.
ISSN 0167-6105, http://dx.doi.org/10.1016/j.jweia.2004.07.006.

Hooff, T.V., & Blocken, B. (2010). Coupled urban wind flow and indoor natural ventilation modelling on a high-resolution grid: A case study for the Amsterdam ArenA stadium. *Environmental Modelling & Software*, 25 (1), 51-65.
ISSN 1364-8152, http://dx.doi.org/10.1016/j.envsoft.2009.07.008.

Hooff, T.V. & Blocken, B. (2012). Full-scale measurements of indoor environmental conditions and natural ventilation in a large semi-enclosed stadium: Possibilities and limitations for CFD validation. *Journal of Wind Engineering and Industrial Aerodynamics*, 104–106, 330-341.
ISSN 0167-6105, http://dx.doi.org/10.1016/j.jweia.2012.02.009.

Hooff, T.V., & Blocken, B. (2013). CFD evaluation of natural ventilation of indoor environments by the concentration decay method: CO2 gas dispersion from a semi-enclosed stadium. *Building and Environment*, 61, 1-17.
ISSN 0360-1323, http://dx.doi.org/10.1016/j.buildenv.2012.11.021.

Hooff, T.V., Blocken, B., Aanen, L., & Bronsema, B. (2012). Numerical analysis of the performance of a venturi-shaped roof for natural ventilation: Influence of building width. *Journal of Wind Engineering and Industrial Aerodynamics*, 104–106, 419-427,
ISSN 0167-6105, http://dx.doi.org/10.1016/j.jweia.2012.02.013.

Huang, H., Ooka, R., Chen, H., & Kato, S. (2009). Optimum design for smoke-control system in buildings considering robustness using CFD and Genetic Algorithms. *Building and Environment*, 44(11), 2218-2227.
ISSN 0360-1323, http://dx.doi.org/10.1016/j.buildenv.2009.02.002.

Huang, S., Li, Q.S., & Xu, S. (2007). Numerical evaluation of wind effects on a tall steel building by CFD. *Journal of Constructional Steel Research*, 63 (5), 612-627.
ISSN 0143-974X, http://dx.doi.org/10.1016/j.jcsr.2006.06.033.

Jakeman, A.J., Letcher, R.A., & Norton, J.P. (2006). Ten iterative steps in development and evaluation of environmental models. *Environmental Modelling & Software*, 21 (5), 602-614.
ISSN 1364-8152, http://dx.doi.org/10.1016/j.envsoft.2006.01.004.

Janssen, W.D., Blocken, B., & Hooff, T. V. (2013). Pedestrian wind comfort around buildings: Comparison of wind comfort criteria based on whole-flow field data for a complex case study. *Building and Environment*, 5, 547-562.
ISSN 0360-1323, http://dx.doi.org/10.1016/j.buildenv.2012.10.012.

Kaijima, S., Bouffanais, R., & Willcox, K. (2013). Computational Fluid Dynamics for Architectural Design. *In Open Systems: Proceedings of the 18th International Conference on Computer-Aided Architectural Design Research in Asia*, 169-178. CAADRIA. Hong Kong, SAR: The Association for Computer-Aided Architectural Design Research in Asia, 2013.

Karava, P., Athienitis, A.K., Stathopoulos, T., & Mouriki, E. (2012). Experimental study of the thermal performance of a large institutional building with mixed-mode cooling and hybrid ventilation. *Building and Environment*, 57, 313-326.
ISSN 0360-1323, http://dx.doi.org/10.1016/j.buildenv.2012.06.003.

Kataoka, H., & Mizuno, M. (2002). Numerical flow computation around aeroelastic 3D cylinder using inflow turbulence. *Wind and Structures*, 5 (2), 379-392.

Kortelainen, J. (2009). Meshing Tools for Open Source CFD – A Practical Point of View. VTT, Espoo, Finland, Tech. Rep. Retrieved from
http://www.csc.fi/english/pages/lscfd/Documents/MeshingToolsForOpenSourceCFD.pdf.

Kobayashi, T., Chikamoto, T., & Osada, K. (2013). Evaluation of ventilation performance of monitor roof in residential area based on simplified estimation and CFD analysis. *Building and Environment*, 63, 20-30.
ISSN 0360-1323, http://dx.doi.org/10.1016/j.buildenv.2013.01.018.

Lateb, M., Masson,C., Stathopoulos, T., & Bédard, C. (2013). Comparison of various types of k–ε models for pollutant emissions around a two-building configuration. *Journal of Wind Engineering and Industrial Aerodynamics*, 115, 9-21.
ISSN 0167-6105, http://dx.doi.org/10.1016/j.jweia.2013.01.001.

Launder, B.E., & Spalding, D.B. (1974). The numerical computation of turbulent flows. *Computer Methods in Applied Mechanics and Engineering*, 3 (2), 269-289.
ISSN 0045-7825, http://dx.doi.org/10.1016/0045-7825(74)90029-2.

Levitan, M.L., Mehta, K.C., Vann, W.P., & Holmes, J.D. (1991). Field measurements of pressures on the Texas tech building. *Journal of Wind Engineering and Industrial Aerodynamics,* 38, 227-234.
ISSN 0167-6105, http://dx.doi.org/10.1016/0167-6105(91)90043-V.

Li, X.X., Liu, C.H., Leung, D.Y.C., & Lam, K.M. (2006). Recent progress in CFD modeling of wind field and pollutant transport in street canyons. *Atmospheric Environment*, 40, 5640-5658. ISSN 1352-2310, http://dx.doi.org/10.1016/j.atmosenv.2006.04.055.

Li, Y., & Stathopoulos, T. (1997). Numerical evaluation of wind-induced dispersion of pollutants around a building. *Journal of Wind Engineering and Industrial Aerodynamics*, 67-68, 757-766. ISSN 0167-6105, http://dx.doi.org/10.1016/S0167-6105(97)00116-5.

Li, W.W., & Meroney, R.N. (1983). Gas dispersion near a cubical model building. Part I. Mean concentration measurements.*Journal of Wind Engineering and Industrial Aerodynamics*, 12 (1), 15-33.
ISSN 0167-6105, http://dx.doi.org/10.1016/0167-6105(83)90078-8.

Liseikin, V.D. (2010). *Grid Generation methods*, Springer, Russia.

Liu, Z., Smith, J., Masters, F., & Reinhold, T. (2009). Assessment of wind storm facility at the Insurance Center for Building Safety Research. *The Seventh Asia-Pacific Conference on Wind Engineering*, Nov 8-12 2009, Taipei, Taiwan.

Lo, L.J., Banks, D., & Novoselac, A. (2013). Combined wind tunnel and CFD analysis for indoor airflow prediction of wind-driven cross ventilation. *Building and Environment*, 60, 12-23. ISSN 0360-1323, http://dx.doi.org/10.1016/j.buildenv.2012.10.022.

Mayne, T. (2008). The New Federal Building. *Design Management Review*, 19(4), 56-64.

Menter, F., Hemstrom, B., Henrikkson, M., Karlsson, R., Latrobe, A., Martin, A., Muhlbauer, P., Scheuerer, M., Smith, B., Takacs, T., & Willemsen, S. (2002). CFD Best Practice Guidelines for CFD Code Validation for Reactor-safety Applications. Report EVOLECORA-D01, Contract No. FIKS-CT-2001-00154, 2002.

Meroney, R.N., Leitl, B.M., Rafailidis, S., & Schatzmann, M. (1999). Wind-tunnel and numerical modeling of flow and dispersion about several building shapes. *Journal of Wind Engineering and Industrial Aerodynamics*, 81, 333-345.
ISSN 0167-6105, http://dx.doi.org/10.1016/S0167-6105(99)00028-8.

Mirzaei, P. A. & Carmeliet, J. (2012). Dynamical modeling of stochastic wind flow in street canyons. *International High Performance Buildings Conference*, 66. Retrieved from: http://docs.lib.purdue.edu/ihpbc/66

Molina-Aiz, F.D., Fatnassi, H., Boulard, T., Roy, J.C., & Valera, D.L. (2010). Comparison of finite element and finite volume methods for simulation of natural ventilation in greenhouses. *Computers and Electronics in Agriculture*, 72 (2), 69-86.
ISSN 0168-1699, http://dx.doi.org/10.1016/j.compag.2010.03.002.

Montazeri, H., & Blocken, B. (2013). CFD simulation of wind-induced pressure coefficients on buildings with and without balconies: Validation and sensitivity analysis. *Building and Environment*, 60, 137-149.
ISSN 0360-1323, http://dx.doi.org/10.1016/j.buildenv.2012.11.012.

Montazeri, H., Blocken, B., Janssen, W.D., & Hooff, T.V. (2013). CFD evaluation of new second-skin facade concept for wind comfort on building balconies: Case study for the Park Tower in Antwerp. *Building and Environment*, 68, 179-192.
ISSN 0360-1323, http://dx.doi.org/10.1016/j.buildenv.2013.07.004.

Moonen, P., Dorer, V., & Carmeliet, J. (2012). Effect of flow unsteadiness on the mean wind flow pattern in an idealized urban environment. *Journal of Wind Engineering and Industrial Aerodynamics*, 104–106, 389-396.
ISSN 0167-6105, http://dx.doi.org/10.1016/j.jweia.2012.01.007.

Morrison, M., Brown, T., & Liu Z. (2012 a). Comparison of field and full-scale laboratory peak pressures at the IBHS research center. *Advances in Hurricane Engineering*, 1109-1124.
http://dx.doi.org/10.1061/9780784412626.097.

Morrison, M.J., Cope, A.D., and Reinhold, T.A. (2012 b). *Performance of the Acrylife Roof Vent*. Technical report: IBHS-12XX01.

Morrison, M., & Kopp, G. (2011). Performance of toe-nail connections under realistic wind loading, *Engineering Structures*, 33(1), 69-76.
ISSN 0141-0296, http://dx.doi.org/10.1016/j.engstruct.2010.09.019.

Moukalled, F., & Darwish, M. (2000). A unified formulation of the segregated class of algorithms for fluid flow at all speeds. *Numerical Heat Transfer, Part B: Fundamentals: An International Journal of Computation and Methodology*, 37(1), 103-139. DOI:10.1080/104077900275576

Murakami, S. (1993). Comparison of various turbulence models applied to a bluff body. *Journal of Wind Engineering and Industrial Aerodynamics*, 46–47, Pages 21-36.
ISSN 0167-6105, http://dx.doi.org/10.1016/0167-6105(93)90112-2.

Murakami, S. (1998). Overview of turbulence models applied in CWE–1997. *Journal of Wind Engineering and Industrial Aerodynamics*, 74–76(1), 1-24.
ISSN 0167-6105, http://dx.doi.org/10.1016/S0167-6105(98)00004-X.

National Program for Applications-Oriented Research in CFD. (2012). NPARC Alliance CFD verification and validation. Retrieved from
http://www.grc.nasa.gov/WWW/wind/valid /tutorial/process.html

Norton, T., Grant, J., Fallon, R., & Sun, D.W. (2010). Optimising the ventilation configuration of naturally ventilated livestock buildings for improved indoor environmental homogeneity. *Building and Environment*, 45(4), 983-995.
ISSN 0360-1323, http://dx.doi.org/10.1016/j.buildenv.2009.10.005.

Oliveira, G., Santos, L., Martins, A., Becker, G., Reis, M., Spogis, N., & Silva, R. (2008). A tool for parametric geometry and grid generation for aircraft configurations, *Proceedings of 26th congress of the international council of the aeronautical sciences*, Anchorage, Alaska, 14-19 September 2008, pp ICAS 2008-2.5.3.

Ono, Y., Tamura, T., & Kataoka, H. (2008). LES analysis of unsteady characteristics of conical vortex on a flat roof. *Journal of Wind Engineering and Industrial Aerodynamics*. 96, 2007-2018.
ISSN 0167-6105, http://dx.doi.org/10.1016/j.jweia.2008.02.021.

Patton, M. (2002). *Qualitative Research and Evaluation Methods*, Sage Publications, USA.

Patankar, S. V., & Spalding, D. B. (1972). A calculation procedure for heat, mass and momentum transfer in three-dimensional parabolic flows. *International Journal of Heat and Mass Transfer*, 15 (10), 1787-1806.
ISSN 0017-9310, http://dx.doi.org/10.1016/0017-9310(72)90054-3.

Pielke Jr., R.A., Gratz, J., Landsea, C.W., Collins, D., Saunders, M.A., & Musulin, R. (2008). *Normalized hurricane damage in the United States: 1900–2005*. Nat. Hazard. Rev. 9, 29–42, http://dx.doi.org/10.1061/1527-69889:1.

Pieterse, J.E., & Harms, T.M. (2013). CFD investigation of the atmospheric boundary layer under different thermal stability conditions. *Journal of Wind Engineering and Industrial Aerodynamics*, 121, 82-97.
ISSN 0167-6105, http://dx.doi.org/10.1016/j.jweia.2013.07.014.

Ramponi, R., & Blocken, B. (2012). CFD simulation of cross-ventilation for a generic isolated building: Impact of computational parameters. *Building and Environment*, 53, 34-48.
ISSN 0360-1323, http://dx.doi.org/10.1016/j.buildenv.2012.01.004.

Reinhold, T. (1982). *Wind tunnel modeling for civil engineering applications*. Cambridge: Cambridge University Press.

Robson, B.J., Hamilton, D.P., Webster, I.T., & Chan, T. (2008). Ten steps applied to development and evaluation of process-based biogeochemical models of estuaries. *Environmental Modelling & Software*, 23 (4), 369-384.
ISSN 1364-8152, http://dx.doi.org/10.1016/j.envsoft.2007.05.019.

Rowley, J.(2002). Using Case Studies in Research. Management Research News, 25 (1), 16 -27. doi:0.1108/01409170210782990.

Rui, Z., Guangbei, T., & Jihong, L. (2008). Study on biological contaminant control strategies under different ventilation models in hospital operating room. *Building and Environment*, 43(5), 793-803.
ISSN 0360-1323, http://dx.doi.org/10.1016/j.buildenv.2007.01.018.

Scott, T., Banks, D. & Mishra, A. (2006). Introduction to applied Computational Fluid Dynamics for the biological safety environment. *Journal of the American Biological Safety Association*, 11(4), 188-196. Retrieved from http://www.absa.org/

Saathoff, P.J., Stathopoulos, T., Dobrescu, M. (1995). Effects of model scale in estimating pollutant dispersion near buildings. *Journal of Wind Engineering and Industrial Aerodynamics*, 54-55, 549-559.
ISSN 0167-6105, http://dx.doi.org/10.1016/0167-6105(94)00071-K

Sengupta, A., Haan, F., Sarkar, P., & Balaramudu, V. (2008). Transient loads on buildings in microburst and tornado winds. *Journal of Wind Engineering and Industrial Aerodynamics*, 96 (10–11), 2173-2187.
ISSN 0167-6105, http://dx.doi.org/10.1016/j.jweia.2008.02.050.

Sester, C., Deroy, O., Sutan, A., Galia, F., Desmarchelier, J.F., Valentin, D., & Dacremont, C. (2013). "Having a drink in a bar": An immersive approach to explore the effects of context on drink choice. *Food Quality and Preference*, 28 (1), 23-31.
ISSN 0950-3293, http://dx.doi.org/10.1016/j.foodqual.2012.07.006.

Shepherd, J.F., & Johnson, C.R. (2008). Hexahedral mesh generation constraints. *Engineering with Computers*, 24 (3), 195-213. DOI 10.1007/s00366-008-0091-4.
ISSN 0177-0667 (Print), ISSN 1435-5663 (Online). Springer-Verlag.

Shih, T.H., Liou, W.W., Shabbir, A., Yang, Z., & Zhu, J. (1995). A new k-ε eddy viscosity model for high reynolds number turbulent flows. *Computers & Fluids*, 24 (3), 227-238.
ISSN 0045-7930, http://dx.doi.org/10.1016/0045-7930(94)00032-T.

Six Phases of Your Project, AIA Pittsburgh. Retrieved from
http://aiapgh.org/aia-architects/working-with-an-architect/six-phases-of-your-project/

Sodja, J. (2007). Turbulence models in CFD. Internal Report, Department of Physics, University of Ljubljana, 2007. Retrieved from
www-f1.ijs.si/~rudi/sola/Turbulence-models-in-CFD.pdf

Souza, A.D. (2005). *How to understand computational fluid dynamics jargon*. NAFEMS Ltd.

Stake, R.E. (1995). *The art of case study research*. London: Sage Publications Ltd.

STAR-CCM+ user guide 8.04

Stathopoulos, T. (1984). Wind loads on low-rise buildings: a review of the state of the art. *Engineering Structures*, 6 (2), 119-135.
ISSN 0141-0296, http://dx.doi.org/10.1016/0141-0296(84)90005-1.

Stathopoulos, T. (1997). Computational wind engineering: Past achievements and future challenges. *Journal of Wind Engineering and Industrial Aerodynamics*, 67–68, 509-532.
ISSN 0167-6105, http://dx.doi.org/10.1016/S0167-6105(97)00097-4.

Stathopoulos, T., Hajra, B., & Bahloul, A. (2008). Analytical evaluation of dispersion of exhaust from roof top stacks on buildings. IRSST research report R-576, Institut de recherché Robert-Sauve´ en sante´ et en securite´ du travail, Montreal, Canada.

Suaris, W., & Irwin, P. (2010). Effect of roof-edge parapets on mitigating extreme roof suctions. *Journal of Wind Engineering and Industrial Aerodynamics*, 98 (10–11), 483-491.
ISSN 0167-6105, http://dx.doi.org/10.1016/j.jweia.2010.03.001.

Tamura, T., Nozawa, K., & Kondo, K. (2008). AIJ guide for numerical prediction of wind loads on buildings. *Journal of Wind Engineering and Industrial Aerodynamics*, 96(10–11), 1974-1984.
ISSN 0167-6105, http://dx.doi.org/10.1016/j.jweia.2008.02.020.

Tieleman, H., Hajj, M., & Reinhold, T. (1998). Wind tunnel simulation requirements to assess wind loads on low-rise buildings. *Journal of Wind Engineering and Industrial Aerodynamics*, 74–76 (1), 675-685.
ISSN 0167-6105, http://dx.doi.org/10.1016/S0167-6105(98)00061-0.

Tominaga, Y., Murakami, S., & Mochida, A. (1997). CFD prediction of gaseous diffusion around a cubic model using a dynamic mixed SGS model based on composite grid technique. *Journal of Wind Engineering and Industrial Aerodynamics*, 67–68, 827-841.
ISSN 0167-6105, http://dx.doi.org/10.1016/S0167-6105(97)00122-0.

Tominaga, Y., & Stathopoulos, T. (2007) Turbulent Schmidt numbers for CFD analysis with various types of flowfield. *Atmospheric Environment*, 41 (37), 8091-8099.
ISSN 1352-2310, http://dx.doi.org/10.1016/j.atmosenv.2007.06.054.

Tominaga, Y., Mochida, A., Yoshie, R., Kataoka, H., Nozu, T., Yoshikawa, M., & Shirasawa, T. (2008). AIJ guidelines for practical applications of CFD to pedestrian wind environment around buildings. *Journal of Wind Engineering and Industrial Aerodynamics*, 96(10–11), 1749-1761.
ISSN 0167-6105, http://dx.doi.org/10.1016/j.jweia.2008.02.058.

Tominaga, Y., & Stathopoulos, T. (2009). Numerical simulation of dispersion around an isolated cubic building: Comparison of various types of k–ε models. *Atmospheric Environment*, 43 (20), 3200-3210.
ISSN 1352-2310, http://dx.doi.org/10.1016/j.atmosenv.2009.03.038.

Tominaga, Y., & Stathopoulos, T. (2010). Numerical simulation of dispersion around an isolated cubic building: Model evaluation of RANS and LES. *Building and Environment*, 45 (10), 2231-2239.
ISSN 0360-1323, http://dx.doi.org/10.1016/j.buildenv.2010.04.004

Tominaga, Y., & Stathopoulos, T. (2011). CFD modeling of pollution dispersion in a street canyon: Comparison between LES and RANS. *Journal of Wind Engineering and Industrial Aerodynamics*, 99 (4), 340-348.
ISSN 0167-6105, http://dx.doi.org/10.1016/j.jweia.2010.12.005.

Uddin, N. (2008). Turbulence modeling of complex flows in CFD (Doctoral dissertation). Retrieved from http://elib.uni-stuttgart.de/opus/volltexte/2008/3638/

Udoewa, V., & Kumar, V. (2012). Computational Fluid Dynamics, Applied Computational Fluid Dynamics, Prof. Hyoung Woo Oh (Ed.), ISBN: 978-953-51-0271-7, InTech, DOI: 10.5772/28614. Retrieved from: http://www.intechopen.com/books/applied-computational-fluid-dynamics/computational-fluid-dynamics

Veress, A. & Rohács, J. (2012). Application of Finite Volume Method in Fluid Dynamics and Inverse Design Based Optimization, Finite Volume Method - Powerful Means of Engineering Design, PhD. Radostina Petrova (Ed.), ISBN 978-953-51-0445-2, InTech, DOI: 10.5772/38786. Retrieved from: http://www.intechopen.com/books/finitevolume-method-powerful-means-of-engineering-design/application-of-finite-volume-method-in-fluid-dynamicsand-inverse-design-based-optimization.

Versteeg, H. & Malalasekera, W. (1995). *An introduction to computational fluid dynamics: The finite volume method*. England: Pearson Education Ltd.

Wainwright, J. & Mulligan, M. (Eds.). (2004). *Environmental Modelling Finding Simplicity in Complexity*. England: John Wiley & Sons Ltd.

Watakabe, M., Ohashi, M., Okada, H., Okuda, Y., Kikitsu, H., Ito, S., Sasaki, Y., Yasui, K., Yoshikawa, K., & Tonagi, M. (2002). Comparison of wind pressure measurements on tower-like structure obtained from full-scale observation, wind tunnel test, and the CFD technology. *Journal of Wind Engineering and Industrial Aerodynamics*, 90 (12–15), 1817-1829.
ISSN 0167-6105, http://dx.doi.org/10.1016/S0167-6105(02)00290-8.

Werner, H., & Wengle, H. (1993). Large eddy simulation of turbulent flow over and around a cube in plane channel. *In: Proceedings of 8th symposium on turbulent shear flows*, pp.155-168.
Wong, N.H., & Heryanto, S. (2004). The study of active stack effect to enhance natural ventilation using wind tunnel and computational fluid dynamics (CFD) simulations. *Energy and Buildings*, 36 (7), 668-678.
ISSN 0378-7788, http://dx.doi.org/10.1016/j.enbuild.2004.01.013.

Yin, R. K. (1994). *Case study research*. Thousand Oaks, CA: Sage Publications

Zeng, Z., Li, X., Li, C., & Zhu, Y. (2012). Modeling ventilation in naturally ventilated double-skin façade with a venetian blind. *Building and Environment*, 57, 1-6.
ISSN 0360-1323, http://dx.doi.org/10.1016/j.buildenv.2012.04.007.

Zhang, A., & Gu, M. (2008). Wind tunnel tests and numerical simulations of wind pressures on buildings in staggered arrangement. *Journal of Wind Engineering and Industrial Aerodynamics*, 96 (10–11), 2067-2079.
ISSN 0167-6105, http://dx.doi.org/10.1016/j.jweia.2008.02.013.

Zhang, L.P., & Wang, Z.J. (2004). A block LU-SGS implicit dual time-stepping algorithm for hybrid dynamic meshes. *Computers & Fluids*, 33(7), 891-916.
ISSN 0045-7930, http://dx.doi.org/10.1016/j.compfluid.2003.10.004.

Zhang, Z., Chen, X., Mazumdar, S., Zhang, T., & Chen, Q. (2009). Experimental and numerical investigation of airflow and contaminant transport in an airliner cabin mockup. *Building and Environment*, 44(1), 85-94.
ISSN 0360-1323, http://dx.doi.org/10.1016/j.buildenv.2008.01.012.

Zhai, Z., & Chen, Q.Y. (2004). Numerical determination and treatment of convective heat transfer coefficient in the coupled building energy and CFD simulation. *Building and Environment*, 39 (8), 1001-1009.
ISSN 0360-1323, http://dx.doi.org/10.1016/j.buildenv.2004.01.023.

APPENDICES

Appendix A: CFD procedures

In general, a CFD analysis is typically composed of three phases: pre-processing, solving and post-processing. Pre-processing consists of importing the building geometry from CAD, creating a computational domain, mesh generation, defining boundaries and initial conditions, and setting numerical controls. Once the computational conditions have been set, the analysis will proceed using commercial CFD codes such as STAR-CD and STAR CCM+ *(CD-Adapco)*, FLUENT and CFX *(ANSYS, Inc),* OpenFOAM, or COVERFLOW. The results can take the form of color plots, contour plots, and numerical reports in the post-processing phase. The specific process involved in performing a CFD analysis is outlined in detail in *NPARC Alliance CFD Verification and Validation* (2012):

1) Formulate the Flow Problem
2) Model the Geometry and Flow Domain
3) Establish the Boundary and Initial Conditions
4) Generate the Grid
5) Establish the Simulation Strategy
6) Establish the Input Parameters and Files
7) Perform the Simulation
8) Monitor the Simulation for Completion
9) Post-Process the Simulation to get the Results
10) Make Comparisons of the Results
11) Repeat the Process to Examine Sensitivities
12) Document

Appendix B: CFD fundamentals

1. Governing equations

According to the book *Computational Fluid Dynamics: The Basics With Applications* (Anderson, 1995), CFD utilizes the fundamental governing equations of fluid dynamics as represented by the continuity, momentum, and the energy equations. These are based on three fundamental physical principals:

(1) Mass is conserved;
(2) F = ma (Newton's second law); and
(3) Energy is conserved (Anderson, 1995, p.38).

These are summarized in the Navier–Stokes equations for incompressible flow:

$$\frac{\partial u_i}{\partial x_i} = 0$$ Equation 1- The conservation of mass

$$\frac{\partial(\rho u_i)}{\partial t} + \frac{\partial(\rho u_i u_j)}{\partial x_j} = -\frac{\partial p}{\partial x_i} + \frac{\partial}{\partial x_j}\left(\mu \frac{\partial u_i}{\partial x_j}\right) + S_i$$ Equation 2 - A momentum equation

where x_i (i = 1, 2, 3) are the three coordinate directions, u_i (i = 1, 2, 3) are the velocities in these directions, p is pressure, ρ is density and μ is viscosity. Equation 1 expresses the conservation of mass, while Equation 2 is a momentum equation where the first term on the left-hand side represents the variation with time and the second is the convection term; on the right-hand side the terms are the pressure gradient, a diffusion term and the source term, respectively (Wainwright & Mulligan, 2004). In general, the Navier-Stokes equations comprise a system of nonlinear partial differential equations and provide the highest level approximations for the flow physics approaching the continuum-mechanics based flow regime (Veress & Rohács, 2012).

2. Initial conditions

At an early stage of the CFD process, the initial conditions must be determined. These conditions are sensitive to the selection of the turbulence model to be utilized. The number of iterations is set up for steady flow problems, but for the case of unsteady flow problems, time steps are needed. A more detailed explanation of how the turbulence model is selected is provided below in Section 5.

3. Grid generation

The geometric domain to be modeled using CFD must be divided up or *discretized* into cells. The combination of all the cells is regarded as the grid or computational domain. For example, three dimensional cells are usually hexahedral or tetrahedral in shape (Scott et al., 2006). The process of determining the grid is referred to as *grid*, or *mesh generation*. Anderson (1995) pointed out that the grid generation is a significant consideration in the CFD process and an appropriate determination of the type of grid is essential if a valid numerical solution is to be obtained. This process has a significant impact on the efficiency and accuracy of CFD, as the element or cell shape and size influences both the computation speed and numerical accuracy (Kortelainen, 2009).

Based upon the connectivity of the mesh or on the type of elements two types of meshes, structured and unstructured, have been defined as shown in Figure 1. According to Bern and Plassmann (2000), all the interior vertices of a structured mesh are topologically alike and the vertices of an unstructured mesh may be arbitrarily different for local neighborhoods. They also noted that a hybrid mesh can be made up of a number of small structured meshes in an overall unstructured pattern, as shown in Figure 2. While a structural mesh is simple and easy to access, an unstructured mesh generally provides a better fit for complicated domains and offers more convenient mesh adaptivity (Oliveira et al., 2008). A high-quality hybrid mesh can take advantage of both these approaches. In addition, both structured and unstructured meshes must

remove unnecessary details in the geometry to ensure robustness and mesh quality (Oliveira et al., 2008).

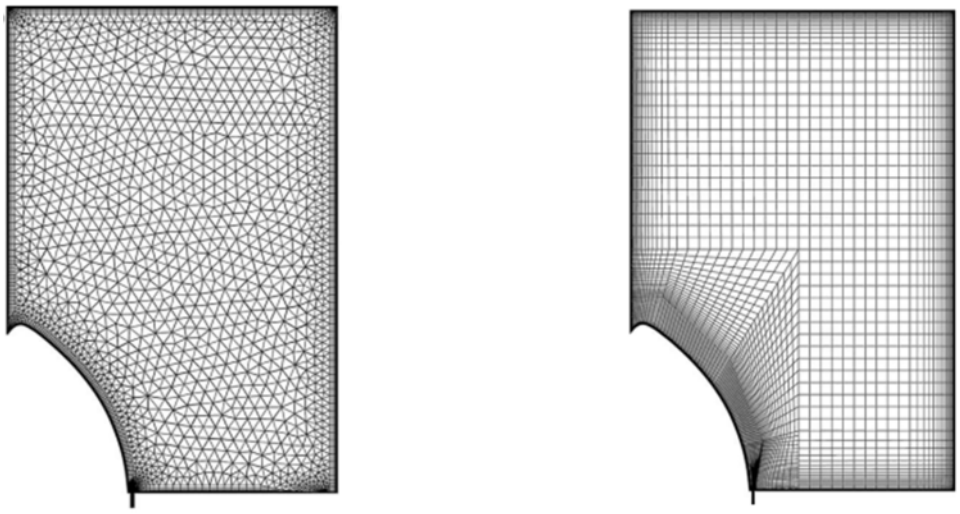

a. Unstructured mesh b. Structured mesh

Figure 1 - The two different mesh types (Bosbach et al. ,2006)

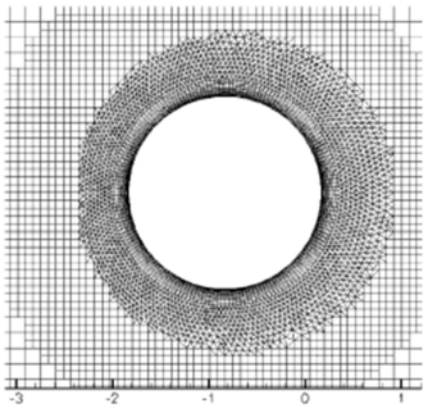

Figure 2 - Close-up view of a hybrid computational grid (Zhang & Wang, 2004)

4. Discretization

Once the cell types have been determined, the next step is to divide the flow domain into small computational volumes called *elements* or *cells* that cover the domain completely but do not

overlap one another (Kortelainen, 2009). Depending upon the type of discretization method utilized, computational grids can be either structured or unstructured. Anderson defined *discretization* as:

the process by which a closed-form mathematical expression, such as a function or a differential or integral equation involving functions, all of which are viewed as having an infinite continuum of values throughout some domain, is approximated by analogous (but different) expressions which prescribe values at only a finite number of discrete points or volumes in the domain (1995, p.125).

Various numerical discretization methods have been developed for the solution of non-linear Partial Differential Equations (Uddin, 2008). According to Veress and Rohács (2012), three discretization methods are normally used in commercial CFD codes: the Finite Difference method, the Finite Element method and the Finite Volume method. Other discretization methods such as the Spectral, Boundary element, Vorticity type and Lattice gas or Lattice Boltzmann methods have been rarely, if ever, used for this purpose.

The characteristics of the three most frequently used methods can be summarized as follows (Udoewa & Kumar, 2012; Veress & Rohács, 2012):

1) The *Finite Difference* method (FDM) is the most traditional and oldest method of the three and is only suitable for structured grids. The mesh size and properties such as stretch ratio, aspect ratio and skewness have a significantly impact on its accuracy. This method is not widely used because of the geometric limitations it imposes on applications, but it is the easiest discretization method of the three.

2) The *Finite Element* method (FEM) provides greater flexibility for dealing with complex geometries than the Finite Difference method. The mesh in the Finite Element method can be either structured or unstructured. While this method is more stable than the Finite Volume method, it requires more computing memory than the Finite Volume method.

3) The *Finite Volume* method (FVM) calculates the partial differential equations over finite volumes created as parts of one or more cells that can be either overlapped or non-overlapped. In this method, it is possible to modify the shape and location of the control volumes to allow greater freedom in the choice of the functional representation of the flow field. The Finite Volume Method permits the use of irregular grids while retaining computational simplicity.

As shown in Figure 3, while FEM separates the continuum region of interest into a number of simply shaped regions, FVM subdivides the domain of interest into a finite number of contiguous control volumes based on a grid (Molina-Aiz et al., 2010).

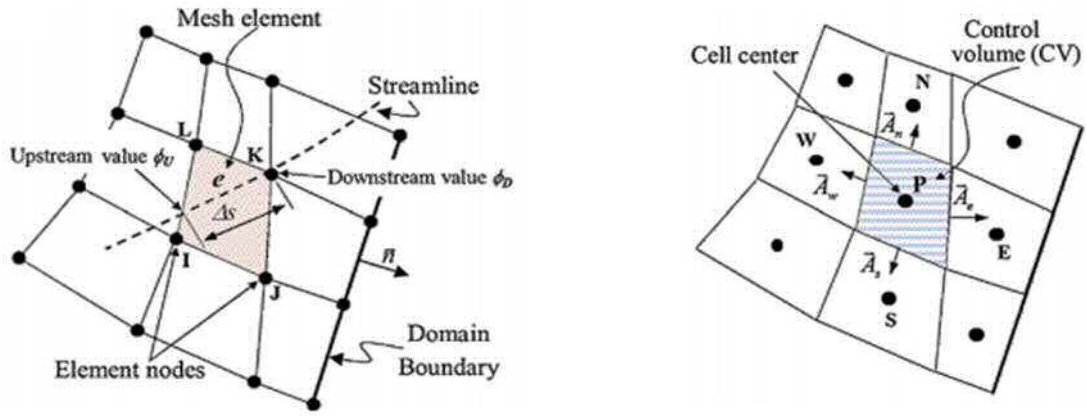

a. FEM b. FVM

Figure 3 - Structured meshes for the two main discretization methods (Molina-Aiz et al., 2010)

5. Turbulence models

A fundamental phenomenon in this field of study is turbulence. Generally, turbulence is a complicated phenomenon that occurs over a wide range of time scales and length scales. Most CFD researchers deal with this by selecting a certain length scale and time scale for the range of turbulence anticipated since turbulence acts over such a wide range of length scales and its periodicity manifests over similarly wide ranges of time periods (Udoewa & Kumar, 2012). Udoewa and Kumar explained that resolving turbulence means computing and calculating

turbulent quantities such as vorticity, velocities and pressures in turbulent regions and noted that modeling turbulence creates the effect of fully resolved turbulence on unknown values such as velocity and pressure based on the effect of the equation to which an expression is added. Turbulence modeling is difficult and represents the most important challenge facing CFD (Wainwright & Mulligan, 2004) and successfully modeling turbulence greatly enhances the quality of numerical simulations (Sodja, 2007).

There are three popular approaches for the analysis of a turbulent flow problem, namely *Direct Numerical Simulation* (DNS), *Large Eddy Simulation* (LES) and models based on *Reynolds Averaged Navier-Stokes* (RANS) equations (Udim, 2008). The characteristics of these three approaches are summarized by Wainwright & Mulligan in their book *Environmental Modeling: Finding Simplicity in Complexity* as follows:

For DNS, it is possible to predict all the eddy structures from the large ones down to the smallest but it requires significant computing resources for practical flows. In LES approach, it uses a length scale to differentiate between larger and smaller eddies. The larger eddies are resolved directly but the smaller eddies are not predicted directly. The smaller eddies are accounted for through a subgrid-scale model. When applying this approach, appropriate filter or grid size should be considered in order to achieve accurate results. However it is less expensive than DNS, LES still requires high computing power and needs fine grids for practical flows. On the other hand, the most widely used approach is the turbulence models based on RANS equations. The most popular option is the k - ε model which is usually the default option in CFD software. k represents the kinetic energy in the turbulent fluctuations and ε represents the rate of dissipation of k (2004, pp.338).

In addition, Udim (2008) mentioned that the RANS approach predicts only the mean flow field and can be applied to achieve a sufficiently accurate prediction in many cases. However, this does fail to represent the true flow physics.

In sum, although both the DNS and LES approaches provide better results, they require far greater computer resources than turbulence models based on RANS methods. Furthermore, there are a number of different versions of turbulence models based RANS methods now available commercially (Udoewa & Kumar, 2012).

6. Solution algorithm

CFD simulations are constructed around numerical algorithms that can deal with fluid flow problems. For example, consider the numerical algorithms used to resolve the coupling that arises in the solution of Navier-Stokes equations between velocity, density and pressure (Moukalled & Darwish, 2000). The SIMPLE (Semi-Implicit Method for Pressure Linked Equations) type of algorithm is commonly used in CFD studies (Patankar & Spalding, 1972), but over the years, a number of modified versions of the SIMPLE algorithm have been suggested including the SIMPLER, SIMPLEC and PISO algorithms (Moukalled & Darwish, 2000).

Versteeg and Malalasekera (1995) compared those four algorithms in their book *An Introduction to Computational Fluid Dynamics: The Finite Volume Method*. The SIMPLE algorithm was originally proposed by Patankar and Spalding (1972) and is essentially a guess-and-correct procedure for the calculation of pressure on a staggered grid arrangement. This method is relatively straightforward and has been successfully used in numerous CFD procedures. The SIMPLER (SIMPLE-Revised) algorithm is an improved version of the SIMPLE algorithm that utilizes pressure corrections only to correct velocity fields. Consequently, this algorithm is very effective in calculating the pressure field correctly and solving the momentum equations while at the same time reducing the computing resources required. The book also introduces the SIMPLEC and PISO algorithms. The SIMPLEC (SIMPLE-Consistent) algorithm follows the same steps as the SIMPLE algorithm but defines the coefficients in the pressure-correlation equation differently. The PISO algorithm, where the acronym PISO stands for Pressure Implicit with Splitting of Operators, and implements a pressure‑velocity calculation procedure for the non-iterative computation of unsteady compressible flows. Versteeg and Malalasekera consider that although the SIMPLEC and PISO algorithms have proved that they are as efficient as the

SIMPLER algorithm for certain types of flows, it is not clear whether they are better overall than the SIMPLER algorithm.

7. Boundary conditions

After choosing a suitable mathematical model for the physical phenomenon, boundary conditions must be chosen. For boundary-value problems, it is essential to assign values along the boundary of the domain that will permit the problem to be solved throughout the entire 2D or 3D space. There are two types of boundary conditions, namely *Dirichlet* and *Neumann* boundary conditions. For a Dirichlet boundary condition, the fixed value of the unknown on the boundary is specified for some flow problems; this is referred to as a direct boundary condition. In contrast, when the value of a derivative of the unknown is specified, this is called a Neumann or natural boundary condition. These boundaries are spatial boundaries (Udoewa & Kumar, 2012).

According to Wainwright & Mulligan (2004), it is common for the velocity to be fixed at an inlet and outlet. For an inlet, turbulence quantities must be correctly specified and inlet profiles consistent with the definition of roughness along the boundaries of the domain. For the outlet condition, careful consideration must be given to the question of whether the outflow should equal the inflow or whether the flow profile should be uniform along the stream direction in order to avoid poor convergence or solutions that are not physically feasible.

8. Numerical parameters for controlling the calculation

Numerical parameters must be specified in order to control the calculation and reduce the computational resources needed. These parameters include the relaxation factor, monitoring residuals, different numerical schemes, the number of iterations for steady flow, number of time steps for unsteady flow, and the choice between single and double precision.

Appendix C: Definitions of several CFD terms

CFD is a computer based mathematical modeling tool that is based upon the fundamental governing equations of fluid dynamics. However, terms within CFD are often not obvious to non-experts to that field (Souza, 2005). Thus, it is important to introduce and describe CFD terms to them. While the most commonly used parameters of CFD will be introduced in this chapter, several terms of CFD simulation will be introduced briefly in this section.

1. Aspect ratio

This is ratio of longest edge length to shortest edge length and it is a measure of quality for a computational grid. In order to avoid convergence problems, the cell aspect ratios should be kept as small as possible (Souza, 2005; STAR-CCM+ user guide 8.04).

2. Boundary conditions

The spatial or temporal specification of variable values or behavior to produce an unique solution (Souza, 2005).

3. Convergence criteria

Through the iterations, the magnitude of the velocity divergence is reduced below some absolute numerical value that tends to a single answer (Souza, 2005)

4. Divergence

The progression of a numerical scheme away from any single solution (Souza, 2005).

5. Grid / mesh

This is the outcome of discretizing the computational domain into a number of elements or cells defining the discrete points at which the numerical solution is computed (Souza, 2005).

6. Grid density

This term means the number of cells in a given volume. A higher grid density should be applied in regions of interest where the variables change rapidly so that their gradients can be computed and represented accurately. In the case of lower grid density, it is generally used where the solution is changing less in order to reduce the computational resources (Souza, 2005).

7. Invalid cell

When each cell interior face belongs to exactly two cells, this is considered as valid cell. If the arrays storing the cell connectivity and vertices have entries that make reference to faces or vertices that fall outside the expected range of values, invalid cells occur (STAR-CCM+ user guide 8.04).

8. No-slip wall

This term means that the fluid velocity at the wall equals the wall velocity. The wall can rest or a tangential wall velocity in the form of a velocity vector with respect to the laboratory coordinate system can be specified (STAR-CCM+ user guide 8.04).

9. Schmidt number

A dimensionless number that is the ratio of kinematic viscosity to diffusivity (STAR-CCM+ user guide 8.04).

10. Skewness

This term is an important measure of cell quality and it is designed to reflect whether the cells on either side of a face are formed in such a way as to permit diffusion of quantities without these quantities becoming unbounded (STAR-CCM+ user guide 8.04).

11. Slip wall

This term means that the fluid velocity at the wall is different with the wall velocity (STAR-CCM+ user guide 8.04).

12. Structured grid

This grid forms a regular pattern. Its grid lines are continuous across the domain and are usually aligned with the co-ordinate directions. For this grid, hexahedra in three dimensions or quadrilaterals in two dimensions are included (Souza, 2005).

13. Unclosed cell

Generally a topologically closed volume cell consists of edges that are connected to exactly two faces, and faces with normals pointing outwards. When a cell is missing a face, or the outward normals are inconsistent, it is regarded as unclosed mesh (STAR-CCM+ user guide 8.04).

14. Unstructured grid

Unlike structured grid, this grid forms an irregular pattern. This grid allows highly complex geometries to be modeled with relative ease compared to structured grids (Souza, 2005).

15. Wall functions

This function has been used to describe the effects of turbulent boundary layers in the region adjacent to a wall, without resolving details of the near wall flow and eliminating the need for high grid resolution in the viscous sub-layer (Souza, 2005).

Appendix D: The commercial CFD codes

Many commercial CFD codes such as STAR-CD and STAR CCM+ *(CD-Adapco)*, FLUENT and CFX *(ANSYS, Inc.)* or OpenFOAM have been used to simulate physical processes. These commercial CFD packages include pre-processors to construct grids, and apply initial conditions, processing algorithms that permit segregated or coupled, steady or unsteady state flows and a variety of turbulence models, and post-processors that display results in a manner that enhance interpretation. Among commercial codes, the characteristics of FLUENT and STAR-CCM+ have been reviewed.

1. FLUENT

FLUENT is a most commonly used commercial CFD code. FLUENT solves the conservative form of the Navier-Stokes equations using the finite volume method on an unstructured, non-orthogonal, curvilinear coordinate grid system. Combinations of elements in a variety of shapes are permitted, such as quadrilaterals and triangles for 2-D simulations and hexahedra, tetrahedra, polyhedra, prisms and pyramids for 3-D simulations. Meshes can be created using mesh generators (GAMBIT) or by several third-party CAD packages. FLUENT allows the following file formats for importing are summarized in table 1 (*ANSYS* FLUENT, 12.0 User's Guide).

Table 1 - File formats for importing into FLUENT (*ANSYS* FLUENT, 12.0 User's Guide)

ABAQUS .inp, .fil, and .odb files
Mechanical APDL .inp, .cdb, .rst, .rmg, and .rfl files.
ANSYS CFX .def and .res files
CGNS files
EnSight files
ANSYS FIDAP Neutral files
GAMBIT files
HYPERMESH ASCII files.
NASTRAN Bulk Data files
PATRAN Neutral files.
PLOT3D mesh and result files.

Turbulent flow models including several popular k–epsilon and k–omega models, and the Reynolds stress model (RSM) are available. Moreover, large eddy simulation (LES) and the more economical detached eddy simulation (DES) turbulence models can be employed (*ANSYS* FLUENT, 12.0 User's Guide).

2. STAR-CCM+

STAR-CCM+ includes the general characteristics of FLUENT. In addition, STAR-CCM+ has a single environment for whole CFD process such as solid modeling, mesh generation, post-processing, etc. Moreover, STAR-CCM+ has a comprehensive suite of geometry creation and preparation tools. For meshing, STAR-CCM+ employs the technology of hexahedral, dodecahedral and arbitrary polyhedral cells and produces boundary trimmed meshes that conform to geometry, as well as high quality prism layer meshes for accuracy. The following file formats that can be imported into STAR-CCM+ are summarized in table 2 (STAR-CCM+ user guide 8.04).

Table 2 - File formats for importing into STAR-CCM+ (STAR-CCM+ user guide 8.04)

Parasolid .x_t , .x_b
IGES .iges, .igs
STEP .stp, .step
Stereo lithography file .stl
PATRAN shells .pat
NASTRAN shells .nas
CATIA V4 .model, .exp, .session / CATIA V5 .catpart, .cadproduct
SolidWorks .sldprt, .sldasm
PRO/Engineer .prt, .asm
Autodesk Inventor .ipt, .iam

For turbulence models, various models that provide closure of the RANS equations, LES and DES model are also available (STAR-CCM+ user guide 8.04).

3. The selection of CFD code

Reviewing manuals, similarities and differences between FLUENT and STAR-CCM+ in their physics conditions such as turbulence types, grid discretization, and solving methods were obtained. Although FLUENT is widely used and initially considered as a potential candidate for this study, it has difficulties in creating models and meshes from other tools such as GAMBIT. Moreover, the cost of its license ranges from $2,000 to $ 10,000 per year. In the case of STAR-CCM+, it provides a single environment in which users can perform CAD creation to post-processing and allows various types of file formats to be imported. In addition, free academic license is provided. Thus, STAR-CCM+ was employed for this present study.